

NIST GCR 14-917-28



Review of Past Performance and Further Development of Modeling Techniques for Collapse Assessment of Existing Reinforced Concrete Buildings

NEHRP Consultants Joint Venture
*A Partnership of the Applied Technology Council and the
Consortium of Universities for Research in Earthquake Engineering*



Disclaimers

This report was prepared for the Engineering Laboratory of the National Institute of Standards and Technology (NIST) under the National Earthquake Hazards Reduction Program (NEHRP) Earthquake Structural and Engineering Research Contract SB134107CQ0019, Task Order 11177. The contents of this publication do not necessarily reflect the views and policies of NIST or the U.S. Government.

This report was produced by the NEHRP Consultants Joint Venture, a joint venture of the Applied Technology Council (ATC) and the Consortium of Universities for Research in Earthquake Engineering (CUREE). While endeavoring to provide practical and accurate information, the NEHRP Consultants Joint Venture, the authors, and the reviewers assume no liability for, nor express or imply any warranty with regard to, the information contained herein. Users of information contained in this report assume all liability arising from such use.

Unless otherwise noted, photos, figures, and data presented in this report have been developed or provided by NEHRP Consultants Joint Venture staff or consultants engaged under contract to provide information as works for hire. Any similarity with other published information is coincidental. Photos and figures cited from outside sources have been reproduced in this report with permission. Any other use requires additional permission from the copyright holders.

Certain commercial software, equipment, instruments, or materials may have been used in the preparation of information contributing to this report. Identification in this report is not intended to imply recommendation or endorsement by NIST, nor is it intended to imply that such software, equipment, instruments, or materials are necessarily the best available for the purpose.

NIST policy is to use the International System of Units (metric units) in all its publications. In this report, however, information is presented in U.S. Customary Units (inch-pound), as this is the preferred system of units in the U.S. earthquake engineering industry.

Cover photo – Damage to the Four Seasons Apartment Building resulting from the 1964 earthquake in Anchorage, Alaska (courtesy of the Karl V. Steinbrugge Collection, University of California, Berkeley, NISEE, 2013a, with permission).

NIST GCR 14-917-28

Review of Past Performance and Further Development of Modeling Techniques for Collapse Assessment of Existing Reinforced Concrete Buildings

Prepared for
U.S. Department of Commerce
National Institute of Standards and Technology
Engineering Laboratory
Gaithersburg, MD 20899

By
NEHRP Consultants Joint Venture
*A partnership of the Applied Technology Council and the
Consortium of Universities for Research in Earthquake Engineering*

December 2013



U.S. Department of Commerce
Penny Pritzker, Secretary of Commerce

National Institute of Standards and Technology
*Patrick D. Gallagher, Under Secretary of Commerce for
Standards and Technology and Director*

Participants

National Institute of Standards and Technology

John (Jack) R. Hayes, Jr., Director, National Earthquake Hazards Reduction Program
Steven L. McCabe, Deputy Director, National Earthquake Hazards Reduction Program

NEHRP Consultants Joint Venture

Applied Technology Council
201 Redwood Shores Parkway, Suite 240
Redwood City, California 94065
www.ATCouncil.org

Consortium of Universities for
Research in Earthquake Engineering
1301 S. 46th Street, Building 420
Richmond, California 94804
www.CUREE.org

Joint Venture Management Committee

James R. Harris
Robert Reitherman
Christopher Rojahn
Andrew Whittaker

Joint Venture Program Committee

Jon A. Heintz (Program Manager)
Michael Constantinou
C.B. Crouse
James R. Harris
William T. Holmes
Jack Moehle
Andrew Whittaker

Project Management

Christopher Rojahn
Jon P. Kiland

Project Review Panel

JoAnn Browning
Gregory Deierlein
James O. Jirsa
Laura N. Lowes
Nicholas Luco
Terry Lundein
Mike Mehrain

Project Technical Committee

Kenneth J. Elwood (Project Director)
Jack Baker
Craig D. Comartin
William T. Holmes
Jack Moehle
Peter Somers

Preface

In 2007, the National Institute of Standards and Technology (NIST) awarded the NEHRP Consultants Joint Venture, a partnership of the Applied Technology Council (ATC) and the Consortium of Universities for Research in Earthquake Engineering (CUREE), a National Earthquake Hazards Reduction Program (NEHRP) “Earthquake Structural and Engineering Research” task order contract (SB1341-07-CQ-0019) to conduct a variety of tasks. In 2011, NIST initiated Task Order 11177 entitled “Development of a Collapse Indicator Methodology for Existing Reinforced Concrete Buildings.” The purpose of this project was to initiate the first phase of work related to the development of a methodology for identifying older reinforced concrete buildings that are at risk of collapse, as outlined in NIST GCR 10-917-7, *Program Plan for the Development of Collapse Assessment and Mitigation Strategies for Existing Reinforced Concrete Buildings* (NIST, 2010b).

The first phase of work of the *Program Plan*, documented in this report, included the identification of critical deficiencies, refinement of the list of common deficiencies, and development of collapse mitigation strategies for older reinforced concrete buildings. To facilitate the anticipated analysis program that is envisioned for developing collapse indicators, this phase also included identification of the latest analysis, modeling, and collapse simulation techniques for reinforced concrete components and systems. Because analytical capabilities are rapidly evolving, and the *Program Plan* includes several research initiatives related to improving collapse simulation that won’t be completed for many years, a key strategy in this effort was the conduct of a Collapse Simulation Workshop. In this workshop, leading researchers and practitioners were assembled to review and discuss current state-of-the-art techniques, and to define recommendations for analyzing and simulating degrading response of reinforced concrete systems, which can be used in the near term.

The NEHRP Consultants Joint Venture is indebted to the leadership of Ken Elwood, Project Director, and to the members of the Project Technical Committee, consisting of Jack Baker, Craig Comartin, Bill Holmes, Jack Moehle, and Peter Somers, for their significant contributions in the development of this report and the resulting recommendations. Technical review and comment at key developmental stages of the project were provided by the Project Review Panel, consisting of JoAnn Browning, Greg Deierlein, Jim Jirsa, Laura Lowes, Nico Luco, Terry Lundein, and Mike Mehrain. The invited experts who attended the Collapse Simulation Workshop

were instrumental in identifying interim techniques for nonlinear collapse simulation included in this report. The names and affiliations of all who contributed to this project are provided in the list of Project Participants.

The NEHRP Consultants Joint Venture also gratefully acknowledges Jack Hayes (NEHRP Director) and Steve McCabe (NEHRP Deputy Director) for their input and guidance in the preparation of this report, Christopher Rojahn and Jon Kiland for ATC project management services, and Bernadette Hadnagy and Amber Houchen for ATC report production services.

Jon A. Heintz
Program Manager

Table of Contents

Preface	iii
List of Figures	ix
List of Tables.....	xiii
1. Introduction	1-1
1.1 Background.....	1-1
1.2 Program Plan.....	1-3
1.2.1 Conceptual Methodology.....	1-4
1.2.2 Work Plan	1-9
1.3 Goals and Report Structure.....	1-10
2. Critical Deficiencies Based on Collapse Case Studies.....	2-1
2.1 Methodological Approach	2-2
2.1.1 Design and Construction Characteristics Affecting Seismic Performance	2-2
2.1.2 Building Selection.....	2-7
2.1.3 Data Assembly.....	2-8
2.1.4 Review and Interpretation.....	2-9
2.2 Building Summaries	2-10
2.2.1 Bullock's Department Store.....	2-10
2.2.2 CTV Building	2-11
2.2.3 Four Seasons Apartment Building.....	2-12
2.2.4 Imperial County Services Building.....	2-13
2.2.5 Olive View Medical Center Main Building.....	2-15
2.2.6 Olive View Psychiatric Clinic	2-16
2.2.7 Olive View Stair Towers	2-17
2.2.8 Pyne Gould Building	2-18
2.2.9 Royal Palm Resort	2-19
2.3 Common Characteristics Among the Buildings.....	2-21
2.3.1 Characteristics Affecting Damage States and Collapse Modes	2-21
2.3.2 Common Design and Construction Characteristics Among Example Buildings.....	2-23
2.3.3 Interaction of Characteristics and the Effect on Performance	2-28
2.4 Conclusions and Implications	2-29
2.4.1 Practical Applications	2-30
2.4.2 Case Histories	2-30
2.4.3 Collapse Analysis Techniques for Engineering Practice	2-31
2.4.4 Physical Testing.....	2-31
2.4.5 Limitations	2-31

3.	Collapse Mitigation Strategies.....	3-1
3.1	Introduction	3-1
3.2	Existing Resources for Building Seismic Retrofit	3-2
3.3	Retrofit Strategies Focused on Collapse Mitigation.....	3-4
3.3.1	Configuration	3-4
3.3.2	Gravity Load-Carrying System	3-5
3.3.3	Shear-Critical Vertical Elements.....	3-6
3.3.4	Load-Path Continuity	3-7
3.3.5	Axial Load in Vertical Elements.....	3-7
3.3.6	Overall System Strength	3-8
4.	Summary of Modeling Techniques for Collapse Assessment of Concrete Buildings	4-1
4.1	Columns	4-2
4.1.1	Future Research.....	4-3
4.2	Beam-Column Joints	4-4
4.2.1	Future Research.....	4-6
4.3	Masonry Infilled Concrete Frames.....	4-6
4.3.1	Future Research.....	4-9
4.4	Walls	4-9
4.4.1	Future Research for Walls.....	4-11
4.5	Load-history Effects.....	4-12
4.5.1	Future Research.....	4-14
4.6	Gravity Load Failures in Collapse Simulation.....	4-15
4.6.1	Future Research.....	4-16
4.7	Ground Motion Selection	4-16
4.7.1	Future Research.....	4-19
4.8	Summary and Cross-Cutting Themes	4-19
5.	Recommended Adjustments to the Program Plan	5-1
5.1	Summary of Recommended Adjustments.....	5-1
Appendix A: Collapse Simulation Workshop		A-1
A.1	Objectives.....	A-1
A.2	Description	A-1
A.3	Workshop Mini-Papers	A-4
A.4	Workshop Breakout Groups.....	A-4
Appendix B: Column Models for Collapse Simulation		B-1
B.1	Introduction	B-1
B.2	Model Considerations	B-1
B.3	Available Models	B-2
B.3.1	Summary of Model 1	B-3
B.3.2	Summary of Model 2	B-5
B.3.3	Summary of Model 3	B-6
B.4	Pros and Cons of Modeling Approaches.....	B-7
B.4.1	Analytical Framework.....	B-7
B.4.2	Behavioral Models	B-8
B.5	Summary and Conclusions.....	B-8

Appendix C: Recommendations for Simulating the Response of Beam-Column Joints in Reinforced Concrete Building Frames	C-1
C.1 Introduction.....	C-1
C.2 Models for Interior Beam-Column Joints in 2D Frames	C-4
C.2.1 Recommendations for Modeling Interior Joints in 2D Frames.....	C-6
C.3 Models for Exterior Beam-Column Joints in 2D Frames	C-8
C.3.1 Recommendations for Modeling Exterior Joints in 2D Frames.....	C-8
C.4 Models for Knee-Joints in 2D Frames	C-8
C.5 Models for Joints in 3D Frames.....	C-11
C.5.1 Interior Joints in 3D Frames	C-12
C.5.2 Exterior Corner Joints in 3D Frames	C-12
Appendix D: Modeling Gravity Load Failure in Collapse Simulations.....	D-1
D.1 Abstract.....	D-1
D.2 Gravity Load Failure Modeling	D-1
D.3 Detection of Gravity Load Failure for Columns	D-5
D.4 Detection of Gravity Load Failure for Beam-Column Joints	D-6
D.5 Detection of Gravity Load Failure for Slab-Column Joints.....	D-9
D.5.1 Explicit Modeling of Gravity Systems	D-9
D.6 General Modeling Guidance	D-9
D.6.1 Fiber Section Modeling	D-9
D.6.2 Infill Wall Modeling	D-10
D.6.3 Monte Carlo Simulations.....	D-10
D.7 Closure	D-11
Appendix E: Assessing the Effects of Displacement History on the Seismic Response of Reinforced Concrete Structures.....	E-1
E.1 Introduction.....	E-1
E.2 Example 1: Effect of Displacement History on Column Lateral-Load Carrying Capacity	E-2
E.2.1 Columns Controlled by Flexure.....	E-2
E.2.2 Columns Controlled by Shear.....	E-3
E.3 Example 2: Effect of Displacement History on Column Axial-Load Carrying Capacity	E-4
E.3.1 Question 1	E-5
E.3.2 Question 2	E-5
E.3.3 Discussion.....	E-8
E.4 Other Topics that Require Further Discussion.....	E-9
E.5 Conclusion	E-9
Appendix F: Collapse Simulation of Masonry-Infilled Reinforced Concrete Frames	F-1
F.1 Introduction.....	F-1
F.2 Failure Mechanisms of Infilled Frames and Causes of Collapse.....	F-1
F.3 Nonlinear Finite Element Models.....	F-4
F.4 Simplified Analysis Method	F-7
F.5 Thoughts on Collapse Simulation.....	F-10
F.6 Summary of Collapse Simulation Method and Research Needs	F-12
F.6.1 Proposed Simulation Method.....	F-12

F.6.2	Further Research and Development	F-12
Appendix G: Reinforced Concrete Structural Wall Modeling for Collapse		
Assessment Utilizing Monte Carlo Simulations		G-1
G.1	Introduction	G-1
G.2	Modeling Approaches for Structural Walls.....	G-1
G.2.1	Axial-Bending Behavior	G-1
G.2.2	Rebar Buckling.....	G-3
G.2.3	Shear Behavior.....	G-6
G.2.4	Three-Dimensional Responses.....	G-10
G.2.5	Axial Failure.....	G-11
G.2.6	Splices	G-11
G.2.7	Sliding Shear at Wall Base.....	G-12
G.3	Summary	G-14
References		H-1
Project Participants.....		I-1

List of Figures

Figure 1-1	Approach for establishing collapse indicator limits based on the relative changes in the collapse fragilities with respect to changes in the collapse indicator parameter	1-9
Figure 1-2	Recommended schedule for development of Guidance Documents	1-10
Figure 2-1	Bullock's Department Store earthquake damage.....	2-11
Figure 2-2	CTV Building earthquake damage.....	2-12
Figure 2-3	Four Seasons Apartment Building earthquake damage	2-13
Figure 2-4	Imperial County Services Building. Earthquake damage occurred in the first-story columns at the east end of the building	2-14
Figure 2-5	Olive View Medical Center Main Building earthquake damage	2-16
Figure 2-6	Olive View Psychiatric Clinic earthquake damage.....	2-17
Figure 2-7	Olive View Stair Towers earthquake damage.....	2-18
Figure 2-8	Pyne Gould Building earthquake damage.....	2-19
Figure 2-9	Royal Palm Resort damage.....	2-20
Figure 4-1	Recommended column models: (a) Haselton et al. (2008) for $V_p/V_n \leq 0.6$, (b) Elwood (2004) for $V_p/V_n \geq 0.8$. V_p/V_n is the ratio of column strength, controlled by flexure (plastic shear demand at flexure yielding), to column shear capacity	4-2
Figure 4-2	Recommended joint models in 2D frames.....	4-4
Figure 4-3	Recommended joint model in 3D frames	4-5
Figure 4-4	Schematic illustration of infill frame behavior and relative collapse risk	4-7
Figure 4-5	Simplified analytical model for infill frame, with one diagonal (top figure) and two struts (bottom figure)	4-8
Figure 4-6	Model for shear strength degradation versus curvature ductility.....	4-11
Figure 4-7	Haselton et al. (2008) lumped plasticity model: (a) calibration from symmetric loading of a test specimen (numbers in parentheses denote steps in the calibration process); (b) prediction of the model under ground-motion excitation.....	4-13

Figure 4-8	Incremental Dynamic Analysis results: (a) illustration; (b) Intensity Measure (<i>IM</i>) values at collapse, as observed from the Incremental Dynamic Analysis (IDA) results, and a collapse fragility function fitted to the data	4-17
Figure A-1	Agenda Day 1 – Collapse Simulation Workshop	A-2
Figure A-2	Agenda Day 2 – Collapse Simulation Workshop	A-3
Figure C-1	OpenSees model of an interior joint subassemblage	C-3
Figure C-2	OpenSees model of an exterior joint subassemblage.....	C-3
Figure C-3	Relationship of ductility classification to design joint shear stress, τ , and average bond stress, λ	C-4
Figure C-4	Column shear versus drift for a brittle beam-column joint specimen	C-5
Figure C-5	Column shear versus drift for a limited-ductility beam-column joint specimen	C-5
Figure C-6	Column shear versus drift for a ductile beam-column joint specimen	C-6
Figure C-7	Column shear versus drift for an anchorage-controlled exterior joint specimen	C-9
Figure C-8	Column shear versus drift for a shear-controlled exterior joint specimen	C-9
Figure D-1	Element removal algorithm	D-3
Figure D-2	Response of a system with nonductile columns experiencing axial failure from shaking table tests and analyses with and without element removal.....	D-5
Figure D-3	Overview of unreinforced beam-column joint model.....	D-7
Figure D-4	Axial capacity model for beam-column joints.....	D-8
Figure D-5	Contribution of different components to beam tip displacement in a beam-column joint test.....	D-8
Figure D-6	Gravity system contribution to vertical capacity	D-9
Figure D-7	Construction of a Tornado diagram.....	D-12
Figure E-1	Range of variation of inferred values of λ reported for 12 columns out of 255 in the full sample	E-3
Figure E-2	Ratios of computed to estimated shear strength	E-4
Figure E-3	Comparison of the peak drift reached at or before axial failure for four columns	E-5

Figure E-4	Friction coefficients estimated using Equation E-1, compared to test data	E-6
Figure E-5	Drift ratio at axial failure	E-8
Figure F-1	Failure mechanisms of infilled frames.....	F-2
Figure F-2	Failure mechanism (b) exhibited in a quasi-static cyclic loading test.....	F-2
Figure F-3	Nonductile reinforced concrete frames with failure mechanism (a) and failure mechanism (b) from Figure F-1	F-2
Figure F-4	Influence of vertical load in nonductile RC frames exhibiting failure mechanism (b) from Figure F-1	F-3
Figure F-5	Collapse of masonry infill in 2008 Wenchuan earthquake	F-4
Figure F-6	Collapse of masonry infill with a window opening in a shaking-table test	F-4
Figure F-7	Finite element modeling of a masonry-infilled RC frame	F-5
Figure F-8	Analysis of an infilled frame subjected to quasi-static cyclic loading	F-6
Figure F-9	Analysis of a three-story infilled frame tested on a shaking table	F-7
Figure F-10	Strut model and shear, V , and axial, N , forces on an infill from finite element analysis	F-8
Figure F-11	Strut model with zero-thickness springs	F-8
Figure F-12	Load, Q , versus displacement, δ , envelope for an infilled fame	F-9
Figure F-13	Frame analysis using equivalent diagonal struts.....	F-10
Figure G-1	Definition of ε_p	G-4
Figure G-2	ε_p^* versus S_h/D	G-4
Figure G-3	BC-Fiber modeling of rebar buckling: (a) well detailed; (b) poorly detailed.....	G-5
Figure G-4	Load-displacement response for wall specimens tested by Massone (2006).....	G-6
Figure G-5	Wall pier test for $P = 0.10A_g f'_c$	G-7
Figure G-6	Model for shear strength degradation versus curvature ductility.....	G-9
Figure G-7	Load-displacement response at top of wall predicted by the model: (a) flexure; (b) shear	G-9
Figure G-8	Lateral load versus top lateral displacement and corresponding damage for specimen RWS.....	G-12

Figure G-9	Conventionally reinforced wall details and associated damage.....	G-13
Figure G-10	Conventionally reinforced wall base overturning moment versus roof displacement responses (structural wall direction)	G-13
Figure G-11	Wall spandrel test with sliding.....	G-14

List of Tables

Table 1-1	Component and System-Level Seismic Deficiencies Found in Pre-1980 Reinforced Concrete Buildings	1-5
Table 1-2	Examples of Collapse Indicators	1-7
Table 1-3	Recommended Work Plan - Summary of Tasks	1-11
Table 2-1	Design and Construction Characteristics (Global Level)	2-4
Table 2-2	Design and Construction Characteristics (Component Level).....	2-6
Table 2-3	Bullock's Building and Event Summary	2-10
Table 2-4	CTV Building and Event Summary	2-11
Table 2-5	Four Seasons Apartment Building and Event Summary	2-13
Table 2-6	Imperial County Services Building and Event Summary	2-14
Table 2-7	Olive View Medical Center Main Building and Event Summary	2-15
Table 2-8	Olive View Psychiatric Clinic and Event Summary	2-16
Table 2-9	Olive View Stair Towers and Event Summary	2-18
Table 2-10	Pyne Gould Building and Event Summary	2-19
Table 2-11	Royal Palm Resort and Event Summary.....	2-20
Table 2-12	Global Level Design and Construction Characteristics for all Example Buildings, with the Potential for these Characteristics to Cause Collapse During a Major Earthquake.....	2-24
Table 2-13	Component Level Design and Construction Characteristics for all Example Buildings, with the Potential for these Characteristics to Cause Collapse During a Major Earthquake	2-25
Table 2-14	Frequency of Design and Construction Characteristics Found Likely or Possible in More than One Third of all Example Buildings	2-26
Table 2-15	Frequency of Most Common Design and Construction Characteristics Found Within the Group of Six Buildings that Collapsed	2-26
Table 4-1	Collapse Simulation Research Recommendations.....	4-21
Table A-1	Workshop Mini-Papers, Authors, and Appendix References	A-4
Table A-2	Workshop Breakout Groups – Day 1	A-5

Table A-3	Workshop Breakout Groups – Day 2.....	A-5
Table B-1	Summary of Models	B-4
Table C-1	Response Models for Interior Beam-Column Joints.....	C-7
Table C-2	Response Models for Exterior Beam-Column Joints.....	C-10
Table D-1	Advantages and Disadvantages of Different Gravity Load Failure Modeling Methods.....	D-3
Table E-1	Ranges of the Data Plotted in Figure E-4	E-7

Chapter 1

Introduction

1.1 Background

Reinforced concrete buildings designed and constructed prior to the introduction of seismic design provisions for ductile response (commonly referred to as *nonductile* concrete buildings) represent one of the largest seismic safety concerns in the United States and the world. The California Seismic Safety Commission (CSSC, 1995) stated, “many older concrete frame buildings are vulnerable to sudden collapse and pose serious threats to life.” The poor seismic performance of nonductile concrete buildings is evident in recent earthquakes, including those in: Northridge, California (1994); Kobe, Japan (1995); Chi Chi, Taiwan (1999); Izmit, Düzce, and Bingol, Turkey (1999, 1999, 2003); Sumatra (2004); Pakistan (2005); China (2008); Haiti (2010); Chile (2010); Christchurch, New Zealand (2011); and Tohoku, Japan (2011).

The exposure to life and property loss in a major earthquake near an urban area is immense. Nonductile concrete buildings include residential, commercial, critical business, and essential (emergency) services buildings, many of which are high occupancy structures. Partial or complete collapse of nonductile concrete structures can result in significant loss of life. Severe damage can lead to loss of critical building contents and functionality, as well as the risk of financial ruin for business occupancies. Without proactive steps to understand and address these types of structures, the risks they pose will persist.

On the basis of detailed surveys and extrapolation across California, the Concrete Coalition¹ (2013) estimates there are approximately 1,500 pre-1980 concrete buildings in Los Angeles, 3,000 in San Francisco, and 20,000 in the 33 most seismically active counties state-wide. Outside of California, nonductile concrete buildings are widespread nationally and worldwide. These numbers portend the scale of the problem nationally and globally, where nonductile concrete buildings are more prevalent.

¹ The Concrete Coalition (<http://www.concretecoalition.org/>), a program of the Earthquake Engineering Research Institute (EERI), is a network of volunteer individuals, governments, institutions, and agencies with an interest in assessing the risk associated with nonductile concrete buildings and promoting the development of policies and procedures for mitigating that risk. Concrete Coalition projects include the development of an inventory of concrete buildings in California and the assembly of case histories describing the performance of concrete buildings in past earthquakes. Currently, the group is assisting San Francisco and Los Angeles in subdividing their inventories into subcategories to facilitate seismic safety programs in each location.

Based on these initial efforts and interactions with various stakeholders, the Concrete Coalition, among others, has identified an emerging critical need to begin development of more efficient procedures for assessing the collapse potential of nonductile concrete buildings and identifying particularly dangerous buildings for detailed evaluation and retrofit.

Evidence from earthquake reconnaissance efforts world-wide shows that strong earthquakes can result in a wide range of damage to nonductile concrete buildings, ranging from minor cracking to collapse (Otani, 1999). Current guidelines and standards for seismic assessment of existing concrete buildings (ASCE, 2013) are not sufficiently refined to enable engineers to quickly and reliably distinguish between buildings that might be expected to collapse and those that might not collapse but would be expected to sustain moderate to severe damage. Consequently, structural engineers have tended towards conservative practices in seismic evaluation and retrofit of structures. The associated guidelines and standards have also tended to be conservative.

Conservative evaluation techniques applied to nonductile concrete buildings almost always indicate that there is a risk of collapse, and that extensive retrofit is needed to mitigate that risk. Recent policy efforts demonstrate the difficulties in legislating large-scale retrofit programs encompassing nonductile concrete buildings without adequate resources or reliable engineering tools. In the case of the California hospital retrofit program (OSHPD, 2009), for example, almost all nonductile concrete buildings were categorized as high risk, needing costly retrofit.

Considering the challenges and limitations associated with funding seismic retrofit, this situation (thousands of buildings, with a vast majority classified as high risk) is not tenable. This “always bad” message is not credible, and it fosters an environment in which retrofitting of reinforced concrete buildings at high risk of collapse does not occur quickly enough, given the large inventory of high-risk buildings identified. To achieve a meaningful reduction in the seismic risk posed by nonductile concrete buildings, jurisdictions and engineers have a need for guidelines that reliably identify the subset of buildings that are most vulnerable to collapse, and that provide cost-effective retrofit solutions for these buildings.

In 2006, the National Science Foundation (NSF) awarded the George E. Brown, Jr. Network for Earthquake Engineering Simulation (NEES), Grand Challenge Project, *Mitigation of Collapse Risks in Older Reinforced Concrete Buildings*” (NSF Award CMMI-0618804, Jack Moehle, Principal Investigator). The Grand Challenge project was tasked with using NEES resources to develop comprehensive strategies for identifying seismically hazardous older reinforced concrete buildings, enabling prediction of the collapse of such buildings, and developing and promoting cost-effective hazard mitigation strategies for them. While the Grand Challenge research

project developed new knowledge about these buildings, additional applied research and technology transfer activities are needed to transition this knowledge into guidelines that can be used in engineering practice.

With support from the National Institute of Standards and Technology (NIST) and the Federal Emergency Management Agency (FEMA), the Applied Technology Council (ATC) and the Consortium of Universities for Research in Earthquake Engineering (CUREE) joined forces to initiate multi-phase projects with this primary objective: development of nationally accepted guidelines for assessing and mitigating the risk of collapse in older nonductile concrete buildings. The projects leverage research results from the NEES Grand Challenge project and the efforts of the Concrete Coalition. The following sections summarize the long-term program plan and proposed methodology developed from these multi-phase projects.

1.2 Program Plan

The first stage was to establish a long-term program plan for the development of collapse assessment and mitigation guidelines for nonductile concrete buildings. The program plan is described in detail in the NIST GCR 10-917-7 document, *Program Plan for the Development of Collapse Assessment and Mitigation Strategies for Existing Reinforced Concrete Buildings*, (NIST, 2010b), herein referred to as the *Program Plan*, and summarised briefly below. The *Program Plan* identifies the following critical needs for addressing the collapse risk associated with older reinforced concrete construction:

- Improved procedures for identifying building systems vulnerable to collapse, including simple tools that do not require detailed analysis;
- Updated acceptance criteria for reinforced concrete components based on latest research results; and
- Identification of cost-effective mitigation strategies to reduce collapse risk in existing reinforced concrete buildings.

To address these needs, the development of a series of eight guidance documents, under the umbrella title *Guidance for Collapse Assessment and Mitigation Strategies for Existing Reinforced Concrete Buildings*, was recommended:

1. Assessment of Collapse Potential and Mitigation Strategies;
2. Acceptance Criteria and Modeling Parameters for Concrete Components: Columns;
3. Acceptance Criteria and Modeling Parameters for Concrete Components: Beam-Column Joints;

4. Acceptance Criteria and Modeling Parameters for Concrete Components: Slab-Column Systems;
5. Acceptance Criteria and Modeling Parameters for Concrete Components: Walls;
6. Acceptance Criteria and Modeling Parameters for Concrete Components: Infill Frames;
7. Acceptance Criteria and Modeling Parameters for Concrete Components: Beams; and
8. Acceptance Criteria and Modeling Parameters for Concrete Components: Rehabilitated Components.

The first document will focus on building system behavior, providing improvements to both efficient identification of collapse vulnerable buildings and detailed collapse assessment based on building analyses. Documents 2 through 8 will be largely based on the collection of existing experimental data according to a consistent methodology for the selection of acceptance criteria and modeling parameters based on these data. Document 1 therefore requires the development of a methodology using sophisticated collapse simulations and the collection of data from buildings collapsed or critically damaged in past earthquakes to identify building parameters, termed here *collapse indicators*, correlated with an elevated probability of collapse. The proposed methodology for the identification of collapse indicators is briefly described in the following section.

1.2.1 Conceptual Methodology

The NIST *Program Plan* proposed a conceptual methodology for selecting collapse indicators and limits for the identification of vulnerable buildings with unacceptable collapse potential. Since other sections of this report provide guidance for the collapse simulation studies to be conducted as part of the collapse indicator methodology, it is necessary to first introduce the basic concepts of the methodology.

The methodology description in the NIST *Program Plan* identified a list of critical deficiencies contributing to the collapse vulnerability of reinforced concrete buildings (Table 1-1). Each deficiency has been found to contribute to collapse or partial collapse of reinforced concrete buildings in past earthquakes. As indicated in the *Program Plan*, the order of deficiencies listed in Table 1-1 does not imply a level of importance or frequency. Deficiencies A through D are component deficiencies that can limit the ability of a structure to resist seismic loading without collapse. Deficiencies E through J are system-level deficiencies that, alone or in combination with component deficiencies, can elevate the potential for collapse of a structure during strong ground shaking.

Table 1-1 Component and System-Level Seismic Deficiencies Found in Pre-1980 Reinforced Concrete Buildings (based on Moehle, 2007 and NIST, 2010b).

Deficiency A: Shear-critical columns  <p>Shear and axial failure of columns in a moment frame or gravity frame system.</p>	Deficiency F: Overall weak frames  <p>Overall deficient system strength and stiffness, leading to inadequacy of an otherwise reasonably configured building.</p>
Deficiency B: Unconfined beam-column joints  <p>Shear and axial failure of unconfined beam-column joints, particularly corner joints.</p>	Deficiency G: Overturning mechanisms  <p>Columns prone to crushing from overturning of discontinuous concrete or masonry infill wall.</p>
Deficiency C: Slab-column connections  <p>Punching of slab-column connections under imposed lateral drifts.</p>	Deficiency H: Severe plan irregularity  <p>Conditions (including some corner buildings) leading to large torsional-induced demands.</p>
Deficiency D: Splice and connectivity weakness  <p>Inadequate splices in plastic hinge regions and weak connectivity between members.</p>	Deficiency I: Severe vertical irregularity  <p>Setbacks causing concentration of damage and collapse where stiffness and strength changes. Can also be caused by change in material or seismic-force-resisting-system.</p>
Deficiency E: Weak-story mechanism  <p>Weak-column, strong-beam moment frame or similar system prone to story collapse from failure of weak columns subjected to large lateral deformation demands.</p>	Deficiency J: Pounding  <p>Collapse caused by pounding of adjacent buildings with different story heights and non-coincident floors.</p>

Many older reinforced concrete buildings contain one or more of the deficiencies identified in Table 1-1. While these conditions can lead to collapse, there are many examples of buildings that survive strong shaking without collapse. The challenge is to identify when these deficiencies will lead to building collapse and when they will not.

Ideally there should be a spectrum of collapse indicators, ranging from those appropriate for quick assessment of collapse potential to others used to identify collapse potential based on results of detailed nonlinear analysis. Collapse indicators for quick assessment must consist of simple parameters, which can be established from basic information available from a quick survey of the building, engineering drawings, or other sources. Conversely, collapse indicators for detailed collapse assessment can make use of results from additional sources including engineering calculations and specifically nonlinear analyses. It is proposed to categorize collapse indicators into two fundamental types:

- **Design Parameter Collapse Indicators.** These collapse indicators are determined based on design features of a reinforced concrete building, including reinforcement details, structural system layout, and relative strength and stiffness of members. These indicators can be further sub-categorized as “rapid assessment” (RA) or “engineering calculation” (EC) collapse indicators, where the former can be determined from a quick survey of the building or engineering drawings, and the latter requires some calculation of capacities and demands based on engineering drawings. RA and EC collapse indicators will be useful for refining the seismic evaluation procedures in ASCE/SEI 41, *Seismic Evaluation and Retrofit of Existing Buildings* (ASCE, 2013).
- **Response Parameter Collapse Indicators.** These collapse indicators reflect the response of the structure based on results from building analysis (BA). Generally the most refined collapse indicators are expected to be derived from results of nonlinear analysis and provide system-level acceptance criteria for the Collapse Prevention performance level.

Table 1-2 provides a list of potential collapse indicators. These collapse indicators have been grouped based on the classification described above, and further grouped as system level or component parameters. Component Building Analysis indicators shown in Table 1-2 (e.g., RA-C1) can be interpreted as equivalent to component acceptance criteria in ASCE/SEI 41. It is anticipated that relationships may exist among the indicators, as vectors of indicators may be found to provide a better indication of collapse potential than any one indicator. For example, if the average minimum column transverse reinforcement ratio for each story (RA-C1) is less than a specific value, and the maximum ratio of column-to-floor area for two adjacent stories (RA-S1) is greater than a specific value, then collapse potential is expected to be high.

Table 1-2 Examples of Collapse Indicators (NIST, 2010b)

Collapse Indicator ¹	System-level		Component-level	
Rapid Assessment (RA) Quantities that can be determined from a survey of the building or review of engineering drawings.	RA-S1.	Maximum ratio of column-to-floor area ratios for two adjacent stories (Deficiencies E and G)	RA-C1.	Average minimum column transverse reinforcement ratio for each story (Deficiency A)
	RA-S2.	Maximum ratio of horizontal dimension of the SFRS ² in adjacent stories (Deficiencies E and I)	RA-C2.	Minimum column aspect ratio (Deficiency A)
	RA-S3.	Maximum ratio of in-plane offset of SFRS from one story to the next to the in-plane dimension of the SFRS (Deficiency I)	RA-C3.	Misalignment of stories in adjacent buildings (Deficiency J)
	RA-S4.	Plan configuration (L or T shape versus rectangular) (Deficiency H)		
	RA-S5.	Minimum ratio of column area to wall area at each story ³		
Engineering Calculations (EC) Quantities that require some calculation of capacities and demands based on engineering drawings, but do not result from nonlinear building analyses.	EC-S1.	Maximum ratio of story stiffness for two adjacent stories (Deficiency E)	EC-C1.	Maximum ratio of plastic shear capacity ($2M_p/L$) ⁴ to column shear strength, V_p/V_n (Deficiency A)
	EC-S2.	Maximum ratio of story shear strength for two adjacent stories (Deficiency E)	EC-C2.	Maximum axial load ratio for columns with $V_p/V_n > 0.7$ (Deficiency A)
	EC-S3.	Maximum ratio of eccentricity (distance from center of mass to center of rigidity or center of strength) to the dimension of the building perpendicular to the direction of motion (Deficiency H)	EC-C3.	Maximum ratio of axial load to strength of transverse reinforcement (45 degree truss model) (Deficiency A)
	EC-S4.	Portion of story gravity loads supported by columns with ratio of plastic shear demand to shear capacity > 0.7 (Deficiency A)	EC-C4.	Maximum ratio of joint shear demand (from column bar force at yield) to joint shear capacity for exterior joints (Deficiency B)
			EC-C5.	Maximum gravity shear ratio on slab-column connections (Deficiency C)
Building Analysis (BA) Quantities for detailed collapse prevention assessment using the results from nonlinear building analyses.	BA-S1.	Maximum degradation in base or story shear resistance (Deficiencies A-B,D-I)	BA-C1.	Maximum drift ratio (Deficiencies A-F, H-I)
	BA-S2.	Maximum fraction of columns at a story experiencing shear failures (Deficiencies A, H-I)	BA-C2.	Maximum ratio of deformation demands to ASCE/SEI 41 limits for columns, joints, slab-column connections, and walls (Deficiencies A-I)
	BA-S3.	Maximum fraction of columns at a story experiencing axial failures (Deficiencies A, H-I)		
	BA-S4.	Minimum strength ratio (as defined in ASCE/SEI 41) ⁶ (Deficiency F)		
	O-S1.	Weak soils likely to result in overturning or large deformation demands in the building		
Other				

¹Collapse indicator notation: RA = Rapid Assessment; EC = Engineering Calculation; BA = Building Analysis; O = Other; S = System; C = Component. Deficiencies are described in Table 1-1.

²May not result in collapse but could help prevent collapse if a mechanism forms.

³SFRS: seismic force resisting system.

⁴ $2M_p/L = 2 \times$ the plastic moment of a column divided by the clear length.

⁵ V_p/V_n = ratio of plastic shear demand (controlled by flexure) to column shear capacity.

⁶ASCE/SEI 41 standard, *Seismic Rehabilitation of Existing Buildings* (ASCE, 2006)

Since the preliminary list of these potential collapse indicators relied on engineering judgment and experience with collapse analyses, it is anticipated that this list will evolve as further experience is gained from the collapse analyses described below.

Collapse simulation studies are necessary to establish a correlation between building design and response parameters and the probability of collapse. In order to identify appropriate and reliable collapse indicators, analytical models using research oriented structural analysis software (e.g., OpenSees, 2013) are needed. Using these models, building characteristics (e.g., dimensions, geometry, and mass) can be varied parametrically to explore effects on building response and collapse probability. Such studies would be used to identify quantitative limits on collapse indicators that have strong correlation with collapse potential.

The use of building prototype models (full building nonlinear models to explore parametric variations on building characteristics and their effects on response) allows explicit consideration of collapse probability, based on loss of gravity load carrying capacity, lateral dynamic instability, modeling uncertainty, and ground motion record-to-record variability. Since absolute probability of collapse is difficult to determine, the emphasis should be on relative probabilities of collapse, or changes in probability of collapse due to changes in building characteristics.

Unlike ductile structures that are typically assumed to collapse due to side-sway, nonductile concrete buildings can undergo gravity-load collapse due to loss of gravity load carrying capacity, prior to development of a side-sway collapse mode.

Nonlinear building prototype models used in this study must incorporate elements capable of approximating loss of gravity load carrying capacity for critical gravity-load supporting components, such as columns (Elwood, 2004) and slab-column connections (Kang et al., 2009), and must account for P-Delta² effects. One significant challenge that must be overcome in the analysis is the distinction between gravity-load collapse and non-convergence due to numerical instability in the model. As envisioned in this study, collapse would be detected based on a comparison of floor-level gravity load demands and capacities (adjusted at each time step to account for member damage and load redistribution). Gravity collapse would be defined as the point at which gravity load demand exceeds the total gravity load capacity at a given floor, and non-convergence of the analysis prior to significant degradation in the capacity to resist gravity loads would not necessarily be considered as collapse.

One approach for selection of design parameter collapse indicators is illustrated in Figure 1-1. In this approach, limits are selected based on the relative changes in the collapse fragilities with respect to changes in the collapse indicator parameter.

² P-Delta is an effect where significant axial load combined with lateral deflection causes additional lateral deflection and, under sufficient lateral deflection, causes lateral instability.

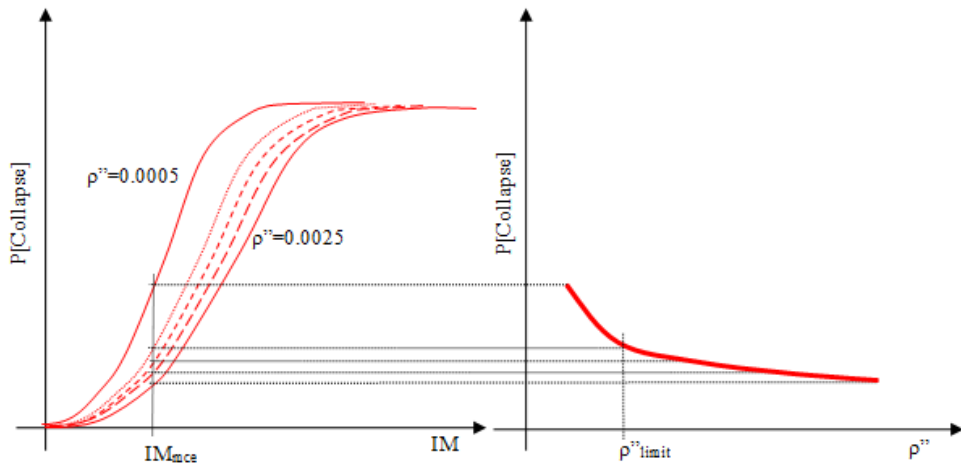


Figure 1-1 Approach for establishing collapse indicator limits based on the relative changes in the collapse fragilities with respect to changes in the collapse indicator parameter ($P[\text{Collapse}]$ = probability of collapse; ρ'' = transverse reinforcement ratio; IM = Intensity Measure) (NIST, 2010b).

Figure 1-1 shows example collapse fragilities for changes in a selected collapse indicator (e.g., average column transverse reinforcement ratio, collapse indicator RA-C1). The curves in the figure suggest that once the transverse reinforcement ratio decreases below approximately 0.001, the probability of collapse increases rapidly. In this example, 0.001 could be selected as an appropriate limit for this collapse indicator. This assessment would be repeated for several different building types and different hazard levels, and the resulting limits would be compared. An ideal collapse indicator would have only limited variation in the limits suggested by different building types. For response parameter collapse indicators, the envisioned process would be similar.

As implemented in a performance assessment, response parameter collapse indicator limits would be compared with responses determined from nonlinear analysis of a building, while design parameter collapse indicator limits would be compared with the relevant design features of a building. Since assessment using design parameter indicators will not directly consider the seismic response of the building in question, it is expected that greater computational effort (i.e., more building prototypes) will be needed to develop reliable design parameter collapse indicators than will be needed to develop response parameter collapse indicators.

1.2.2 Work Plan

The risk associated with older nonductile concrete buildings is significant, and the development of improved technologies for mitigating that risk is a large undertaking. Furthermore, the proposed methodology, as described above, requires considerable computational effort as the collapse simulations must be repeated for multiple ground

motions, multiple hazard levels, multiple values of collapse indicators, and multiple building prototypes with multiple building periods. A multi-phase, multi-year effort is needed to complete all eight recommended guidance documents. Figure 1-2 indicates the recommended timeline for the development of the proposed guidance documents as depicted in the *Program Plan* (NIST, 2010b). The individual tasks proposed by the *Program Plan* to achieve the 8 guidance documents are summarised in Table 1-3.

Document	Year 1	Year 2	Year 3	Year 4	Year 5	Year 6	Year 7
1 - Collapse Indicators	◆				◆		
2 - Columns	◆	◆					
3 - Beam-Column Joints	◆	◆	◆				
4 - Slab-Column Systems		◆	◆				
5 - Walls		◆	◆	◆	◆		
6 - Infill Frames			◆	◆	◆	◆	
7 - Beams				◆	◆	◆	
8 - Rehabilitated Components					◆	◆	◆

Figure 1-2 Recommended schedule for development of Guidance Documents (NIST, 2010b).

1.3 Goals and Report Structure

This report summarizes initial work on Phase 1 of the *Program Plan* related to the development of a collapse indicator methodology. In particular, the goals of the current study included:

- Identification of critical deficiencies based on collapse case studies;
- Identification of collapse mitigation strategies;
- Identification of collapse modeling techniques for reinforced concrete buildings; and
- Refinement of the *Program Plan* based on results of ongoing studies.

Chapter 2 assists in the identification of critical deficiencies for older reinforced concrete buildings through a detailed review of reinforced concrete building collapse case studies. The case studies enable the comparison among the selected buildings of design and construction characteristics and observed seismic performance. This information indicates that current simplified evaluation procedures fail to capture the collapse vulnerability of buildings because there is not adequate attention paid to the vulnerability of the gravity load system.

Chapter 3 identifies current collapse mitigation strategies through a review of the state-of-practice of retrofit techniques typically used for a collapse prevention performance level.

Table 1-3 Recommended Work Plan - Summary of Tasks (NIST, 2010b)

Phase	Document	No.	Task
1	1	1	Development of Collapse Indicator Methodology
		1.1	Identification of critical deficiencies and mitigation strategies
		1.2	Selection of building prototypes
		1.3	Identification of ground motions and component models for collapse simulation
		1.4	Evaluation of methodology for selection of collapse indicators
		1.5	Development of implementation plan for collapse indicators in seismic rehabilitation process
		1.6	Report on collapse indicator methodology
2	1	2	Development of Response Parameter Collapse Indicators
		2.1	Conduct of building prototype analyses for response parameter collapse indicators
		2.2	Report on response parameter collapse indicators
3	1	3	Development of Design Parameter Collapse Indicators
		3.1	Conduct of simplified analyses for initial identification of design parameter collapse indicators
		3.2	Conduct of building prototype analyses to confirm design parameter collapse indicators
		3.3	Report on design parameter collapse indicators
4	2,3	4	Development of Initial Component Acceptance Criteria and Modeling Parameters
		4.1	Selection of column acceptance criteria and modeling parameters
		4.2	Report on acceptance criteria and modeling parameters for reinforced concrete columns
		4.3	Selection of beam-column joint acceptance criteria and modeling parameters
		4.4	Report on acceptance criteria and modeling parameters for reinforced concrete beam-column joints
5	4-8	5	Development of Additional Component Acceptance Criteria and Modeling Parameters
		5.1	Data collection and database development
		5.2	Selection of acceptance criteria and modeling parameters
		5.3	Report on acceptance criteria and modeling parameters for additional reinforced concrete components

Chapter 4 provides further guidance on ground motions and component models for collapse simulations, and identifies short- and long-term research gaps in this field. This guidance is derived from input solicited from experts in the field of reinforced concrete structural design and dynamic response simulation of such buildings.

To achieve the goals of the *Program Plan*, i.e., development of guidance documents for collapse assessment of reinforced concrete buildings, it is necessary to modify / adapt the tasks of the *Program Plan* according to evolving knowledge gained from this and other on-going studies. This report concludes with recommendations for

possible refinements to the *Program Plan* (see Chapter 5), based on the conclusions of the previous chapters and results from on-going studies funded by FEMA through the ATC-78 project series (see ATC, 2012).

Chapter 2

Critical Deficiencies Based on Collapse Case Studies

Collapse of reinforced concrete buildings during earthquakes is a complex phenomenon influenced by numerous factors. The identification of critical deficiencies, the first task of the NIST *Program Plan* (NIST, 2010b), is best accomplished by considering real case studies of collapse, or near-collapse, where such factors have clearly combined to produce poor seismic performance. This chapter provides a summary of nine case study buildings which collapsed, or experienced near-collapse performance, during past earthquakes.

The goals and objectives of the study were as follows:

- **Systematically review available data on selected buildings that collapsed or partially collapsed during earthquakes.** A group of buildings known to have collapsed, or experienced near-collapse performance, during past earthquakes is discussed in Section 2.1. This effort included the assembly and development of a generic checklist comprising design and construction characteristics affecting seismic performance. The formulation and application of this list is described in Section 2.1.
- **Determine the factors leading to collapse in each building.** The list of design and construction characteristics is used as a metric to document the presence or absence of these characteristics and their impact on the observed performance of the select group of buildings (see Section 2.2 for individual building summaries).
- **Identify critical deficiencies that led to collapse.** Comparison among the selected buildings with respect to design and construction characteristics and observed seismic performance is the subject of Section 2.3.
- **Summarize implications for broader effort to identify collapse-prone buildings.** Conclusion and recommendations are summarized in Section 2.4. Key questions addressed in this study include:
 - Are there key factor(s) that could be used to assess collapse risk without detailed analyses?
 - What is the overall efficacy of a checklist approach to the evaluation of collapse risk?

2.1 Methodological Approach

This section describes the basic approach used to identify key generic aspects of performance and collapse, to select and collect data for case-study examples, to review data, and to interpret results as they apply to the goals and objectives of the project. The effort comprised several interrelated tasks. After categorizing and discussing the types of information to be collected, several example buildings were selected. Data were collected from the literature and organized in a standard format for each example to generate a database of case histories. Each individual case was reviewed, discussed, and refined by the Project Technical Committee (PTC). Finally, the case histories were compared with each other to formulate conclusions and recommendations. Although summarized below as individual tasks, the work did not progress completely in sequence from task to task. The overall process was somewhat iterative. As participants gained experience and insights, the basic tasks were re-visited and adjustments were made to improve overall results.

2.1.1 *Design and Construction Characteristics Affecting Seismic Performance*

The Project Technical Committee recognized the importance of establishing a procedure to compile and compare factors that could affect collapse potential in reinforced concrete buildings. For this purpose the PTC, in conjunction with the Concrete Coalition, developed a list of building characteristics thought to be significant with respect to collapse potential. The PTC and the Concrete Coalition then used this “checklist” platform to systematically categorize data on selected buildings, from which they could designate the significance of each characteristic to the collapse of each specific building. In this manner, common characteristics were sought among the examples.

2.1.1.1 Existing Compilations

Several existing lists of potential design and construction characteristics applicable to the seismic evaluation of reinforced concrete buildings have been compiled by various entities. Although these compilations have been used for different purposes, they reflect potential deficiencies that could affect damage and performance. Many of these compilations identify common characteristics (e.g., soft/weak stories, shear critical behavior modes, or torsion). Compilations considered in this study included:

- **ASCE/SEI 31 and ASCE/SEI 41.** The initial stages of the evaluation of existing buildings in accordance with the ASCE/SEI 31 and ASCE/SEI 41 (ASCE, 2003; ASCE, 2006b) use a series of checklists for each building type. These lists address design and construction characteristics that may affect the performance of the building type during seismic shaking. The evaluation procedures use the checklist primarily to identify the need for further analysis to

determine what impact the characteristic might, or might not, have on performance.

- **The Top Ten List.** The Concrete Coalition worked with representatives from the Pacific Earthquake Engineering Research Center to develop a preliminary list of reinforced concrete building characteristics that seemed to contribute to seismic collapse potential. This list, known as *The Top Ten List* (Moehle, 2007), was subsequently included in the NIST GCR 10-917-7 report, (NIST, 2010b, Chapter 4). The purpose of the list (reproduced herein as Table 1-1) was to aid in the communication among practitioners, researchers, and the general public about the potential for collapse.
- **NEHRP.** The National Earthquake Hazard Reduction Program (NEHRP) publishes guidelines that form the basis for codes and standards for new construction, such as FEMA P-750, *NEHRP Recommended Seismic Provisions for New Buildings and Other Structures* (FEMA, 2009b). Included in the guidelines are lists of vertical and plan irregularities in building design and construction that may adversely affect seismic performance. If these characteristics are present, the guidelines generally call for more stringent design restrictions than would otherwise be required.
- **OSHPD.** In California, the design and construction of hospitals fall under the jurisdiction of the Office of Statewide Health Planning and Development (OSHPD). In order to facilitate the evaluation of existing hospitals for seismic performance, the agency has developed a version of the FEMA regional loss modeling software program HAZUS (FEMA, 2006). The OSHPD version is meant to be applied to individual buildings to predict seismic performance. The modeling and damageability of a building are modified based upon a required list of “Significant Structural Deficiencies,” which comprise design and construction characteristics that affect seismic performance (see OSHPD, 2010). The objective is to provide uniformity among analyses of a number of different buildings (with a variety of owners) subject to OSHPD regulation.

2.1.1.2 Consolidation and Development of Current Compilation

Design and construction characteristics affecting the seismic performance of reinforced concrete buildings, primarily from the sources noted above in Section 2.1.1.1, have been assembled into a consolidated list for the purpose of evaluating the example buildings. The list was modified based on observations over the course of assembling and reviewing data on the example buildings. During this process it was apparent that the characteristics fell into two general categories. First, there are characteristics that address performance at a system or Global Level. These are tabulated and explained in Table 2.1. Second, as shown in Table 2-2, there are

Table 2-1 Design and Construction Characteristics (Global Level)

Characteristics	Description	Source(s)
Site related		
Pounding	Damage at misaligned floor/roof plates	ASCE 31 ¹ , Top Ten ² , OSHPD ³
Permanent ground displacement	Evidence of lateral and/or vertical offset of structure; liquefaction, landslide, fault rupture	Top Ten
Materials and construction quality		
Materials		
Concrete	Low strength; evidence of deterioration	ASCE 31, OSHPD
Lightweight concrete	Low shear strength	OSHPD
Reinforcement/post-tensioned reinforcement	Smooth bars; brittle metal	ASCE 31, OSHPD
Execution		
Conveyance/placement of concrete	Rock pockets; lack of plumb and true	ASCE 31
Reinforcement/post-tensioned reinforcement	Out of place; lack of adequate cover	ASCE 31
Field variance with design documents	Construction conditions differ from those specified by design	
Configuration		
Plan irregularities		
Torsion	Offset between center of mass and lateral resistance	ASCE 31, NEHRP ⁴ , Top Ten, OSHPD
Perimeter boundary	Excessively non-uniform floor/roof outline; floor/roof plate re-entries	NEHRP
Vertical irregularities		
Soft story	Level with obviously lower stiffness than others	ASCE 31, NEHRP, Top Ten, OSHPD
Weak story	Level with obviously lower strength than others	ASCE 31, NEHRP, Top Ten, OSHPD
Mass distribution	Significantly larger or smaller seismic mass at one or more levels compared to others	ASCE 31, NEHRP, OSHPD
Interstory masses and/or lateral stiffening elements	Partial story, platform, or mezzanine; stairways or conveyances capable of iteration with lateral system	ASCE 31
Setbacks	Building exterior plane(s) change with height	
Out-of-plane discontinuity	Lateral elements do not align vertically; components are missing or moved in or out of the plane of the lateral resisting element from one floor to another	ASCE 31, NEHRP, OSHPD

Table 2-1 Design and Construction Characteristics (Global Level) (continued)

Characteristics	Description	Source(s)
In-plane discontinuity	Lateral elements do not align vertically; components are missing or moved within the vertical plane of the lateral resisting elements from one floor to another	ASCE 31, NEHRP, OSHPD
Lateral resisting system		
Strength		
Overall lack of strength	Structure with low elastic strength versus local demand	Top Ten
Strength		
Extreme flexibility	Structure with little horizontal stiffness	Top Ten
Load path		
Collectors/struts	Absence of identifiable element(s)	ASCE 31
Anchorage of nonstructural elements	No positive attachment to structure	
In-plane connection of walls to diaphragm	Inadequate capacity to transfer shear parallel to wall	
Out-of-plane connection of walls to diaphragm	Inadequate capacity to transfer tension / compression perpendicular to wall	ASCE 31, OSHPD
Diaphragm chords	High aspect ratio with no apparent reinforcing	ASCE 31
Diaphragm openings	Excessively large segments without reinforcing mechanisms	NEHRP, ASCE 31, OSHPD
Gravity load system		
Deformation capacity	Overall capability of gravity system elements (e.g. slabs, beams, columns, walls) to maintain gravity load capacity in conjunction with lateral displacement demand	Top Ten, OSHPD
Load redistribution capability	Lack of observable alternative load paths in cases of local failures (e.g. two way framing, Vierendeel action in frames, transfer through walls above, catenary action in horizontal framing)	Top Ten

¹ ASCE 31 Standard, *Seismic Evaluation of Existing Buildings* (ASCE, 2003).² Moehle's Top Ten List (Moehle, 2007)³ Office of Statewide Health Planning and Development (OSHPD) List of Structural Deficiencies (see OSHPD, 2010).⁴ NEHRP (FEMA, 2009b).

Table 2-2 Design and Construction Characteristics (Component Level)

Characteristics	Description	Source(s)
Frames		
Columns		
Shear strength	Inadequate transverse reinforcement	ASCE 31 ¹
Lap slices in long reinforcing	Inadequate for full development; potential for slippage	ASCE 31, Top Ten ²
Axial load ratio ($P/A_g f'_e$)	Compressive demands greater than 20%	
"Gravity" load columns drift capacity	Localized drift incompatibility	ASCE 31, Top Ten, OSHPD ³
Captive/"short" columns	Possible pre-emptive shear failure	ASCE 31, Top Ten, OSHPD
Beams/flat slabs		
Strength relative to columns	Adverse strong beam/weak column behavior	ASCE 31, Top Ten, OSHPD
Loss of gravity load capacity	Lateral response combined with gravity loads results in shear behavior	ASCE 31
Continuity of longitudinal reinforcing	Discontinuity or inadequate development at joints	ASCE 31, Top Ten
Joints (beam-col. or slab-col.)		
Interior (concrete on four sides)	Loss of horizontal/vertical (gravity) load capacity	ASCE 31, Top Ten
Exterior (concrete on three sides or fewer)	Loss of horizontal/vertical (gravity) load capacity	ASCE 31, Top Ten
Infills		
Interference with frame action	Evidence of strut action; distress in frame members at openings	Top Ten
Out-of-plane	Blowouts of infill	
Attachment to framing	Lack of separation or lack of attachment to frame for composite behavior	ASCE 31
Shear walls		
Shear		
Diagonal tension/compression	Diagonal cracking or crushing	ASCE 31
Sliding shear	Horizontal cracking and crushing with possible movement	
Connection to diaphragm	Separation/damage at floor/floor plates	ASCE 31
Flexure		
Compression zone buckling capacity	Out-of-plane buckling	
Boundary capacity	Crushing/buckling/fracturing/splice failure of reinforcing openings	
Discontinuity of wall	Not continuous with or without supporting columns	ASCE 31, Top Ten
Boundary reinforcing at openings	Buckling/fracturing/splice failure of reinforcing openings	ASCE 31
Foundation behavior	Excessive rocking: pile/pier failure	ASCE 31

¹ ASCE 31 Standard, *Seismic Evaluation of Existing Buildings* (ASCE/SEI 2003).² Moehle's Top Ten List (Moehle, 2007)³ Office of Statewide Health Planning and Development (OSHPD) List of Structural Deficiencies (see OSHPD, 2010).

characteristics that relate to individual structural features at the element or Component Level.

2.1.1.3 Application to Observations of Performance

During the assembly and review of the example buildings, the design and construction characteristics affecting seismic performance were used to categorize the factors that led to observed performance. For each building, each characteristic was considered and noted according to the following:

- **Likely** - Characteristic is present and noted as a factor likely contributing to observed damage.
- **Possible** - Characteristic is present and noted as a possible factor contributing to observed damage.
- **Unlikely** - Characteristic is present but was not noted as a factor contributing to observed damage.
- **Unknown** - Unknown if the characteristic is present or whether the characteristic was a factor in the observed damage.
- **N/A** - Apparent that characteristic is not present (not applicable).

2.1.2 Building Selection

The Project Technical Committee developed and discussed suggestions for examples of buildings from past earthquakes. There were several objectives in culling these lists into those that are included in this report. In order to have enough information on a variety of buildings to allow some general observations and cross-comparisons, the number of case histories needed to be sufficiently large. This need had to be satisfied with a practical limit on the amount of time and resources available. The following criteria were also considered:

- There was a priority for buildings from the United States and other developed countries with similar, comparable design and construction practices. This differed from the Concrete Coalition effort that included buildings from many countries.
- While focus of the effort was on collapsed buildings, data from buildings that did not collapse during strong shaking were very important to the development of a generic understanding of collapse.
- The PTC selected buildings for which there is a relatively large amount of information, recognizing the amount of detailed information available for specific buildings is often sparse.

2.1.3 Data Assembly

Interns working for the Concrete Coalition assembled the initial data on the examples. They were guided by experienced volunteer mentors, as well as members of the Project Technical Committee. Internet sources produced readily available information. The interns and mentors supplemented these initial data through discussions with, and documents from, practitioners and researchers offline. When recording the data, the interns and mentors primarily noted the observations and opinions of the sources. If there was a difference of opinion on an issue, both perspectives were recorded. At this stage, interpretation of the data as it related to performance were minimized. An effort was made to not interject any speculation or bias into the process.

The information from the examples has been compiled in a common format organized by each individual building, and archived in a Building Performance Database. Information includes:

Basic information

- Building name and location
- Height
- Code
- Geometry
- Lateral system
- Gravity system
- Photographs
- Drawings

Damage

- Description
- Photographs
- Design and construction characteristics affecting performance

Ground motion

- Date
- Magnitude
- Epicentral distance
- Local intensity
- Accelerations

- Strong ground-motion records and recording stations
- Response spectra

References

- Construction drawings
- Investigative reports
- Papers and articles
- Analyses
- Research reports

2.1.4 Review and Interpretation

As noted in the previous section, there was an ongoing review of experienced engineers in the data assembly process. This resulted in some important improvements in the process itself. Most notably, the list of design and construction characteristics affecting performance was expanded and refined as discussed above in Section 2.1.1.

The PTC interpreted the individual case-history data for each example building, with respect to the cause of collapse, and for all the buildings in aggregate. This process began with the distribution of the data to individual members for their personal review. A meeting was then conducted for exchange of viewpoints and discussion. As a result of the meeting, each of the nine examples was assigned to a two person team for a detailed review and interpretation of the performance. This interpretive process allowed for the injection of expert opinion on the classification and significance of the information. There was, however, an effort to avoid unsubstantiated judgments. Some of the situations encountered included:

- The data and previous evaluations for a specific example were consistent with respect to the interpretation of performance. In these cases the PTC reported the findings with a minimum of modification.
- The interpretation of the data with respect to performance differed in whole or in part among those who had previously evaluated the example building. In these cases the PTC reported the different interpretations so long as they were not at odds with observed data.
- Data were available for a specific example, but no credible interpretive opinions were found. In these situations the PTC provided one or more possible interpretations based on the data.

After vetting and refining the individual examples, the PTC then met to review and compare the results as a group. As a result of the discussions, there emerged some

general observations with respect to important factors on collapse potential. These were apparent from similarities and differences when the cases histories were compared to one another (see Section 2.3). Based on these observations (on important factors impacting collapse potential), the PTC formulated the conclusion and recommendation in accordance with the objectives of this effort (see Section 2.4).

2.2 Building Summaries

This section provides a brief summary of information on each building that was collected for the Building Performance Database. These buildings are listed in alphabetical order by name, and all but three totally collapsed.

2.2.1 Bullock's Department Store

The Bullock's Department Store was a 3-story structure located at the Northridge Fashion Centre in Northridge, California (see Table 2-3 for additional building information). Constructed in 1970 as a slab-frame system, the San Fernando earthquake of 1971 prompted engineers to add shear walls in several locations in the structure as a retrofit. The walls were discontinuous below the 2nd level and were poorly attached to the adjacent columns. The building store was located approximately 3 km to the north of the epicenter of the 1994 Northridge earthquake (see Table 2-3 for additional earthquake parameters) and suffered collapse in the southern end of the structure on the 2nd and 3rd stories as a result of the shaking (Figure 2-1). Strut action in the walls appears to have contributed to a punching failure of the slab during the seismic shaking.

Table 2-3 Bullock's Building and Event Summary

Building information		Event information	
Location:	Northridge, California, USA	Earthquake date:	January 17, 1994
Primary use:	Retail	Moment Magnitude:	6.7
No. of stories:	3	Epicentral distance:	3km
Height:	51 ft	Local shaking intensity*:	IX
Size:	230,000 sq ft	PGA**:	-0.5g
Year built:	1970 (1971 retrofit)		
Code:	1967 <i>Uniform Building Code</i>		
Lateral load system:	Shear walls		
Gravity load system:	Two-way waffle slab on columns		

*Modified Mercalli Intensity

**Peak ground acceleration

Date sources: CSSC (1996); EERC (1994); EERI (1996); and Todd et al., (1994)



Figure 2-1 Bullock's Department Store earthquake damage (NISEE, 2013a, Photo NR222).

2.2.2 CTV Building

The CTV Building in Christchurch, New Zealand was originally designed as an office building but changed use over time to include an education facility and radio and television studios for Canterbury Television (see Table 2-4 for additional building information). The building was rectangular in plan, and was founded on pad and strip footings bearing on silt, sand, and gravel. Lateral load resistance was provided by a reinforced concrete wall-tower surrounding the stairs and elevators at the north end and by a reinforced concrete coupled wall on the south face. Precast concrete spandrel panels were placed between columns at each level above the ground floor on the south, east, and north faces. In 1991, collectors were installed at the upper levels in an effort to improve the connections between the floor slabs and the walls of the north. After the September 2010 earthquake and the December 2010

Table 2-4 CTV Building and Event Summary

Building information		Event information	
Location:	Christchurch, New Zealand	Earthquake date:	February 22, 2011
Primary use:	Office	Moment Magnitude:	6.1
No. of stories:	6	Epicentral distance:	6.4 km
Height:	55-71 ft	Local shaking intensity*:	VIII-IX
Size:	47,400 sq ft	PGA**:	~0.5g
Year built:	1987		
Code:	NZS 4203:1984 NZS 3101:1982		
Lateral load system:	Shear walls		
Gravity load system:	Composite steel deck and slab, precast beams, CIP columns.		

*Modified Mercalli Intensity

**Peak ground acceleration

Data sources: CESMD (2011); GeoNet (2011); NZBDH (2011); and USGS (2011)



Figure 2-2 CTV Building earthquake damage (New Zealand Herald, 2011).

aftershock, no significant structural damage was observed. In the February 2011 aftershock, the building completely collapsed with only the north core remaining standing (Figure 2-2). It appeared that the internal structure collapsed first, pulling the slab away from the north tower and pulling down the entire south wall.

2.2.3 Four Seasons Apartment Building

The Four Seasons Apartment Building in Anchorage, Alaska was a 6-story prestressed lift slab structure (see Table 2-5 for additional building information). At the time of the 1964 earthquake, the building was structurally complete and approximately one month away from occupancy. Lateral forces were to be primarily resisted by two separate concrete cores forming the elevator and stair shafts. The post-tensioned slabs were supported on steel columns with lift collars. During the earthquake the structure suffered complete collapse, with both elevator cores falling over and the slabs detaching from the cores to fall one upon another. Although the concrete elevator cores were relatively intact above the second story, they suffered severe damage between the ground and the second story where subsequent analysis revealed insufficient lap splice lengths of the primarily vertical reinforcement. However, there were several observations supporting the conclusion that the floor slabs actually came down before the towers. The slab had no mild steel and had extremely high stresses at the anchors of the post-tensioning strands. Most of the strands failed and shot out of the slabs while they were still elevated. Steel column

collars punched through the slab. There were marks on the towers that indicated that the slabs came straight down vertically (Figure 2-3).

Table 2-5 Four Seasons Apartment Building and Event Summary

Building information		Event information	
Location:	Anchorage, Alaska	Earthquake date:	March 27, 1964
Primary use:	Residential	Moment Magnitude:	9.2
No. of stories:	6	Epicentral distance:	130 km
Height:	52 ft	Local shaking intensity*:	VIII-X
Size:	60,000 sq ft	PGA**:	~0.15g
Year built:	1964		
Code:	1961 <i>Uniform Building Code</i>		
Lateral load system:	Concrete shear walls		
Gravity load system:	Post-tensioned lift-slab on steel columns		

*Modified Mercalli Intensity

**Peak ground acceleration

Data sources: Benuska and Clough (1973); Reuter (1964); and USGS (2012)



Figure 2-3 Four Seasons Apartment Building earthquake damage (Steinbrugge Collection, NISEE, 2013b, Image S2214).

2.2.4 Imperial County Services Building

The Imperial County Services Building in El Centro, California was relatively new at the time of the Imperial Valley earthquake in 1979 (see Table 2-6 for additional building information). The building was extensively instrumented by the U. S. Geologic Survey with thirteen strong motion accelerometers throughout the building, and another three free-field accelerometers near the site (Rojahn and Mork, 1982). The seismic resisting system consisted of moment frames along the interior gridlines in the east-west direction and shear walls in the north-south direction. However, the shear walls were not continuous, with four shorter walls on the first floor transitioning to two large walls on either end of the building. The building was damaged by overturning during the earthquake and the structure was eventually

demolished, even though the building could have been repaired. Most of the damage was concentrated in the columns on the east side of the building at the ground floor, where they exhibited damage at their bases. The failure of four columns resulted in the easternmost bay of the structure dropping approximately 12 inches (Figure 2-4). The structure also showed cracking (both shear and flexure) and spalling of concrete, with the damage generally being more severe toward the east end of the building. Significantly, in spite of the damage, the building did not collapse; a result of a robust gravity load system.

Table 2-6 Imperial County Services Building and Event Summary

Building information		Event information	
Location:	EI Centro, California	Earthquake date:	October 15, 1979
Primary use:	Office	Moment Magnitude:	6.5
No. of stories:	6	Epicentral distance:	26 km
Height:	84 ft	Local shaking intensity*:	IX
Size:	70,000 sq ft	PGA**:	~0.35g
Year built:	1971		
Code:	1967 <i>Uniform Building Code</i>		
Lateral load system:	N-S Shear walls, E-W moment-resisting frame		
Gravity load system:	Cast-in-place slabs, beams, columns		

*Modified Mercalli Intensity

**Peak ground acceleration

Data sources: EERI (1980); Kojic et al., (1984); Kreger and Sozen (1983); Kreger and Sozen (1989); Pauschke et al. (1981); and Zeris (1984)



Figure 2-4 Imperial County Services Building. Earthquake damage occurred in the first-story columns at the east end of the building (photo right) (NISEE, 2013a, Collection Godden J76, Bertero, 1979).

2.2.5 Olive View Medical Center Main Building

The Olive View Medical Center Main Building in Sylmar, Los Angeles, California was a 6-story reinforced concrete structure consisting of symmetric wings set around a central courtyard (see Table 2-7 for additional building information). On the south and most of the east side of the building, the second floor slab extended over the ground floor as a canopy, with heavy landscaping loads on top. Large reinforced concrete shear walls provided lateral resistance in the upper four floors, but these were discontinuous and did not extend below the second floor. Moment resisting concrete frames were provided at the lower levels, supporting the shear wall system above. The stairwell and elevator core walls that extended through the lower two stories were detailed to allow horizontal movement. The moment frame columns in the lower two stories were spirally reinforced, while the gravity only columns in those stories were tied. The lower floors of the building were heavily damaged in the 1971 San Fernando earthquake. The structure remained standing, despite considerable residual drift in the first two stories. Relatively little structural damage, but extensive non-structural damage, were observed in the upper four stories of the building. In the bottom two floors, many tied columns failed completely, resulting in the collapse of the canopy surrounding the building (Figure 2-5). In addition, some spiral columns failed horizontally with top and bottom hinges and joint damage, but they did not lose gravity load carrying capability.

Table 2-7 Olive View Medical Center Main Building and Event Summary

Building information		Event information	
Location:	Los Angeles, California	Earthquake date:	February 9, 1971
Primary use:	Hospital	Moment Magnitude:	6.6
No. of stories:	6	Epicentral distance:	10 km
Height:	80 ft	Local shaking intensity*:	VIII-XI
Size:	500,000 sq ft	PGA**:	-0.5g
Year built:	1969		
Code:	1964 <i>Uniform Building Code</i>		
Lateral load system:	Shear walls and moment resisting frame		
Gravity load system:	Flat slabs with drop panels		

*Modified Mercalli Intensity

**Peak ground acceleration

Data sources: Mahin et al., (1976); Steinbrugge et al., (1971); and USGS and NOAA (1971)



Figure 2-5 Olive View Medical Center Main Building earthquake damage
(Steinbrugge Collection, NISEE, 2013b, Image S4007).

2.2.6 Olive View Psychiatric Clinic

The Olive View Psychiatric Clinic in Sylmar, Los Angeles, California was a 2-story, lightweight concrete building that was part of the greater Olive View Medical Center, although separate from the other buildings (see Table 2-8 for additional building information). The building was configured in a "T" shape, with significant setbacks from the first to second stories. The lateral system was designed as a concrete moment resisting frame, but the irregularity of the plan, in addition to requirements for large open spaces within the clinic, led to the design of large beams relative to the columns at the second floor. Additionally, there were concrete masonry infill block walls in the first and second stories. In the 1971 San Fernando earthquake, the first

Table 2-8 Olive View Psychiatric Clinic and Event Summary

Building information		Event information	
Location:	Los Angeles, California	Earthquake date:	February 9, 1971
Primary use:	Clinic	Moment Magnitude:	6.6
No. of stories:	2	Epicentral distance:	10 km
Height:	28 ft	Local shaking intensity*:	VIII-XI
Size:	56,000 sq ft	PGA**:	~0.5g
Year built:	1969		
Code:	1964 <i>Uniform Building Code</i>		
Lateral load system:	Concrete moment resisting frame		
Gravity load system:	Lightweight concrete slab, beams, and columns		

*Modified Mercalli Intensity

**Peak ground acceleration

Data sources: Chan (1972); Mahin et al., (1976); Steinbrugge et al. (1971); Tashkandi and Selna (1972); and USGS and NOAA (1971)



Figure 2-6 Olive View Psychiatric Clinic earthquake damage (NISEE, 2013a, Collection Godden J74, Bertero, 1971).

story collapsed completely, while the second story suffered only minor damage to the columns (Figure 2-6). During collapse the structure had also rotated considerably. However, it is not clear that this was caused by torsional lateral response. It could have been caused by the sequence of column failures.

2.2.7 Olive View Stair Towers

The four Olive View Stair Towers serviced the main hospital building of the Olive View Medical Center in Sylmar, Los Angeles, California (see Section 2.2.5), but they separated above the 2nd floor slab by a 4 inch seismic joint and attached at the 2nd floor slab to the main building (see Table 2-9 for additional building information). Towers A, B, and D consisted of a 6-story shear wall box sitting on tied columns at the ground floor, while Tower C had a slab on grade at the 2nd story of the main building. During the 1971 San Fernando earthquake, Towers A, B, and D all collapsed, with the shear box overturning and coming to rest on the ground (Figure 2-7). Tower C did not collapse completely, but instead came to rest at an angle of approximately 5 degrees from vertical. Towers A, B, and D overturned and collapsed completely, falling away from the main building in their shorter direction, but at slight angles, suggesting that the movement of the main building interacted with them to some extent. Very small amounts of damage were observed in the upper (shear wall) portions of these towers. The columns supporting the base of the tower were destroyed. Because the shear walls rested on the ground at Tower C, no column failures took place, although some damage was observed in the shear walls.

Table 2-9 Olive View Stair Towers and Event Summary

Building information		Event information	
Location:	Los Angeles, California	Earthquake date:	February 9, 1971
Primary use:	Stairway and exit	Moment Magnitude:	6.6
No. of stories:	7	Epicentral distance:	10 km
Height:	90 ft	Local shaking intensity*:	VIII-XI
Size:	7,000 sq ft each (four total)	PGA**:	~0.5g
Year built:	1969		
Code:	1964 <i>Uniform Building Code</i>		
Lateral load system:	Shear walls on concrete moment resisting frame		
Gravity load system:	Reinforced concrete slab		

*Modified Mercalli Intensity

**Peak ground acceleration

Data sources: Bertero and Collins (1973); Mahin et al. (1976); Steinbrugge et al., (1971); USGS and NOAA (1971)



Figure 2-7 Olive View Stair Towers earthquake damage (NISEE, 2013a, Robert A. Olsen Collection, R0441).

2.2.8 Pyne Gould Building

The Pyne Gould Building in Christchurch, New Zealand was designed in 1963 (see Table 2-10 for additional building information). Primary lateral resistance was provided by reinforced concrete shear walls. Above the 2nd floor level, the walls formed a rectangular core that was nearly symmetric along the north-south center line but offset on the east-west axis. Below the 2nd floor level, there was significantly greater length of wall and shear resistance in the east-west direction than in the core above. In the September 2010 earthquake, the building suffered minor structural and some non-structural damage; in the December 2010 aftershock; no significant additional damage was recorded. In the February 2011 earthquake, the building collapsed (Figure 2-8). The shear-core rotated about the north-south axis of the building with a final resting position at approximately 68 degrees to the horizontal.

The shear-core east and north walls were destroyed between Level 1 and Level 2. The floor slabs were stacked on top of one another with a horizontal offset to the east of 0-4 meters between each slab. Very little rotation in plan occurred.

Table 2-10 Pyne Gould Building and Event Summary

Building information		Event information	
Location:	Christchurch, New Zealand	Earthquake date:	February 22, 2011
Primary use:	Office	Moment Magnitude:	6.1
No. of stories:	5	Epicentral distance:	6 km
Height:	65 m	Local shaking intensity*:	VIII-IX
Size:	4,200 sq m	PGA**:	-0.7g
Year built:	1966		
Code:	NZSS 95; NZS 4203:1992		
Lateral load system:	Shear walls core		
Gravity load system:	CIP slab, beams, cols.		

*Modified Mercalli Intensity

**Peak ground acceleration

Data sources: CESMD (2011); GeoNet (2011); NZBDH (2011); and USGS (2011)



Figure 2-8 Pyne Gould Building earthquake damage (Elwood, 2011).

2.2.9 Royal Palm Resort

The Royal Palm Resort in Anaga, Guam was a 220-unit, 12-story hotel and condominium complex that opened for occupancy just 18 days before the 1993 Guam earthquake (see Table 2-11 for additional building information). The main portion of

the complex consisted of three structurally separate but functionally interdependent structures: Wing A, which contained the hotel rooms; Wing B, which contained the condominiums; and the Elevator Wing. The resort sustained damage ranging from light to extensive in various portions of the structure. The heaviest damage occurred in Wing A, where failures of columns, joints, beams, and concrete-masonry-unit infills resulted in partial collapse, primarily in the southwest portion of the first and second stories (Figure 2-9). The building dropped as much as 1.5 meters at these locations and leaned toward the south with a total residual roof displacement of about 2.7 meters to the south. Damage to B-Block was light to moderate.

Table 2-11 Royal Palm Resort and Event Summary

Building information		Event information	
Location:	Agana, Guam	Earthquake date:	August 8, 1993
Primary use:	Hospitality/residential	Moment Magnitude:	8.1
No. of stories:	12	Epicentral distance:	60 km
Height:	130 ft	Local shaking intensity*:	IX
Size:	390,000 sq ft	PGA**:	~0.2g
Year built:	1993		
Code:	1988 <i>Uniform Building Code</i>		
Lateral load system:	Concrete moment frames		
Gravity load system:	R/C slab, beams, cols.		

*Modified Mercalli Intensity

**Peak ground acceleration

Data sources: EERI (1995); Hamburger (2004); Moehle (1997); Moehle (2003); Priestley and Hart (1994); Ross et al., (2000); and Somerville (1997)



Figure 2-9 Royal Palm Resort damage (Moehle, 2003).

2.3 Common Characteristics Among the Buildings

The data assembled on the example buildings provide an opportunity to compare design and construction characteristics affecting performance for the database group. Although the number of buildings included in this study is too small to support broadly applicable conclusions, the comparison of characteristics provides insight on which characteristics may be relatively more indicative of collapse potential.

2.3.1 Characteristics Affecting Damage States and Collapse Modes

At the onset, the example buildings were selected as well-known examples of “collapse.” Collapse is generally taken to mean that the building fell, completely or partially, to the ground. This definition of “collapse” can be expanded into two different modes (FEMA, 2009c):

- *Gravity load collapse*: A large majority of buildings that collapsed in past earthquakes did so because of failure of gravity load carrying component(s), which causes the building to collapse without excessive sway. Most structural analyses use models that do not include the simulation of gravity load component failure. Consequently this behavior is sometimes called “non-simulated” (FEMA, 2009a) for analysis purposes.
- *Lateral dynamic instability*: Even if the structure maintains the capacity to support gravity loads, it can still collapse in a sidesway mode due to dynamic instability resulting from lateral strength degradation. Collapse results when the structure loses a sufficient portion of its capacity to resist excessive lateral displacement. This mode is modeled in nonlinear structural analyses.

While all the case-study buildings were demolished after the causative earthquake event, three out of the nine example buildings did not actually collapse by the definition above. These are:

- **Royal Palm Resort**. Although many columns in the lower floors lost gravity load capability, the structure exhibited only a partial collapse and remained standing, preventing loss of life or major injuries to the occupants. The column failures resulted from unintended localized short- column effects, possibly exacerbated by inadequate joint reinforcing in the concrete, or by torsion from the interference of masonry infill with frame action. Without these conditions, the building probably would have performed better.
- **Imperial County Services Building**. Major damage to the base of columns at one end of the building caused a vertical “shortening” in the vicinity. The shortening was the result of large overturning motions, overloading the columns. There were no other signs of serious distress and the building remained standing. The column damage was due to a poor reinforcement detail at an offset in longitudinal reinforcing and the unintended interference of the surrounding grade

condition. Without these conditions, the building likely would have exhibited adequate performance.

- **Olive View Hospital Main Building.** In spite of a previous reputation as a poor performer, this building actually had some redeeming features that prevented collapse. The original design anticipated the soft-story effects of the transition from shear walls to frame action at the base. This is evident from the fact that elevator core walls were detailed to slide at the transition level. Between the 2nd level and grade, many poorly confined columns failed due to gravity load. However, the columns with spirals did not fail and prevented collapse. Although plastic hinges and joint distress were evident in many of the remaining columns, the spiral columns, acting in conjunction with their remaining lateral strength, kept the structure stable. It seems likely that the closing and sliding of the horizontal joint in the elevator core walls played a role in the lateral stability at large displacements.

It could be argued that these three buildings would have collapsed if shaking had been only slightly stronger or longer in duration. However, this seems improbable for the Imperial County Services Building. While it is difficult to speculate on the potential for collapse of the Olive View Hospital Main Building and the Royal Palm, given the recorded ground motions, it seems apparent that all three buildings would have had a much higher potential for collapse had it not been for their relatively robust gravity load carrying systems.

Although these three buildings did not collapse, the inclusion of these examples in the study is fortuitous. They provide valuable points of comparison with those buildings that did collapse, as discussed in subsequent sections of this report.

For the remaining six buildings the collapse modes are summarized as follows:

- **Bullock's Department Store.** The interior floors of the building collapsed without excessive side sway in a gravity load collapse mode. There were no signs of lateral dynamic instability.
- **CTV Building.** The floors of the building collapsed without excessive side sway in a gravity load collapse mode. There were no signs of lateral dynamic instability.
- **Four Seasons Apartment Building.** Although the central concrete cores fell laterally, there is compelling evidence that the post-tensioned slabs collapsed without excessive side sway prior to the cores. Collapse due to lateral instability would have necessitated the overturning of the towers despite the development of a relatively stable rocking mechanism after splice failure. Lateral dynamic instability, while possible, seems unlikely given these observations.

- **Olive View Psychiatric Clinic.** It is apparent that the reinforced concrete tied columns failed to support the gravity loads of the building. Furthermore, it can be seen that the building rotated in plan as it collapsed onto the ground. This rotation may have been caused by the first floor columns failing in sequence.
- **Olive View Stair Towers.** The three towers all toppled horizontally away from the building, essentially in one piece above the 2nd floor. It is apparent that frame action at this level below the discontinuous walls played a role in the collapse. If the columns below the walls had failed abruptly (e.g., shear or compression) and lost vertical (gravity load) capability, the tower would have become rotationally unstable under its own weight. As another possibility, if the columns had failed in flexure, they might have maintained the gravity load, in which case the collapse would have been due to lateral dynamic instability. In this case, it seems that the mode of collapse could have been a combination of gravity load collapse (column failure) and subsequent instability.
- **Pyne Gould Building.** The central core rotated and the rest of the building translated to the side during collapse. This failure appears to have been caused by a massive failure of the core walls at the 2nd level above grade. As a result, the core became unstable under its own weight and pushed the floor and roof slabs over to the side. It seems unlikely that lateral dynamic instability played a significant role.

2.3.2 Common Design and Construction Characteristics Among Example Buildings

Tables 2-12 and 2-13 tabulate the design and construction characteristics for all the buildings and the effects that each characteristic may have had on the final damage state. Table 2-14 lists the characteristics that were found to be likely or possible for at least a third of all case-study buildings. Table 2-15 lists the characteristics most common among those that actually collapsed. From these comparisons, the following general characteristics emerge as key factors in the performance of the example buildings.

2.3.2.1 Global Level Observations

For the example buildings, site-related characteristics did not emerge as important to behavior and performance. This is, however, due solely to the selection of the examples and is not significant in a general sense. For some buildings these characteristics could be very important to performance. For the example buildings, the following global characteristics emerged relatively more often than others:

Plan irregularities. Plan torsion was noted as a characteristic in seven of the nine examples. Of these, five collapsed. In reviewing the actual collapse mechanisms of these five, it seems that the absence of torsional response would not have precluded

Table 2-12 Global Level Design and Construction Characteristics for all Example Buildings, with the Potential for these Characteristics to Cause Collapse During a Major Earthquake
 (Outcomes are measured In terms of Likely, Possible, Unlikely, Unknown, and Not Applicable (N/A)).

Global Level	Bullock's	CTV Building	Four Seasons	Imperial County Services Bldg	Olive View Main Bldg	Olive View Psych Clinic	Olive View Stair Towers	Pyne Gould Building	Royal Palm Resort
Site-related									
Pounding	Unknown	N/A	N/A	N/A	Possible	Possible	Likely	N/A	Unlikely
Permanent ground displacement	N/A	Unlikely	Unlikely	N/A	Unlikely	Unlikely	Unlikely	Unlikely	Unknown
Materials and construction quality									
Materials									
Concrete	Unlikely	Possible	Unknown	Unlikely	Unlikely	N/A	Unlikely	Unlikely	Possible
Light-weight concrete	Possible	N/A	N/A	Unlikely	Unlikely	Possible	N/A	N/A	Unknown
Reinforcing/PT steel	Unknown	N/A	Unknown	Unlikely	Unlikely	Unknown	Unlikely	Unlikely	Unknown
Execution									
Conveyance/placement of concrete	Unknown	N/A	Unknown	Unlikely	Unknown	Unknown	Unknown	Unlikely	Unknown
Rebar/PT	Unlikely	Possible	Unknown	Unlikely	Unknown	Unknown	Unknown	Unlikely	Unknown
Field variance with design documents	Unknown	Likely	Unknown	Unlikely	Unknown	Unknown	Unknown	Unknown	Likely
Configuration									
Plan irregularities									
Torsion	Unlikely	Likely	N/A	Possible	Possible	Possible	Unlikely	Likely	Likely
Perimeter boundary	Unlikely	Unlikely	N/A	N/A	Possible	Unlikely	Unlikely	N/A	Unlikely
Vertical irregularities									
Soft story	Possible	N/A	Unlikely	Unlikely	Likely	Possible	Likely	Unlikely	Possible
Weak story	Likely	N/A	Unlikely	Unlikely	Likely	Likely	Likely	Unlikely	Likely
Mass distribution	Unlikely	N/A	Unlikely	N/A	Possible	Unlikely	Unlikely	Unlikely	Unlikely
Inter-story masses and/or lateral stiffening elements	Unknown	N/A	N/A	N/A	N/A	Unknown	Possible	Unlikely	Unknown
Setbacks	Unknown	N/A	N/A	N/A	Unlikely	Possible	N/A	N/A	N/A
Out-of-plane discontinuity	Possible	N/A	N/A	Possible	N/A	Unlikely	N/A	Possible	N/A
In-plane discontinuity	Likely	N/A	N/A	Unlikely	Likely	Likely	Likely	Unlikely	N/A
Lateral resisting system									
Strength									
Overall lack of strength	Possible	Unlikely	Unlikely	Unlikely	Possible	Likely	Likely	Likely	Unlikely
Stiffness									
Extreme flexibility	Unlikely	Unlikely	Unlikely	Unlikely	Unlikely	Unlikely	Unlikely	Unlikely	Unlikely
Load path									
Collectors/struts	Unlikely	Likely	Unlikely	Unlikely	Unlikely	Unlikely	Unlikely	Unlikely	Unlikely
Anchorage of nonstructural elements	Unlikely	Unknown	Unlikely	N/A	Unknown	Possible	Unlikely	Unlikely	Unknown
In-plane connection of walls to diaphragm	Possible	Possible	Possible	Unlikely	Unlikely	Unlikely	Unlikely	Possible	Unlikely
Out-of-plane connection of walls to diaphragm	Unlikely	Possible	Possible	Unlikely	Unlikely	Unlikely	Unlikely	Possible	Unlikely
Diaphragm chords	Unlikely	Unlikely	Unlikely	Unlikely	Unlikely	Unlikely	Unlikely	Unlikely	Unlikely
Diaphragm openings	Unlikely	Likely	Unlikely	Unlikely	Unlikely	Unlikely	Unlikely	Unlikely	Unlikely
Vertical load system									
Deformation capacity	Likely	Likely	Likely	Unlikely	Unlikely	Likely	Likely	Likely	Unlikely
Load redistribution capability	Likely	Likely	Likely	Unlikely	Unlikely	Likely	Likely	Likely	Unlikely

Table 2-13 Component Level Design and Construction Characteristics for all Example Buildings, with the Potential for these Characteristics to Cause Collapse During a Major Earthquake
 (Outcomes are measured In terms of Likely, Possible, Unlikely, Unknown, and Not Applicable (N/A)).

Component Level		Bullock's	CTV Building	Four Seasons	Imperial County Services Bldg	Olive View Main Bldg	Olive View Psych Clinic	Olive View Stair Towers	Pine Gould Building	Royal Palm Resort
Frames										
Columns										Sum of Likely or Possible Ratings
Shear strength	Unlikely	Possible	N/A	Likely	Likely	Likely	Likely	Possible	Likely	7
Lap slices in longitudinal reinforcing	Unlikely	Possible	N/A	Unlikely	Unknown	Unknown	Unknown	Possible	Possible	3
$\frac{P}{A_g f'_c}$	Unlikely	Likely	N/A	Likely	Possible	Unlikely	Unlikely	Unlikely	Possible	4
"Vertical" load columns drift capacity	Unlikely	Likely	Possible	Likely	Likely	N/A	N/A	Possible	Likely	6
Captive/"short" columns	Unlikely	Possible	N/A	Likely	N/A	Unlikely	N/A	N/A	Likely	3
Beams/flat slabs										
Strength relative to columns	Unlikely	Likely	N/A	Unlikely	Possible	Likely	Possible	Possible	Likely	6
Loss of vertical capacity	Unlikely	Unlikely	N/A	Unlikely	Unlikely	Unknown	Unlikely	Unlikely	Unknown	0
Continuity of longitudinal reinforcing	Unlikely	Likely	N/A	Unlikely	Unknown	Unlikely	Unlikely	Unlikely	Unknown	1
Joints (beam-col. or slab-col.)										
Interior (concrete on four sides)	Likely	Likely	Likely	Unlikely	Possible	Possible	Unknown	Likely	Likely	7
Exterior (concrete on three sides or fewer)	Likely	Likely	Likely	Unlikely	Possible	Possible	Unknown	Likely	Likely	7
Infills										
Interference with frame action	Likely	Possible	N/A	N/A	N/A	Possible	N/A	N/A	Likely	4
Out-of-plane	Unlikely	N/A	N/A	N/A	N/A	Unknown	N/A	N/A	Unlikely	0
Attachment to framing	Likely	N/A	N/A	N/A	N/A	Possible	N/A	N/A	Unlikely	2
Shear walls										
Shear										
Diagonal tension/compression	Unlikely	Unlikely	Unlikely	Unlikely	Unlikely	N/A	Unlikely	Likely	N/A	1
Sliding shear	Likely	Unlikely	Unlikely	Unlikely	Unlikely	N/A	Unlikely	Unlikely	N/A	1
Connection to diaphragm	Possible	Possible	Possible	Unlikely	Unlikely	N/A	Unlikely	Likely	N/A	4
Flexure										
Compression zone buckling capacity	Unknown	Unlikely	Unlikely	Unlikely	Unlikely	N/A	Unlikely	Likely	N/A	1
Boundary capacity	Unknown	Unlikely	Likely	Unlikely	Unlikely	N/A	Unlikely	Possible	N/A	2
Discontinuity of wall	Likely	Unlikely	N/A	Likely	Likely	N/A	Likely	Possible	N/A	5
Boundary reinforcing at openings	Unlikely	Unlikely	Unlikely	Unlikely	Unlikely	N/A	Unlikely	Unlikely	N/A	0
Foundation behavior	Unlikely	Possible	Unlikely	Unlikely	Unlikely	N/A	Possible	Unlikely	N/A	2

¹ P = axial load; A_g = gross area of column (section); f'_c = strength of concrete.

normally used by engineers, designates a story that has less horizontal strength relative to others in the building. All of the five buildings that were classified as having soft stories also can be classified as having horizontally weak stories by this definition. Of these five example buildings, three collapsed.

Interpretation of the behavior that can result from soft and/or weak stories requires some clarification of these conventional designations with respect to performance. Soft stories tend to increase drifts at that story, leading to relatively larger component displacements in the story. Weak stories tend to develop inelastic behavior prior to other stories, thereby concentrating inelastic horizontal drift at the weak level. Thus, the initial consequences of soft and weak stories are similar in concept. However, the important point is that neither necessarily signals collapse. The performance of a building with a soft or weak story depends upon several subsequent factors as discussed in Section 2.3.3 below.

Table 2-14 Frequency of Design and Construction Characteristics Found Likely or Possible in More than One Third of all Example Buildings

		Buildings										Percentage of Likely or Possible Ratings
Level	Category	Performance Impact										Percentage of Likely or Possible Ratings
		Characteristic	Unlikely	Likely	N/A	Possible	Possible	Possible	Unlikely	Likely	Likely	
Global	Plan irregularities	Torsion	Unlikely	Likely	N/A	Possible	Possible	Possible	Unlikely	Likely	Likely	67%
	Vertical load system	Deformation capacity	Likely	Likely	Likely	Unlikely	Unlikely	Likely	Likely	Likely	Unlikely	67%
	Vertical load system	Load redistribution capability	Likely	Likely	Likely	Unlikely	Unlikely	Likely	Likely	Likely	Unlikely	67%
	Vertical irregularities	Soft story	Possible	N/A	Unlikely	Unlikely	Likely	Possible	Likely	Likely	Unlikely	56%
	Vertical irregularities	Weak story	Likely	N/A	Unlikely	Unlikely	Likely	Likely	Likely	Likely	Unlikely	56%
	System strength	Overall lack of strength	Possible	Unlikely	Unlikely	Unlikely	Possible	Likely	Likely	Likely	Unlikely	56%
	Vertical irregularities	In-plane discontinuity	Likely	N/A	N/A	Unlikely	Likely	Likely	Likely	Unlikely	N/A	44%
	Load path	In-plane connection of walls	Possible	Possible	Possible	Unlikely	Unlikely	Unlikely	Unlikely	Unlikely	Possible	44%
	Site-related	Pounding	Unknown	N/A	N/A	N/A	Possible	Possible	Likely	N/A	Unlikely	33%
	Vertical irregularities	Out-of-plane discontinuity	Possible	N/A	N/A	Possible	N/A	Unlikely	N/A	Possible	N/A	33%
Component	Load path	Out-of-plane connection of walls	Unlikely	Possible	Possible	Unlikely	Unlikely	Likely	Unlikely	Possible	Unlikely	33%
	Columns	Shear strength	Unlikely	Possible	N/A	Likely	Likely	Likely	Likely	Possible	Likely	78%
	Joints (beam-col. or slab-col.)	Exterior (concrete on three sides or fewer)	Likely	Likely	Likely	Unlikely	Possible	Possible	Unknown	Likely	Likely	78%
	Joints (beam-col. or slab-col.)	Interior (concrete on four sides)	Likely	Likely	Likely	Unlikely	Possible	Possible	Unknown	Likely	Likely	78%
	Columns	"Vertical" load columns drift capacity	Unlikely	Likely	Possible	Likely	Likely	N/A	N/A	Possible	Likely	67%
	Beams/flat slabs	Strength relative to columns	Unlikely	Likely	N/A	Unlikely	Possible	Likely	Possible	Possible	Likely	67%
	Shear walls	Discontinuity of wall	Likely	Unlikely	N/A	Likely	Likely	N/A	Likely	Possible	N/A	56%
	Columns	$\frac{P}{A_g f'_c}$ ¹	Unlikely	Likely	N/A	Likely	Possible	Unlikely	Unlikely	Unlikely	Possible	44%
	Infills	Interference with frame action	Likely	Possible	N/A	N/A	N/A	Possible	N/A	N/A	Likely	44%
	Shear walls	Connection to diaphragm	Possible	Possible	Possible	Unlikely	Unlikely	N/A	Unlikely	Likely	N/A	44%
	Columns	Lap slices in longitudinal reinforcing	Unlikely	Possible	N/A	Unlikely	Unknown	Unknown	Unknown	Possible	Possible	33%
	Columns	Captive/"short" columns	Unlikely	Possible	N/A	Likely	N/A	Unlikely	N/A	N/A	Likely	33%

¹ P = axial load; A_g = gross area of column (section); f'_c = strength of concrete.

Table 2-15 Frequency of Most Common Design and Construction Characteristics Found Within the Group of Six Buildings that Collapsed

		Buildings										Percentage of Likely or Possible Ratings
Level	Category	Performance impact										Percentage of Likely or Possible Ratings
		Characteristic	Likely									
Global	Vertical load system	Deformation capacity	Likely	100%								
	Vertical load system	Load redistribution capability	Likely	100%								
	System strength	Overall lack of strength	Possible	Unlikely	Unlikely	Likely	Likely	Likely	Likely	Likely	Likely	67%
	Load path	In-plane connection of walls to diaphragm	Possible	Possible	Possible	Possible	Unlikely	Unlikely	Unlikely	Possible	Possible	67%
	Plan irregularities	Torsion	Unlikely	Likely	N/A	Possible	Possible	Unlikely	Likely	Likely	Likely	50%
	Vertical irregularities	Soft story	Possible	N/A	Unlikely	Possible	Likely	Likely	Likely	Unlikely	Likely	50%
	Vertical irregularities	Weak story	Likely	N/A	N/A	Likely	Likely	Likely	Likely	Unlikely	Likely	50%
	Vertical irregularities	In-plane discontinuity	Likely	N/A	N/A	Likely	Likely	Likely	Likely	Unlikely	Likely	50%
Component	Load path	Out-of-plane connection of walls to	Unlikely	Possible	Possible	Possible	Unlikely	Unlikely	Unlikely	Possible	Possible	50%
	Joints (beam-col. or slab-col.)	Exterior (concrete on three sides or fewer)	Likely	Likely	Likely	Possible	Unlikely	Unknown	Likely	N/A	Likely	83%
	Columns	Shear strength	Unlikely	Possible	N/A	Likely	Likely	Likely	Likely	Possible	Possible	67%
	Beams/flat slabs	Strength relative to columns	Unlikely	Likely	N/A	Likely	Possible	N/A	N/A	Possible	Possible	67%
	Shear walls	Connection to diaphragm	Possible	Possible	Possible	N/A	N/A	Unlikely	Likely	N/A	Possible	67%
	Joints (beam-col. or slab-col.)	"Vertical" load columns drift capacity	Unlikely	Likely	Possible	N/A	N/A	N/A	N/A	N/A	Possible	50%
	Shear walls	Interior (concrete on four sides)	Likely	Likely	Likely	Unknown	Unknown	Unknown	Unknown	Unknown	Unknown	50%
	Infills	Discontinuity of wall	Likely	Unlikely	N/A	N/A	Likely	Likely	Unlikely	Possible	Possible	50%

Lateral system. With respect to the lateral system characteristics, overall lack of strength relative to demand was found relatively frequently in the example buildings. Although information on ground motion was gathered at each example building, the level of detail for this parameter is inconsistent among the sites. This precludes a reliable quantitative comparison of horizontal capacity relative to demand.

Nonetheless, five of the example buildings could be characterized qualitatively as horizontally weak compared to the actual ground motion. Of these, four collapsed. One example that was not characterized as weak relative to demand did collapse. Consequently, this characteristic was not completely reliable as a precursor to collapse for these examples.

Gravity system. When studying the performance of buildings specifically selected as examples of collapse, it should not be completely surprising that the robustness of the gravity load system is a key factor contributing to whether collapse was observed or not. The study gauged two related characteristic parameters:

1. ***Overall gravity load capacity of floor/roof levels in the presence of large lateral drifts.*** This characteristic played a role in all of the buildings that collapsed. In at least one case (Olive View Psychiatric Clinic), there were column shear failures at most of the columns (at a single level). For several others (Bullocks, CTV, and Four Seasons), gravity load failures of beam-column or beam slab joints caused collapse. These are further discussed at the component level below.
2. ***Presence and Reliability of the Gravity Load Redistribution Mechanisms.*** Gravity load redistribution capability was absent in all example buildings that collapsed. Notably, this capability was present in all three examples buildings that did not collapse:
 - The Olive View Main Hospital Building had a sufficient number of spiral columns to support all gravity loads. Furthermore, closure of the sliding joint at the base of the elevator walls likely provided additional lateral and gravity load support at the large residual drift.
 - The exterior columns at one end of the Imperial County Services Building shortened but did not lose gravity load capacity. When these columns failed, much of their gravity loads were redistributed by framing throughout the height of the building; this provided an alternative load path for the gravity loads initially supported by the failed columns, thus preventing collapse.
 - A large proportion of columns on one side of the Royal Palm Resort lost gravity load capacity at the lower level, causing the building to tilt dramatically. In spite of this, the gravity load capacity of the remaining framing and the relatively deep spandrels above and below the failed columns prevented general collapse.

2.3.2.2 Component Level Observations

Column strength and drift capacity. Column capacity in terms of both strength and displacement is an important characteristic of all the example buildings. Since the buildings were selected as examples of collapse, this observation is expected. Column strength relative to the strength of beams or slabs is an important issue; in this sample set of collapsed buildings, weak columns existed in four of the six actual collapses. These observations confirm that column strength characteristics are important considerations for performance and collapse.

Beam or slab connection to columns. Most of the examples exhibit characteristics indicating unfavorable beam or slab connection to columns. Based on the review of the data from the examples, it is evident that these characteristics are ambiguous, making it difficult to distinguish between lateral and gravity load capacities. Furthermore, the fact that joints lose lateral capacity does not necessarily mean that they lose the capability to sustain gravity load. For example, there is evidence that some of the beam column joints in the Olive View Hospital Main Building may have lost lateral capacity, but still maintained gravity load capacity. This factor is particularly significant since these joints seem to have contributed to the capacity of the building to avoid collapse.

Shear wall discontinuity. Five of the example buildings had discontinuous walls; of these, three collapsed. This tends to confirm the prevailing concern with this characteristic as it affects performance and collapse.

Interference of infill with frame action. In those buildings that included infill masonry, it is evident that wall infill interferes with frame action and could have contributed to collapse. One of the most convincing examples is found in the Royal Palm Resort, where “nonstructural” infills significantly altered the intended structural behavior. Though these infills led to severe damage to components, the building remained standing.

Connection of walls to diaphragms. Several of the examples that fully collapsed show signs of a weak connection of shear walls to diaphragms. Design and construction details confirm these weaknesses. However, it is difficult to interpret the implication of this observation since it is not known whether the damage was a cause or result of collapse.

2.3.3 Interaction of Characteristics and the Effect on Performance

The review of the characteristics of the nine example buildings in aggregate leads to the conclusion that design and construction characteristics affecting collapse are interdependent and interactive. No single deficiency is a clear-cut indicator of collapse potential in and of itself. It is also evident that the characteristics fall into two broad categories.

- First, the global-level characteristics, for the most part, relate to factors that can increase lateral deformation demands at the component level. For example, the twisting associated with torsional response magnifies elastic and inelastic story displacements, which in turn lead to larger column distortions.
- Second, the component-level characteristics relate to conditions that decrease component lateral deformation capacities. For example, lack of adequate transverse reinforcement in columns leads to brittle loss of lateral and axial-load capacity at smaller column distortions.

For the purpose of improving the capability to identify collapse risk, the most significant observation from these examples is the importance of the robustness of the gravity load carrying system. This observation may seem trivial and self-fulfilling on the surface; however, engineers and researchers alike tend to focus on lateral response and capacity. All of the current seismic analysis and design evaluation procedures for structures are based predominantly in the horizontal force and displacement domain. Of the three example buildings that did not collapse, each had global characteristics that increased lateral demand and component characteristics that decreased lateral capacity. Their ability to remain standing was due to the fact that the gravity load system in these buildings had the capability to maintain gravity load support in spite of many “failures” in lateral load capacity. In contrast, all of the collapsed examples had gravity load systems that lacked deformation capacity and/or gravity load redistribution capability.

2.4 Conclusions and Implications

The results of this study of nine reinforced concrete buildings that collapsed due to earthquake shaking lead to several key conclusions with respect to the development of a simplified evaluation of collapse potential.

- Reinforced concrete buildings generally collapse due to loss of the gravity load carrying capability after sustaining damage caused by lateral (horizontal) distortions, rather than lateral dynamic instability. Current simplified evaluation procedures do not focus directly on the capability of the gravity load system.
- Existing lists of deficiencies and checklists in ASCE/SEI 41-13 (ASCE, 2013) are useful for identifying the presence of design and construction characteristics that may increase lateral seismic demand or decrease lateral capacity. They can also be used to determine the potential locations of damage due to horizontal distortions. While this information may be useful, it is insufficient to predict collapse risk and other performance risks more generally.
- The compilation and organization of design and construction characteristics developed for this study consider the gravity load capacity of subject buildings, including the ability to redistribute loads. These design and construction

characteristics capture the key factors leading to damage resulting from horizontal distortion and its effect upon gravity load carrying capability of the building.

- The characterization of the gravity system capacity, when subject to damage from lateral distortions, has not been developed formally for the purposes of this study. Thus the assessments of adequacy are necessarily based upon engineering judgment (of the PTC). In the cases examined here, the inadequacies were reasonably obvious, but this is not likely the case for all buildings.

Based on these conclusions, it is clear that the issue of post-damage gravity system capacity is vitally important to assessing collapse risk. It is also apparent that procedures for evaluating this capacity systematically and reliably are currently not available. Consequently, the recommendations outlined below are directed toward improvements aimed at this aspect of collapse risk.

2.4.1 Practical Applications

Engineering practitioners should recognize the inherent limitations of currently available checklists to “evaluate” reinforced concrete buildings. Although useful for preliminary purposes and to guide subsequent analyses, in their present form they should not be used to quantify collapse risk. Practitioners should also consider the inherent capacity of the gravity load system, particularly under expected lateral deformation demands, when investigating the seismic performance of structures.

This study did not use ASCE/SEI 41-13 to evaluate the expected seismic performance of the case-study buildings. The buildings in this study should be subjected to the Tier 1 procedures in ASCE/SEI 41-13 to see how they would fare. It is possible that modifications to improve the standard would emerge from this review.

2.4.2 Case Histories

This study illustrates the usefulness of reviewing and comparing actual case histories of damage to buildings in past earthquakes. Further comparison of other case studies may better determine if the presence or absence of a robust gravity load carrying system is related to collapse performance. Examining more buildings that did not collapse when subject to strong shaking should provide valuable data as well. The EERI Concrete Coalition is about to release an online database documenting the seismic performance of reinforced concrete buildings. The format is oriented toward case histories and focuses on individual buildings. Currently the database comprises approximately 60 buildings, including those covered in this study and report. Other efforts to assemble and catalog building performance data are also progressing, including those of investigators at NIST involved in the NIST Disaster and Failure

Studies Program (NIST, 2013b) and those of investigators at the Applied Technology Council and Purdue University involved in data archival activities at NEEScomm (Hortacus et al., 2012).

It is also worth noting that there are quite a few reinforced concrete buildings that have been evaluated and retrofitted. Many of these would have valuable analysis and evaluation data that could contribute to a more generalized understanding of performance. An effort to garner this data, particularly from well qualified firms, should supplement information gathered by reconnaissance teams after earthquakes.

2.4.3 Collapse Analysis Techniques for Engineering Practice

It is a challenging research problem to include the effect of loss of gravity load capacity in individual components in nonlinear response history analysis (as described in detail in Chapter 4 of this report). Reliable modeling and solution strategies are not yet available for practical application. It may be possible to estimate the effects of gravity load capacity loss by investigating a simple linear analysis for gravity loads. This model could be evaluated in parallel with the nonlinear analysis for earthquake shaking. If the nonlinear model resulted in major damage to gravity load carrying components, these could be removed from the linear model to investigate the consequences with respect to global collapse. The linear model could be two- or three-dimensional to capture the capability of the structure to redistribute gravity loads to components that maintain gravity load capacity.

2.4.4 Physical Testing

Past tests of assemblies that included gravity systems should be re-examined to glean whatever useful information about gravity capacity that may already exist. Particularly pertinent are tests on large-scale structures. The design of future tests should include consideration of gravity load transfer in the test assembly and the data recovery/instrumentation strategy.

2.4.5 Limitations

As mentioned throughout this chapter, the small number of example buildings limits the degree to which generalizations about the causes of seismically induced collapse can be made based upon these results. This limitation warrants caution when applying the observations in the evaluation of the seismic performance of buildings *a priori*.

Chapter 3

Collapse Mitigation Strategies

3.1 Introduction

For many years, it has been common practice to utilize a “Life Safety” seismic performance objective for the design of seismic retrofits of potentially hazardous older buildings, including nonductile concrete structures. The original seismic designs of these older buildings were also designed to a life safety objective, although the criteria then used were less advanced than today’s requirements, making the buildings less earthquake resistant, in many cases substantially less earthquake resistant. Similarly, the understanding of earthquake ground motions (i.e., earthquake demand) was much less advanced than it has been in recent years, as a result of the proliferation of earthquake ground motion records over the last several decades.

Since the late 1990s, a life safety performance objective has often been used for either voluntary or building code-mandated seismic retrofits. Though there are several different definitions in practice, the Life Safety performance objective essentially specifies seismic performance in which there is an adequate margin of safety against building collapse and building occupants are able to exit the building following an earthquake with a relatively low risk of life-threatening injury.

“Collapse Prevention” seismic performance, in accordance with ASCE/SEI 41, *Seismic Evaluation and Retrofit of Existing Buildings* (ASCE, 2013), is defined as “the post-earthquake damage state in which a structure has damaged components and continues to support gravity loads but retains no margin against collapse.” Compared to Life Safety, this implies more structural damage and less residual lateral capacity.

Because of the margin against collapse associated with Life Safety performance, and the potentially extensive scope of retrofit required to achieve this performance level in nonductile concrete structures, there is a need to consider mitigation strategies that focus more directly on avoiding collapse. In other words, retrofit strategies that address the characteristics contributing to the greatest risk of building collapse, while potentially not addressing some deficiencies that may result in significant damage at the design level earthquake, are needed. These strategies should focus on eliminating the most significant collapse-inducing deficiencies, while potentially allowing other deficiencies to remain as long as they are not judged to be a contributor to a high risk of large scale, sudden, and brittle collapse.

An important concept pertaining to collapse prevention is global collapse, as compared to failure of some localized individual elements that would not necessarily lead to an elevated risk of collapse of the entire structure. Concern with localized failure is one of the main tenants of current practice, whereas many reinforced concrete structures are inherently redundant and can develop several possible load paths for resisting both gravity and lateral loads.

Commonly available resources for designing building seismic retrofits that would be of use in developing collapse-mitigation strategies for older reinforced concrete buildings are provided below, along with potential mitigation strategies for common collapse-inducing deficiencies.

3.2 Existing Resources for Building Seismic Retrofit

Resources for developing building seismic retrofits for collapse mitigation have been developed and updated under a variety of Federal, state, and private-sector programs over the last several decades, including those of the Federal Emergency Management Agency, the California Seismic Safety Commission, the Structural Engineering Institute of the American Society of Civil Engineers, and the American Concrete Institute. Such resources provide important technical information and criteria that should be considered in the development of collapse-mitigation strategies for older reinforced concrete buildings. These resources include those listed below:

ATC-40, *Seismic Evaluation and Retrofit of Concrete Buildings*. Funded by the California Seismic Safety Commission, the ATC-40 report (ATC, 1996), provides systematic guidance, in the form of methodology and commentary, for the seismic evaluation and retrofit design of existing concrete buildings. Developed synergistically with the FEMA 273 *NEHRP Guidelines for the Seismic Rehabilitation of Existing Buildings* (FEMA, 1997a), the ATC-40 report introduced (along with FEMA 273) the concept of a two-part performance objective, consisting of a defined damage state and a defined level of seismic hazard. This 2-volume document is both broad and comprehensive, providing guidance on determination of deficiencies, development of retrofit strategies, quality assurance procedures, and other facets of seismic retrofit. At the least, review of this document would provide perspective on the range of issues that need to be considered when developing collapse-mitigation strategies for older concrete buildings.

FEMA 274, *NEHRP Commentary on the Guidelines for the Seismic Rehabilitation of Existing Buildings*. FEMA 274 (FEMA, 1997b) provides commentary for the concurrently-developed companion FEMA 273 report, *NEHRP Guidelines for the Seismic Rehabilitation of Existing Buildings* (FEMA, 1997a), which was replaced by the FEMA 356 *Prestandard and Commentary for the Seismic Rehabilitation of Buildings* (FEMA, 2000), and subsequently the ASCE/SEI 41-06 standard, *Seismic*

Rehabilitation of Existing Buildings (ASCE/SEO, 2006), and more recently ASCE/SEI 41-13 standard, *Seismic Evaluation and Retrofit of Existing Buildings* (ASCE, 2013). Much of the detailed commentary in FEMA 274, which was not included in the commentaries of the more recent documents, may be useful in targeting analysis and seismic retrofit measures for collapse mitigation.

FEMA 547, Techniques for the Seismic Rehabilitation of Existing Buildings.

FEMA 547 (FEMA, 2006) is a thorough retrofit guideline for most common building types. It includes chapters specific to reinforced concrete-frame and shear-wall buildings and covers a wide range of performance objectives and mitigation strategies. It also provides example details for various elements of common mitigation strategies. Using the techniques presented in the guideline, together with a seismic retrofit scope focused on mitigating the significant collapse risks, can lead to an effective retrofit strategy.

ASCE/SEI 31, Seismic Evaluation of Existing Buildings. ASCE/SEI 31 (ASCE, 2003) is primarily an evaluation standard and does not include a Collapse Prevention performance objective, but the Tier 1 checklists are a good way of identifying deficiencies in reinforced concrete buildings that could pose a high risk of collapse. Furthermore, the commentary may be helpful in determining methods for mitigation of hazards. This standard has been updated and combined with ASCE/SEI 41 into a single standard (ASCE/SEI 41-13) that is scheduled to be available in 2014.

ASCE/SEI 41-13, Seismic Evaluation and Retrofit of Existing Buildings.

ASCE/SEI 41-13 (ASCE, 2013) contains provisions for and commentary on developing retrofits to achieve Collapse Prevention performance of reinforced concrete buildings. The simplified rehabilitation provisions, though not intended to be used for Collapse Prevention performance, contain useful information on retrofit methods for specific deficiencies.

ACI 369, Guide for Seismic Rehabilitation of Existing Concrete Frame Buildings and Commentary. ACI 369 (ACI, 2011) is a supplement to ASCE/SEI 41-06, with guidelines specific to reinforced concrete frame buildings. The guide contains primarily technical provisions, but the guide-based format allows the introduction of new technical content more quickly than through the standards process. It could therefore be used as a resource for cutting-edge analysis techniques to develop collapse mitigation retrofits.

International Existing Building Code (IEBC), Appendix A5. IEBC, Appendix A5, “Earthquake Hazard Reduction in Existing Concrete Buildings” (ICC, 2012b), contains “hazard reduction” provisions for reinforced concrete buildings, primarily using references to ASCE/SEI 31, ASCE/SEI 41, and the *International Building Code* (ICC, 2012a).

EERI Concrete Coalition Building Performance Database. Discussed in more detail in Chapter 1 and Chapter 2, the Earthquake Engineering Research Institute's Concrete Coalition has assembled a database of case histories describing the performance of reinforced concrete buildings in past earthquakes. These case histories can be useful in understanding the deficiencies that most likely to lead to building collapse and, consequently, those that should be the focus of a collapse mitigation program.

3.3 Retrofit Strategies Focused on Collapse Mitigation

Mitigation should focus on the most severe of collapse indicators and should minimize the likelihood or severity of those deficiencies. The focus should not generally be on improving overall building behavior or eliminating all deficiencies that could, for instance, be identified in an ASCE/SEI 31 Life Safety seismic evaluation.

3.3.1 Configuration

Certain configuration irregularities, such as those that cause severe torsion, weak stories, and in-plane discontinuities, can be significant deficiencies that contribute to the likelihood of building collapse. Where collapse mitigation is the goal of a retrofit program, the strategy should focus on reducing the effect of these irregularities without necessarily considering other global characteristics, such as overall lateral strength. Depending on the specific conditions in a building, one or more of the following strategies could be considered.

- **Add strength or stiffness to a weak or soft story.** A seismic retrofit could focus on providing more uniform strength and stiffness distribution to the adjacent stories, rather than considering overall lateral strength. For example, a mitigation program could involve adding additional shear wall(s) or braced frames to a tall first floor, where strength and stiffness would be designated relative to the upper floors, rather than only as a criterion of overall lateral strength.
- **Eliminate vertical discontinuities or strengthen elements supporting the discontinuity.** The collapse mitigation strategy should account for the strength of the elements above the discontinuity. An example is locally strengthening concrete columns below a discontinuous shear wall for the capacity of the wall above.
- **Mitigate a severe plan irregularity.** Similar to the weak-story condition, new lateral elements should be added locally in order to balance the lateral system (reducing torsion) in addition to considering global lateral strength.

- **Soften existing elements.** Rather than adding strength or stiffness, an option for mitigating a vertical or horizontal deficiency may be reducing the stiffness and strength of selected existing elements. As long as this does not lead to an unsafe reduction in the gravity load-carrying system, or excessively reduce the overall lateral strength, softening the elements that create the deficiency can be an effective low-impact strategy. For example, if a structure has a solid wall on one end and a highly perforated wall on the other end, new openings could be created in the solid wall to reduce the stiffness and the torsional response. Of course, care should always be taken when reducing the strength of an existing building.
- **Remove or separate portions of building that cause the irregularity.** If a significant vertical or horizontal irregularity is created by vertical or plan offsets, a strategy could be to remove the offset portion of the building, thus leaving an intact, more regular structure. Alternatively, adding structural separations in an irregularly-shaped plan could be used as a method to remove irregularity. These strategies require careful consideration of the completeness and the deformation capability of the gravity load-carrying system at the potential seismic separation locations.

3.3.2 Gravity Load-Carrying System

Failures in the gravity system, either due to lack of deformation capacity or lack of load redistribution capacity, were significant factors in the behavior of most of the sample buildings described in Chapter 2. Adding supplemental gravity support systems to mitigate gravity collapse associated with lateral deformation or localized failures has been a common practice in the retrofit of unreinforced masonry buildings, and the same concepts could apply to reinforced concrete buildings. Some strategies include:

- **Add secondary support framing.** Providing secondary support columns, beams, or brackets with reliable deformation capacity can be a relatively simple strategy for mitigating this type of deficiency. These systems can be designed for a reduced live load and for lower factors of safety to provide added gravity load capacity for the expected loads in order to resist collapse.
- **Improve poor connectivity.** Inadequate connections between discontinuous elements of the gravity system can be improved by local strengthening and the addition of connections.
- **Mitigate punching shear in flat slab systems.** Reducing the collapse risk associated with punching shear in flat slab systems with insufficient deformation capacity can be accomplished by adding column capitals, or brackets, or by other means to strengthen the slab-to-column interfaces.

- **Add lateral stiffness to reduce deformation demand.** Although this strategy is generally considered as a global retrofit strategy for improved performance, it can be more cost effective than locally improving connections or adding support framing, since it can be a localized upgrade. For example, shear walls can be added at specific locations rather than improving every slab-column connection throughout the building.

3.3.3 Shear-Critical Vertical Elements

Failure of shear-critical columns or slender wall piers is a well-documented cause of collapse in reinforced concrete buildings. There is evidence of buildings that have suffered significant shear failures and have not collapsed, but the post-earthquake stability of elements with shear failures is difficult to predict. The mitigation strategy could involve either strengthening the shear-critical element or providing a reliable gravity-load-carrying system if a shear failure occurs. Mitigation strategies include the following:

- **Strengthen shear-critical elements.** Shear-critical columns or wall piers can be strengthened by means of concrete overlays, fiber-reinforced polymer (FRP) overlay, or steel jacketing. The added elements will provide additional shear capacity and confinement in order to improve the deformation capacity of the element. It should be noted that this strategy can be difficult if the deficient elements are on the building perimeter and are integrated with cladding or glazing systems.
- **Provide a secondary gravity support system.** Similar to the mitigation strategy presented in Section 3.3.2, secondary support elements can be added to mitigate the collapse risk associated with shear-critical elements. This strategy does not improve the post-yield behavior of the building as an element strengthening strategy does, but it can be effective in reducing the risk of collapse.
- **Globally stiffen the building.** The addition of concrete shear walls or braced frames to stiffen the lateral system can be effective in reducing the likelihood of shear failures in shear-critical elements by reducing potential deformations. As discussed in Section 3.3.2, this strategy can be cost effective compared to a more extensive upgrade of all shear-critical elements.
- **Locally stiffen shear-critical elements.** As with the previous strategy, localized strengthening should be added to mitigate shear-critical elements. For example, adding infill to openings between narrow, shear-critical wall piers will result in a solid wall rather than individual piers.
- **Soften elements.** Shear-critical behavior caused by short concrete elements, such as columns or wall piers in systems with deep spandrel beams, can be mitigated by reducing the depth of the spandrels, thus making the vertical

elements taller or longer. Either the spandrels can be reduced or slots can be created at the ends to separate them from the vertical column elements. This strategy requires confirmation that the reduced spandrel beams have sufficient capacity to resist gravity loads. The overall lateral strength and stiffness of the resulting structure should be checked to confirm adequacy.

3.3.4 Load-Path Continuity

Localized gaps in the lateral load path (e.g., those at the interface between diaphragms and vertical elements of the lateral system, or at the interface with foundation elements) can lead to building collapse. There are also other examples of load path deficiencies. In some buildings, shear walls in upper stories are discontinuous at the lower story because of entrance and exit openings. Other buildings may have solid walls at rear property lines adjacent to other buildings and extensive window openings or curtain walls at street sides for natural light and view. Barring other significant deficiencies, localized mitigation of these load path deficiencies can be effective in reducing the risk of collapse. Some examples of specific load-path deficiencies and mitigation measures follow:

- **Collector connections to shear walls.** Where the shear walls in a building have little or no direct connection to the floor and roof diaphragms (for example, at exterior stairwells or other building appendages), a serious load path discontinuity can exist if collector elements are not provided. Mitigation strategies include adding collector elements to provide interconnection or providing additional lateral elements elsewhere in the building.
- **Lateral element connections to foundations.** Especially in buildings with deep foundations and significant overturning or uplift demands, lack of adequate interconnection at the foundation can lead to an elevated risk of collapse. Improving the connection with foundation elements can be difficult and extremely intrusive, so providing additional lateral elements could be a more economical strategy.
- **Locally stiffen shear-critical elements.** Provide localized strengthening to mitigate shear-critical or missing load path elements.

3.3.5 Axial Load in Vertical Elements

Failures in columns and slender walls subject to high axial loads have been significant factors in building collapse. As with previously discussed deficiencies, mitigation of the collapse risk of vertical elements could be either local or global in nature. Examples of such mitigation strategies include:

- **Add capacity or confinement.** Added axial strength and/or confinement using concrete encasement, fiber reinforced polymers (FRP), or steel jacketing can improve the behavior of high axial load elements.
- **Add lateral elements.** Instead of increasing strength, adding shear walls or braced frames to globally stiffen and strengthen a building can reduce the axial demand. Note that this strategy is less effective when high axial stress due to gravity loads is a significant factor in the expected behavior of these elements.

3.3.6 Overall System Strength

Reinforced concrete buildings with an overall lack of adequate lateral strength can suffer collapse, though it is not always clear whether the relative lateral weakness is the primary cause or a secondary effect exacerbating other deficiencies. It does seem reasonable, however, to assume that at some minimum ratio of lateral strength to seismic demand, the risk of collapse becomes significant, especially for brittle systems and elements. Mitigation strategies for this condition are similar to measures commonly used for seismic retrofits for a range of performance levels. They include:

- **Addition of lateral elements.** Improve the overall lateral strength with the addition of shear walls or braced frames.
- **Mass reduction.** Reduce seismic demands by altering the building (for example, by removing a story).
- **Seismic isolation and supplemental damping.** Reduce seismic demands by adding seismic isolation or supplemental damping to the building. These measures can be effective in reducing the risk of collapse in relatively weak buildings, but they can be very intrusive and costly to implement.

Chapter 4

Summary of Modeling Techniques for Collapse Assessment of Concrete Buildings

Reliable collapse assessment of reinforced concrete buildings requires the selection of appropriate nonlinear component and simulation models, assessment criteria, ground motions, and the use of robust and accurate modeling software. This chapter focuses on modeling techniques appropriate for the collapse simulation studies identifying collapse indicators (as observed in case studies in Chapter 2). These studies will involve Monte Carlo simulations of building prototypes up to the stage of collapse; therefore, they require nonlinear models that are computationally efficient yet capable of reasonably representing critical failure modes, including loss of gravity load support for nonductile concrete components.

To solicit input from the research community on this challenging and rapidly evolving discipline, thirty-three earthquake engineering specialists, including experts in simulation of reinforced concrete structures under significant loading causing nonlinear response and in earthquake ground motion selection, were invited to a Collapse Simulation Workshop held in San Francisco, on January 17-18, 2013 (see Appendix A). Participants in the Workshop reviewed the findings of the NEES Grand Challenge project on nonductile concrete buildings and other relevant research on existing nonlinear analysis models for collapse simulation of reinforced concrete buildings. The Workshop discussions addressed component models and assessment criteria for concrete columns, beam-column joints, walls, slab-column connections, and other components deemed critical to the results of collapse simulations within the context of the methodology for identification of collapse indicators. Procedures proposed for the selection of appropriate ground motions, including consideration of duration and spectral shape, in collapse simulation studies, were also discussed.

This chapter provides a summary of recommendations for collapse modeling of reinforced concrete buildings based on the discussions at this Workshop, with an emphasis on models appropriate for collapse indicator studies where Monte Carlo simulations are performed for prototype buildings with varying characteristics. Since collapse simulation is a rapidly evolving field, the recommendations are accompanied by future research needs, including short- and long-term objectives, to achieve improved collapse modeling techniques for reinforced concrete buildings. Six

technical papers prepared for the Workshop are included in Appendices B through G. The Workshop papers provide more details on the recommendations summarized below, although the recommendations in those papers may not be in full agreement, since the descriptions provided in this chapter reflect the consensus of the Workshop participants, while the Workshop papers reflect only their authors' opinions.

4.1 Columns

Building collapse is frequently precipitated by shear and axial load failure of columns; hence, modeling such failures is critical to the utility of collapse indicator studies. Furthermore, since collapse indicator parameters are varied over a wide range during these studies (see Chapter 2), models must be able to capture transitions between modes of response (i.e., transition between flexure, flexure-shear, and shear-controlled response, without significant step functions in predicted behavior). For current applications, the modeling approach adopted in the ATC-78-1 project (ATC, 2012) is recommended (see Figure 4-1). Use the Haselton, et al. (2008) lumped plasticity model for columns with $V_p/V_n \leq 0.6$ (flexure response, Figure 4.1a) and use the Elwood (2004) model for columns with $V_p/V_n \geq 0.8$ (shear or flexure-shear response, Figure 4.1b). V_p/V_n is the ratio of column strength, controlled by flexure

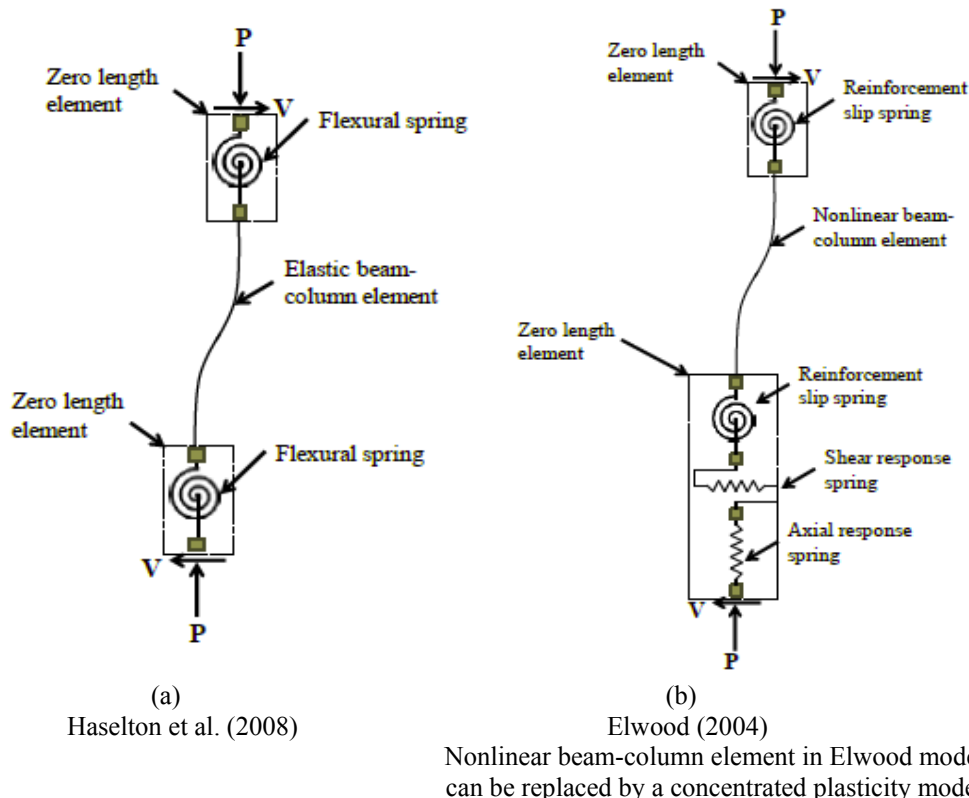


Figure 4-1 Recommended column models: (a) Haselton et al. (2008) for $V_p/V_n \leq 0.6$, (b) Elwood (2004) for $V_p/V_n \geq 0.8$. V_p/V_n is the ratio of column strength, controlled by flexure (plastic shear demand at flexure yielding), to column shear capacity.

(plastic shear demand at flexure yielding) to column shear capacity. It is assumed that a linear interpolation between the two limits of $V_p/V_n = 0.6$ and $V_p/V_n = 0.8$ will provide a reasonable estimate of the transition in response between flexure and flexure-shear behavior.

Models to capture axial load failure (Elwood, 2004) should only be included in the flexure-shear and shear-dominated columns, since this model assumes the development of the diagonal (shear) failure plane.

Newer column models proposed by LeBorgne and Ghannoum (2013) and Baradaran Shoraka and Elwood (2013) may provide improved response prediction over Elwood (2004) for columns without doubly symmetric loading. However, these models have seen limited calibration and use to date, and thus are not currently recommended for collapse indicator studies. Baradaran Shoraka and Elwood (2013) capture flexural failures in addition to flexure-shear and shear failures, thus eliminating the need to transition between element types as V_p/V_n changes, but this capability requires further calibration.

4.1.1 Future Research

Short-term benchmark studies will significantly improve confidence in available column models. For example, the models described above will benefit from further validation with test data, particularly through comparison with shake table tests where columns are subjected to realistic asymmetric loading cycles (see Section 4.5.1). Furthermore, the use of the column models noted above (for the analysis of case-study buildings) will help to identify any potential shortcomings in these models before embarking on collapse indicator studies.

The emphasis on concentrated plasticity elements in Haselton et al. (2008) does not account for the influence of axial load variation (for example, due to overturning demands or vertical ground motion) on the lateral response. While this is clearly a simplification of the true behavior, it is not known if axial load variation has a notable impact on collapse estimates. Short-term studies, requiring less than six months, should be initiated to investigate this phenomenon. These studies will help identify if fiber elements are truly preferred over concentrated plasticity elements for collapse simulation.

Furthermore, column models described above do not account for the presence of short lap splices with poor confinement, a common deficiency in older concrete columns. Column models developed for this purpose (Chowdhury and Orakcal, 2012) have generally seen limited calibration to date. A medium-term research effort (roughly six months to a year to complete) is required to investigate how such models can be used with the preferred column models described above, in order to calibrate these findings with available test data (Melek and Wallace, 2004).

A longer-term research effort (roughly one to two years) is needed to develop and validate a column model that can capture all essential failure modes described above (i.e., flexure, flexure-shear, shear, splice, and axial failures) without the need to change computer modeling finite element types. While such an element is undoubtedly desirable, it is not essential, and collapse simulation studies should proceed even without this all-in-one solution.

4.2 Beam-Column Joints

Beam-column joints should be accurately (comprehensively) modeled to achieve reliable results in collapse simulations of concrete frames. The recommended model, balancing the desire for accuracy and computational efficiency needed for Monte Carlo simulations, is a rotational spring with rigid offsets to define the joint area (see Figure 4-2). A zero-length fiber-type bar-slip section model may be added to the ends of the connecting beams for conditions with expected bar slippage. As shown in Figure 4-3, for three-dimensional (3D) frames, it is currently recommended to include two uncoupled rotational springs to represent the force-deformation response separately in the perpendicular directions.

The beam-column joint model needs to capture:

- Joint flexibility at low demand levels;
- Potential joint shear failure resulting in a rapid loss of lateral-load carrying capacity;
- Strength loss due to pullout of poorly anchored beam reinforcement; and
- Effects of accumulation of joint damage on inelastic deformation capacity of beams and columns.

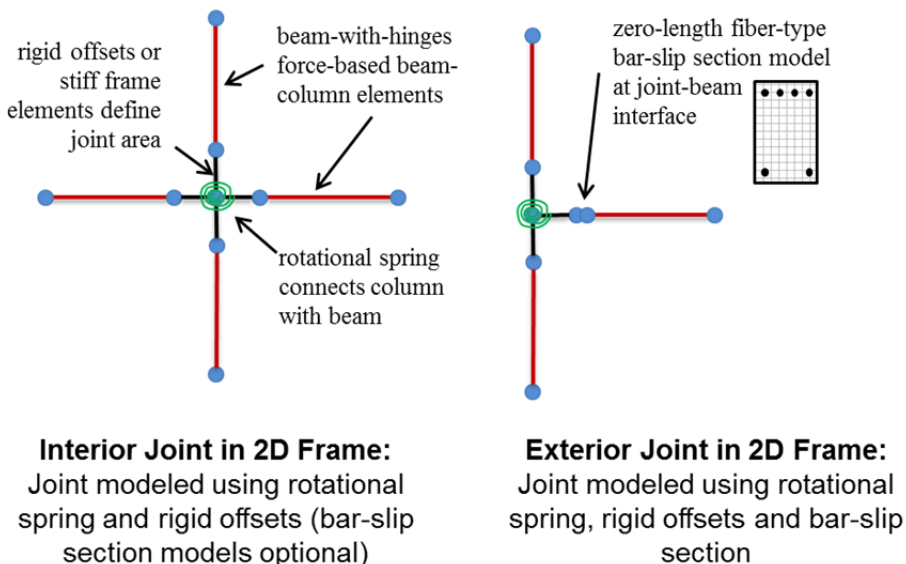
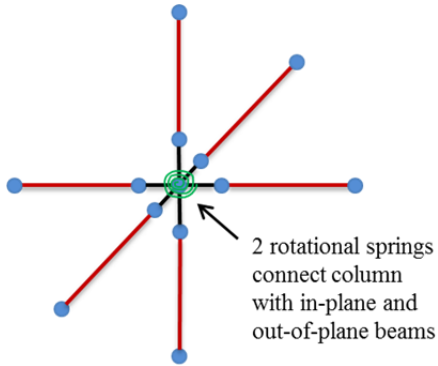


Figure 4-2 Recommended joint models in 2D frames



Interior Joint in 3D Frame:

Joint modeled using 2 rotational springs and rigid offsets (bar-slip section models optional)

Figure 4-3 Recommended joint model in 3D frames.

When using OpenSees (Mazzoni et al., 2009), the rotational springs should be defined using zero-length elements using the Pinching4 (OpenSees, 2013) material model. For all joints, it is recommended that the approach found in the Mitra and Lowes (2007) model be used to define cyclic response parameters for use with a Pinching4 material model. Various models are available in the literature for defining the moment-rotation backbone of the rotational spring. Considering the extent of calibration to joints typical of existing buildings (typically lacking joint transverse reinforcement) and the ease of implementation, the following combination of models are recommended:

For two-dimensional (2D) and 3D interior joints:

- use the method proposed by Kim and LaFave (2009) to define the response envelope to 10% strength loss; and
- use the method proposed by Anderson et al. (2008) to estimate the descending branch of envelope.

This combination is necessary since the method proposed by Kim and LaFave does not include significant strength degradation that is necessary for collapse simulations. It should be recognized that the Kim and LaFave (2009) envelope was calibrated using joint shear stress versus strain data, rather than full joint assembly response. Future work should validate the proposed models using full subassembly test data and typical models for beams and columns. For 2D interior joints, a backbone model by Birely et al. (2012), already calibrated using subassembly load-displacement data and an OpenSees model such as that shown in Figure 4-2, could be used as an alternative to the method proposed by Kim and LaFave.

For 2D exterior joints, use of the method proposed by Sharma et al. (2011) is recommended to define the moment-rotation envelope to the response history.

For corner joints, use of the Hassan (2011) model to define the backbone of the rotational spring is recommended. Despite failures of corner joints noted in earthquake reconnaissance, there is a limited amount of data for corner joints subjected to loading from both orthogonal framing directions.

Current models do not address loss of joint axial load carrying capacity, but this is considered adequate for current purposes. There is little evidence of global building collapse or loss of gravity support directly caused by joint failure. Recent laboratory tests indicate that beam-column subassemblies typically maintain axial load capacity following significant loss of joint shear capacity (Hassan, 2011).

4.2.1 Future Research

The recommendations noted above represent the consensus of the Workshop participants; however, it is recommended that calibration of the combined models using data from recent beam-column joint tests be performed (Lehman et al., 2004; Hassan, 2011).

Limited data is available on the performance of three-dimensional joints, particularly corner joints subjected to bidirectional loading. Furthermore, data is lacking for joints with eccentric beams, even though this configuration is relatively common in existing reinforced concrete buildings. Future experimental testing should focus on the seismic performance of these joint configurations, including the deformation capacity corresponding to axial load of the columns.

4.3 Masonry Infilled Concrete Frames

To assist in providing recommendations for modeling collapse-vulnerable infilled frames, it is useful to first consider the specific characteristics of infill frames that would make them more or less likely to collapse when subjected to strong ground shaking.

Collapse is defined as the loss of vertical support of the concrete frame for one or more stories. For the purposes of this project, failure of the infill that does not result in failure of the concrete frame does not constitute collapse. In addition, if the frame suffers a loss of gravity load-carrying capacity but the infill itself is still capable of providing adequate vertical support for gravity loads, this is not defined as collapse.

Collapse of infill frames can often be attributed to the following behavior:

- Damage of masonry infill walls due to in-plane seismic loading;

- Shear failures in columns or beam-column joints caused by frame-infill interaction under in-plane loading;
- Collapse of damaged infill walls due to shaking and/or out-of-plane loads; and
- Loss of column axial load capacity due to large story drifts.

The collapse behaviors and responses listed above are more likely in infill frames with certain properties. Figure 4-4 summarizes the likelihood of collapse of infill frames given the causes and sequence of collapse risk discussed above. Initial collapse simulation modeling efforts should be focused on infill frames most vulnerable to collapse (as indicated in Figure 4-4).

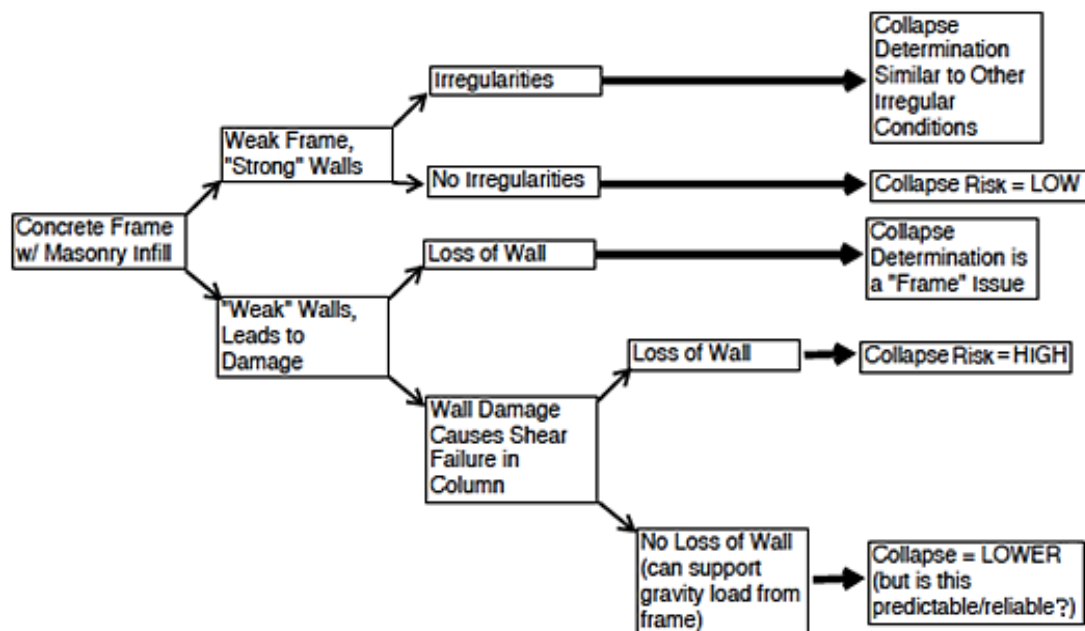


Figure 4-4 Schematic illustration of infill frame behavior and relative collapse risk.

This assessment also points to possible collapse indicator parameters to be considered as specific to infill frames:

- Number or gross area of infill walls/bays;
- Height-to-thickness ratio of infills (as a measure to predict possible wall failure);
- Relative lateral strength of the infill and frame; and
- Relative stiffness of infill and frame.

Infill frame models for collapse simulation need to be able to simulate column failures, cracking and compression failures in masonry infill, and failure of the infill either in-plane or out-of-plane. For Monte Carlo simulations, such behaviors are best represented by phenomenological models using diagonal struts, such as those conceptually illustrated in Figure 4-5. This model consists of beam-column elements representing the frame and one or two diagonal struts representing the masonry infill.

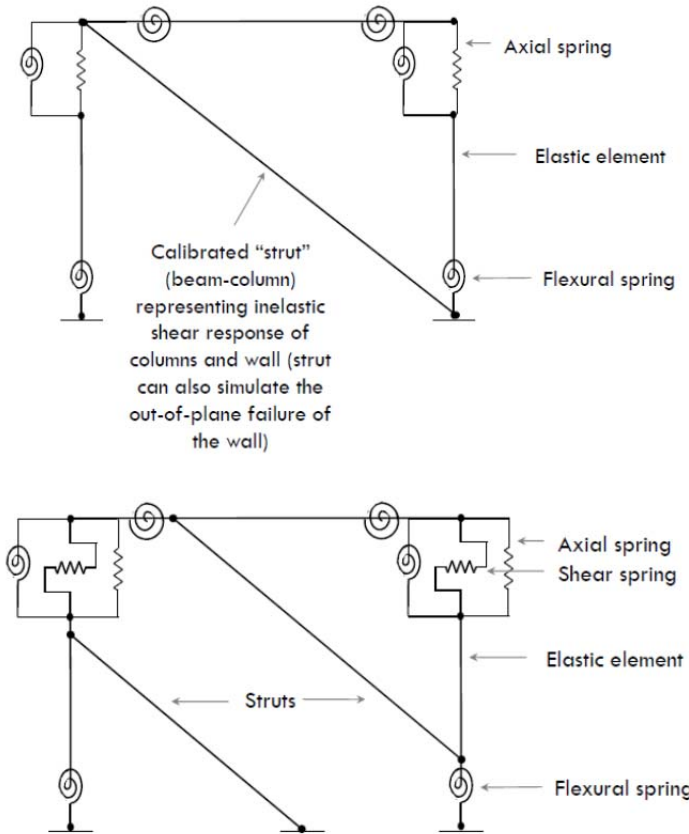


Figure 4-5 Simplified analytical model for infill frame, with one diagonal (top figure) and two struts (bottom figure).

In the model with one strut, the strut has to be calibrated to include the behavior associated with both infill wall failure and column shear failure, both of which are impacted by wide variation in frame and masonry properties. For the model with two struts, the calibration is expected to be somewhat less difficult, since failure of the infill and the frame are modeled separately. The basic model type and configuration can be used for the various types of masonry units.

Because these models must represent complex interactions between concrete frames and the masonry infill, a critical aspect of modeling collapse is calibrating the simplified models. Finite element models (Stavridis and Shing, 2010) may be used for calibration considering the limited data from infill frame testing and the wide variety of infill frame configurations and unit types. The finite element models are useful to predict the load-displacement response up to a severe damage state (on the verge of collapse) without collapse itself. In lieu of model calibration, strut properties may be established based on empirical rules previously established by test data and finite element models. Stavridis (2009) has established such rules for one class of infill frames. These guidelines need to be expanded for different infill and frame properties.

Based on experimental evidence, a 70% to 80% drop of the lateral in-plane load capacity at any story can be considered a reasonable criterion for collapse of infill frames (see Appendix F for additional information).

To simulate the damage and possible collapse of an infill wall caused by out-of-plane loads, a diagonal strut can be modeled with two 3-D fiber-section beam-column elements, which can account for the out-of-plane bending and the arching mechanism developed in an infill wall (Kadysiewski and Mosalam, 2009).

4.3.1 Future Research

Recommendations for future research for infill frames are extensive due to the complex failure mechanisms and the wide range of factors influencing the collapse of infill frames. Recommendations include:

- Development of guidelines to calibrate strut models;
- Further development and experimental verifications in modeling in-plane and out-of-plane interaction of walls;
- Studies to validate the collapse criteria for detecting collapse of infill frames in collapse simulations;
- Better calibration of strut models and enhanced finite element models to simulate the full collapse of infill walls, including out-of-plane failures; and
- Acquisition of more experimental data on collapse.

All of these recommendations are likely to involve medium- or long-term effort and need to be coordinated in a more comprehensive plan to better identify, model, and calibrate the various behaviors that can lead to collapse in masonry infill frame structures.

4.4 Walls

Reinforced concrete wall systems in existing buildings have the potential for loss of lateral load carrying capacity; this loss will place large deformation demands on the gravity system and will lead to increased collapse potential. While the loss of axial load capacity in walls is possible, particularly for lightly reinforced squat walls responding in shear, it is recommended that axial load failure of walls should not be considered at the present time. The following recommendations focus on modeling the lateral load response of reinforced concrete walls in order to adequately predict displacement demands on the gravity system.

Recommendations for the modeling of reinforced concrete walls depend on the primary mode of response: flexural deformations, or shear deformations, or as transition walls with a combination of flexural and shear deformations. Walls may be approximately categorized into these response bins based on their shear span-to-

length ratio: greater than 1.5 for flexure, less than 1.0 for shear, and all others considered transition walls.

Beam-column elements with fiber-discretized cross-sections are recommended for modeling walls responding primarily in flexure. Such models are preferred because of their ability to capture varying stiffness up the height of the wall with changes in loading and axial-moment interaction (this is particularly important for coupled walls). Displacement-based fiber elements are generally preferred over force-based elements for Monte Carlo simulations, due to their simpler implementation and generally better convergence performance. Force-based elements require calibration of the softening branch of the concrete stress-strain relationship used for concrete fibers to avoid localization of curvatures at one section at large displacement demands. Displacement-based elements will only capture a linear variation of curvatures over the length of a wall element, but this is generally an appropriate approximation for walls responding in flexure.

Capturing bar buckling is also critical to simulating loss of lateral load capacity in walls responding in flexure. While identification of the initiation of bar buckling may be possible by post-processing analysis results, such an approach will lead to conservative assessments of building collapse if analysis is considered unreliable and ignored after buckling is initiated. Bar buckling can be incorporated in the reinforcement fiber stress-strain relationship, but such an approach has seen limited calibration with test data and requires further validation (see future research in Section 4.4.1).

Models with shear springs in series with a stiff flexural element, similar to those recommended for columns (Section 4.1), are recommended for walls responding primarily in shear. The strength and deformation capacity of such walls are controlled by shear failure and are sensitive to axial loads. The backbone for the shear spring should be adjusted based on the axial load due to gravity. ASCE/SEI 41-13 (ASCE, 2013) provides a conservative estimate of this shear response backbone. Such elements may be vulnerable to axial load failure after shear failure; however, as noted previously, the calibration of models for depicting gravity load failures of shear-controlled walls still requires further development (see future research in Section 4.4.1).

Less research has been conducted on transition walls where the initial response is governed by flexural deformations, but strength loss is generally influenced by shear demands. It is recommended that transition walls be modeled in a manner similar to flexure-shear columns (Elwood, 2004), where a shear spring is included in-series with the fiber-element model recommended for flexure-controlled walls. The backbone for the shear spring should be modified to include more shear deformation and loss of shear strength at a critical deformation demand. The critical deformation

demand may be defined based on the curvature ductility demand, as shown in Figure 4-6; however, if curvature ductility is used it is necessary to ensure that the curvatures from the analysis are consistent with the average curvature measurements from the test data used to develop the failure model.

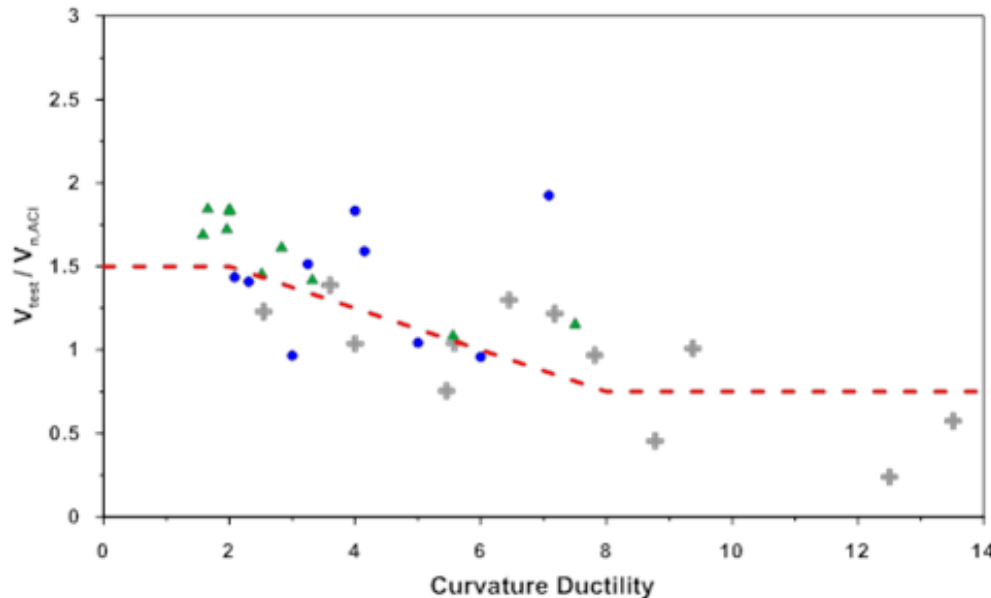


Figure 4-6 Model for shear strength degradation versus curvature ductility (Yang et al., 2012).

4.4.1 Future Research for Walls

Significant research is required to improve the efficacy of wall modeling and the predicted displacement demands on the gravity system required for reliable collapse simulations. Among the research needs, the most important is further calibration of available models with test data. In particular, bar buckling, shear response of transition walls, splice models, and sliding shear models require further calibrations using wall tests. While constitutive relationships for reinforcement fibers capable of capturing bar buckling during analysis have been proposed and implemented in OpenSees (Mazzoni et al., 2009), these have generally seen limited calibration. The shear response of transition walls and the selection of the most appropriate failure criteria require further development and calibration. For existing walls it is particularly important to develop and calibrate models capturing strength loss due to short lap splice lengths, a failure mode that has been given limited attention to date in wall modeling. While short lap splice lengths in reinforced concrete with adequate confinement may be better, in older buildings adequate confinement was not required by code, nor was it provided. Integration of sliding shear models with the modeling techniques described above must also be considered. All these calibration and model development activities are considered medium-term efforts.

Long-term research needs include further consideration of axial failure of lightly reinforced walls. In addition to axial failure of shear-critical walls noted above, through-thickness failure of thin walls with a single layer of reinforcement represents a potentially critical failure mode not generally considered in past research. Such a failure can lead to loss of axial load capacity in the compression zone of the wall, large displacement demands, and potential collapse of the wall system. Experimental testing is required to address this gap in knowledge and enable model development for collapse simulation.

Given the importance of adequately predicting the displacement demands on the gravity system for collapse simulation of wall buildings, the limited amount of shake table test data on wall systems, particularly those typical of older reinforced concrete construction, represents a significant limitation on the validation of wall models.

For collapse indicator studies on wall buildings, a broad range of selected wall characteristics (e.g., shear to flexural strength ratio) should be used to determine the variation in collapse probability associated with changes in the collapse indicator parameter. This will lead to a range of expected failure modes of response and consequent changes in the element model types required above. Research will need to address expected transitions in response prediction ranges as the wall element models and the failure modes of response change (i.e., to address the transition of when a flexure-controlled wall becomes a transition wall and when a transition wall becomes a shear-controlled wall).

4.5 Load-history Effects

The capacity and response of reinforced concrete elements during strong ground shaking can be influenced by the number and symmetry of loading cycles and the direction and rate of loading. Despite this well-established conclusion, determining the extent to which the concrete elements are influenced by load-history effects is challenging, given current models and limited test data exploring the influence of load-history. It is thus recommended that component models not be selected based on the models' ability to capture load history effects; for collapse simulations, load-history effects should generally be a secondary consideration in the selection of preferred models.

Despite the above caution, however, it is important for the analyst to appreciate how load-history effects may influence the validity of collapse simulation results. The discussion below focuses on the following aspects of load history:

- Number of loading cycles;
- Symmetry or asymmetry of loading cycles;
- Direction of loading (i.e., uniaxial vs. biaxial); and

- Rate of loading.

Number of loading cycles. Several experimental studies (Ranf et al., 2006; Takemura and Kawashima, 1997) have shown that increasing the number of cycles typically does not influence the element strength, but it can result in a decrease in the drift at lateral strength degradation. It is important to note two important considerations regarding this observation. First, the number of cycles imposed at large drift levels in most of the studies referenced above frequently exceeded the number of large drift cycles expected for structural components, even during a long duration earthquake. Furthermore, typical loading protocols used in cyclic tests with two or three loading cycles per drift level may already impose more displacement cycles than expected in typical ground motions. Second, lightly loaded shear-critical columns may not be strongly influenced by the number of cycles of loading experienced prior to shear failure, as long as the load cycles do not cause significant flexural degradation. With these two considerations noted, current component models calibrated to typical cyclic tests likely already reflect some degree of reduced drift capacity due to the cyclic loading effects; consequently, further reduction in drift capacity for this aspect of load history may be unwarranted.

Symmetry or asymmetry of loading cycles. Models that capture cyclic deterioration, such as the Ibarra, Medina, and Krawinkler (2005) lumped plasticity model, are typically calibrated using experiments subjected to symmetric loading protocols. Nonetheless, such models will be used to predict collapse under highly asymmetric earthquake loading, as illustrated in Figure 4-7. It is unclear if the cyclic deterioration should be the same for both symmetric and asymmetric loading cases. Some further thought is warranted to determine the reliability of these models to predict cyclic behavior under asymmetric loading.

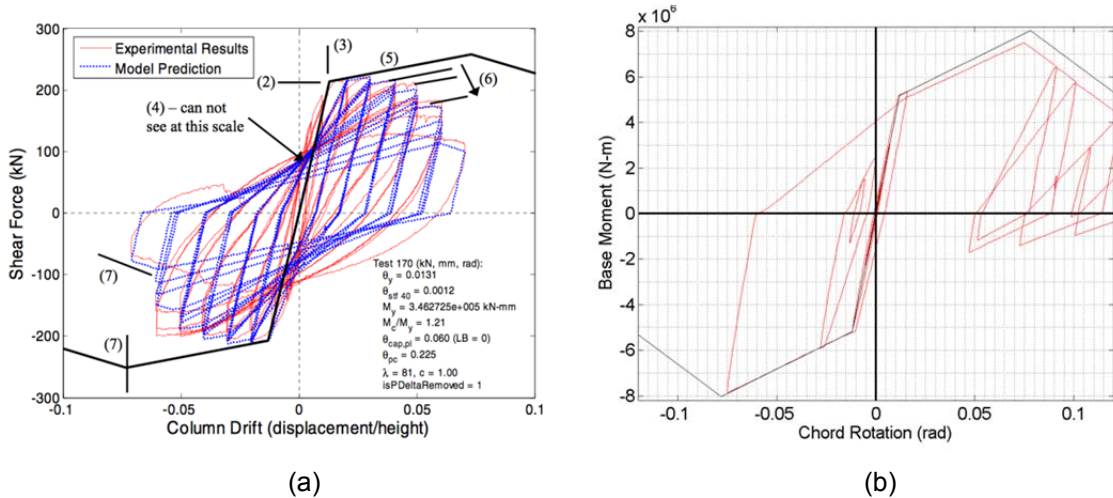


Figure 4-7 Haselton et al. (2008) lumped plasticity model: (a) calibration from symmetric loading of a test specimen (numbers in parentheses denote steps in the calibration process); (b) prediction of the model under ground-motion excitation.

Direction of loading. Two-dimensional models may underestimate column axial loads and corner joint demands. Furthermore, Henkhaus (2010) demonstrated that shear-critical columns loaded uniaxially have larger drift ratios at shear and axial failure than those loaded biaxially. These impacts could be considered, for example, by adjusting the drift capacities of components where three-dimensional demands are expected to be significant. The Workshop paper by Pujol (see Appendix E) suggests that this difference in uniaxial versus biaxial loading can be reasonably captured by reducing the drift capacity at axial load failure by a factor of two. Limited data exists to evaluate the influence of direction of loading on joint or wall behavior.

Rate of loading. Post-earthquake reconnaissance has revealed fracture of reinforcement (e.g., Elwood, 2013), potentially resulting from rapid impulsive loading or from brittle characteristics of reinforcement with high quantities of carbon content. This phenomenon could influence building behavior, but it may not be captured by current component models, which are generally not calibrated using tests with impulsive loading. On the other hand, it is well known that an increase in the rate of loading will typically lead to higher flexural strengths due to strain-rate effects. Further study to better understand this issue would be beneficial.

4.5.1 Future Research

Short-term research would help address the challenges of load-history effects described above, significantly benefiting collapse assessment studies going forward. This research would include the development of alternate ground motion suites for assessments. Supplementing the FEMA P-695 (FEMA, 2009c) ground-motion suite with a long-duration suite, or a directivity suite, for example, would provide additional insights into building behavior under a wider range of conditions, even if the additional ground motions were used only in limited cases.

Medium-term research, would include the validation of currently available models against atypical loading protocols, including asymmetric load cycles and high loading rates, to determine if adjustments to existing models are necessary to account for such load histories. Ideally, to capture the appropriate loading rate and cyclic demands, existing models should be validated for dynamic response prediction using shake table tests. A database of shake table tests of columns is available for this purpose (Li, 2012).

Additional medium-term research could include calibration studies to determine how to incorporate 3D behavior effects in 2D models of buildings. Two types of tests are envisioned. First, 2D models could be run with and without adjustments to column and joint behavior to reflect anticipated 3D behavior in order to determine what effect these adjustments have on collapse capacity. Second, a few buildings could be

modeled with 2D and 3D models to aid in calibrating the adjustments to be used in 2D models.

Longer-term research, would include improvement of cyclic deterioration effects considered in current component models. For example, the Elwood (2004) column model does not predict deterioration under repeated cycles to the same peak displacement; whether this deterioration should be incorporated needs to be evaluated. The lumped plasticity model developed by Ibarra, Medina, and Krawinkler (2005) and calibrated by Haselton et al. (2008) predicts cyclic deterioration via a single parameter, which may not be sufficient.

An important final effort to evaluate the importance of load-history effects on the building system performance would be the careful evaluation of case-study buildings from past earthquakes (see case studies in Chapter 2) to determine if load-history effects may have played a role in such failures. This evaluation may involve developing models with and without consideration of load-history effects and examining discrepancies between the observed and calculated performance. Identifying discrepancies would lead to improved understanding of collapse phenomena and the physics that should be incorporated into component models.

4.6 Gravity Load Failures in Collapse Simulation

While the collapse of ductile systems may be governed by sidesway collapse modes, existing older reinforced concrete buildings are expected to exhibit brittle failure modes, compromising the ability to maintain gravity load support prior to the development of a sidesway collapse mechanism. Such collapse modes, often termed “gravity load collapse,” were observed in all collapsed case-study buildings reviewed in Chapter 3. Examples of critical gravity load failures include axial-load failure of columns and punching shear failure of slab-column connections without sufficient continuity steel. This section describes approaches for simulating gravity load failures and criteria for detecting gravity load collapse.

Two types of simulations are possible for gravity load failures: implicit and explicit simulations. Implicit simulations (sometimes referred to as non-simulated failure modes) involve post-processing the predicted response of the building to detect failures, while explicit simulations involve capturing the gravity load failure of the component during the analysis and changing the component model accordingly. Implicit simulation is appropriate for components whose collapse can be gauged by a simple demand measure, such as drift ratio; failure of the component does not significantly affect dynamic response of the building. An example is a slab-column gravity frame in an otherwise stiff building.

Explicit simulation should be employed where failure of the component is expected to influence the dynamic response of the building (e.g., column failure in a moment

frame). Explicit simulations may be classified into two approaches: element-removal, in which the component is removed once failure is detected (Talaat and Mosalam, 2009), and post-failure modeling, in which component failure is modeled through complete loss of gravity load support (Elwood, 2004). The element-removal approach is applicable to failure modes that tend to be sudden, such as failure of slender columns with high axial load. Post-failure modeling is more appropriate for buildings where gravity load support may not be lost as quickly, such as buildings with shear walls or with pier-like columns. Collapse indicator studies to date (ATC, 2012) have only applied the post-failure modeling approach, but they frequently run across convergence challenges when trying to track the post-failure response of the component. Limited studies have been performed using the element-removal approach (Mosalam et al., 2009); however, while limited, results to date suggest that element removal may lead to fewer convergence problems.

The selection of implicit versus explicit simulation of gravity load failures should also depend on the gravity load transfer mechanisms present in the building. Implicit simulation is likely sufficient for buildings with limited capability to transfer gravity loads after failure of a gravity load supporting component. This may result in a conservative assessment of the collapse capacity; however, this may be appropriate since, as demonstrated in Chapter 2, limited capacity for gravity load redistribution was found to be a common characteristic of collapsed reinforced concrete buildings in past earthquakes.

4.6.1 Future Research

While all three approaches described above (implicit simulation, element removal, and post-failure modeling) are possible using OpenSees, there have been no comparisons of the collapse prediction results of analyses between these three approaches. Such a comparison for a range of building types would be a valuable medium-term research effort. Knowing the conditions in which one approach could be used over another may eliminate considerable effort in collapse simulations.

An assessment of the gravity load redistribution capability of typical floor systems (slab-beam, flat slab, waffle slab) would also assist in the selection of the appropriate simulation technique for gravity load failures. The assessment would involve the selection of archetypical floor systems, including varying reinforcement details (e.g., short bottom beam bar embedment), and large-displacement analysis for sudden loss of a single column. This is also likely a medium-term effort.

4.7 Ground Motion Selection

The selection of ground motions for assessment of collapse risk is important due to the high amplitude of shaking necessary to collapse many engineered structures. One way to quantify collapse risk is by using a fragility function specifying the

probability of collapse given a ground motion with amplitude measured by an Intensity Measure (IM) such as spectral acceleration at a given period. Fragility functions are often obtained by performing Incremental Dynamic Analysis (IDA) using a suite of ground motions, and counting the fraction of the ground motions

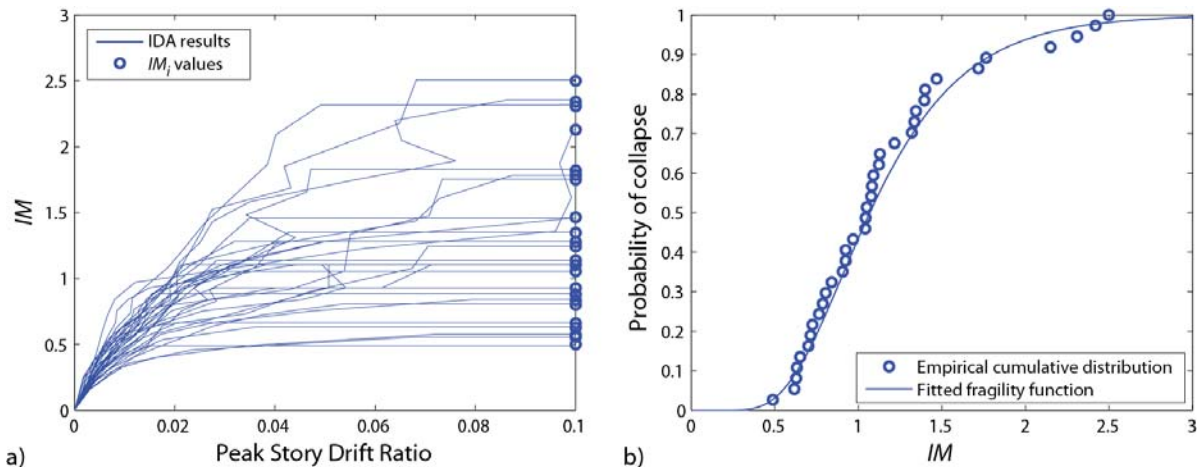


Figure 4-8 Incremental Dynamic Analysis results: (a) illustration; (b) Intensity Measure (IM_j) values at collapse, as observed from the Incremental Dynamic Analysis (IDA) results, and a collapse fragility function fitted to the data (Baker, 2013).

causing collapse at each IM level of interest, as illustrated in Figure 4-8. Within this procedure, there are two ways of viewing the role of ground motions, with differing implications regarding ground motion selection procedures.

From one perspective, ground motions can be viewed as “dynamic loading protocols.” That is, the ground motions are a single re-used “standardized” set of loading conditions to which a structure is subjected, in order to investigate its response. Using consistent ground motion sets simplifies the assessment procedure, since a single set of ground motions can be used in all analysis cases, saving the effort of selecting new ground motions and potentially facilitating “fair” comparisons of collapse capacity across building classes and locations (though, as discussed below, this may not actually be fair in some cases). There are a number of such standardized sets available today (Somerville et al., 1997; Krawinkler et al., 2003; FEMA, 2009c; Baker et al., 2011). These sets are popular because they reduce analysis effort and are useful for cases where a number of building types are being studied or where there is no specific site of interest. The problem with generic ground motions, however, is that they lead to a building being considered equally safe whether it is located in New Madrid, Seattle or Los Angeles, if those sites had similar hazard levels (defined with regard to the Intensity Measure used to specify the collapse fragility). The question is whether the differences in the other properties of strong-ground shaking at those varying locations need more careful consideration.

From an alternate perspective, the ground motions can be viewed as representations of what future ground motions might look like at the site of interest and with the IM level of interest. From this perspective, the ground motions for a given analysis should be representative of the ground motions a specific building may actually undergo. For example, near-fault sites are more likely to experience ground motions with short durations and large velocity pulses; sites in subduction regions, conversely, are more likely to experience long-duration shaking. Likewise, sites with stiff versus soft near-surface materials will experience different types of shaking. Furthermore, low-amplitude ground motions generally have different properties than high-amplitude motions, and so unique motions should be used at each intensity level of interest. Such an analysis is sometimes referred to as Multiple Stripe Analysis. The use of such an approach will make the analysis results more predictive of building behavior at that site. The drawback is that it requires site-specific motions to be selected for each analysis case and requires more information about the site. Nonetheless, the impact of these ground-motion properties on collapse capacity is large enough that it can significantly affect the resulting predictions of collapse risk. For example, Haselton et al. (2011) found a change of a factor of 23 in the predicted collapse rate of an 8-story reinforced concrete frame building in Los Angeles when the spectral shape was based on site-specific analysis, as opposed to when generic ground motions were used. Similarly, Raghunandan and Liel (2013) predicted a 40% decrease in median collapse capacity for a modern concrete frame located in Seattle versus San Francisco, due to the longer duration of shaking expected for intense ground motions in Seattle. Recognizing the impact of these issues, a number of codes and guidelines for assessment of individual structures recommend that some or all of the above properties be considered when selecting ground motions for structural assessment (see NIST, 2011a for a summary of guidance).

Site-specific ground motion issues may matter less for collapse screening procedures where the goal is to obtain a *relative* ranking of collapse risk for a population of buildings with similar seismic hazard, such as all nonductile reinforced concrete buildings in the Los Angeles region (Anagnos et al., 2008). However, site-specific motions may still be important to consider even in these cases. For example, some buildings could be susceptible to short-duration pulses, while in others, weaknesses may arise under high numbers of loading cycles in a long-duration earthquake. If that is the case, using ground motions unrepresentative of motions at a given site may preferentially trigger certain failure mechanisms while hiding others, leading to incorrect relative rankings of building types with differing deficiencies. This example is hypothetical, but its possibility should be considered when using generic ground motions.

When considering treatment of ground motions for general collapse assessment procedures, an option that bridges the two approaches above is to use generic ground

motions for structural analysis but modify the resulting collapse capacities after the fact to reflect anticipated impacts of ground motion properties at a specific site of interest. This creates the benefit of avoiding the effort of site-specific ground motion selection, but at the cost of relying on approximate corrections to account for effects that could be captured directly via a refined treatment of ground motions. This approach was developed in the FEMA P-695 project to account for the anticipated effect of variation in spectral shape from one location to another (Haselton et al., 2011), and was termed a “Spectral Shape Adjustment Factor.” That model, however, includes no adjustments for duration, site conditions, or directivity, and was calibrated only for frame structures. Development of a more general model of this type may be useful to facilitate collapse risk screening procedures.

There is no single approach for treatment of ground motions in all analysis circumstances. Development of consensus regarding appropriate approaches in specific circumstances will depend upon articulation of the objectives of collapse assessment methodologies. Progress will also depend on further research to quantify the impact of various ground motion properties on collapse risk across a range of seismic environments and for a range of building types.

4.7.1 Future Research

While there are mechanics-based reasons to believe that certain collapse indicators might indicate susceptibility, e.g., to pulse-like or long-duration ground motions, there is not yet empirical evidence that such susceptibility exists and is being captured by current modeling techniques. Research to perform collapse simulation of reinforced concrete buildings under varying ground motion types would help to resolve this issue. The findings would quantify the importance of considering the ground motion issues raised above and would also inform decisions regarding load-history effects discussed earlier.

Further development of a general model like the “Spectral Shape Adjustment Factor” developed in FEMA P-695, extended to adjust for other ground motion properties, would facilitate the use of general ground-motion sets for collapse studies while enabling the collapse indicator results to be tailored for the specific site of interest.

4.8 Summary and Cross-Cutting Themes

Collapse simulation of reinforced concrete buildings is a very challenging and rapidly evolving field, particularly when applied to Monte Carlo simulations to investigate the influence of changes to specific building characteristics as proposed in the NIST *Program Plan* (NIST, 2010b). This chapter has offered some recommendations for modeling concrete components and selection of ground motions, largely based on input from experts during a two-day workshop in January 2013. Although the focus

was on identification of current capabilities for collapse simulation, the evolving nature of the topic area also led to the identification of important research topics for improvement of collapse simulation in the near future. A summary of the identified research topics, along with estimates of the effort (time) required to conduct the research, are provided in Table 4-1. The estimated effort for each research topic (right-most column) largely excludes the time required for proposal development, refinement, and review, contract coordination and management, if required, and research results documentation and publication. The estimates roughly correspond to the ranges specified in the above sections on future research, as follows: short term (less than 6 months); medium term (6 months to a year); and longer term (1 to 2 years).

The following important research needs, cutting across multiple topic areas discussed above, were also identified during the Workshop (see also Table 4-1):

- **Development of existing reinforced concrete building inventories.** The Workshop identified a strong need to develop inventories for existing reinforced concrete buildings in high and moderate seismic zones in the United States. Inventories would allow future research to focus on the most relevant modeling needs and future analytical studies to focus on building types of greatest risk exposure. Inventory efforts have been conducted in Los Angeles as part of the NEES Grand Challenge project and in other California municipalities by the Concrete Coalition. These projects have provided important estimates of the total number of pre-1980s reinforced concrete buildings and, where available, the structural systems of such buildings. Future efforts should build on these projects to identify common structural details pertinent to nonlinear modeling.
- **Case studies with real buildings.** The Workshop further recognized the importance of evaluating collapse simulation capabilities through comparisons of simulation results and the performance of real buildings in earthquakes. This may be initiated with the buildings described in Chapter 2.
- **Three-dimensional models.** Collapse involves a three-dimensional response of the building; however, the majority of collapse simulation studies (ATC, 2012; FEMA, 2009c) and shake table testing (Yavari et al., 2013) to date has focused on the response of two-dimensional frames. While challenges still remain in developing robust two-dimensional models for collapse simulation, investigation of the influence of three-dimensional response, including torsional demands and gravity load redistribution through a floor system, should be explored. It is noted that three-dimensional modeling can significantly increase the run-time for collapse simulations, a limitation that must be overcome in order to implement three-dimensional models in collapse indicator studies.

Table 4-1 Collapse Simulation Research Recommendations

Topic	Title	Estimated Effort
Columns	Comparison of models with shake table tests	Less than 6 months
Columns	Influence of axial load variation on column response	Less than 6 months
Columns	Development of column models, including lap splice behavior	6 months – 1 year
Columns	Column model for all failure modes	1 – 2 years
Beam-column joints	Calibration of proposed beam-column joint models	Less than 6 months
Beam-column joints	Testing of corner and eccentric joints	1 – 2 years
Infill frames	Guidelines to calibrate struts in simplified model	Less than 6 months
Infill frames	Improvement of finite element models for infill frames	6 month – 1 year
Infill frames	In-plane/out-of-plane interaction of infill walls	1 - 2 years
Infill frames	Collapse experiments on infill frames	1 - 2 years
Walls	Calibration of models for bar buckling with wall tests	6 months – 1 year
Walls	Calibration of models for shear response with wall tests	6 months – 1 year
Walls	Calibration of models for splices with wall tests	6 months – 1 year
Walls	Calibration of models for sliding shear with wall tests	6 months – 1 year
Walls	Transitions in response predictions for varying failure modes	6 months – 1 year
Walls	Axial failure of thin walls	1 – 2 years
Walls	Shake table tests on wall building systems	1 – 2 years
Load-history	Alternate ground motion suites with different load histories	Less than 6 months
Load-history	Comparison of models with alternate load histories and strain rates	6 months – 1 year
Load-history	Approximate 3D models	6 months – 1 year
Load-history	Improvement of cyclic deterioration effects	1 – 2 years
Gravity-load failures	Comparison of implicit, element-removal and post-failure modeling approaches	6 months – 1 year
Gravity-load failures	Gravity load redistribution for typical floor systems	6 months – 1 year
Cross-cutting	Development of existing reinforced concrete building inventories	Varies depending on extent and detail
Cross-cutting	Case studies with real buildings	6 months – 1 year for 2-3 case studies
Cross-cutting	Comparison of collapse criteria	6 months – 1 year
Cross-cutting	3D models for collapse simulation	1 – 2 years

Collapse criteria. The Workshop identified the need to compare different criteria currently used to detect building collapse in numerical simulations. Currently used criteria include shear failure of a single column (most conservative), a pre-selected percentage of columns experiencing shear failure, a pre-selected percentage drop in lateral load capacity, axial load failure of a percentage of columns at a story, and a story-by-story comparison of gravity load demands and column axial-load capacities (considering degradation in axial-load capacity with drift demand). These criteria can clearly result in a wide range of collapse predictions. A medium-term research effort where building systems are evaluated using the different collapse criteria, and differences in predicted response are identified, would greatly assist in selecting the preferred collapse criteria for future collapse simulation studies.

Chapter 5

Recommended Adjustments to the Program Plan

During the conduct of the project efforts to (1) identify, collect, and archive data on reinforced concrete buildings that collapsed wholly or partially as a result of earthquakes, as described in Chapter 2, and (2) evaluate and improve earthquake-collapse simulation modeling of reinforced concrete buildings, as discussed in Chapter 4, the project team collaborated with participants in a closely related FEMA-funded project investigating and prioritizing collapse indicators in older reinforced concrete buildings, as documented in the ATC-78-1 report (ATC, 2012). The FEMA-funded effort was initiated in part as a result of the recommendations in the NIST GCR 10-917-7 *Program Plan for the Development of Collapse Assessment and Mitigation Strategies for Existing Reinforced Concrete Buildings* (NIST, 2010b). The resulting synergy of the two projects benefited both efforts, and provided a more detailed understanding of the difficulties and complexities involved in identifying reliable collapse indicators in real buildings. These findings compelled a re-examination of the original *Program Plan* to determine accomplishments to date and to identify potential improvements. Those potential improvements are provided below in the form of recommended adjustments to the *Program Plan*.

5.1 Summary of Recommended Adjustments

- Coordination of work programs initiated by multiple stakeholders is critical to the success of the *Program Plan* and to address effectively the significant seismic risk posed by nonductile concrete buildings in the United States. It is recognized that the ongoing FEMA-funded effort by the Applied Technology Council to develop an efficient seismic assessment technique for nonductile concrete frame buildings (ATC-78 project series; see ATC, 2012) fulfills the goals of Phase 3 (development of design parameter collapse indicators) of the *Program Plan*.
- Participants in the Collapse Simulation Workshop recommended several studies that are expected to lead to improvements in modeling of concrete components for collapse simulations. Such studies may be undertaken during Phases 4 and 5 of the *Program Plan* (i.e., development of component acceptance criteria and modeling parameters). While these model improvements will clearly help ongoing numerical studies of structural systems (e.g., the ATC-78 project series), studies should not be halted while component models are refined. It is recommended that component models and acceptance criteria be developed

concurrently with ongoing system studies. The order of component model development should be selected based on current knowledge and needs for system studies. In particular, the building case studies (Chapter 2) should be used to identify the most important needs in terms of model development. The *Program Plan* had recommended the following order for development of the component modeling and acceptance criteria documents:

- Columns
- Beam-column joints
- Slab-column systems
- Walls
- Infill frames
- Rehabilitated components

This order is still appropriate, with the exception that modeling efforts on walls should be moved up to be concurrent with modeling efforts on columns and beam-column joints. This urgency for walls comes from recognizing that many of the buildings considered in the collapse case studies were influenced by wall behavior and that walls are commonly present, at least around elevators or stairs, in most existing buildings. This effort on existing walls will also be synergistic with the high priority placed on the seismic performance of walls in the NIST GCR 13-917-23 report development effort, *Development of NIST Measurement Science R&D Roadmap: Earthquake Risk Reduction in Buildings* (NIST, 2013a).

- Participants in the Collapse Simulation Workshop recommended the evaluation of different collapse criteria (i.e., how to detect collapse during analysis). Results from this evaluation are critical to estimations of probability of collapse from all collapse simulation studies. Such evaluation may involve the comparisons of results from different criteria to determine the variation in collapse predictions with different assumptions. This effort will also be important in indicating the extent of nonlinear response in component models needed to provide reliable estimates of performance. The evaluation of different collapse criteria should be informed by the observations from case-study buildings to ensure the selected criteria are consistent with collapse observations in the field. The evaluation of collapse criteria for collapse simulations should be undertaken as a task within Phase 2 of the *Program Plan* (development of response parameter collapse indicators).
- A key challenge identified in the Collapse Simulation Workshop was the lack of validation of three-dimensional models for collapse predictions. Challenges

include modeling the bidirectional response of critical components such as columns, capturing the torsional response of buildings at large inelastic displacement demands, and modeling the redistribution of gravity loads within a three-dimensional structure after component failures. Phase 2 of the *Program Plan* (development of response parameter collapse indicators) will need to identify limitations on current capabilities to model collapse in three-dimensional models and provide guidance for detailed modeling studies and collapse simulation done in engineering offices. These efforts will require the involvement of engineering practitioners.

- Participants in the Collapse Simulation Workshop also identified the strong need to understand the most common nonductile concrete building systems and components in order to focus model development on the most prevalent cases. Such an investigation should also include an assessment of common combinations of building characteristics influencing collapse behavior. The investigation of existing nonductile concrete building systems and components should be approached from a regional standpoint (considering large metropolitan areas in high seismic zones), with the realization that a full “inventory” of building characteristics may not be necessary (or even possible). The following approach may be considered as a refinement of the development of broadly applicable building prototypes envisioned in the original *Program Plan* (see Table 1-3, Task No. 1.2, Selection of building prototypes):
 - Use high-level inventories of buildings, such as those collected by the Concrete Coalition or the NEES Grand Challenge project, to describe the age and occupancy of buildings in a region.
 - Ask regional consultants to describe common building types and complex conditions (e.g. combination of deficiencies) found in such buildings. Use specific building examples to assist in the discussion, but do not document the details of such examples.
 - Ask regional consultants to develop a consensus on most common buildings of interest from a collapse vulnerability standpoint.
 - Extract typical examples of component details to assist with model development efforts.
- There is a critical need to provide advice to practitioners on the identification of the most collapse-prone buildings. Although the overall *Program Plan* will take several years to complete, guidance in the short-term is still needed. This guidance could take several forms, the first of which is underway:
 - ATC will produce a FEMA report, scheduled to be completed in 2014, on the assessment of nonductile concrete frames.

- A list of “very bad” building types from a collapse vulnerability standpoint should be released as they are identified. Importantly, it must be made clear that this listing does not mean other building types are not in the “very bad” category.
 - A Technical Brief (TechBrief) could be developed on the importance of the gravity load system in the collapse assessment of reinforced concrete buildings. This TechBrief could explain how to assess the deformation capacity and load redistribution capability of the gravity load system. Tools and methodologies from the progressive collapse discipline should be explored in developing guidance on the assessment of load redistribution capability of typical building systems.
 - Interim updates on progress related to collective work on the collapse assessment of reinforced concrete buildings may be useful for the engineering community. EERI, through the Concrete Coalition, could provide web updates as appropriate.
- The collapse indicator methodology proposed by the *Program Plan* to identify an efficient assessment technique and system-level acceptance criteria for nonlinear analysis was largely based on the results of sophisticated collapse simulation studies. In part based on the input from experts at the Collapse Simulation Workshop and the careful evaluation of case study buildings, it is now recognized that (1) more than sophisticated analysis methods are needed to address the goals of the *Program Plan*, and (2) work plans for future phases of the *Program Plan* must incorporate other sources of information and processes. In particular, an ongoing effort to understand the collapse and near-collapse performance of case-study reinforced concrete buildings should continue in parallel with all other phases of the *Program Plan*. The effort to develop a case-study database may leverage the collection of information on nonductile concrete buildings by the Concrete Coalition, although this will require careful review and interpretation of the current dataset. Review of the case-study buildings should be integrated with the modeling efforts to provide a “reality check” on the collapse simulation studies. Expert judgment from the team evaluating the case-study buildings will be a key component in addressing the likely collapse vulnerability of complex buildings outside the scope and capability of analysis studies.
- The case studies can also be used to test assessment techniques, simplified or detailed, proposed by projects stemming from the *Program Plan*; this should be performed for several case study buildings to avoid judging a proposed method based on a single data point.

- Detailed modeling of case study buildings may also provide insights on the capabilities of current models used in any collapse simulation studies and may identify challenges that must be addressed in future phases. However, it is recognized that such efforts can be expensive, with low return on investment.
- Although the *Program Plan* is focused on the collapse assessment of reinforced concrete buildings, the tasks that are completed will likely also provide insights on other damage levels (e.g., repairability). Such insights should be documented, but they are not the focus of the *Program Plan*.

Appendix A

Collapse Simulation Workshop

A.1 Objectives

This appendix describes the structure and organization of a two-day workshop that was convened in San Francisco on January 17-18, 2013, to solicit input from the research community on the collapse simulation of reinforced concrete buildings. The conduct of such a workshop was identified as an early task in the NIST GCR 10-917-7, *Program Plan for the Development of Collapse Assessment and Mitigation Strategies for Existing Reinforced Concrete Buildings*, (NIST, 2010b). The objective of the workshop was defined as:

Identification of appropriate nonlinear component and simulation models, assessment criteria, and ground motions for future collapse simulation studies conducted to identify collapse indicators.

It was envisioned that information obtained from this workshop could be used in subsequent collapse simulation studies to accelerate the identification of collapse indicators for nonductile concrete buildings before other research initiatives in the *Program Plan* were completed.

A.2 Description

The workshop was designed around a series of mini-papers, which are focused summaries of preferred modeling approaches addressing specific topics defined by the workshop organizing committee. Topics included results from the NEES Grand Challenge project on *Mitigation of Collapse Risks in Older Reinforced Concrete Buildings* and other relevant research related to analysis models, failure criteria, and ground motions for collapse simulation of reinforced concrete buildings. Because collapse simulation studies are expected to involve Monte Carlo simulations of building prototypes through collapse, information was focused on nonlinear models that are computationally efficient, yet capable of reasonably representing critical failure modes, including loss of gravity load support.

The workshop structure included plenary sessions and six breakout sessions over two days. The workshop agenda is presented in Figure A-1 and Figure A-2. Workshop attendees are identified in the list of Project Participants.



NEHRP Consultants Joint Venture



COLLAPSE SIMULATION WORKSHOP

January 17-18, 2013

Hotel Kabuki
1625 Post Street, San Francisco, California 94115
Phone: 415-922-3200

Agenda

January 17, 2013

9:00 am	Welcome and Introductory Comments	Rojahn
9:05 am	Overview of Workshop Objectives and NIST Program Plan	Elwood
9:25 am	Summary of Collapse Simulation Studies Conducted under FEMA-funded ATC-78/78-1 Projects, Identification and Mitigation of Seismic Hazards Posed by Non-Ductile Concrete Buildings (FEMA Task Order 1111) <ul style="list-style-type: none">• Overview of Collapse Indicator Methodology (20 minutes)• Example Application of Collapse Indicator Methodology (30 minutes)• Collapse Simulation Challenges in Example Application (30 minutes)	Holmes Moehle Liel
10:45 am	<i>Break</i>	
11:00 am	Ground Motions for Collapse Simulation	Baker
11:30 am	Summary of Topics to be Addressed in Breakout Sessions	Elwood
Noon	<i>Lunch</i>	
1:30 pm	Breakout Sessions (Part 1) <ul style="list-style-type: none">a. Column Modeling (Uni-Directional).<ul style="list-style-type: none">• Identify preferred column model for response from flexure to shear failure (axial failures addressed in separate breakout).• Can the models capture the transition between shear and flexure failures?• Is it preferred to use concentrated plasticity models with hysteretic rules or fiber models?b. Beam-Column Joints Modeling (Uni-Directional).<ul style="list-style-type: none">• What is the preferred method to model joints when joint failure controls the response of a frame building?• How to model joints when beams or columns govern response?• How to transition from beam or column controlled frame response to joint controlled frame response?c. Infill Frames<ul style="list-style-type: none">• Identify preferred model for infill and frame.• How does infill model influence column failure?• Is it important to modify the models for unit type?	
4:30 pm	Day 1 Closure	

Applied Technology Council
201 Redwood Shores Parkway
Suite 240
Redwood City, California 94065
(650) 595-1542

Consortium of Universities for Research
in Earthquake Engineering
1301 S. 46th Street – Bldg. 420
Richmond, California 94804
(510) 665-3529

Figure A-1 Agenda Day 1 – Collapse Simulation Workshop.

January 18, 2013

8:30 am Summaries from Day 1 Breakout Sessions – Part 1

Breakouts (Part 2)

a. Modeling Gravity Load Failures

- Identify preferred method of modeling loss of gravity load support (i.e. treat as non-simulated failure mode or model failure explicitly)
- Do we need to explicitly model axial load failure in columns? In beam-column joints? In slab-column connections? If so, how to detect and degrade response?
- Does the gravity system need to be explicitly modeled?

b. Load History Effects

- In collapse simulation of concrete buildings, is it important to capture bi-directional demands and response of concrete components? If so, how?
- Do cyclic models adequately capture deterioration resulting from long-duration ground motions?
- Is it preferred to use concentrated plasticity models with hysteretic rules or fiber models?

c. Modeling of Walls and Wall-Pier Systems

- What are the preferred wall models to capture the displacement demands on gravity system? What wall systems are most likely to lead to high demands on the gravity system?
- Is the potential for wall axial load failure significant enough to warrant modeling this failure mode? If so, what are some possible approaches? For what types of walls should this failure mode be considered?
- Is it preferred to use concentrated plasticity models with hysteretic rules or fiber models?
- How to model discontinuous walls and supporting columns?

12:30 pm ***Lunch with Presentation:***

Foundation Modeling Considerations (30 minutes)

Stewart

1:45 pm Summaries from breakouts – Part 2

2:45 pm Workshop Conclusions

Elwood

3:00 pm ***Adjournment***

Figure A-2 Agenda Day 2 – Collapse Simulation Workshop.

A.3 Workshop Mini-Papers

To provide background and stimulate discussion in the breakout sessions, mini-papers were requested from six prominent researchers active in the field of modeling existing reinforced concrete buildings. These papers were distributed in advance of the workshop to allow attendees time to prepare for discussion.

The mini-papers and authors are listed in Table A-1. Topics included advanced modeling recommendations for key reinforced concrete components, such as columns, beam-column joints, and frames with masonry infill. Topics also included overarching issues, such as modeling of gravity load failure and assessing the effects of displacement history. The full text of each mini-paper presented at the workshop is provided in Appendix B through Appendix G.

Table A-1 Workshop Mini-Papers, Authors, and Appendix References

Mini-Paper	Author	Appendix
Column Models for Collapse Simulation	Wassim M. Ghannoum University of Texas, Austin	Appendix B
Recommendations for Simulating the Response of Beam-Column Joints in Reinforced Concrete Building Frames	Laura N. Lowes University of Washington	Appendix C
Modeling Gravity Load Failure in Collapse Simulations	K.M. Mosalam, and M.S. Günay University of California, Berkeley	Appendix D
Assessing the Effects of Displacement History on the Seismic Response of Reinforced Concrete Structures	S. Santiago Pujol Purdue University	Appendix E
Collapse Simulation of Masonry-Infilled Reinforced Concrete Frames	P. Benson Shing University of California, San Diego	Appendix F
Reinforced Concrete Structural Wall Modeling for Collapse Assessment Utilizing Monte Carlo Simulations	John W. Wallace University of California, Los Angeles	Appendix G

A.4 Workshop Breakout Groups

Breakout sessions were used to develop consensus on the issues addressed in the mini-papers. Six breakout sessions, one for each mini-paper, were conducted. The topics and assignments for each breakout session are shown in Tables A-2 and A-3. The resulting recommendations from the breakout discussions are summarized in Chapter 4.

Table A-2 Workshop Breakout Groups – Day 1

Assignments	Breakout Topics		
	Columns	Joints	Infills
Moderator 1	Moehle	Jirsa	Liel
Moderator 2	Almufti	Holmes	Somers
Author/Presenter	Ghannoum	Lowes	Shing
Participants	Haselton	Kunnath	Abrams
	Pujol	LaFave	Fleischman
	McKenna	Hueste	Deierlein
	Matamoros	Wiliamson	Mahin
	Lehman	Zareian	Mosalam
	Korolyk	Wallace	Kim
	Baradaran Shoraka	Berkowitz	Comartin
	Baker	Günay	Luco

Table A-3 Workshop Breakout Groups – Day 2

Assignments	Breakout Topics		
	Gravity load failures	Load history	Walls
Moderator 1	Moehle	Baker	Lowes
Moderator 2	Comartin	Kunnath	Holmes
Author/Presenter	Mosalam	Pujol	Wallace
Participants	Wiliamson	Deierlein	Lehman
	Hueste	Haselton	Zareian
	Fleischman	Matamoros	LaFave
	Liel	Shing	Mahin
	McKenna	Ghannoum	Abrams
	Somers	Jirsa	Berkowitz
	Baradaran Shoraka	Korolyk	Almufti
	Günay	Luco	Kim

Appendix B

Column Models for Collapse Simulation

by Wassim M. Ghannoum
University of Texas at Austin
Austin, Texas

B.1 Introduction

Task: Discuss alternatives for modeling concrete columns.

1. Please compare leading models for concrete columns, providing pros and cons in terms of: (a) what they promise to do; and (b) how well they have been tested or validated (note: axial failures are addressed in a separate breakout).
2. Can the models from Question 1 capture the transition between shear and flexure failures?
3. Are the models from Question 1 practical for Monte Carlo collapse simulations where thousands of runs are required?
4. Is it preferred to use concentrated plasticity models with hysteretic rules or fiber models?

B.2 Model Considerations

To accomplish the stated goal of running thousands of simulations up to structural collapse, the following model characteristics are important:

1. Computational efficiency.
 - This requirement limits models to line-elements with either lumped-plasticity or fiber-section implementations.
2. Calibration to a wide range of column failure modes.
 - Since the goal is to generate a comprehensive assessment of collapse vulnerability, all column failure modes need to be represented.
3. Ability to transition between shear and flexure failures.
4. Ability to simulate the full lateral-strength degrading behavior including in-cycle and cyclic degradation.
 - In-cycle degradation (or post-peak negative stiffness) can lead to dynamic instability and increased deformation demands. For structures that rely

mainly on moment frames for lateral stability, simulating the in-cycle degradation is essential to providing realistic collapse simulation results.

- Cyclic degradation can be as important as in-cycle degradation, depending on the ground motion used. For near fault ground motions characterized by a large pulse, cyclic degradation may not play a significant role. On the other hand, for long duration motions with a large number of cycles, cyclic degradation can be more critical than in-cycle degradation; in such cases the column response may degrade to a residual strength with only minimal contact with the envelope force-deformation response.
5. Compatibility with joint and bar-slip models.
 6. Ability to adapt to varying boundary conditions.
 - Lateral-strength behavior of reinforced concrete (RC) columns depends on several parameters that can vary significantly during analyses: axial load, ratio of shear to moment, and plastic rotations. Variations in column boundary conditions can be accentuated in collapse simulations in which adjacent members fail. For example, a column seeing an increase in axial load due to the loss of an adjacent column may have a significant increase in flexural strength. Consequently that column may sustain a shear failure at much lower deformations.
 7. Availability through implementation in analytical software.
 8. Ability to provide uncertainty measures in statistical terms for Monte Carlo simulations.
 9. Compatibility with column axial failure models.
 - Models are available to capture column axial load failure after shear failure (Elwood, 2004); however, such models are not appropriate for columns experiencing flexural failures. Ideally column models should be able to distinguish between flexural and shear failures and trigger axial load failures accordingly.

B.3 Available Models

Numerous models exist that deliver either a maximum shear strength or a limiting deformation, that, if reached, would indicate incipient loss of lateral strength in a reinforced concrete column (e.g., Panagiotakos and Fardis, 2001; Biskinis et al., 2004; Kowalski and Priestley, 2000; Mostafaei and Kabeyasawa, 2007; Aschheim, 2000; Sezen and Moehle, 2004; Pujol et al., 1999; Kato and Ohnishi, 2002). Such models are not treated here as they provide no guidance for simulating behavior once the critical limit state is reached. Three models satisfy most of the criteria discussed above: (1) a model by Haselton et al., 2008; (2) a model by Leborgne and

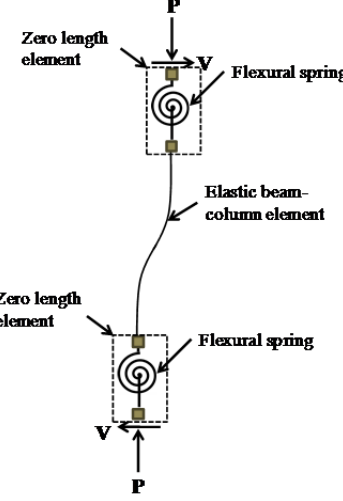
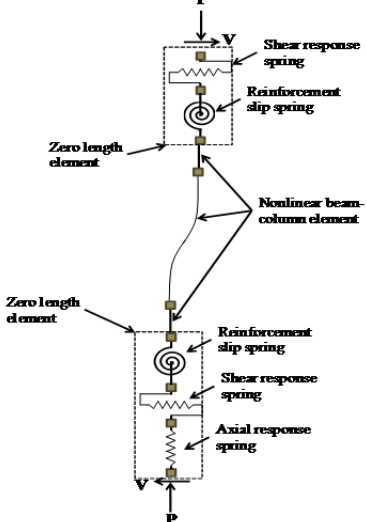
Ghannoum, 2013, and LeBorgne, 2012; and (3) a model by Baradaran Shoraka and Elwood, 2013 (in review). These three models, summarized below, provide regression- and mechanics-based equations for defining the nonlinear modeling parameters for column elements, including cyclic and in-cycle degradation. Note that model numbers in the following sections refer to the models listed in Table B-1.

It is noteworthy that very limited experimental data exists for columns failing due to inadequate lap splices. None of the three models identified treat inadequate lap splices.

B.3.1 Summary of Model 1 (Haselton et al., 2008)

1. Model 1 is implemented through a lumped-plasticity framework with zero-length rotational springs placed at the ends of elastic line-elements. The springs use a non-linear hysteretic model that includes damage accumulation features.
2. The model is calibrated to 255 rectangular column tests: 220 columns tests with flexure failures, and 35 column tests with flexure-shear failures. Both failure types, however, are lumped together to achieve an averaged model. The model is not calibrated for shear failures sustained prior to flexural yielding. A shear failure model could be added to Model 1 using a zero-length shear spring. However, there are no models that treat the full cyclic degrading behavior for this type of failure.
3. This model provides regression-based equations that are used to estimate linear and non-linear parameters based on column properties and loading conditions. The material model includes in-cycle as well as cyclic degrading behaviors. It also provides elastic stiffness estimates for the elastic line elements and includes effects of bar-slip-induced deformations. In the original formulation, it was not possible to distinguish between flexure and flexure-shear failure modes; however, it is possible to recalibrate the regression relationships for any dataset to focus on one specific failure mode. This approach was used in ATC-78-1 (ATC, 2012) to focus only on columns experiencing flexural failures.
4. Model 1 is calibrated for full cyclic behavior, including in-cycle and cyclic degradation. Pinching and stiffness degradation are not treated, but may not be an issue depending on column type.
5. Being implemented through line elements, it is compatible with joint models that are line-element based. Bar-slip induced deformations may need to be adjusted depending whether the joint model accounts for those deformations.
6. All model parameters are fixed by user input at the model building phase. Thus the model does not adjust behavior to varying boundary conditions during analysis.

Table B-1 Summary of Models

	 <p>Model 1: Haselton et al. (2008)</p>	 <p>Model 2: Leborgne and Ghannoum (2013)</p>
Failure types	Flexure, flexure-shear	Shear, flexure-shear
Elements	Elastic beam-column element + zero-length flexural spring	3 nonlinear elements + zero-length shear springs
Calibration Database	255 columns	32 columns
Model Description	The model provides regression-based equations that are used to estimate linear and non-linear parameters of flexural springs based on column properties and loading conditions.	The shear spring model has the ability during analyses to monitor the deformations between two nodes bracketing the plastic hinge region, as well as forces in the adjacent column element. The model compares the shear force in the column with a limiting shear force and the rotation of the plastic hinge region with a limiting rotation.
Cyclic Modeling	The model is calibrated for the full cyclic behavior, including in-cycle and cyclic degradation.	The model can simulate the full degrading behavior, including in-cycle and cyclic degradation.
Input by User versus Adaptive Model	All model parameters are fixed by user input at the model building phase. Thus the model does not adjust behavior to varying boundary conditions during analysis.	The user can either input fixed values for rotation and shear-force limits or use the calibrated version of the model, which automatically evaluates limits during analysis utilizing the ASCE/SEI 41 shear strength equation and a regression-based plastic rotation equation.
OpenSees Material	Pinching4 using hysteretic model by Ibarra el al. (2005)	PinchingLimitState Material described in Leborgne (2012)
P is axial load; V is shear		

P is axial load; V is shear

7. The model utilizes a non-linear material model that is implemented in OpenSees and is thus ready for use.
8. From the regressions performed to calibrate model parameters, uncertainty measures can be extracted for parametric Monte Carlo simulations.
9. Since this model does not distinguish between flexure and flexure-shear failures, it is not appropriate to couple this model with an axial failure model which assumes the development of a diagonal failure plane (e.g., Elwood, 2004). This limits the model applicability to collapse simulations governed by a side-sway mechanism or where non-simulated failure modes are used to terminate analysis at first column axial failure.

B.3.2 Summary of Model 2 (Leborgne and Ghannoum, 2013)

1. Model 2 is implemented through zero-length shear springs placed at the ends of column line-elements. The model can be used with either a fiber-section or lumped-plasticity column element. For the calibrated version of the model, it is recommended to use a fiber-section column element, since the model was calibrated that way. Optionally, zero-length fiber sections can be used at the end of column elements to account for bar-slip induced rotations.
2. Currently the model is only calibrated to 32 rectangular column tests in which flexural yielding occurred prior to shear-induced lateral strength degradation. Work is underway to expand the calibration to a 500-column database covering shear, flexure-shear, and flexure-critical columns. Circular columns will also be included. Given the scope of work, a full model is not expected to be completed for at least a couple of years.
3. The shear spring model has the ability during analyses to monitor the deformations between two nodes bracketing the plastic hinge region, as well as forces in the adjacent column element. The model compares the shear force in the column with a limiting shear force and the rotation of the plastic hinge region with a limiting rotation. Once the first one of these is reached, a degrading behavior is triggered and all model cyclic degrading parameters are defined. Thus the model can seamlessly transition between a shear failure mode driven by a limiting shear force and a flexure-shear failure mode driven by a limiting deformation. Flexural failures are not captured by the model.
4. The model can simulate the full degrading behavior, including in-cycle and cyclic degradation. The material model used has several damage functions that include strength and stiffness degradation. Pinching is also available. All damage parameters are defined in the model using regression-based equations that the model evaluates automatically based on column properties.

5. Being implemented through line elements, it is compatible with joint models that are line-element based. Bar-slip induced deformations may need to be adjusted depending on whether the joint model accounts for those deformations.
6. The user has the choice of either inputting fixed values for rotation and shear-force limits or using the calibrated version of the model that automatically evaluates them utilizing the ASCE/SEI 41 shear strength equation and a regression-based plastic rotation equation. In the latter version, limits are functions of axial load, moment, and shear. The limits are evaluated at each load increment based on current loads in the column element.
7. The model is implemented in OpenSees and is ready to use.
8. From the regressions performed to calibrate model parameters, uncertainty measures can be extracted for parametric Monte Carlo simulations.
9. The model is applicable to columns experiencing shear or flexure-shear failures, and hence can be easily coupled with axial failure models by adding a zero-length spring in series with the column element.

B.3.3 Summary of Model 3 (Baradaran Shoraka and Elwood, 2013)

1. Model 3 is implemented through zero-length shear springs placed at the ends of column line elements. The model must be used in combination with a force-based fiber element.
2. The model is formulated based on modified compression field theory and shear friction concepts. Currently it is validated with 20 rectangular columns tests. The model uses the shear strain demands in the plastic hinge region (assumed to be bounded by the first two integration points) to detect shear failure.
3. The model can represent both shear failure and flexure-shear failure modes and transition between them seamlessly, owing to its compression field background. The model can also detect when shear capacity is sufficient and flexural deformations govern response; however, it does not currently capture flexural failures (i.e., degradation due to rebar buckling/fracture). If the OpenSees Min-Max material is used to impose strain limits, the model will be able to represent all three failure types; however, this detection of flexural failures requires calibration.
4. The model can simulate the full degrading behavior, including in-cycle and cyclic degradation. While the in-cycle negative stiffness is treated in detail in the model, all cyclic parameters are given as the same regardless of column properties.

5. Being implemented using line elements, it is compatible with joint models that are line-element based. Bar-slip induced deformations may need to be adjusted, depending on whether the joint model accounts for those deformations.
6. The model constantly monitors column forces and deformation demands between integration points and adjusts the limit state that triggers strength degradation.
7. The model is implemented in OpenSees and is ready to use.
8. In theory, once the model is validated using more column tests, uncertainty measures can be extracted for parametric Monte Carlo simulations.
9. The model is applicable to columns experiencing shear or flexure-shear failures, and hence can be easily coupled with axial failure models by adding a zero-length spring in series with the column element.

B.4 Pros and Cons of Modeling Approaches

As with most analytical models, the summarized models can be broken into two components: (1) the analytical framework; and (2) the behavioral models governing the analytical parameters.

B.4.1 Analytical Framework

Lumped-plasticity versus fiber-section implementation of flexural deformations:

- Lumped-plasticity models are more efficient computationally than fiber-section models. However, fiber-section models can also be used effectively in Monte Carlo simulations. Moreover, when simulations push structures to large deformations and well into the nonlinear range, the computational time for the lumped-plasticity models is greatly decoupled from the number of degrees of freedom in a structure. The number of iterations for convergence greatly effect computational time, and depend on whether a structure will lose stiffness suddenly (e.g., structures with all columns being identically dimensioned and detailed) or gradually. Fiber-section implementations tend to smooth out structural stiffness changes.
- Lumped-plasticity models are easier to interpret because they contain clear behavioral transitions.
- Fiber-section models can simulate the cyclic flexural behavior more accurately than lumped-plasticity models. Fiber-sections can account for pinching behavior due to flexural degradation and can utilize confined concrete properties at large deformations.
- Perhaps the most notable difference is that fiber-section models adapt their behavior to varying axial loads; both strength and stiffness changes are accounted

for. For end-columns, columns in tall buildings, or in cases of loss of adjacent columns, this feature can make a significant difference.

Pre-defined or adaptive parameters:

- Typical analytical frameworks consist of material models that are inserted into structural elements. Material models require the input of certain parameters that govern the material response. These parameters are typically input when a model is built and remain fixed for the duration of an analysis. Model 1 utilizes this classic framework. Models 2 and 3, on the other hand, utilize a framework that allow the models to monitor key forces and deformations such that its parameters can be evaluated at each load increment and can thus adapt to varying column boundary conditions.

B.4.2 Behavioral Models

- Model 1 is calibrated to a larger dataset than Models 2 and 3. Model 1 elements depict both flexure and flexure-shear critical columns. Models 2 and 3 elements depict shear and flexure-shear critical columns. The overlap between these models can be utilized to get a more comprehensive solution; however, analysts must be aware of possible inconsistencies at the transition between flexure and shear failures if separate models are used for the two failure modes.
- All three models represent the cyclic and in-cycle degradation of the lateral strength of columns. Model 3, however, defines cyclic damage parameters to be the same for all columns.
- Models 1 and 2 utilize regression-based equations to define model parameters. The equations are functions of column geometric and material properties, as well as column loading. Based on regression results, uncertainties can be treated in a similar fashion for both models. Model 3 is theory-based, but comparing its predictions with a large experimental dataset would help generate quantifiable uncertainty measures.

B.5 Summary and Conclusions

In summary, three models that have advanced nonlinear simulation capabilities are discussed. All models can simulate the loss of lateral strength of RC columns using cyclic and in-cycle strength loss algorithms. None of them, unfortunately, covers the full spectrum for column lateral-strength behavior at this stage. Notably, circular columns and inadequate lap-splices are not treated. Model 1 is calibrated to flexure and flexure-shear critical columns, and is appealing from a computational stand point, as it uses a lumped-plasticity framework. Model 2 has more advanced capabilities, but demands more computational effort, since it is based on fiber-section elements. Model 2 is calibrated, at present, to fewer column types than Model 1. Model 3 has only been validated to 20 column tests, and similar to Model 2, treats

shear and flexure-shear critical columns only at this stage. A creative use of these models may need to be pursued to achieve a more comprehensive solution for the problem at hand.

Appendix C

Recommendations for Simulating the Response of Beam-Column Joints in Reinforced Concrete Building Frames

by Laura N. Lowes
University of Washington
Seattle, Washington

C.1 Introduction

The following are recommendations for modeling beam-column joints for nonlinear dynamic analyses of reinforced concrete building frames subjected to earthquake loading. Recommendations are based on a review of models that are currently available in the literature, as well as part of the author's experience developing and using joint models and conducting nonlinear dynamic analyses of concrete frames. The recommendations address joints with detailing typical of pre-1967¹ construction (i.e., no transverse reinforcement) as well as joints designed to achieve performance superior to that of pre-1967 construction, such as those compliant with ACI 318 Code requirements for special moment frames.

In developing the recommendations, the primary objectives were to identify models that can provide:

1. Accurate simulation of the fundamental characteristics of joint response to earthquake loading.
2. Simple implementation of the model in OpenSees using existing element formulations and material models. Existing OpenSees joint and one-dimensional (1D) spring elements are sufficient. The nonlinear response of joints is characterized by a pinched hysteresis as well as stiffness and strength loss under cyclic loading; the OpenSees analysis platform includes material models that are capable of simulating this type of behavior.
3. Numerical robustness and stability, so that analyses are not hampered by failures to converge.

¹ In 1967 UBC provisions changed to include requirements that: (i) joint shear strength defined using the column shear strength equation exceed joint shear demand; (ii) transverse reinforcement be provided in the joint to achieve required shear strength; (iii) the sum of column flexural strengths exceed the sum of beam flexural strengths; and (iv) splices in beam and column longitudinal reinforcement be located away from the joint. Similar revisions were made to the ACI Code in 1971. These Code issues are reflected in drawings for buildings designed for construction on the West Coast from 1923 – 1979.

4. Computational efficiency.
5. Objective calibration procedures, so that the model-building process is as efficient as possible and modeling parameters do not need to be adjusted to define the model for a specific beam-column joint with a specific set of design characteristics.

Modeling of “interior” and “exterior” joints in two-dimensional (2D) frames (Figures C-1 and C-2) is addressed first. These are typically considered to be the most prevalent and most critical building joint configurations. As a result, most experimental research and numerical modeling efforts have focused on these configurations. Recommendations for modeling knee joints in 2D frames are provided; however, few studies have addressed these components, and few data are available for model calibration and validation. Modeling of joints in three-dimensional (3D) frames is addressed second. Fewer experimental investigations and modeling efforts have addressed these joint configurations.

Modeling recommendations address simulation of response through significant loss of joint shear strength; recommendations do not address loss of joint axial load-carrying capacity. This is considered adequate for the proposed study. In the laboratory, beam-column joint subassemblages have typically maintained moderate axial loads following significant loss of joint shear strength. A recent study by Hassan (2011) found that for joints with beam-to-column depth ratios less than 2.5, joint axial load failure was unlikely to precede column axial load failure.

Figures C-1 and C-2 show recommended element configurations for simulating interior and exterior joint response in 2D frames. These include the use of a rotational spring to simulate joint shear stress-strain response and the introduction of zero-length bar slip fiber-section models at the beam-joint (shown in Figure C-2) and/or the column-joint interfaces (not shown). Beam-column joint elements exist in OpenSees; however, these are not recommended for use as they require an intra-element solution², which introduces the potential for numerical problems and reduced numerical robustness and efficiency.

The rotational joint springs shown in Figures C-1 and C-2 require a 1D joint moment versus joint rotation response model. Joint response models are discussed below; however, most of these models define joint shear stress versus strain. Since joints are

² The OpenSees joint elements are essentially small structural subassemblages within the global structural model. These subassemblages comprise multiple nodes and multiple nonlinear springs that are not (explicitly) part of the global structural model. For each iteration to establish equilibrium of the global structural model, it is necessary to solve for equilibrium of the joint subassemblage model. While the user has control over the global solution algorithm with the ability to change the tolerance or step size to improve the rate of convergence, the user has no control over the solution algorithm used to solve the joint subassemblage model. Thus, the user has limited ability to continue the analysis when a “failure to converge” occurs within the joint element.

not subjected to pure shear loading at the geometric perimeter of the joint, Celik (2007) provides equations relating shear stress to joint moment. Joint shear deformation may be assumed to be equal to joint rotation.

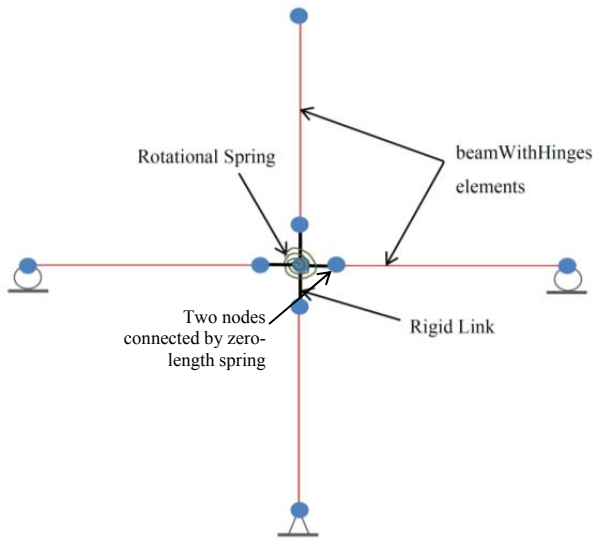


Figure C-1 OpenSees model of an interior joint subassemblage.

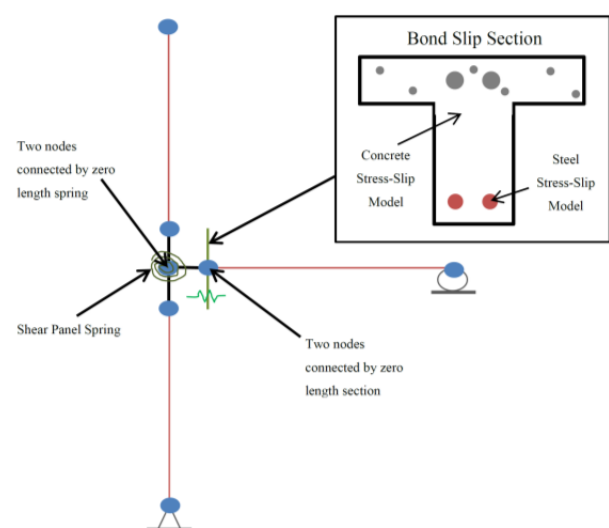


Figure C-2 OpenSees model of an exterior joint subassemblage.

Figure C-2 shows a zero-length bar slip fiber-section model at the beam-joint interface. These models have been used successfully to simulate rotation due to slip of reinforcement anchored in footings (Berry, 2006; Oyen, 2006) and are consistent with the bar slip springs introduced into joint models by Youssef and Ghobarah (2001), and Mitra and Lowes (2007). The bar slip section model may be used to simulate deformation due to bar slip for interior joints with continuous reinforcement, but is likely most relevant for joints in which beam (or column) longitudinal reinforcement terminates within the joint with a short straight anchorage. Berry (2006) provides general guidance on defining the bar slip model; Mitra and Lowes (2007) provide recommendations for bond strength within joints and cyclic response parameters.

The following sections provide recommendations for joint core constitutive models and bar slip models. It is expected that these constitutive models will be used to define input parameters for the 1D OpenSees Pinching4 material model, although other models may be adequate. The Pinching4 model allows for definition of a multi-linear response envelope, simulates the pinched response histories that are typical of beam-column joint stress versus shear strain data, and provides a mechanism for simulating strength and stiffness loss under cyclic loading.

Most of the modeling recommendations below represent the combination of response envelopes developed by one research group with cyclic response quantities

developed by another research group, or they represent the combination of models simulating joint shear response with models simulating anchorage failure. Few of the recommended modeling approaches have been fully validated using experimental datasets. Thus, a limited model validation effort is recommended prior to using these models in extensive collapse simulations to identify collapse indicators.

C.2 Models for Interior Beam-Column Joints in 2D Frames

As suggested in Figure C-1, an interior joint in a 2D frame represents the intersection of a continuous beam and continuous column. For these joints, the primary objectives for modeling are accurate simulation of: (1) joint flexibility; and (2) ductile versus brittle subassemblage response, where a ductile subassemblage exhibits limited inelastic joint deformation with large inelastic deformation concentrated in beams (or columns), and a brittle subassemblage exhibits extensive inelastic joint deformation accompanied by loss of joint strength and limited inelastic action in beams (or columns). Figure C-3 shows a ductility classification for 45 interior joints, with a wide range of design characteristics. Joints are classified as:

- *Ductile* – joint strength is sufficient to develop the yield strength of the beams framing into the joint and load carrying capacity is maintained to a displacement ductility in excess of 4.
- *Brittle* – joint strength is not sufficient to develop the yield strength of the beams framing into the joint.
- *Limited Ductility* – joint strength is sufficient to develop the yield strength of the beams framing into the joint, but strength loss occurs at ductility demands less than 4.

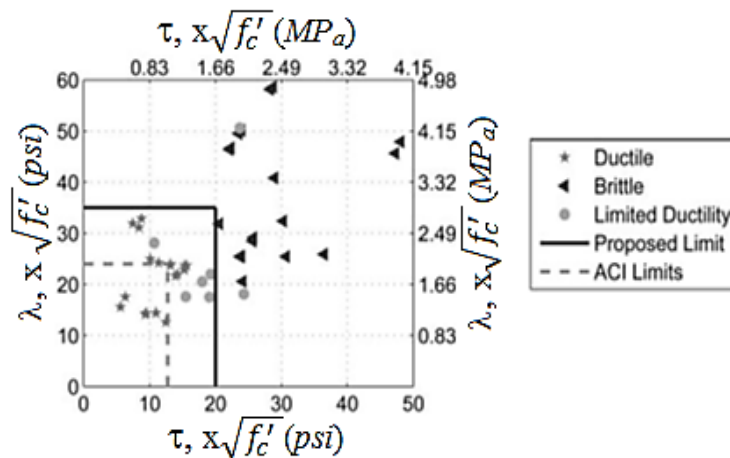


Figure C-3 Relationship of ductility classification to design joint shear stress, τ , and average bond stress, λ (Birely et al., 2012, with permission).

The data in Figure C-3 suggest that subassemblage ductility is determined by τ , the design joint shear stress demand per ACI 352R-02 (ACI, 2002), and λ , the average bond stress demand for beam bars assuming yielding on both sides of the joint. Figures C-4, C-5, and C-6 show column shear versus drift for joint test specimens with no transverse reinforcement (i.e., $\rho_{\text{joint}} = 0\%$), exhibiting brittle, limited-ductility, and ductile response, respectively.

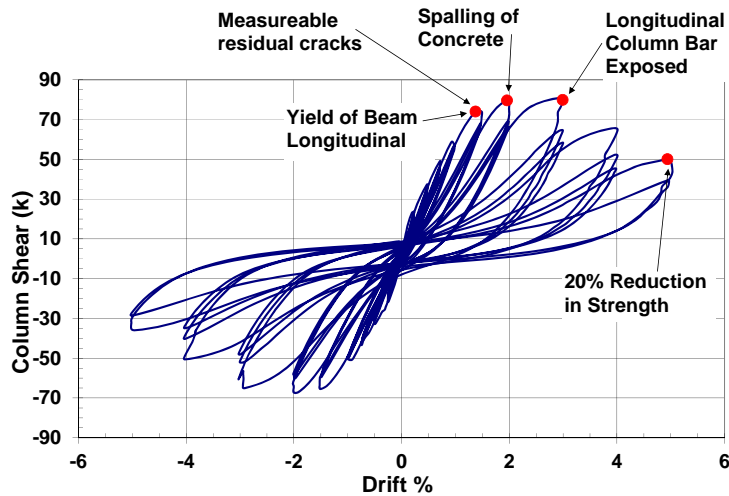


Figure C-4 Column shear versus drift for a brittle beam-column joint specimen (PEER 22, from Walker, 2001) with no joint transverse reinforcement, maximum joint shear stress, $\tau_{\max} = 20.6 \sqrt{f'_c}$, and average bond stress demand, $\lambda = 31.9 \sqrt{f'_c}$. Joint design is not compliant with ACI requirements for special moment frames.

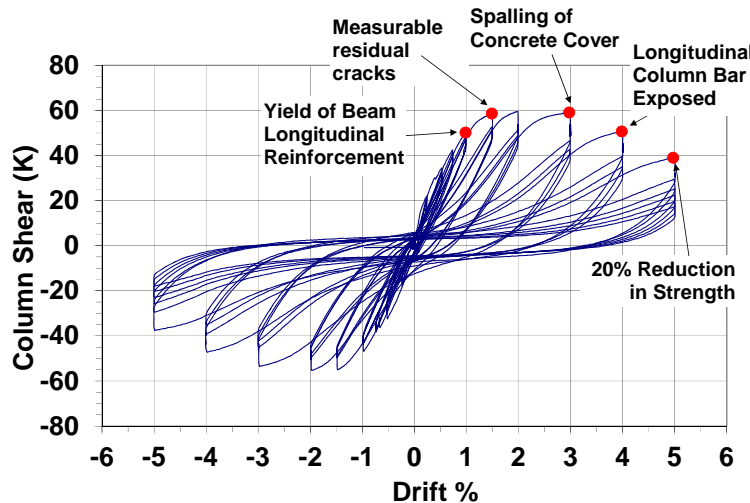


Figure C-5 Column shear versus drift for a limited-ductility beam-column joint specimen (PEER 14, from Walker, 2001) with no joint transverse reinforcement, maximum joint shear stress, $\tau_{\max} = 10.7 \sqrt{f'_c}$, and average bond stress demand, $\lambda = 28.1 \sqrt{f'_c}$. Joint design is not compliant with ACI requirements for special moment frames.

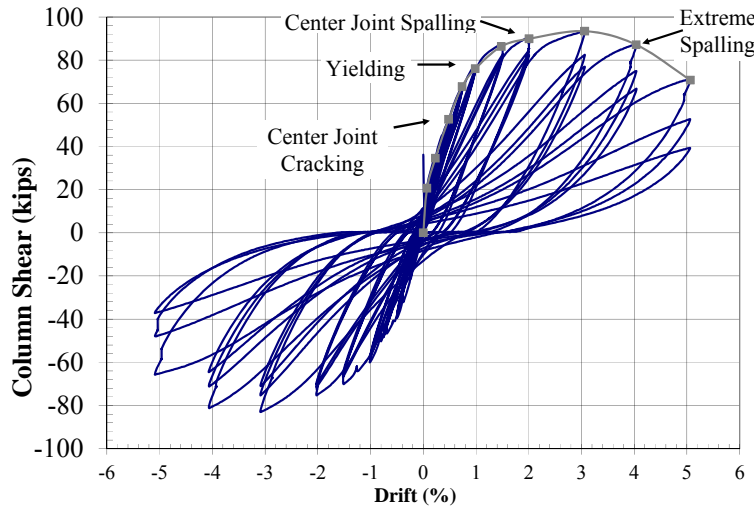


Figure C-6 Column shear versus drift for a ductile beam-column joint specimen (PEER 0995, from Alire, 2002) with no joint transverse reinforcement, maximum joint shear stress, $\tau_{max} = 7.5 \sqrt{f'_c}$, and average bond stress demand, $\lambda = 31.9 \sqrt{f'_c}$. Joint design is not compliant with ACI requirements for special moment frames.

Many models have been proposed for simulating the response of interior joints. Table C-1 provides information about those models considered to be most relevant to the current study.

C.2.1 Recommendations for Modeling Interior Joints in 2D Frames

The models by Birely et al. (2012) and Kim and LaFave (2009) are likely the best models for the current study. Despite the fact that they do not include recommendations for simulation of cyclic response or simulation of response beyond 10% strength loss, these two models provide a relatively simple approach for defining a shear strength versus deformation envelope that is appropriate for use for a range of design configurations and that can provide simulation of ductile as well as nonductile response mechanisms.

Of the Birely, and Kim and LaFave models, the Birely model is preferred for most joint simulations. This model was calibrated using subassemblage load-displacement data and an OpenSees model such as that shown in Figure C-1; thus, the model could be expected to provide accurate simulation of the response envelope for similarly modeled subassemblages. The Kim and LaFave model has not been validated using subassemblage data and nonlinear beam-column element models, and there is the potential that this model neglects bar slip or other deformation, though experimental data suggest that bar-slip deformation is small. The Birely model requires the addition of a post-peak response segment as well as definition of cyclic response quantities. Here, it is recommended that post-peak strength loss be defined as a function of joint shear stress demand, with the ratio of

Table C-1 Response Models for Interior Beam-Column Joints

Reference	Cyclic or Envelope	Defining Characteristics	Pros	Cons
Mitra and Lowes (2007)	Cyclic	- Model includes τ vs. γ for joint core derived from concrete strut model as well as bar-slip springs derived from bond stress capacity	- Validated using large data set (57 specimens) - Developed for OpenSees - Calibrated using data in Figures C-4 through C-6	- Complicated to define model parameters for specific set of joint characteristics - Requires intra-element solution
Andreson et al. (2008)	Cyclic	- τ vs. γ model only - Developed using experimental τ vs. γ data - Joint strength is $0.95 \tau_{ACI}$ - Joint strength degrades with cyclic loading once maximum strength is reached; rate of degradation depends on τ_{ACI} , which is the design joint shear stress computed per ACI 352R-02 (ACI, 2002)	- Developed using data from test specimens with no transverse reinforcement (i.e., older joints) - Demonstrated to provide accurate response of specimen with limited transverse reinforcement - Calibrated using data in Figures C-4 through C-6	- Model definition is relatively complicated - Implementation in OpenSees (i.e., translating model definition in the paper to existing OpenSees material model) will be difficult and likely imperfect - Because beam strength determines joint strength, accurate simulation of post-peak response and impact of τ_{ACI} on response is critical - Has only been validated using joint τ vs. γ data, not subassemblage response data
Kim and LaFave (2009)	Envelope to cyclic response	- τ vs. γ model - Developed using experimental τ vs. γ data - Quadralinear envelope, trilinear to maximum strength and then descending branch to 90% maximum strength - Envelope points are functions of multiple design parameters (e.g., geometry, joint reinforcement ratio, concrete strength)	- Developed using large data set (80+ specimens) - Defines response for joints with a wide range of design parameters - Calibrated using data in Figures C-4 and C-5	- Implementation in OpenSees requires definition of cyclic response quantities (i.e., unloading-reloading response, stiffness loss); these could be taken from Mitra and Lowes (2007) - Model calibration, for individual joint design, requires calculation of a number of design parameters - Requires definition of post-peak response; model only predicts response through 10% strength loss.
Birely et al. (2012)	Envelope to cyclic response	- Joint moment vs. joint deformation model (i.e., includes all non-frame member deformation) - Bilinear to maximum strength/failure; does not include post-peak response	- Simple - Developed using large data set - Joint model includes all non-frame member deformation, so no bar slip model required; model was developed using subassemblage test data - Model validation demonstrates that model can predict joint failure versus beam-yielding - Calibrated using data in Figures C-4 through C-6	- Requires definition of post-peak response. - Requires definition of cyclic response quantities (i.e., unloading-reloading curves including stiffness loss with cyclic loading); these could be taken from Mitra and Lowes (2007) - Model calibration, for individual joint design, requires calculation of beam yield moments

initial stiffness to post-peak stiffness defined per Anderson et al. (2008). Unloading-reloading response may be defined using the recommendations of Mitra and Lowes (2007). It should be noted that Birely et al. (2012) includes also a recommended hinge rotation limit for beams framing into the joint (i.e., rotation at which beam flexural strength loss due to joint damage initiates); however, depending on the way in which beam modeling is accomplished, it may not be possible to introduce this limit into an OpenSees model.

For interior joints in which beam longitudinal reinforcement terminates within the joint with inadequate anchorage, the Kim and LaFave model, in combination with bar slip section models at the beam-joint interface, is preferred.

C.3 Models for Exterior Beam-Column Joints in 2D Frames

As suggested by Figure C-2, an exterior joint in a 2D frame represents the termination of a beam in a continuous exterior column. For exterior beam-column joints, the primary objective for modeling is accurately distinguishing between response controlled by: (1) anchorage failure for beam bottom reinforcement with short embedment lengths; (2) joint shear failure; and (3) beam flexure. Figures C-7 and C-8 show column shear versus drift for exterior beam-column joint test specimens with no transverse reinforcement (i.e., $\rho_{joint} = 0\%$), exhibiting anchorage-controlled response and shear-controlled response, respectively.

Table C-2 provides information about exterior joint response models considered to be most relevant to the current study.

C.3.1 Recommendations for Modeling Exterior Joints in 2D Frames

The model by Sharma et al. (2011) is likely the best model for the current effort. The model is shown to provide acceptably accurate simulation of the response envelope for 13 planar exterior beam-column joints with and without short straight anchorage for beam bottom bars, including those shown in Figures C-7 and C-8. Use of this model will require definition of cyclic response parameters; recommendations provided by Mitra and Lowes (2007) for interior joints will likely require some modification, in particular for exterior joints in which inadequate anchorage for beam bottom bars results in significantly weaker response in one loading direction.

C.4 Models for Knee-Joints in 2D Frames

Knee joints in a 2D frame typically occur at the intersection of an exterior column and the (roof) beam at the top of a frame. The knee joint on the left side of a frame is modeled in OpenSees by removing the top column, and its associated nodes, from the model shown in Figure C-2.

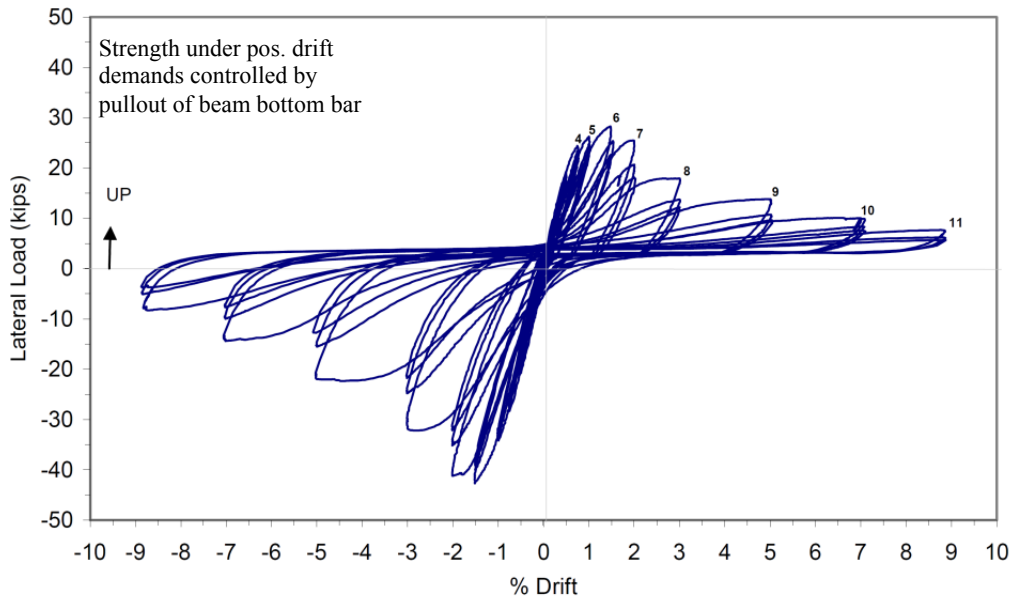


Figure C-7 Column shear versus drift for an anchorage-controlled exterior joint specimen (Unit 2, from Pantelides et al., 2002) with no joint transverse reinforcement, maximum joint shear stress, $\tau_{\max} = 7\sqrt{f'_c}$ (up) and $10.6\sqrt{f'_c}$ (down), beam bottom bar anchorage length of 6 in., and column axial load = $0.25A_g f'_c$. Joint design is not compliant with ACI requirements for special moment frames.

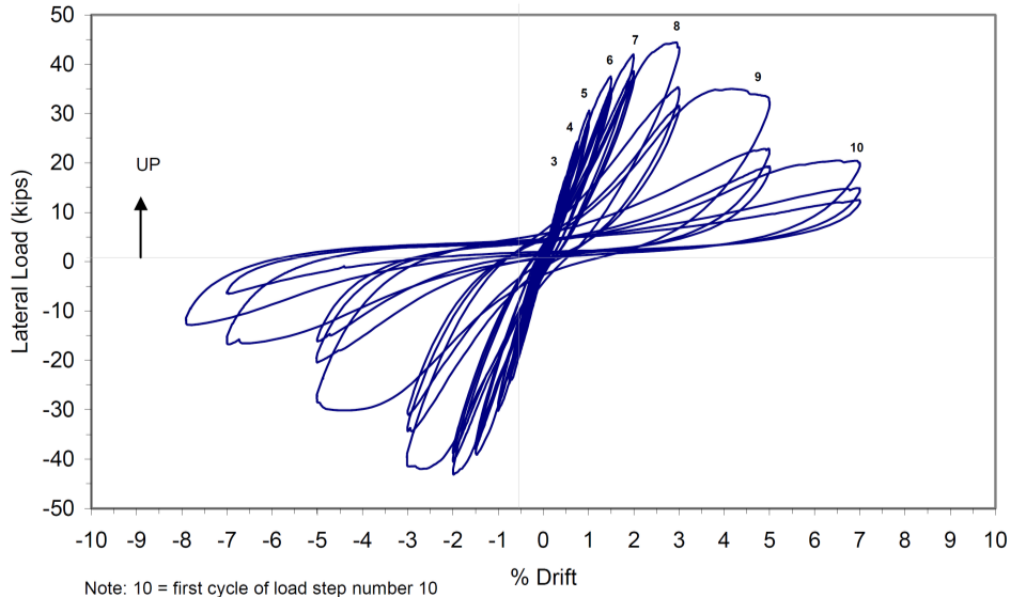


Figure C-8 Column shear versus drift for a shear-controlled exterior joint specimen (Unit 6, from Pantelides et al., 2002) with no joint transverse reinforcement, maximum joint shear stress, $\tau_{\max} = 11.3\sqrt{f'_c}$, beam bar anchorage with 180-degree hooks, and column axial load = $0.25A_g f'_c$. Joint design is not compliant with ACI requirements for special moment frames.

Table C-2 Response Models for Exterior Beam-Column Joints

Reference	Cyclic or Envelope	Defining Characteristics	Pros	Cons
Sharma et al. (2011)	Envelope to cyclic response	<ul style="list-style-type: none"> - Model includes τ vs. γ for joint core derived from Priestley (1997) principal tensile stress model - Maximum tensile stress is empirically calibrated; one strength for well-anchored bars and one strength for bars with 6 in. straight anchorage length 	<ul style="list-style-type: none"> - Simple - Validated using data from 12 joint subassemblage tests; specimens have range of design characteristics and exhibit anchorage and joint failure - Does not require bar slip section 	<ul style="list-style-type: none"> - Model cannot be directly applied to joints with straight beam bar anchorage lengths other than 6 in. - Proposed implementation/spring model is different from that shown in Figure C-2 - Validation was not in OpenSees, used zero-length plastic hinges for beams and columns and used a spring configuration different from that in Figure C-2 - Requires definition of cyclic response quantities; recommendations of Mitra and Lowes (2007) may not be appropriate given as different strengths in +/- directions.
Kim and LaFave (2009)	Envelope to cyclic response	<ul style="list-style-type: none"> - Defines response for joints with well-anchored beam longitudinal reinforcement (90- or 180-degree hooks) - τ vs. γ model - Developed using experimental τ vs. γ data - Quadrilinear envelope, trilinear to maximum strength and then descending branch to 90% maximum strength - Envelope points are functions of multiple design parameters (e.g., geometry, joint reinforcement ratio, concrete strength) 	<ul style="list-style-type: none"> - Developed using large data set - Includes descending branch of response curve, so no additional modeling is required to simulate strength loss 	<ul style="list-style-type: none"> - Implementation in OpenSees requires definition and use of bar slip section model to simulate strength loss due to anchorage failure; this can be defined using Mitra and Lowes (2007) and Berry (2006) - Requires definition of cyclic response quantities; these could be taken from Mitra and Lowes (2007) - Model calibration, for individual joint design, requires calculation of a number of design parameters - Requires definition of post-peak response; model only predicts response through 10% strength loss
Mitra and Lowes (2007); Anderson et al. (2008); Birely et al. (2012)	Envelope to cyclic response history and cyclic	<ul style="list-style-type: none"> - τ vs. γ models for interior beam-column joints - Assume that these can be applied to exterior joints - Employ bar slip section model to simulate pullout of beam bars with short, straight anchorage 	<ul style="list-style-type: none"> - Simple - Allows for use of same model for interior and exterior joints 	<ul style="list-style-type: none"> - Requires validation - Requires definition and use of bar slip section model to simulate strength loss due to anchorage failure - Requires definition of cyclic response quantities; these could be taken from Mitra and Lowes (2007)
Hassan (2011)	Cyclic	<ul style="list-style-type: none"> - τ vs. γ model to simulate joint core response combined with M vs. θ model to simulate bar slip - Developed for exterior joints in 3D frames and applied to 2D joints 	<ul style="list-style-type: none"> - Simple - Developed for use in OpenSees; validated using subassemblage model and test data 	<ul style="list-style-type: none"> - Not validated for exterior joints in which beam bars have inadequate straight anchorage - Validation effort for 2D joints is limited
Park (2010)	Cyclic	<ul style="list-style-type: none"> - Moment, M vs. rotation, θ model to simulate joint response - Developed for exterior joints in 3D frames and applied to 2D joints. 	<ul style="list-style-type: none"> - Simple - Developed for use in OpenSees; validated using subassemblage model and test data 	<ul style="list-style-type: none"> - Does not include simulation of bar slip and cannot simulate failure due to pullout of beam bars with short anchorage lengths - Validation effort for 2D joints is limited

Given that the top story of a frame is typically not a critical region of the frame with respect to collapse under earthquake loading, accurate simulation of response for these components should be considered less important than for interior or exterior joints. Relatively little research has addressed the earthquake response of knee joints in older, or modern, building frames. For knee joints, joint shear demands are likely similar in magnitude to those in exterior joints; for older joints, inadequate anchorage detailing for beam and/or column bars terminating in the knee joint likely controls response. Kim and LaFave (2009) provide a joint shear stress, τ , versus joint shear strain, γ , model for the envelope of the cyclic response history for knee joints with transverse reinforcement and adequate anchorage detailing for beam and column reinforcement. Recommendations are provided for extending this model to the case of no transverse reinforcement with adequate anchorage detailing, but no data exist for validation. The Kim and LaFave model could be extended for use in cyclic loading using the recommendations of Mitra and Lowes (2007).

For the current study, the Kim and LaFave model is recommended for simulating the response of modern joints. This model in combination with bar slip section models at the beam-joint and column-joint interfaces is recommended for simulating the response of older knee-joints with inadequate straight bar anchorages for beam and/or column longitudinal reinforcement anchored in the joint.

C.5 Models for Joints in 3D Frames

In 3D frames, the interior, exterior, and knee joints described above are extended to include continuous or terminating beams in the out-of-plane direction, and are subjected to loading in the out-of-plane direction. The addition of beams framing into the joint is typically understood to improve joint core response by providing additional confinement of the core. However, 3D loading may increase joint damage and reduce joint deformation capacity. Relatively few experimental studies have addressed joints in 3D frames. Model development activities have employed data from 3D joint tests to calibrate 2D joint response models such as those described above; however, 3D joint models in which in-plane and out-of-plane response are coupled do not exist.

Joints in 3D frames may be modeled in OpenSees using the configurations shown in Figures C-1 and C-2 with the addition of another node at the center of the joint, a second rotational spring to simulate the joint response in the out-of-plane direction, and, depending on the number of beam segments extending in the out-of-plane direction, one or two rigid links within the joint volume extending in the out-of-plane direction(s) and one or two beam-column elements in the out-of-plane direction(s). Using this modeling approach, joint behavior in the in-plane and out-of-plane directions is not coupled.

C.5.1 Interior Joints in 3D Frames

Interior joints in 3D frames represent the intersection of a continuous column, a continuous beam, and either a second continuous beam or a beam that terminates at the joint. Relatively few experimental or numerical studies have addressed these joint configurations; no experimental studies have addressed interior joints in 3D frames without transverse reinforcement. Beams and columns framing into all sides (or all but one side) of the joint could be expected to provide some additional confinement of the joint core and improve performance; however, interior joint subassemblages with transverse reinforcement in 3D frames have exhibited joint failure prior to beam yielding in the laboratory. Given the potential for joint failure, simulation of the nonlinear response of interior joints, including reduced stiffness as well as strength loss, is required for the current study. The model developed by Kim and LaFave can be extended to interior joints from 3D frames; but only a few data exist for validation of the model for joints with transverse reinforcement and no data exist for validation of the model for joints with no transverse reinforcement. For the case of older interior beam-column joints with three beam segments framing into the joint, it is likely that anchorage of beam reinforcement is inadequate and will control response. In this case, the model by Kim and LaFave should be supplemented by a bar slip section model at the joint-beam interface.

C.5.2 Exterior Corner Joints in 3D Frames

Recent research at the University of California, Berkeley (Park, 2010; Hassan, 2011) has addressed the earthquake response of older exterior joints in 3D frames and, in particular, older exterior corner joints in 3D frames. This research included experimental tests of exterior corner joints to investigate the impact on response of column axial load, beam-to-column depth ratio, joint shear demand/beam longitudinal reinforcement ratio, and load history. Modeling efforts addressed definition of joint strength as well as development of joint cyclic response models. Two models by Park (2010) and Hassan (2011) were developed using OpenSees, and validated using OpenSees models of subassemblages and experimental data for exterior joints and exterior corner joints in 3D frames. They provide acceptably accurate simulation of measured response. The model by Park does not explicitly separate deformation due to joint shear response and bar slip, while the model by Hassan does. Neither model addresses simulation of response for joints in which beam bars have inadequate, straight anchorage within the joint; in this case, the models should be combined with bar slip fiber section models at the joint-beam interface.

Appendix D

Modeling Gravity Load Failure in Collapse Simulations

by K.M. Mosalam, and M.S. Günay
University of California, Berkeley
Berkeley, California

D.1 Abstract

This paper investigates the different options that can be used for modeling gravity load failure of critical structural components of nonductile reinforced concrete (RC) buildings. The considered options are non-simulated failure and the three approaches for explicit modeling of gravity load failure, namely element removal, assignment of low stiffness to a failed element, and representation of the post-failure response of failed elements with degradation. This paper presents advantages and disadvantages of the different options, along with the models that can be used for failure detection in explicit modeling and a brief note on explicit modeling of gravity systems. The last section of the paper consists of brief comments/guidance on fiber section modeling, infill wall modeling (including collapse), and Monte Carlo simulations. In this part of the paper, a deterministic sensitivity analysis, the so-called tornado diagram, is presented as a method to reduce the number of variables involved in Monte Carlo simulations. Benefiting from this analysis, research efforts and resources can be strategically allocated for further investigations on critical issues in collapse simulation of nonductile RC buildings.

D.2 Gravity Load Failure Modeling

In order to model the gravity load failure of the critical structural components of nonductile reinforced concrete buildings, there are two alternative options that can be considered. The first option is the explicit modeling of gravity load failure, while the second option is the determination of gravity failure of the components through post-processing, without the explicit modeling of gravity failure (non-simulated failure). In the second approach, engineering demand parameters, such as drifts, obtained as a result of the analyses can be used to determine collapse by comparing these engineering demand parameters with the limits provided by the available gravity loss models (e.g., Elwood and Moehle, 2005). To determine the more suitable option to be used in collapse simulations, it is useful to consider one of the collapse indicators mentioned in the NIST report, *Program Plan for the Development of Collapse Assessment and Mitigation Strategies for Existing Reinforced Concrete Buildings*, (NIST, 2010b). The considered collapse indicator from the *Program Plan* is the

“maximum fraction of columns at a story experiencing axial failures,” which requires the identification of the number of columns experiencing gravity load failures. Such identification could be inaccurate if executed by post-processing of results without explicit consideration of gravity load failure, because the gravity load failure of a column (or a beam-column joint) is likely to affect response of the other columns and the overall system. Accordingly, it is preferable to explicitly model the gravity load failure of critical components for an accurate determination of collapse indicators and the collapse probability.

Non-simulated failure could only be feasible in cases where the first column axial failure is sufficient to define global collapse. Such a case may occur when all the columns at a story have similar properties and failures of all columns are likely to take place almost simultaneously. In this case, there is no need to explicitly consider the consequences of an axially failed column.

Explicit modeling of gravity load failure consists of two stages. The first stage is the detection of gravity load failure. Available models in literature for columns and beam-column joints that can be used for this purpose are mentioned in the following section of this paper. The second stage is the post-failure modeling, which include the following possible options: (1) element removal, (2) assigning low stiffness to a collapsed element; and (3) representing the post-failure response with degradation. The first approach consists of the direct removal of the element from the structural model upon failure of the element (e.g., Talaat and Mosalam, 2007; 2009). The second approach consists of reducing the stiffness of the collapsed element using a small multiplier (e.g., Grierson et al., 2005) in order to eliminate its contribution to the global structural stiffness matrix. The third approach consists of representing the post-failure response with a degraded force-displacement relationship (e.g., Elwood and Moehle, 2005). Advantages and disadvantages of these three methods are summarized in Table D-1 along with the non-simulated gravity load failure approach mentioned above.

The element removal approach of Talaat and Mosalam (2007) is based on dynamic equilibrium and the resulting transient change in system kinematics. It constitutes the basis of a corresponding progressive collapse algorithm. This algorithm is implemented in OpenSees for automatic removal of collapsed elements during an ongoing simulation, represented in Figure D-1. The implementation is carried out as a new OpenSees module, designed to be called by the main analysis module after each converged integration time step to check each element for possible violation of its respective removal criteria. The relevant models presented in the next section can be used for defining these removal criteria. A violation of a pre-defined removal criterion triggers the activation of the algorithm on the violating element before returning to the main analysis module. Activation of the element removal algorithm includes updating nodal masses, checking if the removal of the collapsed element

Table D-1 Advantages and Disadvantages of Different Gravity Load Failure Modeling Methods

Component Failure Method	Advantages	Disadvantages
Element removal	<ol style="list-style-type: none"> 1. Eliminates numerical problems associated with ill-conditioned stiffness matrices. 2. Enforcing dynamic equilibrium enables: <ul style="list-style-type: none"> - the computation of the resulting increase in nodal accelerations - the inclusion of the system's complete kinematic state at time of element collapse in determining if it can survive to a new equilibrium state. 3. Can track motion of the collapsed element relative to the damaged system to estimate the time and kinetics of a subsequent collision with the intact part. 4. Eliminates the numerical convergence problems related to the iterative formulation of some element and material types by removing them (see Disadvantages of "Non-simulated failure"). 	<ol style="list-style-type: none"> 1. Requires additional book-keeping operations to update the nodal masses and to check nodal forces, constraints, restraints, dangling nodes, and floating elements. 2. Introduces an additional computational burden by redefining degrees of freedom of a structural model and the corresponding connectivity. 3. Results in convergence problems, not on the element or material levels, but on the numerical integration level, because of the sudden updating of mass, stiffness, and damping matrices, as well as the local vibrations triggered as a consequence of the resulting transient effect (refer to discussions on the methods to overcome these convergence problems).
Assigning low stiffness to a failed element	<ol style="list-style-type: none"> 1. Avoids additional tasks related to the element removal process (Items 1 and 2 in Disadvantages of "Element Removal"). 	<ol style="list-style-type: none"> 1. Introduces numerical problems associated with ill-conditioned stiffness matrices. 2. Fails to explicitly consider the consequences of component failure (Items 2 and 3 in Advantages of "Element Removal").
Degraded post-failure response	<ol style="list-style-type: none"> 1. Avoids additional tasks related to the element removal process (Items 1 and 2 in Disadvantages of "Element Removal"). 	<ol style="list-style-type: none"> 1. Introduces numerical convergence problems related to the iterative formulation of some element, e.g., force-based beam-column, and material types, e.g., Bouc-Wen, since the failure state generally occurs at a negatively sloped portion of the constitutive relationship. 2. Fails to explicitly consider the consequences of component failure (Items 2 and 3 in Advantages of "Element Removal").
Non-simulated failure	<ol style="list-style-type: none"> 1. Becomes suitable for fast and simplified analyses in some special cases (e.g., having similar columns in a story). 	<ol style="list-style-type: none"> 1. Produces inaccurate results due to the lack of realistic representation of post-failure response.

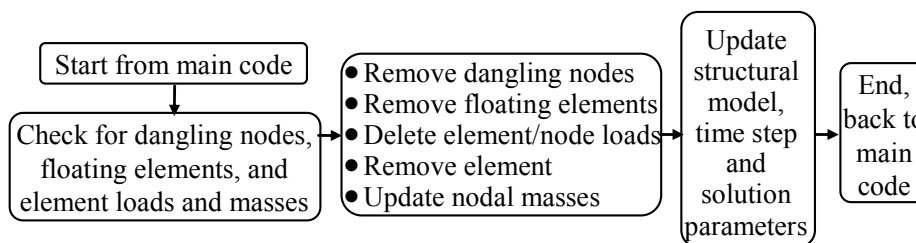


Figure D-1 Element removal algorithm (Talaat and Mosalam, 2007).

results in leaving behind dangling nodes or floating elements which must be removed as well, and removing all associated element and nodal forces, imposed displacements, and constraints.

Since the structural elements lose their ability to support gravity loads after gravity load failure, the removal of a failed element is the most representative approach to model gravity load failure. Hence, the discussion in the following two paragraphs compares the element removal approach (Option 1) with Options 2 and 3. It should be mentioned that the approach of Option 1 assumes that the gravity load support is lost instantaneously. As previously mentioned, the first stage of gravity load failure explicit modeling is the detection of this failure. Such detection is based on equations derived from tests where the loss of the gravity load support of the specimen is defined by a single point, and there are no data obtained from the tests beyond this point. Accordingly, the assumption of instantaneous gravity load failure is dictated by the gravity failure detection models. Alternately, the detection equations can be constructed with a probability distribution (e.g., in the form of a set of equations for the median and median plus/minus a dispersion). However, these types of equations require further tests.

The removal of a collapsed element requires several book-keeping operations to update the nodal masses and to check nodal forces, constraints, restraints, dangling nodes, and floating elements. There is an additional computational burden introduced by the redefinition of degrees of freedom of a structural model and the corresponding connectivity. Option 2 (which consists of assigning low stiffness to failed elements) avoids such additional tasks. However, there are three important advantages of Option 1 compared to Option 2. First, it avoids numerical problems due to ill-conditioned stiffness matrices. Second, enforcing dynamic equilibrium enables: (1) the computation of the resulting increase in nodal accelerations; and (2) the inclusion of the system's complete kinematic state at time of element collapse to determine if the structure can successfully redistribute the forces from the removed element and survive to a new equilibrium state. Third, the motion of the collapsed element can be tracked relative to the damaged system to estimate the time and kinetics of a subsequent collision with the intact part.

Although representing the post-failure response with a degraded force-displacement relationship in Option 3 is realistic for most of the failed components, it may introduce numerical problems. The failure state generally corresponds to a negatively sloped portion of the constitutive relationship, where the iterative formulation of some element (e.g., force-based beam-column), and the material types (e.g., Bouc-Wen (Baber and Wen, 1981)) are likely to experience convergence problems. The removal of such elements automatically eliminates the associated numerical problems. Analyses conducted to estimate the responses obtained from shaking table tests of a nonductile RC frame showed that the analyses considering

and not considering the element removal were both successful in predicting the observed collapse of the nonductile members (Mosalam et al., 2009). On the other hand, the response after collapse was rather jagged and close to being unstable for the case without element removal. In contrast, analysis for the case with element removal provided a more reasonable response, see Figure D-2. It should be noted that the analyses without the element removal used the degraded post-failure approach (Option 3).

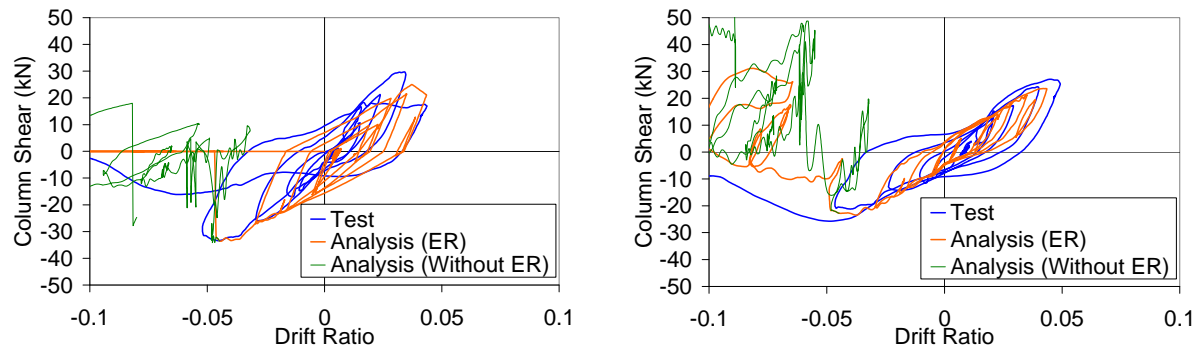


Figure D-2 Response of a system with nonductile columns experiencing axial failure from shaking table tests and analyses with and without element removal, ER (Mosalam et al., 2009).

Element removal may introduce convergence problems, not on the element or material levels, but on the numerical integration level, as a result of the sudden updating of mass, stiffness, and damping matrices, and the triggered local vibrations resulting from transient effect. Possible solution to such convergence problems include the adaptive switching of solver type and convergence criteria and the reduction of integration time steps (Talaat and Mosalam, 2007). It should be noted that this strategy was used for the analyses of the nonductile reinforced concrete frame mentioned in the above paragraph. Another effective solution is the use of transient integrators that do not require iterations, e.g., operator-splitting methods (Hughes et al., 1979). Recent preliminary analyses conducted on bridge systems showed that the operator splitting method results in exactly the same solution with the commonly used implicit Newmark integration, even for cases with highly nonlinear response.

D.3 Detection of Gravity Load Failure for Columns

One of the models that can be used to detect the gravity load failure of columns is the one proposed by Elwood and Moehle (2005), where the drift at axial failure of a shear-damaged column is represented as follows:

$$\left(\frac{\Delta}{L}\right)_{\text{axial}} = \frac{4}{100} \frac{1 + (\tan \theta)^2}{\tan \theta + P \left(s / \left(A_{st} f_{yt} d_c \tan \theta \right) \right)} \quad (\text{D-1})$$

where $(\Delta/L)_{axial}$ is the column drift ratio at axial failure, P is the column axial force, A_{st} is the area of transverse reinforcement, f_{yt} is the yield strength of transverse reinforcement, s is the spacing of transverse reinforcement, d_c is the column core depth (center to center of tie), and θ is the critical crack angle from the horizontal (assumed 65 degrees).

Elwood and Moehle (2005) stated that this axial failure model is based on data from 12 columns, where all columns were constructed of normal strength concrete, were the same in height-to-width ratio, were designed to yield longitudinal reinforcement prior to shear failure, and were tested in uniaxial bending. Despite these limitations, Fardipour et al. (2011) mentioned that the drifts estimated with a modified version of Equation D-1 were in reasonable agreement with the test results of four cantilever columns with axial load ratios of 20% to 40%, a nominal transverse bar ratio of 0.07%, and a vertical bar ratio of 0.5% to 1%. The modifications of Fardipour et al. (2011) to Equation D-1 consisted of: (1) change of the crack angle to $55 + 35P/P_o$ for $P/P_o < 0.25$, and 59 for $P/P_o > 0.25$, where P_o is the axial force capacity of the undamaged column; and (2) addition of the yield drift to calculate the drift corresponding to axial failure. However, it is to be noted that change of the crack angle is inappropriate due to the way that the equation was developed.

This axial capacity model is implemented in OpenSees as a limit state material model and used as a spring connected to a column end. Removal of the corresponding spring is also implemented in OpenSees (although not in the latest version of the program). When the drift during a simulation reaches the drift corresponding to axial failure, the spring in question is removed using the element removal algorithm.

D.4 Detection of Gravity Load Failure for Beam-Column Joints

Beam column joints of old nonductile reinforced concrete buildings (i.e., those designed in the 1960s) are generally unreinforced. The beams connected to such joints rotate relative to the columns (i.e., the right angle between the beam and column is not maintained due to joint shear failure and corresponding deformation). Joint panel flexibility can be modeled by using a rotational spring located between the beam and column end nodes. As illustrated in Figure D-3, rigid end offsets are used at the beam and column ends to model the physical dimensions of the joints.

The rotational spring is defined by a nonlinear constitutive relationship, which is characterized by a backbone curve and a set of hysteresis rules (Park and Mosalam, 2013b). These characteristics are empirically developed based on the measured joint responses and visual observations from the recent tests of four corner joint specimens (Park and Mosalam, 2013a) and verified by comparison with other exterior and interior beam-column joint tests. Accordingly, a strength model is developed to determine the peak force of the backbone curve, which also corresponds to the joint

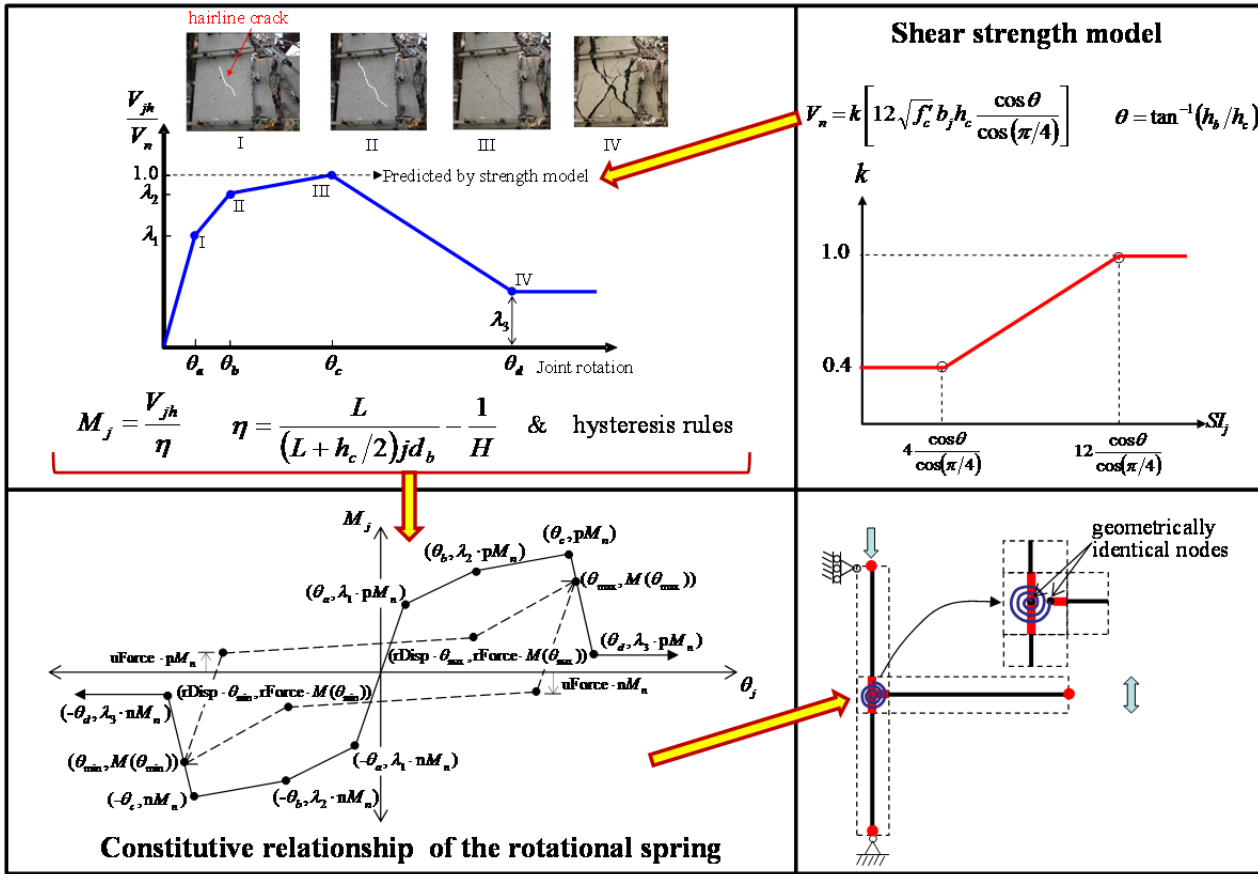


Figure D-3 Overview of unreinforced beam-column joint model (Park and Mosalam, 2012a). Refer to source for definition and use of these parameters.

shear strength (Park and Mosalam, 2009; 2012a). This practical strength model accounts for the effects of: (1) the joint aspect ratio defined as the ratio of beam to column cross-sectional heights; and (2) the beam reinforcement ratio, as its main parameters. The model is verified by its accurate predictions of various beam-column joint test results available in the literature (Park and Mosalam, 2012a, 2012c).

The rotational spring and the constitutive relationship mentioned above can be used to represent the axial failure and corresponding removal of a beam-column joint using the proposed extension by Hassan (2011). He proposed an axial capacity model for beam-column joints where the drift (i.e., beam tip displacement normalized by the beam length, in reference to the testing setup in Park and Mosalam, 2012b), at axial collapse, is represented as a function of the axial force and the beam bottom reinforcement strength (see Figure D-4).

Equation D-2 is suitable to be used to remove a beam-column joint as a part of the progressive collapse algorithm when the drift in this equation is replaced by joint rotation of the considered analytical model as shown in the bottom-left of Figure D-3.

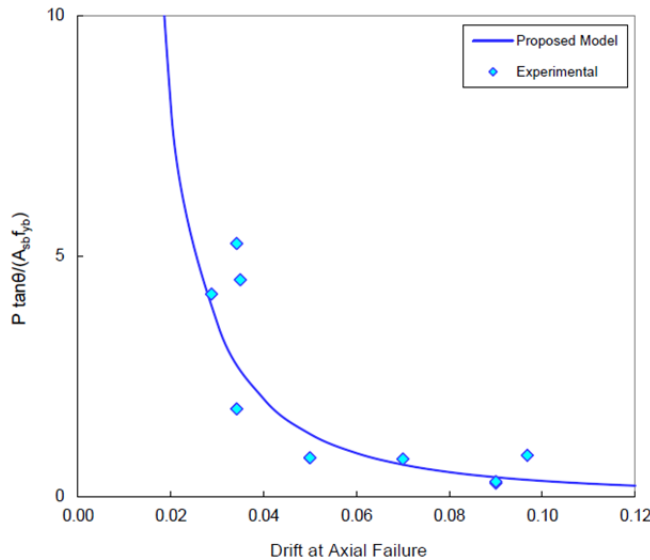


Figure D-4 Axial capacity model for beam-column joints (Hassan, 2011).

$$\theta_{axial} = 0.057 \left(\frac{P \tan \theta}{A_{sb} f_{yb}} \right)^{-0.5} \quad (D-2)$$

where θ_{axial} is the joint rotation at joint axial failure, P is the axial force, A_{sb} is the area of the beam bottom reinforcement, f_{yb} is the yield strength of the beam bottom reinforcement, and θ is the crack angle.

Note that the difference between the joint rotation and the above-mentioned drift in the tests of Hassan (2011) is the sum of the flexural deformation of the beam and the displacement due to column rotation (Figure D-5). However, it should be noted that this expression is based on a rather small joint axial failure database. Therefore, more joint axial failure tests are needed to further verify the relationship. Hassan (2011) also mentioned that the case of high axial load on a joint, where the beam flexural capacity is much smaller than the direct joint failure capacity, is excluded from the application of this model.

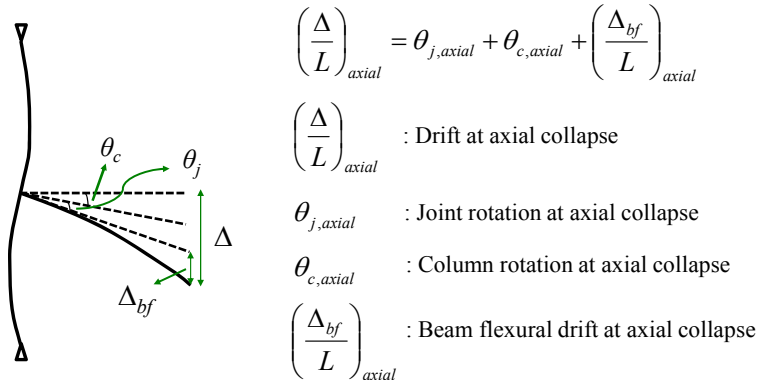


Figure D-5 Contribution of different components to beam tip displacement in a beam-column joint test.

The removal of a beam-column joint has not yet been implemented into OpenSees. However, the idea is similar to the case of column failure. When the rotation of the spring (representing the joint) during a simulation reaches the rotation corresponding to axial failure (Equation D-2), the joint (i.e., the rotational spring and rigid end offsets) is removed using the element removal algorithm.

D.5 Detection of Gravity Load Failure for Slab-Column Joints

Gravity support loss in slab-column joints can be defined with punching shear failure. In order to detect a punching shear failure, available limit models in literature, such as Elwood et al. (2007) or Hueste and Wight (1999), can be used. In these models, drift or plastic rotation values corresponding to the punching shear failure are determined as functions of the gravity shear ratio, which is defined as the value of the vertical gravity shear divided by the punching shear strength of the connection.

D.5.1 Explicit Modeling of Gravity Systems

Explicit modeling of the gravity system is a natural prerequisite for explicit modeling of gravity failure. As shown in Figure D-6, gravity support may not be completely lost after the lateral and axial failures of the primary system. Therefore, explicit modeling of the gravity system generally leads to a more accurate and realistic determination of global collapse.

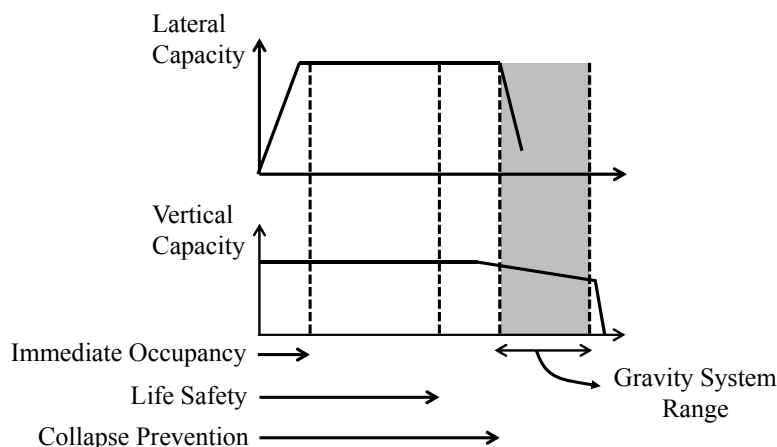


Figure D-6 Gravity system contribution to vertical capacity (Holmes, 2000).

D.6 General Modeling Guidance

This section provides brief comments and guidance about fiber section modeling, infill wall modeling, and Monte Carlo simulations.

D.6.1 Fiber Section Modeling

In nonlinear response history analyses, it is useful to consider bi-directional ground motions to correctly capture the column axial force and biaxial bending, especially

for corner columns. Accordingly, fiber discretization of column sections is more beneficial and accurate than the moment-curvature/interaction diagram representation of column sections. However, fiber discretization of beam sections may lead to artificial axial forces when rigid diaphragm constraints are present (OpenSeesWiki, 2012). Hence, it is preferred to define the force-deformation of beam sections in the form of moment-curvature relationships, which can be used along the full length of a member, thus allowing the consideration of distributed plasticity.

D.6.2 Infill Wall Modeling

Earthquakes in the last two decades (e.g., the 1999 earthquake in Kocaeli, the 2008, earthquake in Wenchuan, and the 2009 earthquake in L'Aquila) led to several observations related to unreinforced masonry (URM) infill walls. First, URM infill walls contribute to the stiffness and strength of the frames, as evidenced by the weak/soft story damage of the open ground story buildings and the torsional response created by the non-uniform distribution of infill walls around the building perimeter. Second, URM infill wall failure is a combination of in-plane and out-of-plane effects; this is evidenced by some of the URM infill wall failures occurring at the upper stories, where the story shear forces are the highest, instead of the lower stories. Third, the failure of infill walls at a story lead to the formation of weak/soft stories during the earthquake, which may result in the failure of a story, as evidenced by intermediate story collapses. Fourth, infill walls interact with the frame members, as evidenced by shear cracks and failures of columns and beam-column joints in infilled bays (Mosalam and Günay, 2012).

URM infill walls can be modeled to consider these observations. The first and second observations can be reflected by employing a practical model that considers in-plane and out-of-plane interaction of infill walls (Kadysiewski and Mosalam, 2008). The third observation can be considered by removing failed infill walls where detection of failure is based on a combination of in-plane and out-of-plane displacements (OpenSeesWiki, 2010). Finally, the fourth observation can be taken into account by modeling nonlinear shear springs at the column ends to consider the effect of additional horizontal forces transferred from the infill walls to the columns, following the partial separation of the infill walls from the frames. Such modeling of infill walls, considering the mentioned observations, has recently been used for the investigation of the structural response of buildings designed according to modern seismic codes (where infill walls are considered nonstructural in the design process), under the effect of earthquake ground motions (Mosalam et al., 2013).

D.6.3 Monte Carlo Simulations

In the NIST *Program Plan*, the key parameters that can be used to define collapse (i.e., collapse indicators), and their limits, are determined using collapse fragility curves. The development of fragility curves requires an extensive number of

analyses based on the Monte Carlo simulations of various random variables, including concrete strength, longitudinal and transverse reinforcement yield strength, concrete and masonry modulus of elasticity, masonry compressive and shear strengths, damping ratio, story mass, and ground motion parameters, including record-to-record variability. Consideration of all the relevant parameters as random variables may lead to an extensive and impractical number of simulations. However, uncertainties in some of these parameters may have insignificant effects on the variability of the structural response and, consequently, on collapse fragility curves. To identify and rank the effect of parameter uncertainties on response variability, it is possible to use a Tornado Analysis (Lee and Mosalam, 2006). Thus, parameters with insignificant effect can be treated as deterministic, thereby eliminating the burden of unnecessary simulations.

The tornado diagram, commonly used in decision analysis, has been used in sensitivity analysis in earthquake engineering (Porter et al., 2002). The diagram consists of a set of horizontal bars, referred to as swings, one for each random variable (i.e., considered parameter). The length of each swing represents the variation in the output (i.e., engineering demand parameters), due to the variation in the respective random variable. Thus, a variable with larger effect on the engineering demand parameter has larger swing than those with lesser effect. In a tornado diagram, swings are displayed in a descending order from top to bottom. This wide-to-narrow arrangement of swings resembles a tornado. In order to determine the swing due to a considered parameter, two extreme values (e.g., 10th and 90th percentiles), corresponding to pre-defined upper and lower bounds of the assumed probability distribution for the parameter, are selected. Considered engineering demand parameters are determined as a result of nonlinear response history analysis using the upper and lower bound values of the considered parameter, while the other input random variables are set to their best estimates, such as the medians. This process yields two bounding values of the engineering demand parameter variation for each input parameter. The absolute difference of these two values is the swing of the engineering demand parameter corresponding to the selected input parameter. This process is repeated for all the input parameters to compute the swings of the engineering demand parameters (Figure D-7). Finally, one builds the tornado diagram by arranging the obtained swings in descending order as mentioned above. The resulting tornado diagram generally provides an indicative picture for the selection of the necessary random variables to be used in the Monte Carlo simulations to develop the fragility curves (Lee and Mosalam, 2005).

D.7 Closure

Nonductile RC buildings are one of the main seismic safety concerns worldwide. Conservative seismic assessment of these buildings results in impractical decisions of extensive rehabilitation, which slows down the retrofitting operations and leaves the

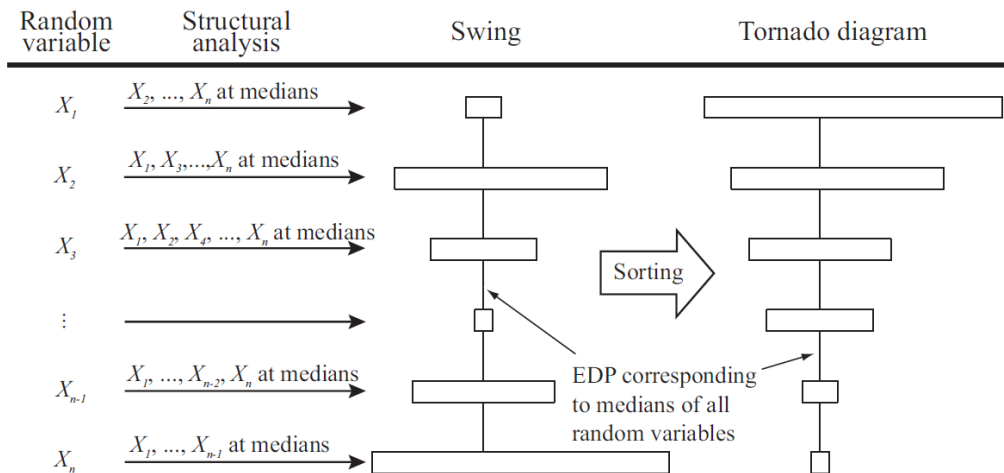


Figure D-7 Construction of a Tornado diagram (Lee and Mosalam, 2006).
EDP: engineering demand parameter.

buildings that are really under the risk of collapse vulnerable for a longer duration. Accordingly, there is a need to define methods for more refined seismic assessment of these buildings. Towards this basic objective, two issues are presented herein, namely: (1) the modeling of gravity load failure; and (2) a method for generating the Tornado diagram, to identify the influential uncertain parameters on the response variability and eliminate the burden of unnecessary simulations by treating the parameters with insignificant influence as deterministic. The first and second issues are useful to facilitate the accurate and efficient application of the refined seismic assessment, respectively.

Appendix E

Assessing the Effects of Displacement History on the Seismic Response of Reinforced Concrete Structures

by Santiago Pujol
Purdue University
West Lafayette, Indiana

E.1 Introduction

This workshop mini-paper discusses a deceptively simple question: can our best tools for numerical simulation accurately capture the effect of displacement history on the response of reinforced concrete structures? Displacement history here refers to number and amplitude of displacement reversals and to direction of displacement. Displacement refers exclusively to lateral displacement.

If we were at a stage in which common material properties inferred from uniaxial tests of isolated material coupons, geometry, and equilibrium sufficed to produce accurate estimates of structural response, the question could then possibly be addressed as a general question. But we do not seem to have reached that stage yet, as demonstrated by the abundance of alternative formulations used to understand element response. We have models for beam-columns, models for beam-column joints, models for slab-column connections, models for deep beams, and models for walls, to mention what first comes to mind. And then each type of structural element can exhibit radically different responses to a given displacement history, depending on whether the element is vulnerable to the effects of shear, the effects of combined flexure and axial load, or to both types of effects. One could even argue that torsion should be also considered. And to make matters worse, element response can be affected by nonstructural components such as infill walls. It follows that the question above would have to be asked for each component, structural or not, deemed critical to the seismic response of reinforced concrete structures, and it would have to be asked for each type of expected response. From that point of view, answering is simply daunting.

This paper is merely an invitation to consider the implications of the question. With that in mind, two admittedly narrow examples are provided. Because this note is being submitted to a workshop on collapse simulation, the examples chosen relate to

the most critical elements in frame structures in matters related to collapse: the columns. The first example addresses displacement-history effects on column lateral-load carrying capacity. The second example addresses displacement-history effects on column axial-load carrying capacity for columns likely to fail in shear, a clearly critical condition.

E.2 Example 1: Effect of Displacement History on Column Lateral-Load Carrying Capacity

E.2.1 *Columns Controlled by Flexure*

The fact that displacement history may have a dramatic effect on lateral-load carrying capacity has been known since the 1970s, when the first load-displacement curves from cyclic and monotonic tests were compared. The critical matter is that displacement capacity (i.e., the displacement at which lateral-load carrying capacity decreases permanently past a given threshold) is sensitive to the applied displacement history. The decrease in strength (and/or stiffness) can occur within a given displacement cycle or from one cycle to the next. There are many options to choose from when it comes to selecting a set of rules to represent cyclic or hysteretic response. One option that: (1) is receiving the attention of the profession today; (2) considers explicitly the strength/stiffness decay described; and (3) is readily available for numerical simulation on widely available software, is the ingenious model proposed by Haselton et. al. (2008). The model describes a set of hysteretic rules and includes six parameters to idealize hysteretic response. Each parameter is expressed as a function of geometric and material properties of the column through calibration against data from 255 column tests. The size of the database shows categorically that the development of the formulation took great effort. 86% of the columns in the database failed in flexure. All were reported to have reached their flexural capacities. Explicit measures of the dispersion of each parameter were provided so that the model can be used in Monte Carlo simulations (Liel et al., 2009).

Ideally, the efficacy of the model should be assessed through a systematic evaluation of its ability to reproduce easily quantifiable measures of column toughness. One clear choice should be drift capacity. It would be interesting to estimate drift capacity from the test results and then estimate it again from hysteretic curves generated numerically in a “pretend blind test.” Before making such an evaluation, it is difficult to state with certainty whether this or similar formulations “capture accurately” the effects of load reversals. Nevertheless, to motivate the workshop participants to investigate the potential of the chosen, or similar, formulation(s), the results of a simple exercise are presented. In this formulation one parameter represents the effects of load reversals: the cyclic deterioration rate, λ . The parameter was estimated by its proponents to be mainly a function of axial load level and tie spacing, which seems sensible as both parameters are related to the softening of the

concrete core described forty years ago by Wight and Sozen (1975). From the 255 column tests studied, Haselton et al. (2008) inferred values of λ varying from 10 to 150, in most cases. This range of variation is expected to represent a broad range of conditions and displacement histories. Figure E-1 shows the range of variation of inferred values of λ reported for 12 columns out of the 255 in the full sample. These columns were nominally identical, except for the fact that some had closer tie spacing than others. The only other differences among them were common deviations in measured concrete strength (not exceeding 20% of the mean) and the applied displacement history.

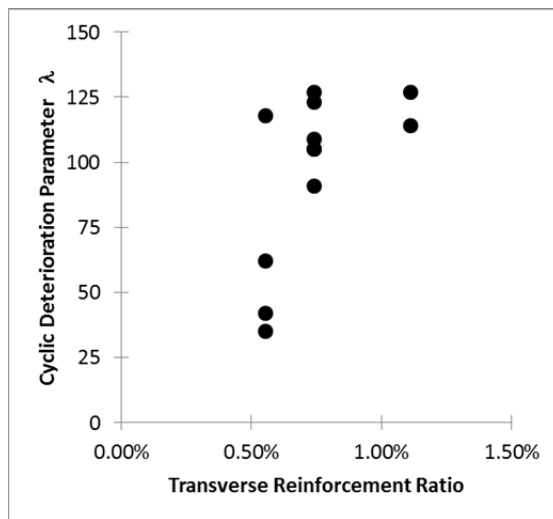


Figure E-1 Range of variation of inferred values of λ reported for 12 columns out of 255 in the full sample (NISEE, 2013b).

For a transverse reinforcement ratio of 0.6%, with all other column properties essentially constant, λ (the parameter meant to quantify the effect of cycles) was inferred to vary within a range nearly as large as the range of variation observed for the entire sample (of 255 columns). This suggests a simple fact: the task at hand is not simple. If models similar to the one discussed are used to estimate collapse vulnerability, their results need to be interpreted very carefully. To the knowledge of the writer, whether a more detailed model, perhaps one in which the hysteresis is defined at the material level instead of the element level, yields better results remains to be proven through systematic comparisons of measured and predicted drift capacity (or other measures of toughness). Until that is accomplished, the most efficient modeling techniques should be favored over other alternatives.

E.2.2 Columns Controlled by Shear

Henkhaus (2010) reported ratios of computed to estimated shear strength (Figure E-2). He considered columns: (1) subjected to nine different displacement histories; and (2) with shear strengths smaller than or similar to the shear associated with flexural capacity. Three of the displacement histories considered included cycles

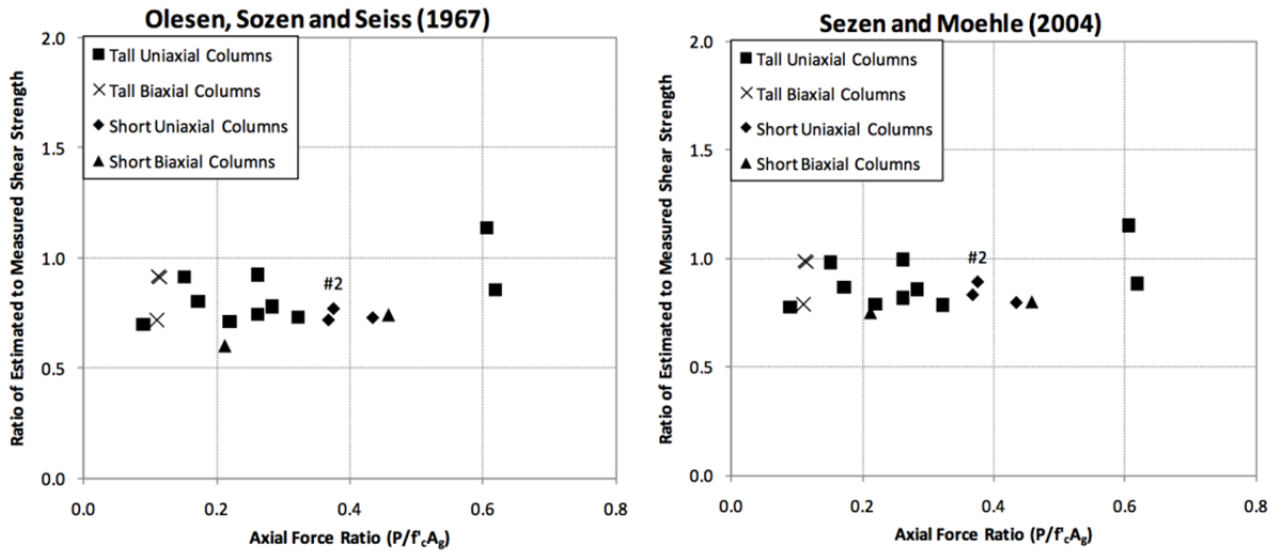


Figure E-2 Ratios of computed to estimated shear strength (Henkhaus, 2010).

along two perpendicular axes. Shear strength was computed in two different ways: (1) using a formulation calibrated using results from monotonic tests (Olesen et al., 1967); and (2) using a formulation calibrated using results from uniaxial cyclic tests (Sezen and Moehle, 2004). The results in Figure E-2 do not suggest that shear strength is critically sensitive to displacement history. From this, nevertheless, it does not follow that displacement capacity is not sensitive to number and direction of cycles. This sensitivity is not always high. Ranf et al. (2006) observed the drift at shear failure in circular columns with light transverse reinforcement to decrease by no more than 35% when the total number of cycles (of increasing amplitude) were increased from 6 to 75. The columns were reported to fail in shear after reaching their full flexural capacities.

E.3 Example 2: Effect of Displacement History on Column Axial-Load Carrying Capacity

This section addresses two questions:

1. If a column can resist axial load through displacement cycles applied after shear failure, is this resistance sensitive to displacement history (i.e., the number, amplitude, and direction of the cycles)?
2. How can it be quantified through analysis the effect of displacement history on the peak drift reached before or at axial failure?

A clear answer is provided for the first question, but no crisp answer is provided for the second question because the available information is not conclusive.

E.3.1 Question 1

The capacity of a column to resist axial load through displacement cycles applied after shear failure is indeed sensitive to displacement history. The tests by Sezen (2002) and Henkhaus (2010) showed this clearly. Figure E-3 compares the peak drift reached at or before axial failure for four columns. The columns represented by crosses were subjected to displacement cycles along two perpendicular axes. The columns represented by solid squares were tested along a single axis. Otherwise, the four columns represented in the chart were nominally identical. The plot shows that the columns subjected to more cycles (whether along a single axis or along two axes) failed at drift ratios approaching half the drift ratio reached by column 2CLD12, which was subjected to 7 cycles. The evidence seems clear in this case; it indicates that peak drift is indeed sensitive to displacement history.

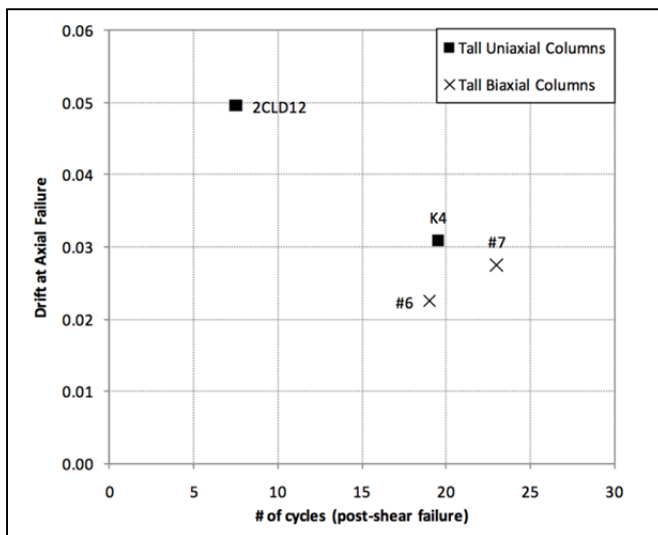


Figure E-3 Comparison of the peak drift reached at or before axial failure for four columns (Henkhaus, 2010).

E.3.2 Question 2

How to quantify the effect of displacement history on peak drift reached before or at axial failure?

The data in Figure E-3 can be interpreted to suggest that the increase in the number of cycles causes a decrease in the “effective coefficient of friction” associated with the inclined plane(s) that eventually leads (lead) to collapse. Elwood and Moehle (2005) estimated this coefficient as:

$$\mu = \frac{P - \frac{A_{st}f_{yt}d_c}{s}}{\frac{P}{\tan(\theta)} + \frac{A_{st}f_{yt}d_c}{s} \tan(\theta)} \quad (\text{E-1})$$

where μ is effective friction coefficient, P is applied axial load, A_{st} is area of transverse reinforcement, f_{yt} is yield stress of transverse reinforcement, d_c is the depth of concrete core, s is spacing of transverse reinforcement, and θ is the approximate angle between a horizontal line and the critical inclined crack (taken as the smaller of 65 degrees and the arctangent of the ratio of height to depth). Effective friction coefficients estimated using Equation E-1, compared with test data, are shown in Figure E-4.

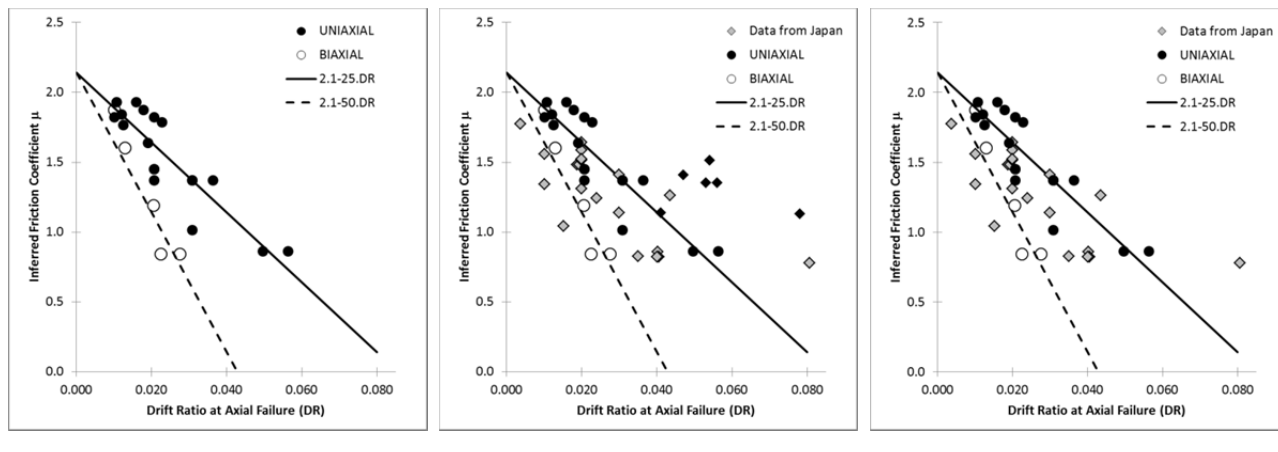


Figure E-4 Friction coefficients estimated using Equation E-1, compared to test data.

Figure E-4(a) shows results reported by Henkhaus (2010), Sezen (2002), and Lynn et al. (1996), and suggests that the reduction in effective friction coefficient with increasing peak drift demand accelerates in the case of biaxial loading.

Figure E-4(b) includes data produced by Japanese researchers. The black diamonds in Figure E-4(b) represent Japanese data from monotonic tests or tests in which the column failed in a monotonic “push” applied after a few initial cycles. The fact that these tests tend to yield larger peak drift ratios confirms the sensitivity of the response to number of cycles.

Figure E-4(c) excludes columns that failed in a monotonic “push.” Observe that a number of points representing uniaxial tests from Japan fall near the results from biaxial tests reported by Henkhaus. The total number of cycles applied in these Japanese tests was not larger than the number of cycles applied by Henkhaus. These observations indicate that the effect of displacement history may be as critical as the effects of other variables not considered in the formulation of Equation E-1. The ranges of the data plotted in Figure E-4 are shown in Table E-1.

Observe that the columns tested in Japan tended to have smaller ratios of height to depth. Nevertheless, no clear correlation between peak drift ratio and height-to-depth ratio was observed in the data, which include specimens with height-to-depth ratios

Table E-1 Ranges of the Data Plotted in Figure E-4

Parameter	U.S. Tests			Tests from Japan		
	Minimum	Median	Maximum	Minimum	Median	Maximum
<i>General Properties</i>						
Height-to-Depth Ratio	3.2	6.4	6.4	2.0	3.0	6.5
Axial Load Ratio	0.07	0.22	0.62	0.18	0.23	0.65
<i>Material Properties</i>						
Concrete Strength [MPa]	17	26	33	14	26	41
Longitudinal Reinf. Yield Stress [MPa]	330	440	490	340	400	450
Transverse Reinf. Yield Stress [MPa]	370	400	480	290	390	590
<i>Reinforcement Properties</i>						
Longitudinal. Reinf. Ratio	1.5%	2.5%	3.1%	1.0%	2.3%	4.8%
Transverse Reinf. Ratio	0.07%	0.07%	0.18%	0.08%	0.21%	1.02%
Tie Spacing/Depth	0.44	1	1	0.13	0.33	2.2
Tie Spacing/Long. Bar Diameter	9.2	14	21	2.8	6.3	20

as low as 3 reaching peak drift ratios as high as 8%. The columns tested in Japan also tended to have more and better distributed transverse reinforcement, but it is unlikely that this would have caused the low drift ratios shown in Figure E-4. All the data discussed here are accessible at NEEHub (NEES, 2012).

The two lines in Figure D-4(c) represent bounds for approximately two thirds of the data. They lead to this equation to estimate the drift ratio, DR , at axial failure:

$$DR = C \frac{1 + \tan^2(\theta)}{\tan(\theta) + P \frac{s}{A_{st} f_{yt} d_c \tan(\theta)}} \% \quad (\text{E-2})$$

where C is a coefficient discussed below, θ is the approximate angle between a horizontal line and the critical inclined crack (taken as the smaller of 65 degrees and the arctangent of the ratio of height to depth), P is the column axial load, A_{st} is the area of transverse reinforcement, f_{yt} is the yield stress of transverse reinforcement, s is spacing of transverse reinforcement, and d_c is depth of concrete core.

The solid line in Figure E-4 leads to $C = 4$. The broken line leads to $C = 2$. Within the range $2 \leq C \leq 4$, Equation E-2 captures two thirds of the data available for drift at

axial failure (Figure E-5). The initial idea at the time this note was drafted was to justify the variations in C in terms of the direction of the displacement cycles. But the spread of the data in Figure E-5 does not support that justification. Instead, the simplest option seems to be to say that C varies only in part as a function of displacement history. If Equation E-2 is to be used in analysis to detect axial failure, one needs to ask whether there may be scenarios in which the displacement history may deviate drastically from what was included in the calibration presented. Considering that the data produced by Henkhaus (2010) include results from columns subjected to as many as 30 cycles at drift ratios of 1% or more, that seems unlikely, but to use the analysis results to confirm this opinion would not be a waste of time.

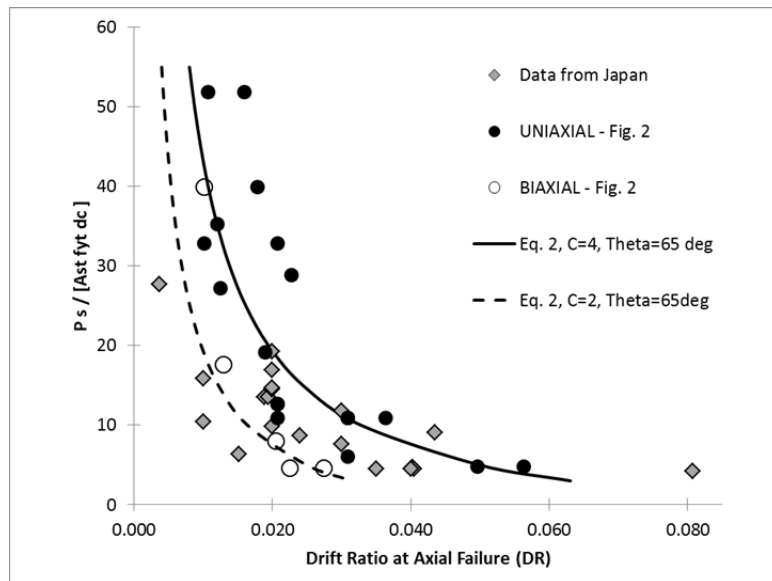


Figure E-5 Drift ratio at axial failure.

E.3.3 Discussion

In view of the uncertainties revealed by the data discussed in this section, it is prudent to ask: what is the goal of the desired but elusive formulation to quantify displacement-history effects? Certainly, we cannot predict confidently what may occur to a given group of vulnerable buildings during a future earthquake. The objective must therefore be to classify said buildings according to their vulnerability or to identify ranges of parameters within which collapse is more likely. If that is the case, one could assign a probability distribution to C (Equation E-2) and treat it as a “random” parameter in suites of nonlinear analyses. Given the data discussed here, the suggested variation in C would account for both the effects of number and direction of loading cycles and the effects of relevant parameters that we cannot yet identify. If the expectations are correct, 2D analysis should suffice for assessment of frames with vulnerable columns. But given that the margin between shear and axial failures is narrow (an average difference in drift ratio of 0.5% according to Henkhaus, 2010), we may also want to explore the option of concentrating on the

drift at shear failure (instead of the peak drift reached before or at axial failure) as an alternative vulnerability index. In the case of drift at shear failure we have much more experimental information available.

E.4 Other Topics that Require Further Discussion

The examples presented only scratch the surface of the problem this paper was meant to address. The participants of the workshop are asked to contribute by considering the cases described and these additional cases/issues:

- Slab-column connections.
- Beam-column joints.
- Structural walls.
- “Asymmetric” displacement histories (i.e., cases in which the drift reached in one direction is much larger than the drift reached in the other direction).
- The advantages and disadvantages of 3D analysis versus 2D analysis.

E.5 Conclusion

This paper is an invitation to consider one question: can our best tools for numerical simulation accurately capture the effect of displacement history on the response of reinforced concrete structures? The paper provides admittedly insufficient facts to help the reader answer confidently and completely. But the few facts provided and the uncertainties discussed indicate that:

- Simpler and computationally inexpensive numerical formulations are preferable over more detailed formulations, and
- Although numerical simulation may not yet yield accurate results, it can be used to rank a given set of structures and to identify ranges in which collapse may be more likely.

Appendix F

Collapse Simulation of Masonry-Infilled Reinforced Concrete Frames

by P. Benson Shing
University of California, San Diego
La Jolla, California

F.1 Introduction

The collapse simulation of masonry-infilled reinforced concrete frames presents a significant challenge because of their complicated failure mechanisms and the number of factors that could affect their behavior. There is also a lack of experimental studies in which such structures were tested to collapse. This paper summarizes possible failure mechanisms and causes of collapse of these structures, and presents a method to construct and calibrate a simplified analysis model that can be used for Monte Carlo collapse simulations. Additional research and development work needed to improve collapse simulations is also discussed. The information presented here is largely based on research supported by the National Science Foundation (NSF) under the Network for Earthquake Engineering Simulation (NEES) program.

F.2 Failure Mechanisms of Infilled Frames and Causes of Collapse

Under earthquake loading, the interaction of a reinforced concrete frame with masonry-infill walls can result in one of several possible failure mechanisms, depending on the strength and stiffness of the walls as compared to those of the frame. Figure F-1 shows three failure mechanisms that have been frequently observed in laboratories and in the field (Mehrabi et al., 1994; 1996).

Failure mechanism (a) may occur when infill walls develop profuse horizontal sliding shear cracks because of weak mortar joints; mechanism (b) may occur in nonductile reinforced concrete frames infilled with relatively strong masonry that tends to develop localized horizontal and/or diagonal cracks, as shown in Figure F-2; and mechanism (c) may occur in walls constructed of weak masonry units, such as hollow clay tile, which is vulnerable to compressive failure. Since the resistance of both the frame and the wall can be affected by the frame-wall interaction and the resulting failure modes, the lateral load resistance of an infilled frame is not a simple sum of those of a bare frame and a masonry wall acting independently.

Failure mechanisms

- (a) Horizontal sliding
- (b) Diagonal crack
- (c) Panel crushing

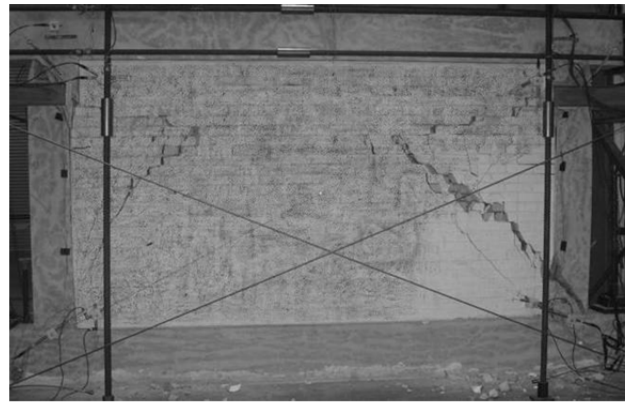
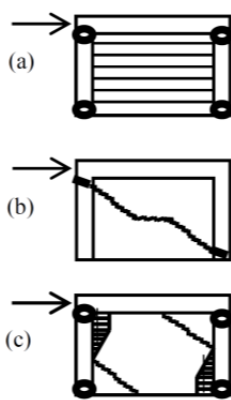
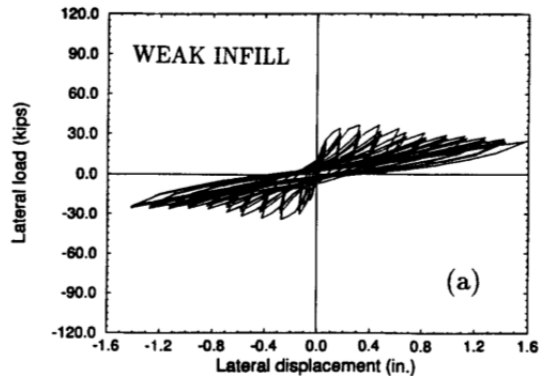


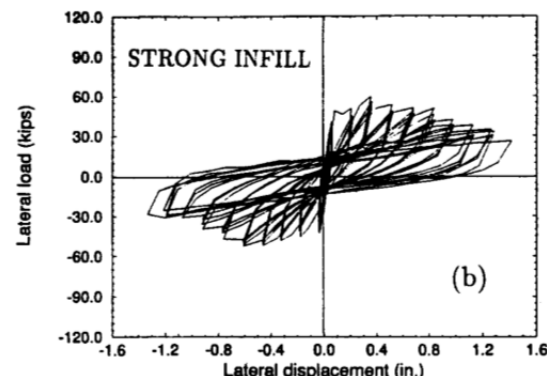
Figure F-1 Failure mechanisms of infilled frames (Mehrabi et al., 1996).

Figure F-2 Failure mechanism (b) exhibited in a quasi-static cyclic loading test (Blackard et al. 2009).

The ability of an infilled frame to resist earthquake loads depends not only on its strength but also on its ductility. As shown in Figure F-3, a frame exhibiting failure mechanism (a) tends to be more ductile than that mechanism (b). Furthermore, as shown in Figure F-4, increasing the axial load on an infilled frame governed by failure mechanism (b) can increase its lateral load resistance but reduce its ductility.



Mechanism (a)



Mechanism (b)

Figure F-3 Nonductile reinforced concrete frames with failure mechanism (a) and failure mechanism (b) from Figure F-1 (Mehrabi et al., 1996).

This can be explained by the fact that masonry-infill is the main load-resisting element of an infilled frame, and the lateral resistance of a masonry wall is largely governed by the shear resistance of the bed joints, which depends on the joint compressive stress. A higher axial load on the frame will have a higher compressive stress transmitted to the bed joints, and will, thereby, result in a higher shear resistance. Nevertheless, masonry units will be more susceptible to crushing failure when subjected to higher axial and shear stresses. Such crushing can occur in the interior of a wall (which is different from mechanism (c)) and will lead to more rapid

load degradation. The proportion of the gravity load carried by an infill wall depends on the construction sequence, which affects the load transfer, the ratio of the elastic axial stiffness of the wall to that of the reinforced concrete (RC) columns, the creep and shrinkage of the RC columns with respect to that of the wall, and the expansion of clay units due to moist absorption. A method to estimate the effect of creep on the gravity load distribution in an infilled frame can be found in Koutromanos et al. (2011).

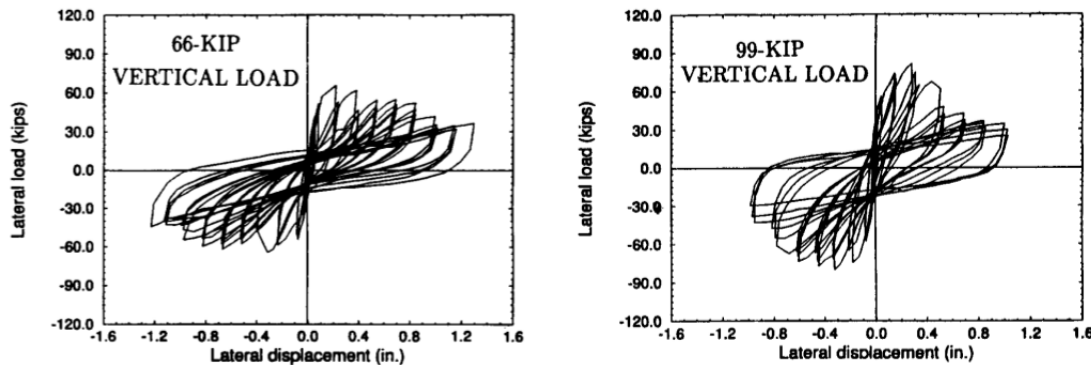


Figure F-4 Influence of vertical load in nonductile RC frames exhibiting failure mechanism (b) from Figure F-1 (Mehrabi et al., 1996).

Hence, it can be expected that the performance of an infilled frame and its susceptibility to collapse during earthquakes depend on many factors, including the strength and quality of the masonry infill, the locations of infill walls in the frame, the reinforcing details of the frame, and the resistance of the resulting system as compared to the seismic load demand.

Even though an infilled frame may exhibit an undesired failure mode (e.g., failure mechanism (b) shown in Figure F-1) and the falling debris of damaged masonry can be a major life-safety concern, both field observations from past earthquakes and laboratory studies (e.g., Stavridis et al., 2012) have shown that masonry-infill walls could significantly enhance the lateral resistance of a nonductile RC frame and protect it from major damage or collapse in a severe earthquake. The collapse of infilled RC frames in earthquakes was often associated with a weak-story mechanism, which could be attributed to the lack of infill walls in the bottom story or to the severe damage and loss of infill during strong shaking. Studies have shown that infill walls could develop a strong resistance to out-of-plane loads because of the arching mechanism that could develop with the bounding frame (Dawe and Seah, 1989; Angel et al., 1994; Mander et al., 1993; Bashandy et al., 1995; and Flanagan and Bennett, 1999). However, the effectiveness of the arching mechanism and the stability of a wall depend on its span-to-thickness (slenderness) ratio, and could be compromised by the damage and crushing failure of masonry under in-plane loads (see Figure F-5) and the presence of an opening in the wall (see Figure F-6).



Figure F-5 Collapse of masonry infill in 2008 Wenchuan earthquake (courtesy of P. Shing, with permission).



Figure F-6 Collapse of masonry infill with a window opening in a shaking-table test (Stavridis et al., 2012).

Therefore, to simulate the collapse of a masonry-infilled reinforced concrete frame, it is important that the model can directly or indirectly account for the following behaviors at the component and structural levels:

Component Level

1. The inelastic behavior of reinforced concrete members, including flexural hinging, diagonal shear failure, axial load failure of reinforced concrete columns, and failure of beam-to-column joints.
2. The inelastic behavior of masonry walls, including the cracking and shear sliding of mortar joints and the crushing failure of masonry units.
3. The loss of stability and out-of-plane collapse of infill walls, considering the influence of the arching mechanism, wall damage under in-plane loads, and wall openings.

Structural Level

1. Frame-wall interaction and the resulting failure mechanism.
2. The $P-\Delta$ (axial load-deformation) effect on the reinforced concrete frame.
3. The three-dimensional response under multi-axial ground motions.

F.3 Nonlinear Finite Element Models

A detailed nonlinear finite element model can capture the global as well as local failure behavior of an infilled frame. However, these models require a significant computational effort and are not suited for Monte Carlo simulations. They can be used, however, to calibrate simplified models to be used for that purpose.

There are two general finite element modeling approaches to simulate the fracture behavior of quasi-brittle materials, such as concrete and masonry. They are the

smeared and discrete crack approaches. The smeared crack approach has been often used to model diffused tensile cracks as well as the compressive failure of concrete in reinforced concrete structures. However, this approach suffers from several inherent limitations, including stress locking (Rots, 1991; Lotfi and Shing, 1991) that limits its ability to simulate the brittle behavior of a reinforced concrete member failing in diagonal shear and the shear sliding behavior of masonry joints. This limitation can be overcome by representing cracks in a discrete manner using zero-thickness interface elements. Hence, combining the smeared and discrete approaches is necessary to model the failure behavior of infilled frames in a realistic way (Stavridis and Shing, 2010; Koutromanos et al., 2011). An example of this is shown in Figure F-7, in which zero-thickness interface elements are used to model flexural and diagonal shear cracks in reinforced concrete columns and cracks in masonry joints. Smeared crack elements are used to model diffused damage, including compressive failure, in the concrete members and brick units.

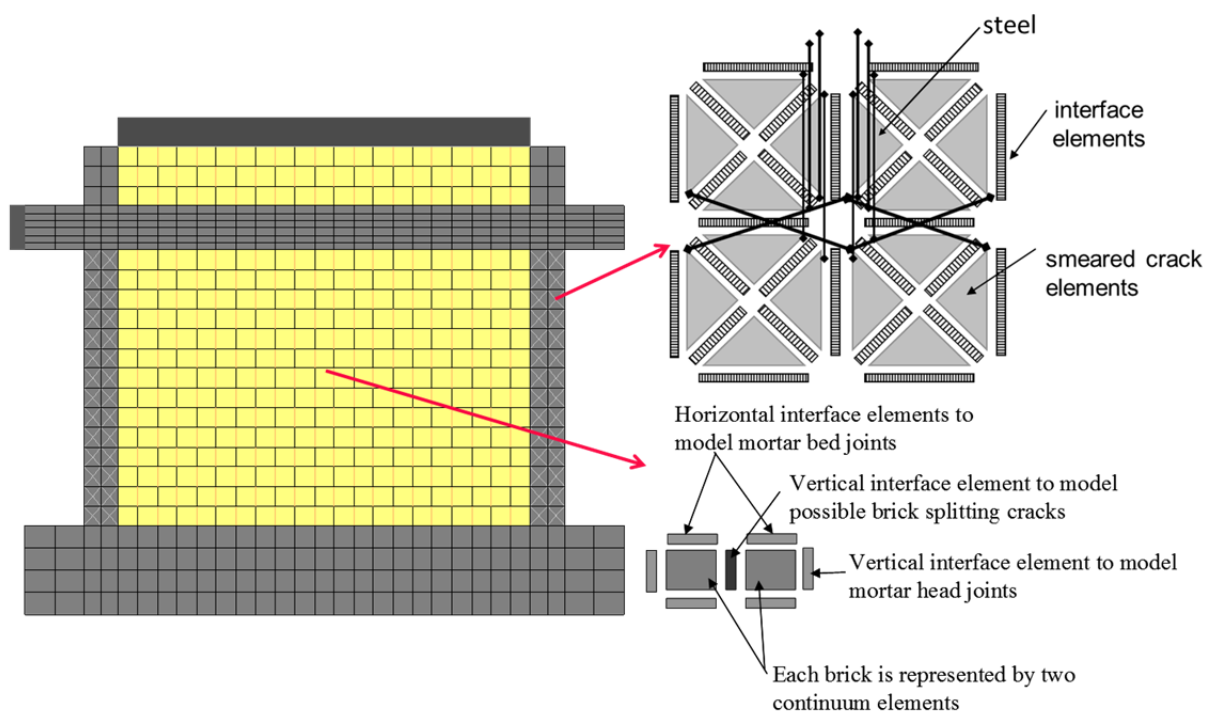


Figure F-7 Finite element modeling of a masonry-infilled RC frame.

Constitutive laws that can be used for the smeared crack and zero-thickness interface elements are described in Koutromanos (2011) and Koutromanos et al. (2011). Koutromanos (2011) has developed a cohesive crack constitutive law for the zero-thickness interface. This modeling approach has proven to be able to accurately capture the failure mechanism and load-displacement response of infilled frames up to a severe failure state, which normally corresponds to a story drift ratio beyond 1% and a lateral load degradation exceeding 50%. Figure F-8 shows the validation of

such a model with a quasi-static test conducted by Blackard et al. (2009), including the crack pattern developed in the model. A picture of the damaged specimen is shown in Figure F-2.

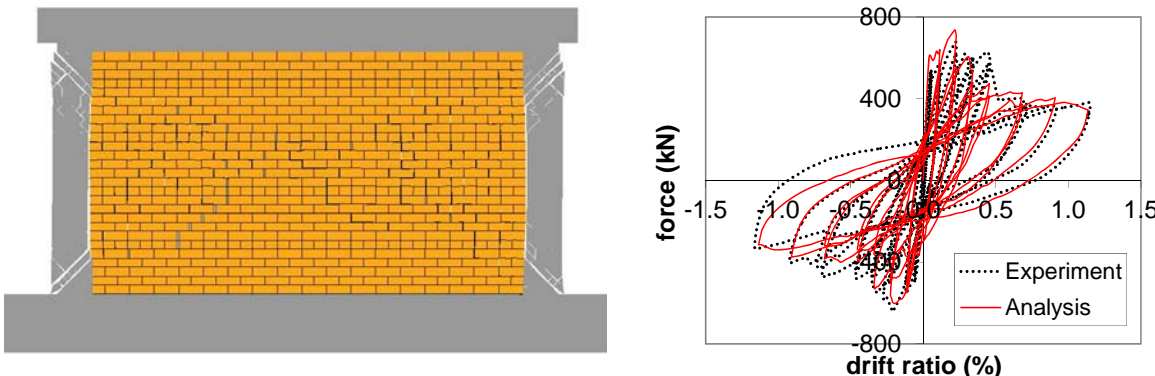
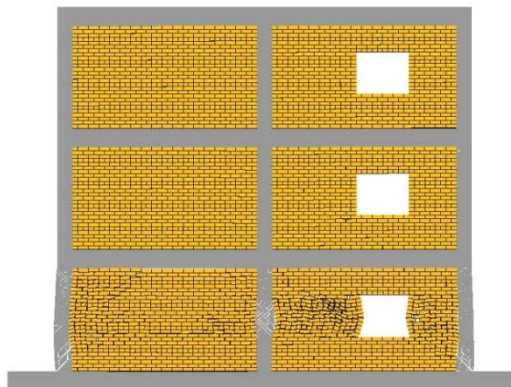


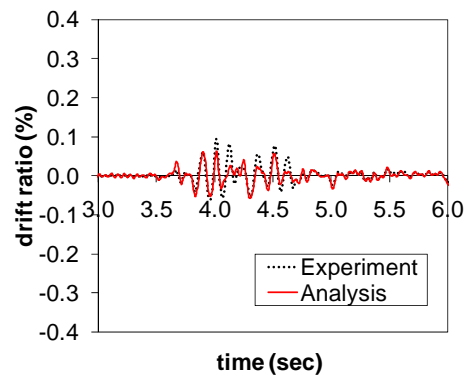
Figure F-8 Analysis of an infilled frame subjected to quasi-static cyclic loading (Koutromanos et al., 2011).

This modeling method has been successfully applied by Koutromanos et al. (2011) to simulate the response of a three-story masonry-infilled nonductile reinforced concrete frame tested on a shaking table by Stavridis et al. (2012). As shown in Figure F-9, the model is able to accurately capture the failure mechanism, response time histories, and base shear vs. bottom story drift relations of the structure through the second last run on the shaking table with the Gilroy motion (from the 1989 Loma Prieta earthquake) scaled to 120%. The specimen collapsed out-of-plane in the subsequent run with the 250% El Centro motion (from the 1940 Imperial Valley Earthquake) after severe diagonal shear failures had developed in the bottom story columns, and the bottom-story infill wall with a window had partially collapsed (as shown in Figure F-6). However, neither the out-of-plane collapse of the frame nor the collapse of the wall can be simulated by the model. This is because of the plane-stress formulation and the small displacement assumption used in the model.

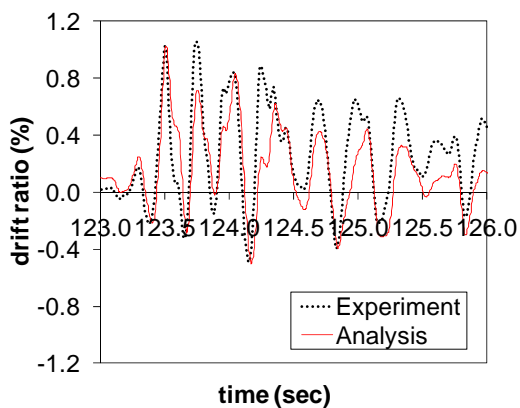
The constitutive models presented here can be extended to three dimensions to simulate the out-of-plane collapse of a frame and that of a masonry-infilled wall. While this extension is conceptually straightforward, it can significantly increase the computational effort. Furthermore, to simulate the collapse of a masonry wall due to brick dislocation and the axial load collapse of an RC column due to shear failure, the cohesive crack model for the zero-thickness interface element needs to be enhanced to account for the loss of contact due to shear sliding.



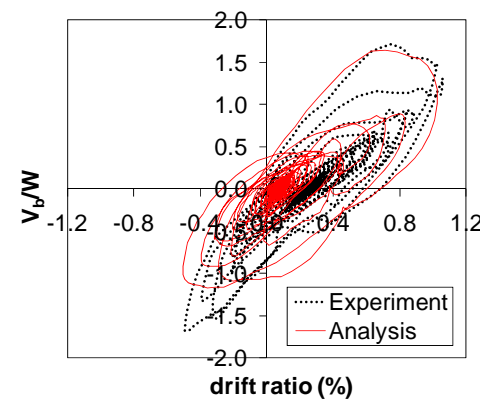
(a) Crack Pattern for 120% Gilroy motion



(b) Bottom-story drift time history for Gilroy motion scaled to 67%



(c) Bottom-story drift time history for Gilroy motion scaled to 120%



(d) Base shear vs. story drift for Gilroy motion scaled to 120%

Figure F-9 Analysis of a three-story infilled frame tested on a shaking table (Koutromanos et al., 2011).

F.4 Simplified Analysis Method

A simple and efficient approach to model infill walls in frame structures is to use the equivalent diagonal strut concept proposed by Holmes (1961), Stafford Smith (1967), and Mainstone and Weeks (1970). This concept has been investigated and extended by many others in later studies. However, the original equivalent strut theory was based on the observed behavior of small-scale steel frames infilled with brickwork and concrete. For masonry-infilled RC frames, the equivalent strut representation appears to be an over-simplification of the actual behavior, and fails to capture some key failure mechanisms, such as mechanisms (a) and (b) depicted in Figure F-1. A study by Stavridis (2009) based on detailed nonlinear finite element models has demonstrated that the compressive stress field in a masonry-infill wall may not be accurately represented by a single diagonal strut. As shown in Figure F-10, the force distribution developed in an infill wall can be quite different from that introduced by a diagonal strut.

Hence, replacing a wall by a diagonal strut will not lead to a realistic representation of the load transfer from the frame to the wall. Furthermore, it will not account for the possible shear failure of a column that could be induced by the frame-wall interaction. Models to simulate the shear and axial load failures of columns using zero-length springs have been proposed (Elwood, 2004). These elements can be combined with a strut model to account for the axial and shear failures of a column, in the way shown in Figure F-11.

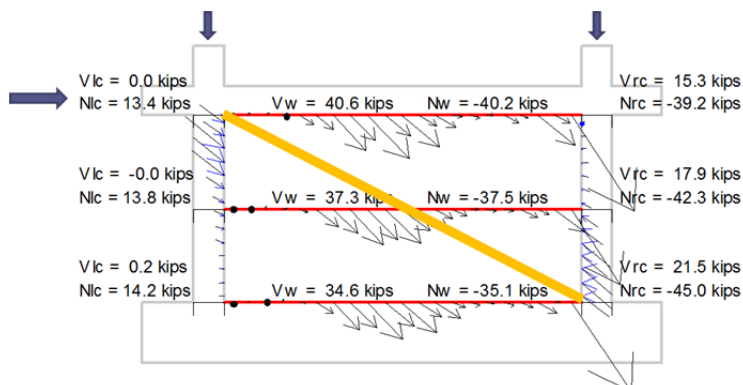


Figure F-10 Strut model and shear, V , and axial, N , forces on an infill from finite element analysis (Stavridis, 2009).

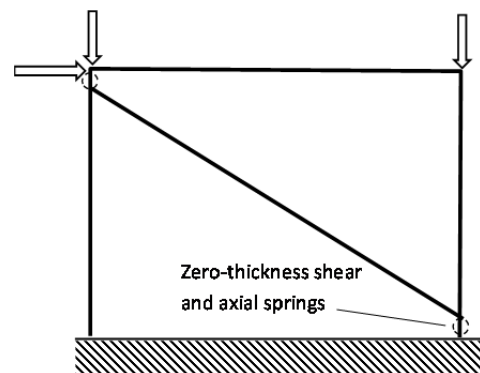


Figure F-11 Strut model with zero-thickness springs.

However, two issues will arise with such a model. One is that it ignores the shear transfer between the beam and the wall, as shown in Figure F-10, and it will thereby induce unrealistically large shear demands on the columns, thus causing their premature shear failure. Another issue is that the shear failure of a column may result in the collapse of the column under the axial load, which will lead to the collapse of the frame, without being able to account for the vertical load carrying capacity of the wall. Moreover, the orientation of the compressive strut forces in a wall can change as damage evolves. Multiple-strut models, as proposed in some studies, might partially overcome this deficiency. Nevertheless, this will increase the complexity of the model, and their benefits remain to be demonstrated.

Despite the aforementioned issues, the use of strut models is probably the best option for Monte Carlo simulations. For this purpose, one can adopt a pragmatic approach by treating diagonal struts as phenomenological models, that have to be calibrated in such a way that they represent not only the behavior of infill walls, but also that of an infilled frame as a whole. To this end, Stavridis (2009) has used experimental data and finite element analysis results to derive a set of simple rules to define ASCE/SEI 41 type pushover curves for infilled frames, as shown in Figure F-12. In the absence of more reliable data, such a curve can be used to determine the load-displacement relation for an equivalent diagonal strut so that it can capture the cyclic load degradation exhibited by an infilled frame; this degradation could result from the shear failure of reinforced concrete columns as well as damage in the infill. It should

be mentioned that the shear failure of one or more of the reinforced concrete columns may not necessarily lead to collapse, as the masonry wall will most likely be able to carry the gravity load shifted from the columns. Nevertheless, as the maximum drift amplitude and the cumulative drift under cyclic load reversals increase, masonry-infill may suffer severe damage and collapse, which can trigger the partial or total collapse of the structure.

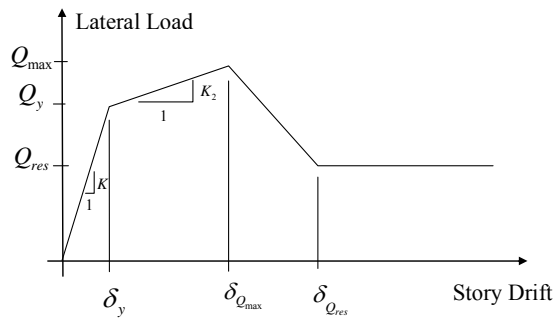


Figure F-12 Load, Q , versus displacement, δ , envelope for an infilled frame.

The above method was attempted to model the response of a three-story infilled frame tested on a shaking table, with the structural configuration shown in Figure F-9. The frame model with equivalent diagonal struts is shown in Figure F-13. The analysis was carried out with the software platform OpenSees. The axial behavior of the diagonal struts was modeled with a constitutive law for concrete. The strut model was calibrated with pushover analyses for six scenarios, representing the six infilled bays in the structure, to mimic the simplified pushover curves defined by empirical rules. The models calibrated for the bottom-story bays are shown in Figures F-13(b) and F-13(c). Figure F-13(b) depicts the solid infill, while Figure F-13(c) depicts the infill with a window opening. In Figure F-13(d), the base shear versus bottom story drift hysteretic curves obtained for the three-story frame with the strut-based model are compared to the test results for a sequence of ground motion records up to the 120% Gilroy motion. The model shows more rapid load degradation than the test results, due to the conservatism introduced in the simplified pushover curves. The quality of the simulation could probably be improved by calibrating the struts using a detailed finite element model in place of the empirical rules.

This type of model can be used for three-dimensional response analysis. The out-of-plane failure of an infill wall can be modeled with fiber-section beam-column elements, which can simulate the arching mechanism as well as out-of-plane bending failure. To model the out-of-plane response, each compression strut can be represented by two beam-column elements. This method has been used by Kadysiewski and Mosalam (2008), and is discussed in Mosalam and Günay (2013) in the context of collapse simulation. Mosalam and Günay (2013) have also proposed an interaction curve for the axial load and out-of-plane bending moment capacities of

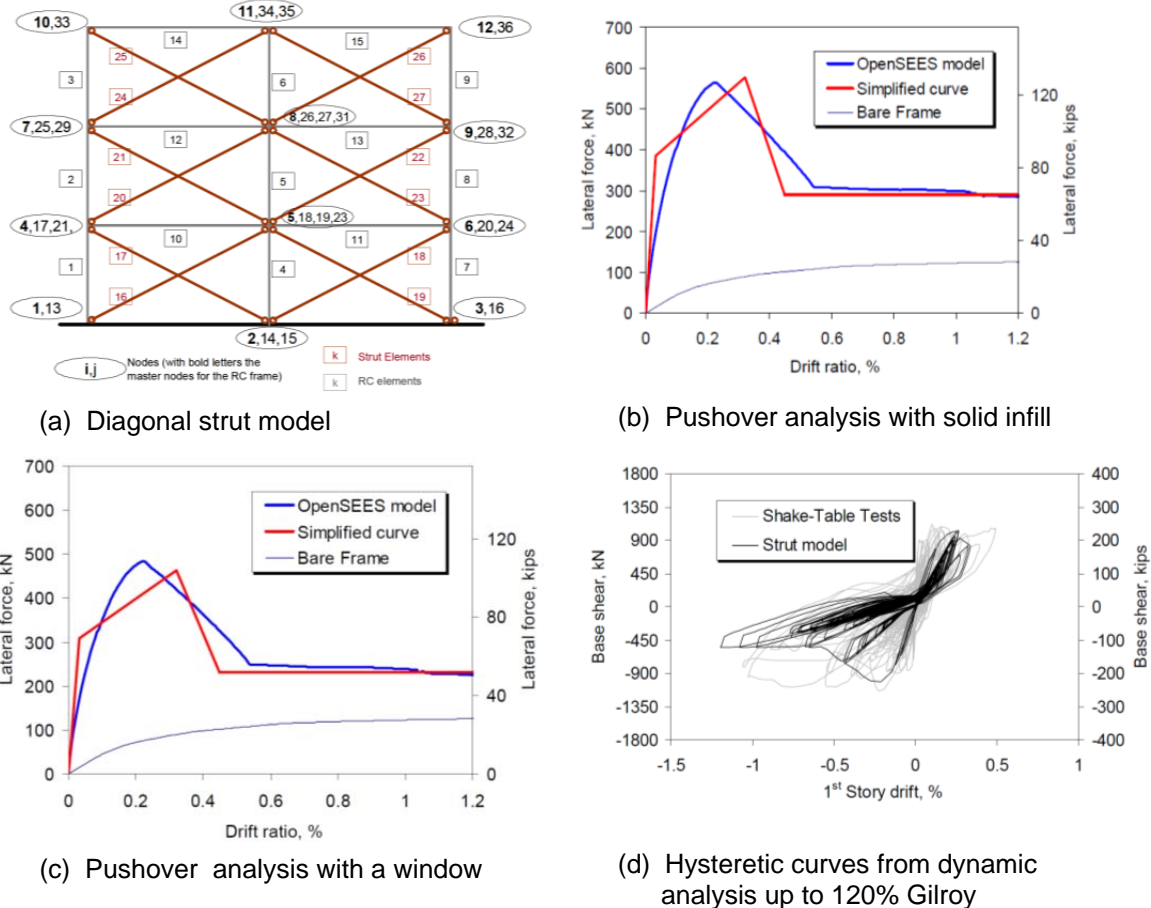


Figure F-13 Frame analysis using equivalent diagonal struts (Stavridis, 2009).

a strut to represent the behavior of a masonry-infilled wall under combined loads. The proposed interaction curve is based on results of finite element analysis. This approach deserves to be further explored and evaluated with experimental data (e.g., the data of Dawe and Seah, 1989; Angel et al., 1994; Mander et al., 1993; Bashandy et al., 1995; and Flanagan and Bennett, 1999). However, it should be noted that if a phenomenological strut model is calibrated so that it emulates the in-plane response of an infilled frame rather than that of a wall alone, a proper account of the interaction of the axial load resistance with the out-of-plane bending moment capacity of a strut may not be conceptually straightforward.

F.5 Thoughts on Collapse Simulation

The detailed finite element modeling and simplified analysis methods presented above can be used to simulate the response of an infilled frame up to a severe damage stage that is close to collapse. Nevertheless, neither method can simulate the actual collapse of an infilled frame in a satisfactory way without further enhancements. Since only a simplified analysis method is practical for Monte Carlo collapse simulations, the discussion here will focus on the simplified approach, but with an

understanding that detailed finite element models are useful for the calibration of simplified models.

One critical issue in a collapse simulation is the definition and identification of collapse. While collapse can be defined as the loss of the vertical load carrying capacity of a structure, one still needs to distinguish between partial and total collapse. This is a definition issue that may warrant further discussion. In any regard, the simulation of the partial or total collapse of an infilled frame is a big challenge because of the possible interaction and load transfer among different elements of the frame, namely, the columns, beams, and walls. Once the reinforced concrete columns in an infilled frame have suffered severe damage, such as shear failure, the gravity load can shift to the infill walls. A severely cracked masonry wall could still carry a significant gravity load even though it might have lost most of its in-plane and out-of-plane lateral load resisting capacity. This can be perceived as an unstable equilibrium state, which has been observed in in-plane quasi-static tests (see Figure F-2) and nonlinear finite element analyses (Koutromanos et al., 2011). Hence, the collapse of an infilled frame will most likely be preceded by the collapse of infill walls as previously discussed. The collapse of infill walls can occur before or after the RC frame has suffered severe damage. The former situation can occur if the masonry is very weak or if a large opening exists in a wall; it will lead to a weak-story mechanism. For this situation, simple models, like those proposed by Elwood (2004) to simulate the collapse of reinforced concrete columns due to shear failures and gravity loads, can be used. Nevertheless, as previously mentioned, combining these models with diagonal struts representing infill walls may lead to the undesired consequence of premature collapse.

In view of the aforementioned modeling challenges and the large margin of uncertainties in the collapse prediction for an infilled frame, it is prudent to treat the first attainment of an unstable equilibrium state of the structure as the total collapse condition. This can be considered as a state in which the infilled frame has lost a significant portion of its lateral in-plane load-carrying capacity due to the failure of the walls at one or more stories. Until more experimental data are available, this state can be conservatively assumed to be reached when the post-peak in-plane resistance of the infilled frame drops to 60% of the peak. The story-drift level at which this load degradation is reached can be taken as the collapse criterion for Monte-Carlo-type simulations. This critical drift level can be identified with a pushover analysis of a planar structure using a detailed finite element model or a simplified model. With this approach, one can avoid the challenging exercise of modeling the progressive collapse of individual elements or the actual collapse of a system, which can be unreliable even with very advanced computational models.

F.6 Summary of Collapse Simulation Method and Research Needs

F.6.1 Proposed Simulation Method

1. Simplified models with equivalent diagonal struts representing infill walls are the best option for Monte Carlo collapse simulations. The in-plane resistance of a strut can be modeled with a phenomenological hysteretic law, which can be calibrated with detailed static 2D finite element analysis of critical frame-wall subassemblies of the system. Reinforced concrete beams and columns can be modeled with appropriate beam-column elements with flexural hinging capabilities. The resulting simplified model is intended to emulate the overall load-displacement relation of an infilled frame, but not the detailed failure mechanism. Calibration must be done for each structural configuration and design. Static finite element analysis of this type can be time-consuming but manageable. Such analyses can also be used as a pre-screening tool to identify the design and material parameters that need to be considered in the Monte Carlo simulation.
2. To simulate the damage and possible collapse of an infill wall caused by out-of-plane loads, a diagonal strut can be modeled with two 3D fiber-section beam-column elements, which can account for the out-of-plane bending and the arching mechanism developed in an infill wall.
3. For Monte Carlo collapse simulation, a convenient criterion for collapse must be determined. This can be a story-drift limit that corresponds to a significant drop of the in-plane lateral resistance of the frame. Until more experimental data are available, this state can be conservatively assumed to be reached when the post-peak in-plane resistance of the infilled frame drops to 60% of the peak. The drift limit corresponding to this load degradation can be established with a detailed finite element model or a simplified model.

F.6.2 Further Research and Development

1. To simplify strut model calibration, it will be desirable to have a set of simple empirical rules that can be used to determine the envelope curves for the load-displacement relations for infilled frames, and rules for the cyclic loading and unloading. The simple guidelines proposed by Stavridis (2009) to define such envelop curves have only been calibrated for one class of infilled frames that have nonductile RC frames and strong brick infill. Further work is needed to expand and improve the guidelines for infilled frame systems with different frame and infill properties.
2. To accurately simulate the interaction of the in-plane and out-of-plane responses of an infill wall and the resulting damage and load degradation, further calibration and validation of strut models for out-of-plane resistance is needed.

For this purpose, existing experimental data can be consulted and new data may need to be acquired.

3. Studies are needed to confirm or improve the proposed criterion for collapse. To this end, existing experimental data on the out-of-plane resistance of infilled walls damaged by in-plane loading can be consulted, and dynamic testing of infilled frames to collapse needs to be conducted. Numerical studies with 3D finite element models that can simulate brick dislocation and infill collapse can also provide more insight to this problem.
4. For further numerical studies and calibration of simplified models, finite element modeling capabilities that can simulate collapse in a detailed fashion are desirable.
5. Other simplified modeling strategies, including element removal methods (Mosalam and Günay 2013), should be considered. Different modeling methods should be compared and evaluated with benchmark examples.

Appendix G

Reinforced Concrete Structural Wall Modeling for Collapse Assessment Utilizing Monte Carlo Simulations

by John W. Wallace
University of California at Los Angeles
Los Angeles, California

G.1 Introduction

Reinforced concrete structural walls, whether in new buildings or older existing buildings, typically provide the primary lateral strength and stiffness to limit lateral displacements. Therefore, the modeling approach and modeling parameters used to capture the load versus deformation behavior of structural walls have a significant impact on the probability of collapse and on the ability to develop economical rehabilitation strategies. This paper briefly reviews various modeling approaches available to assess capabilities and limitations related to assessing collapse.

The focus of this discussion is related to the question of modeling walls and wall piers in existing reinforced concrete buildings:

- What are the preferred wall models to capture the demands on gravity system (i.e., cases where large displacement of the gravity system leads to collapse)? What wall systems are most likely to lead to high demands on the gravity system and how best to model such systems?
- Is the potential for wall axial load failure significant enough to warrant modeling this failure mode? If so, what are some possible approaches to modeling this failure mode? For what types of walls should this failure mode be considered?
- Is it preferred to use concentrated plasticity models with hysteretic rules or fiber models?
- How best to model discontinuous walls and supporting columns?

G.2 Modeling Approaches for Structural Walls

G.2.1 Axial-Bending Behavior

Wall modeling approaches most commonly used for design and assessment include:

- Elastic beam-column elements located at the centroid of the wall cross-section with rigid-plastic hinges at the top and bottom of each floor level;

- Fiber beam-column elements based on uniaxial material models for reinforcement, unconfined concrete, and confined concrete; and
- Detailed finite element models with detailed discretization, ability to model complex interactions, and detailed material models.

For purposes of discussion, the first modeling approach is referred to as BC-Hinge, whereas the second is referred to as BC-Fiber (BC=beam column). Detailed finite element models are not discussed, as they are impractical for the stated goal. Both modeling approaches are based on the assumption that in-plane-sections remain plane during loading and unloading for three unknown response quantities or degrees-of-freedom at each end of a vertical element (for a 2D model), one rotational degree of freedom (θ_z) and two translational degrees of freedom (δ_x and δ_z).

Limitations associated with BC-Hinge models include: (1) empirical rules to define the load-deformation responses; (2) element bending stiffness that does not vary with level of axial load; (3) migration of the neutral axis along the wall cross-section during loading and unloading that does not vary with applied axial load-moment ($P\text{-}M$) interaction, or shear, V ; (4) interaction with connecting beams, both in the plane of the wall and perpendicular to the wall, may not be properly considered; and (5) axial growth that is not considered.

This modeling approach is attractive when a large number of analyses are required and the primary goals are to determine global responses and to compare the sensitivity of responses to variations in model parameters, such as elastic bending stiffness, $P\text{-}M$ yield strength, peak strength (including post-yield hardening), and, in some cases, strength loss and axial load failure. Typically, data are dispersed into bins based on level of axial load, shear, and detailing (e.g., as specified in ASCE/SEI 41); therefore, modeling parameters account for various interactions, such as the potential impact of shear and axial load on the wall rotation capacity at strength loss. However, drawbacks include the lack of data to define (statistically) many of these parameters, especially for walls that do not have well-confined boundary regions, leading to significant uncertainty.

It is attractive to use BC-Fiber models because they address the limitations noted above for BC-Hinge models, as well as the ability to track material strains. However, BC-Fiber models are not without fault, with limitations that include: (1) longer computer run times; (2) generally more stability/convergence issues; (3) sensitivity of results to element size (mesh) and element formulation (i.e., force-based versus displacement-based integration points); and (4) false sense of accuracy given the added level of sophistication. Mesh sensitivity typically leads to the use of element sizes (heights) that are selected to be approximately equal to expected plastic hinge lengths. For BC-Fiber models, parameters are needed to define the uniaxial material relations (concrete and rebar). In most element implementations (especially in

commercially-used programs), interaction between axial-bending behavior and shear behavior and the potential impact of loading history on modeling parameters are not typically considered. Given these issues, knowledge of and experience with BC-Hinge modeling, at least for some modeling parameters, are prerequisites to obtaining reliable results with BC-fiber models. Finally, given the relatively large number of material and modeling parameters compared with BC-Hinge models, and given the impact of variation in these parameters on the dispersion in response quantities (Engineering Demand Parameters), it may be necessary to limit sensitivity studies to a limited number of parameters.

Several variations, or hybrid, approaches to the BC-Fiber model exist and are commonly used. One such approach, the Multiple-Vertical-Line-Element (MVLE) model, addresses some of the concerns associated with element size and stability by using average axial responses over specified element heights. Another approach, the “uniaxial” wall element available in PERFORM 3D (CSI, 2013), uses four-node elements with two displacement degrees-of-freedom at each node point along with a plane-section assumption. This modeling approach simplifies the modeling of complex wall cross-sections, as elements can easily be connected edge-to-edge to create various shapes; however, it also tends to increase computer run times by adding degrees-of-freedom.

G.2.2 Rebar Buckling

To investigate the role of buckling of vertical reinforcement, the procedure presented by Rodriguez et al. (1999) is evaluated. In this study both monotonic and cyclic tests were conducted on isolated rebar coupons for various s/d_b ratios (s is the spacing of transverse reinforcement and d_b is the diameter of transverse reinforcement) to assess the onset of rebar buckling, which was defined as a strain drop of 20% from a prior peak value. The coupon tests indicated that bars subjected to cyclic loading were more prone to buckling failures than bars subjected to monotonic loading. For cyclic loading, Rodriguez et al. (1999) proposed the use of parameter $\varepsilon_p^* = \varepsilon_0^+ - \varepsilon_p$ (defined in Figure G-1) as an indicator of onset of buckling of a reinforcing bar subjected to axial load reversals. The variation of ε_p^* versus S_h/D (equal to s/d_b) ratios are presented in Figure G-2. As expected, the value of the strain indicator ε_p^* drops substantially for large s/d_b ratios. For ratios typically used in older buildings, similar to values used for walls damaged in Chilean buildings in 2010 (e.g., 8 to 11), Figure G-2 suggests very low values of ε_p^* .

Potential shortcomings of this approach include that it defines the onset of buckling (in a nonlinear analysis model) for an isolated rebar test, which is not necessarily well correlated to significant loss of lateral strength of actual structural walls. For large ratios of s/d_b , concrete cover spalling needs to occur prior to bar buckling. Also, buckling of an individual bar or pair of bars at a wall boundary with a fairly large

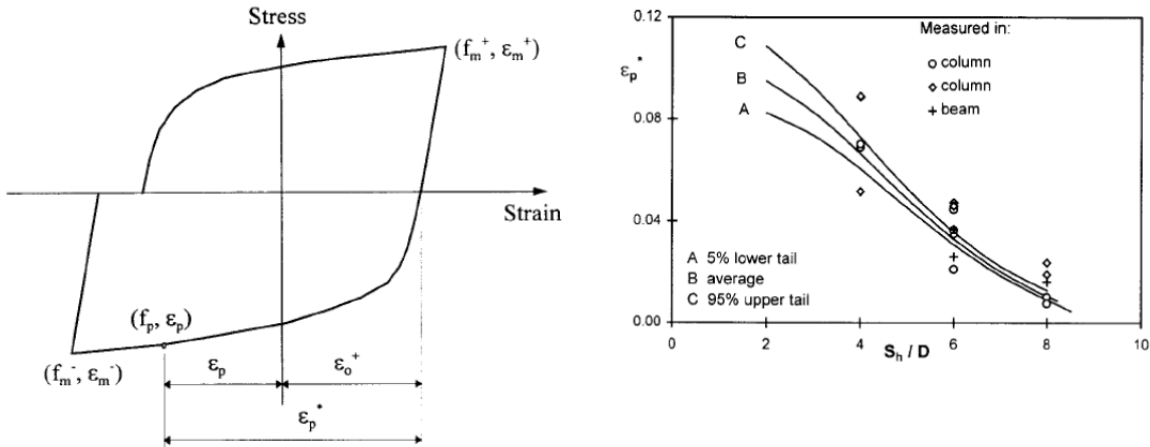


FIG. 11. Cyclic Stress Strain Curve for Steel

$$\varepsilon_p^* = \varepsilon_p^+ - \varepsilon_p^- \quad (7)$$

Figure G-1 Definition of ε_p^* (Rodriguez et al., 1999).

Figure G-2 ε_p^* versus S_h/D (equal to s/d_b) (Rodriguez et al., 1999).

number of longitudinal bars distributed along the wall length may not lead to a significant strength loss. Wall RW1, tested by Thomsen and Wallace (1995; 2004), demonstrates this behavior. In these tests, bar buckling was observed to initiate at about 1.0% drift, and yet the wall was able to sustain several cycles of 2.0% drift prior to significant loss in lateral strength during the first cycle to 2.5% drift.

The buckling indicator proposed by Rodriguez et al. (1999) was used to develop a procedure to assess the onset of buckling for structural walls. The procedure developed was calibrated by comparing results with test results for the four cantilever walls with both rectangular and T-shaped cross section tested by Thomsen and Wallace (1995; 2004), because these tests included drift and strain data for walls with both rectangular and T-shaped cross sections. The comparison with test results indicated that, for the range of values expected for the onset of bar buckling: (1) onset of buckling (very minor out-of-plane displacement of vertical bar) with no observed loss in lateral strength typically was associated with the lower-bound of the range; (2) bar buckling with noticeable out-of-plane displacements and significant concrete cover spalling was associated with the mid- to upper-range of the indicator; and (3) significant loss in lateral strength was generally associated with the high-range of the indicator. Calibration of this approach with a larger test data set is recommended.

Given that use of BC-Fiber and hybrid models are quite common and average rebar strain histories are readily available, the potential to directly assess rebar buckling, or to aid in post-processing of results to assess rebar buckling, is attractive. It is possible to modify rebar stress-strain relations (i.e., stress drop) for individual bars; this has been implemented in some recent studies (e.g., GCR 10-917-8, NIST,

2010a). The NIST GCR 10-917-8 studies were conducted on relatively simple building configurations with limited degrees-of-freedom using OpenSees.

Convergence issues were noted and observed to significantly depend on the modeling and material parameters used (e.g., element heights, integration points, and post-yield hardening slope). Tuna (2012) used a similar approach in PERFORM-3D V5 to assess the role of rebar buckling on the collapse of a 15-story building (Figure G-3(b)). The slope of the descending branch of the rebar stress-strain relation could be selected to initiate stress loss at the onset of buckling using the approach discussed in the prior paragraph and drop to a residual value (e.g., zero) at the upper-bound of the buckling indicator, as rapid strength loss tends to lead to convergence problems. As noted in Figure G-3(b), where four different models were used for reinforcement in compression, current computer programs (OpenSees, PERFORM-3D) do not track the difference (peak values, or the sum of the absolute values) in the maximum tensile and compressive strains recorded. Minor improvements to current models might therefore be possible by enabling tracking of these values. It would be relatively easy to implement model parameters for rebar that could produce degradation if the residual strain reached a specified value, and then compressive strain reached a limiting value. New tests will provide data to help calibrate models.

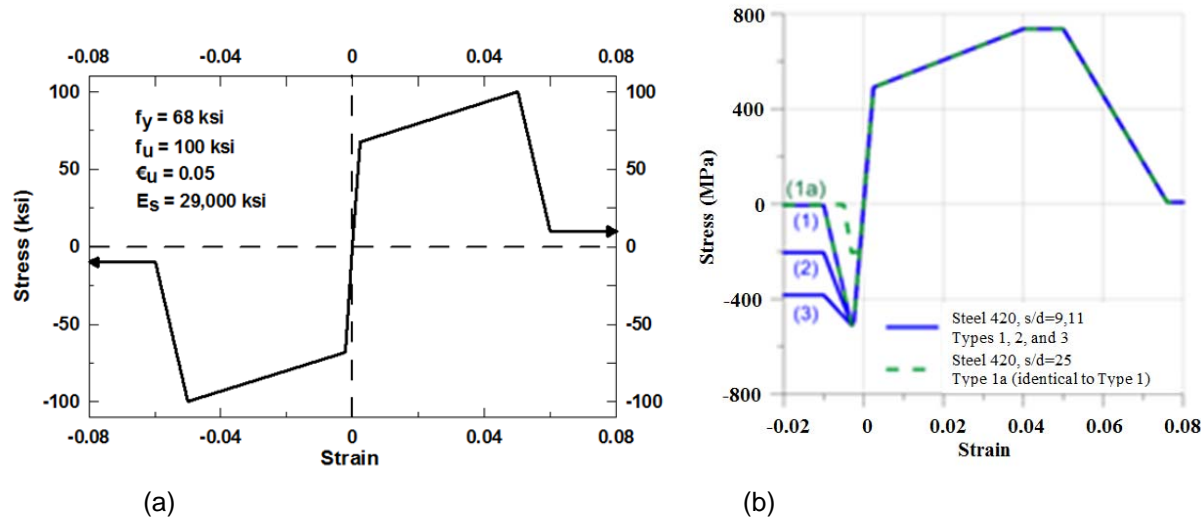


Figure G-3 BC-Fiber modeling of rebar buckling: (a) well detailed; (b) poorly detailed (Tuna, 2012).

For BC-Hinge models, rebar buckling can be treated by manipulating the hinge relations (versus tracking rebar stress-strain relations), with the primary modeling parameters being when to initiate strength loss and the rate of strength loss. This approach can work well in some cases, such as well-detailed coupling beams (Naish et al., 2013a; 2013b), but, as previously noted, the lack of test data for “poorly” confined walls makes this a challenging task.

G.2.3 Shear Behavior

In most structural analysis programs, limited options exist to model nonlinear shear behavior, typically with multi-linear segments used to define key points associated with cracking, yielding, and degrading strength. In some cases, additional points are included to model residual strength and loss of axial load carrying capacity (e.g., ASCE/SEI 41 backbone relations, ASCE, 2013).

For short wall segments controlled by shear, test results for lightly reinforced walls reported by Massone (2006) provide useful information to define the shear force-deformation relation, with uncracked shear modulus approximated as

$G_c = E_c 2(1+\nu) \approx 0.4E_c$, where G_c is the shear modulus of concrete, E_c is the elastic modulus of concrete, ν is the poisons ratio, and shear (inclined) cracking occurs at roughly 2.5 to $3.0 \sqrt{f'_c}$. The yield point, and thus the slope of the line connecting the crack point to the yield point, depends on various factors, such as the level of axial load and the quantity of boundary reinforcement. For example, for wall piers tested with zero axial load, yield occurred at an average strain over the wall pier of about 0.004. However, when the same pier was tested with moderate axial load ($P = 0.05$ and $0.10A_g f'_c$), the strength and stiffness increased substantially as demonstrated in Figure G-4; strength increases by about 50% and post-cracking stiffness approximately doubles. Clearly, demands placed on the gravity system could vary substantially depending on the level of axial load. The most realistic approach would appear to be to model shear using at least a trilinear relation: (a) uncracked, (b) post-cracked, and (c) post-yield, followed by strength loss. [For lightly reinforced walls with modest axial load ($P=0.10A_g f'_c$), with axial failure followed closely by strength loss (shear failure), no reliable residual strength existed (see Figure G-5)]. A couple cycles of reliable residual strength to about 1.0% drift were observed for piers with $P=0.05A_g f'_c$, whereas modest residual strength was observed to drift levels of 3.0%

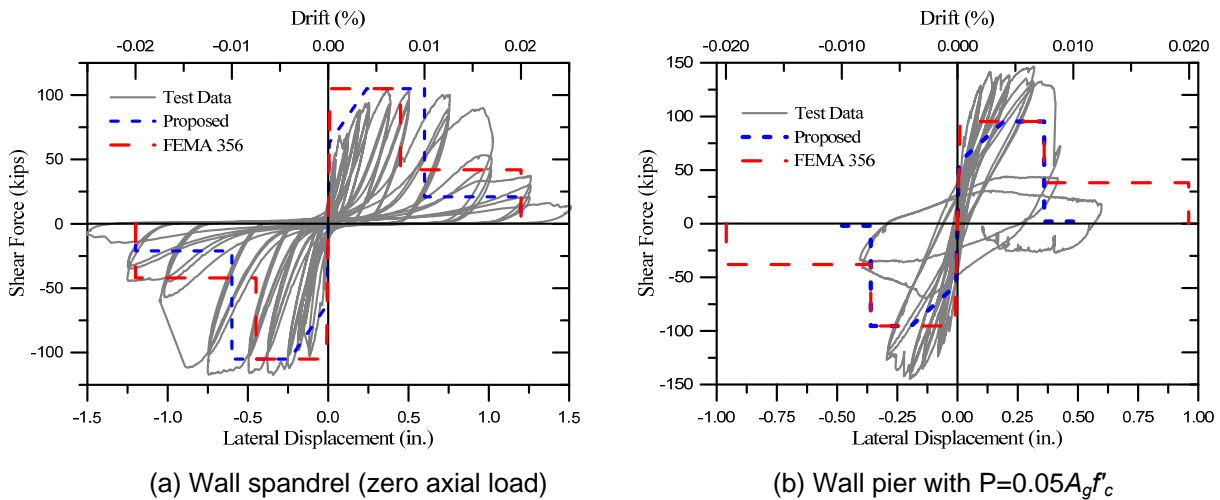
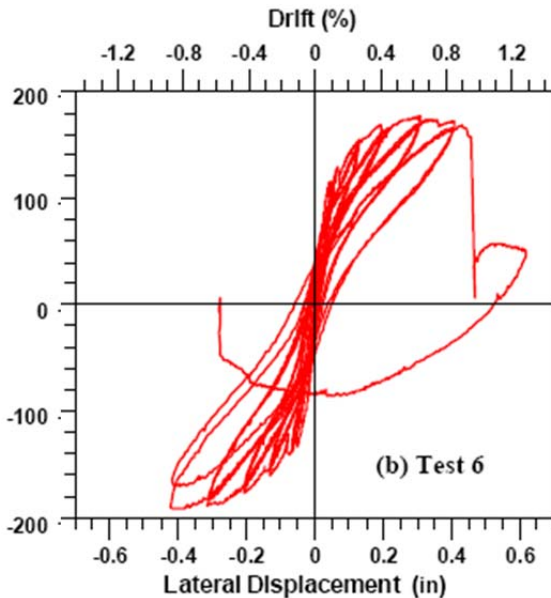
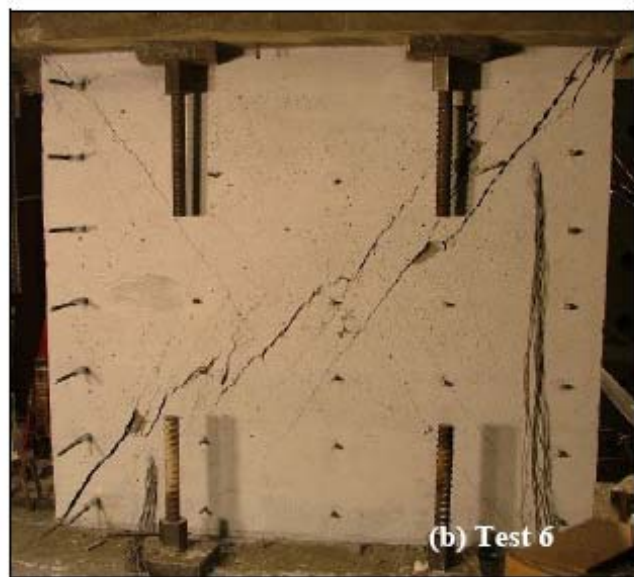


Figure G-4 Load-displacement response for wall specimens tested by Massone (2006).



(a) Load-Displacement Relation



(b) Wall Pier at 1.2% drift

Figure G-5 Wall pier test for $P = 0.10A_g f'_c$ (Massone, 2006).

for zero axial load. The test results also point out the need to use factors that account for “pinching.”

The FEMA 356 curve (FEMA, 2000) is calculated disregarding the ACI provision that requires two curtains of reinforcement. Nominal strengths for the FEMA 356 and proposed curves were calculated using ACI 318-05 (ACI, 2005) strength equations with measured material strengths.

For slender walls, appropriate modeling of the load–deformation behavior may be complicated by shear-flexure interaction, i.e., where nonlinear shear deformations occur for walls with shear strength greater than that required to reach flexural yielding (typically, these are relatively slender walls, with aspect ratios $h_w/l_w > 1.5$).

This interaction between shear and flexure can have various impacts, such as lower shear stiffness after flexural yielding and loss of lateral-load strength and axial-load capacity at lower lateral deformations. Various modeling approaches are available in the literature to address this issue: (a) models based on experimental data that bin tests according to shear demand, axial load, and detailing (e.g., as specified in ASCE/SEI 41); (b) models that reduce the shear stiffness following flexural yield (and could also incorporate (a)); (c) models that reduce shear strength depending on the level of nonlinear flexural demands (e.g., displacement ductility or curvature ductility); and (d) models that directly incorporate shear-flexure interaction.

- (a) Models based on bins of test data (e.g., the ASCE/SEI 41 model): In the near-term, this modeling approach is attractive, since it is both simple and widely

used. However, the lack of data for many conditions common for existing buildings, such as poorly detailed walls, walls with heavy axial stress, and thin walls, imposes severe limits that typically lead to large uncertainty. In addition, this modeling approach is sometimes misused. The ASCE/SEI 41 approach assumes all deformation for a given bin is associated with either shear or flexure backbone relations; however, engineers sometimes include backbone relations for both shear and flexure (since computer programs ask for this information). Given the conservatism of the ASCE/SEI 41 relations, this approach is not an issue; however, if new relations are developed using median estimates, then this would be inappropriate. Databases have recently been assembled to reassess wall modeling parameters (e.g., Tuna, 2012); therefore, sufficient information may be available to establish new (median) modeling parameters in the near future.

- (b) Models with both flexure and shear backbone relations: This modeling approach is a slight variation on the ASCE/SEI 41 model, in that flexural behavior is modeled using an appropriate approach (e.g., BC-Fiber, since backbone relations cannot be input when this approach is used), and the nonlinear shear backbone relation (shear spring) is incorporated. This approach is limited in that calibration studies are needed to define the shear cracking point and the post-crack slope of the shear force-deformation relations for shear-controlled walls (see Figures G-4 and G-5). Tests of relatively slender walls by Thomsen and Wallace (2004), along with calibration studies conducted by Gogus (2010) (see also NIST, 2011a), provide useful information for this modeling approach. The approach described by Gogus (2010) uses an ad hoc approach to soften the post-crack slope of the shear force-deformation relation to account for nonlinear interactions (i.e., increased deformation) that are not considered by the modeling approaches available (i.e., the modeling approaches do not consider interaction; therefore, an ad hoc approach is needed to mimic the interaction).
- (c) Models with shear strength degradation (e.g., the Elwood and Moehle, 2008 column model): A further modification of the modeling approaches described in (a) and (b) involves reducing shear strength as a function of nonlinear flexural demands, such as displacement ductility or curvature ductility (Figure G-6). Although use of displacement ductility is convenient for assessing trends for wall test data, use of curvature, derived from the test results, is more convenient for use in structural analysis programs. Currently, this modeling approach is available in OpenSees for columns, but not in commercial programs.

This approach suffers from the same limitations as the previous two approaches due to the lack of data for a wide range of test conditions. Although more data are becoming available (Tran and Wallace, 2012; Gulec and Whittaker, 2011), a large number of the tests may not be representative of conditions in many collapse-sensitive buildings. For example, the Portland Cement Association

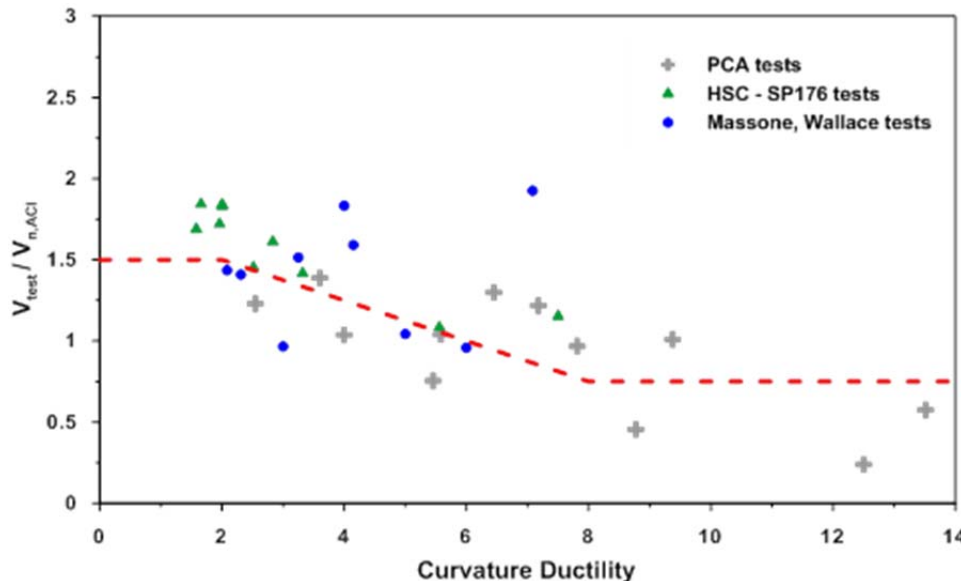


Figure G-6 Model for shear strength degradation versus curvature ductility (Yang et al., 2012).

(PCA) tests (Yang et al., 2012) in Figure G-6 include tests on “barbell-shaped” wall cross sections and for walls that are “well-detailed” at wall boundaries, and some of the recent tests noted above are for “well-detailed” walls.

- (d) Models that incorporate shear-flexure interaction (e.g., Kolozvari, 2012): Over the last several years, new modeling approaches have been developed to directly incorporate shear-flexure interaction. Model calibration with test data also is underway for the tests conducted by Tran and Wallace (2012) (see Figure G-7). It is reasonable to assume that these approaches will become available in research-oriented computational platforms (OpenSees) in the next 6 to 12 months and eventually in commercially used programs. However, it also is reasonable to assume that insufficient test data will exist in the short-term to calibrate these

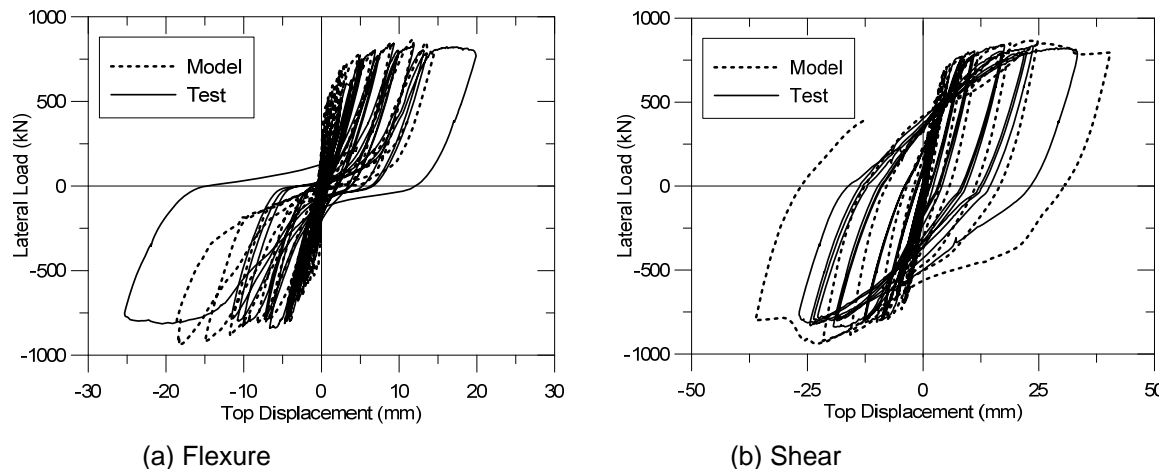


Figure G-7 Load-displacement response at top of wall predicted by the model:
(a) flexure; (b) shear (Tran and Wallace, 2012).

models for a wide-range of conditions (moment/shear \times depth (M/Vd) ratios, axial stress, boundary transverse reinforcement, and load history). Furthermore the added computational effort will likely significantly increase computer run times.

G.2.4 Three-Dimensional Responses

The potential influences of structural wall responses on the overall behavior of a three-dimensional building system has not received much attention, although there are examples in the literature that highlight the impacts, such as the U.S.-Japan 7-story building tested on the University of California, Berkeley shake table in the 1980s (out-of-plane coupling), and the NEES Research, University of California, San Diego building slice test (in-plane coupling). For the most part, these studies have examined the responses of planar walls subjected to shaking parallel to the wall web. A few studies that document the influence of bi-directional loading on the behavior of isolated structural walls have been conducted, (e.g., Japanese studies on high-performance walls in the 1990s, recent tests by Brueggen et al., (2010), and Kabeyasawa et al., (2012)). Preliminary observations from Kabeyasawa et al., (2012) tests indicate a modest reduction in wall deformation capacity for biaxial loading versus uniaxial loading, whereas preliminary results from the NEES testing facility at University of Minnesota (Brueggen et al., 2010) reveal that BC-Fiber wall models calibration with data from uniaxial wall tests reasonably capture results from the biaxial tests (Brueggen et al., 2010). However, all of the studies noted here are for “well detailed” walls; biaxial loading may have a greater impact on the behavior of “poorly detailed” walls where buckling of reinforcement is likely to lead to concentration of damage and subsequent strength loss (e.g., Wallace et al., 2013). To address this issue, the following approaches could be used: (a) for a 2D model using a BC-Hinge wall element model, reduce the hinge rotation capacity modestly to account for biaxial responses; (b) for a 2D model using a BC-Fiber wall element model, reduce the tensile strain value at strength loss to account for biaxial responses (this would require some calibration work); and (c) for a 3D model using a BC-Fiber wall element model, use a biaxial mesh (again, this would require some calibration work to ensure the approach used was producing results that were consistent with the test results).

Modeling of non-planar walls is not adequately addressed in currently available computational platforms. Within OpenSees, wall models have been implemented that focus on capturing the responses of planar walls; modeling of other shapes (e.g., T and L shaped walls) with members framing into the wall sections perpendicular to either primary axes is not readily accomplished. The BC-Fiber modeling approach used in PERFORM-3D appears to circumvent this issue, although it is necessary to use additional beam (horizontal) members to ensure “fixed-end” conditions are properly considered. An added complication arises from the need to consider

effective flange widths. For more slender walls, assuming the entire flange is effective is reasonable; but for shorter walls with long flanges, this is not appropriate. Shorter walls with longer flanges are not very likely to be a collapse risk.

G.2.5 Axial Failure

Models that incorporate loss of axial load carry capacity have been proposed for columns (Elwood and Moehle, 2008) and extended to low-aspect ratio walls (Wallace, et al., 2008). The approach was shown to produce reasonable results for lightly-reinforced, low-aspect ratio wall piers (see Figures G-4 and G-5). Although it is possible to incorporate axial failure with the proposed model into any of the modeling approaches described here, it is currently available only in the OpenSees computational platform for columns using modeling approach (c) discussed in the prior section. Extension of the axial failure of walls required recalibration of the shear friction drift relation proposed for columns; additional tests are now available to revisit this extension (Tran and Wallace, 2012). However, based on observations from post-earthquake reconnaissance conducted over the last 50 years, complete overturning or axial failure of buildings constructed with cast-in-place structural walls is very rare, even when substantial wall damage was observed (Wallace et al., 2008). Therefore, additional emphasis on modeling of collapse-sensitive elements such as columns would appear more fruitful than focusing on walls, unless the walls were the primary problem (e.g., St. John's Hospital in Santa Monica, following the Northridge Earthquake, where substantial spandrel and pier damage was observed, but interior columns were slender and transverse reinforcement consisted of tightly spaced spirals per ACI 318). In recent studies (NIST, 2010a; Gogus, 2010) axial failure of wall elements was assumed to occur at specified drift values (based on judgment). For low-aspect ratio walls, the tests presented in Figures G-4 and G-5 (Massone, 2006) provide some data to establish this drift limit. For more slender walls, data do not exist for poorly detailed walls. However, as noted previously, collapse of buildings with slender walls has rarely occurred, suggesting that the gravity systems in this type of building is the greater concern.

G.2.6 Splices

Johnson (2010) reports test results for isolated, slender (h_w/l_w and $M_u/V_u l_w = 2.67$) cantilever walls carried out to investigate the behavior of anchorage details. Three wall specimens were tested, designated RWN, RWC, and RWS for continuous, coupled, and spliced vertical reinforcement, respectively. Although rectangular wall cross-sections were tested, the quantity of boundary longitudinal reinforcement was varied to represent a wall with a T-shaped cross section. Lateral load versus top lateral displacement relations for specimen RWS are plotted in Figure G-8(a). Results for specimens RWC and RWN are similar.

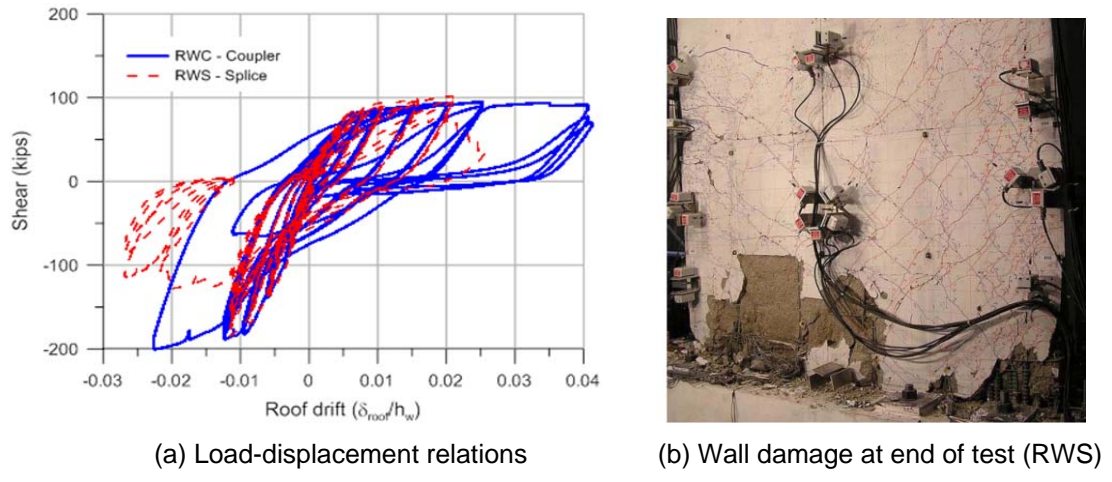


Figure G-8 Lateral load versus top lateral displacement and corresponding damage for specimen RWS (Wallace et al., 2012).

For RWC, the wall reached rotations exceeding +0.035 (#5 in tension) and -0.02 (#9 in tension), whereas for RWS, the wall reached rotations of approximately +0.02 (#5 in tension) and -0.012 (#9 in tension). Damage was concentrated at the foundation-wall interface (Figure G-8(b)), which accounted for about 0.015 of the measured top rotation of 0.02. However, the test results indicate that the presence of the splice significantly reduced the wall lateral deformation capacity. The limited discussion provided here intends to highlight the problem of modeling the behavior of wall splices and the impact of the splice on wall deformation capacity. The test results suggest that wall deformation capacity at loss of lateral strength should be reduced where splices exist. However, strength loss tends to be less drastic than observed for shear failures, with modest residual strength to fairly large drift values.

G.2.7 Sliding Shear at Wall Base

Nagae et al., (2011) reports E-Defense tests on two 4-story buildings, one conventionally reinforced and the other using high-performance reinforced concrete construction, both with rectangular wall cross sections (Figure G-9(a)). The conventionally reinforced wall had confinement exceeding U.S. requirements, with axial load of approximately $0.03A_g f'_c$, yet the compression boundary zone sustained localized crushing and lateral buckling (Figure G-9(b), after Kobe 100% motion).

The base overturning moment versus roof displacement responses are plotted in Figure G-10; base rotations are slightly less than the roof drift ratio (e.g., for Kobe 100%, the base rotation measured over $0.27l_w$ is a little more than 0.02). Following crushing of boundary regions, sliding shear responses increased substantially during the Kobe 100% test (Figure G-10). Sliding displacements in the Takatori 60% test reached the limits of the sensor, +45mm and -60mm with peak shear of +/- 2000 kN.

Lateral load versus wall top lateral displacement relation for a test conducted on a low-aspect ratio wall segment (spandrel) with zero axial load is plotted in

1Fl.	Section			
	B x D	2,500 x 250		
	Rebar	2 x 6-D19	Vertical	D13@300 (W)
	Hoop	(A) 2,3-D10@80 (B) 2,3-D10@100	Horizontal	(A) D10@125 (W) (B) D10@200 (W)
	Joint	2,2-D10@150		



(a) Conventional reinforced concrete wall details
(Nagae et al., 2011)

(b) Wall damage
(Wallace et al., 2012)

Figure G-9 Conventionally reinforced wall details and associated damage.

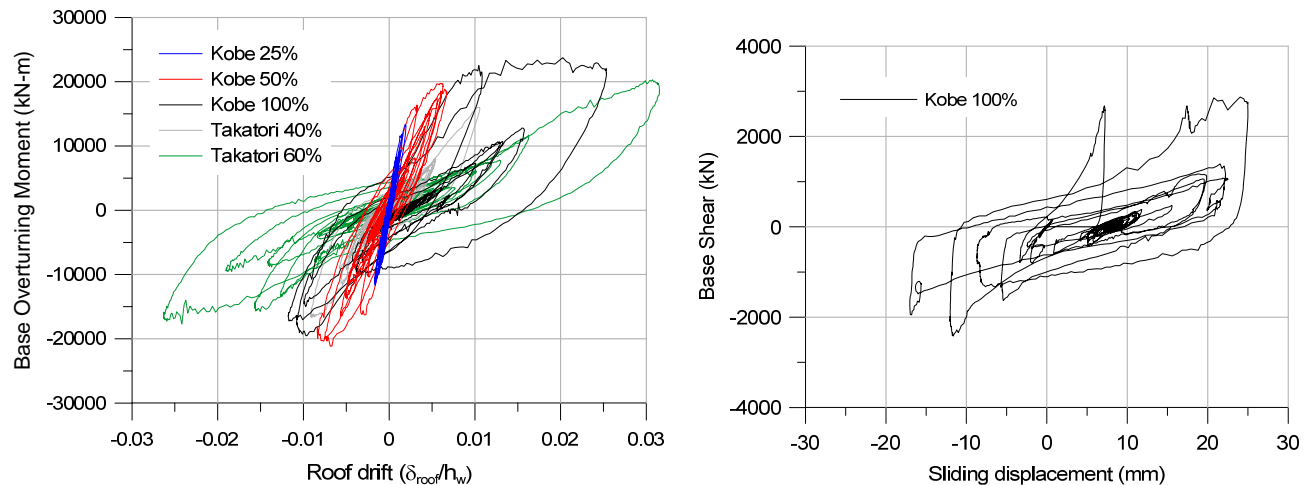


Figure G-10 Conventionally reinforced wall base overturning moment versus roof displacement responses (structural wall direction) (Wallace et al., 2012).

Figure G-11. A weakened plane joint (see Massone, 2006) existed at the base of the wall segment; therefore, under lateral load, sliding occurred, as is evident in Figure G-11. However, since the specimen was not significantly damaged even after it was subjected to large lateral drifts, additional testing was conducted with average axial stress levels of $0.025A_g f'_c$ and $0.05A_g f'_c$. With even modest axial load, the sliding behavior at the wall base resisted substantial lateral load with stable energy dissipation characteristics. The relations plotted in Figure G-10 for the E-Defense test, also with modest axial load (about $0.03A_g f'_c$), and Figure G-11 suggest that sliding behavior provides substantial stiffness, strength, and a stable energy dissipation mechanism. Modeling this behavior might provide additional drift capacity prior to collapse for some structures. For slender walls, slight modifications to existing modeling approaches (BC-Fiber, MLVE) would be needed to enable coupling between strength loss due to crushing at wall boundaries and sliding

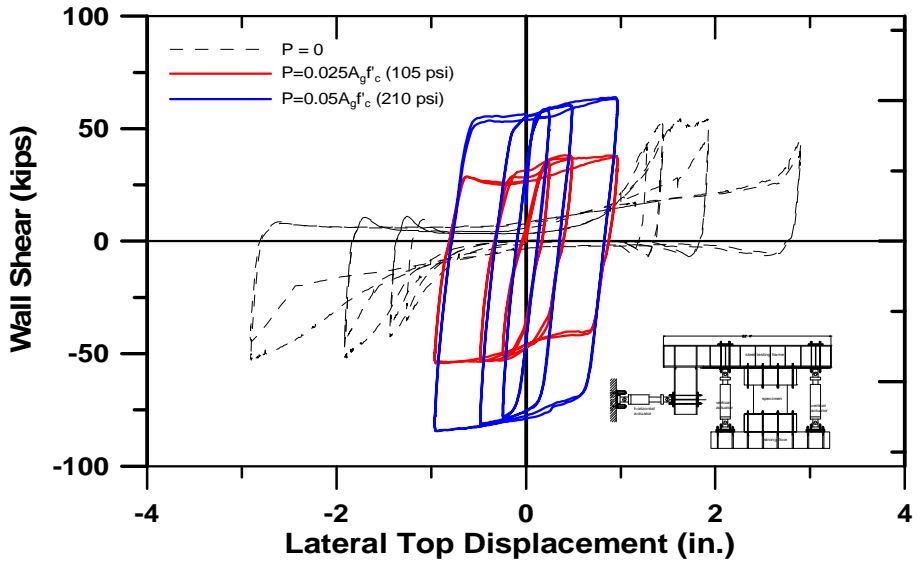


Figure G-11 Wall spandrel test with sliding (courtesy of J. Wallace, with permission)

behavior (e.g., the E-Defense test). For low-aspect ratio walls, a similar approach could be used, i.e., if shear failure does not occur prior to initiation of sliding, then sliding behavior would dominate (or just model the sliding behavior, neglecting the added stiffness that exists prior to sliding).

G.3 Summary

This paper provided an overview of various modeling approaches used to capture axial-bending, rebar buckling, shear, shear-flexure interaction, three-dimensional responses, axial failure, anchorage failure, and sliding shear failure. Currently, approaches to model most of these behaviors exist within the OpenSees computational platform or PERFORM-3D, although in some cases in a simplified form. Potential modeling improvements are suggested for several conditions (e.g., rebar buckling) that would be relatively simple to implement but that also would significantly improve modeling capabilities for collapse simulations. In other instances, such as, shear-flexure interaction and splices, the information presented focuses on presenting test results or behavior models that could be valuable for modelers to understand mechanisms, not modeling approaches that could be used for nonlinear dynamic analysis using currently available tools.

Within the next year or two, modeling capabilities are likely improve to better capture rebar buckling, axial failure, and shear-flexure interaction, again improving modeling capabilities for collapse simulation for buildings with structural walls. Until these new models are implemented, calibrated, and documented, modeling efforts for collapse assessment may require post-processing, which make the process both challenging and typically conservative. The most practical approaches for

collapse simulation studies are BC-Hinge and BC-Fiber models, with the limitation that complex failure modes (e.g., sliding shear and rebar buckling) are treated by simple approaches. The potential to implement simple modeling improvements that would improve our ability to model rebar buckling should be considered. Direct modeling of axial failure is probably not necessary for structural walls, but it should be considered for gravity systems used in combination with walls. Use of the BC-Fiber model (including hybrids) is likely a better option for most studies, as the model is able to account for behavior and interactions that are not captured using a BC-Hinge model. For studies where the advantages of a BC-Fiber model are not needed, then use of a BC-Hinge model is appropriate. As additional model development and test data become available, it may be possible to revisit and refine work on collapse indicators.

References

- ACI, 2002, *Recommendations for Design of Beam-Column Connections in Monolithic Reinforced Concrete Structures*, ACI 352R-02, Joint ACI-ASCE Committee 352, American Concrete Institute, Farmington Hills, Michigan.
- ACI, 2005, *Building Code and Commentary*, American Concrete Institute, ACI 318-05, Farmington Hills, Michigan.
- ACI, 2008, *Building Code and Commentary*, American Concrete Institute, ACI 318-08, Farmington Hills, Michigan.
- ACI, 2011, *Guide for Seismic Rehabilitation of Existing Concrete Frame Buildings and Commentary*, ACI 369R-11, American Concrete Institute, Farmington Hills, Michigan.
- Alire, D., 2002, *Seismic Evaluation of Existing Unconfined Reinforced Concrete Beam-Column Joints*, M.S. Thesis, Department of Civil and Environmental Engineering, University of Washington, Seattle, Washington.
- Anagnos, T., Comerio, M.C., Goulet, C., Na, H., Steele, J., and Stewart, J.P., 2008, "Los Angeles inventory of nonductile concrete buildings for analysis of seismic collapse risk hazards," *Proceedings*, 14th World Conference on Earthquake Engineering, International Association of Earthquake Engineering, Tokyo, Japan.
- Anderson, M., Lehman, D.E., and Stanton, J., 2008, "A cyclic shear stress-strain model for joints without transverse reinforcement," *Engineering Structures* Vol. 30, pp. 941-954.
- Angel, R., Abrams, D., Shapiro, D., Uzarski, J., and Webster, M., 1994, *Behavior of Reinforced Concrete Frames with Masonry Infills*, Report No. UILU-ENG-94-2005, Dept. of Civil Engineering, University of Illinois, Urbana-Champaign, Illinois.
- ASCE, 2003, *Seismic Evaluation of Existing Buildings*, ASCE/SEI 31-03, American Society of Civil Engineers, Reston, Virginia.
- ASCE, 2006a, *Minimum Design Loads for Buildings and Other Structures*, ASCE/SEI 7-05, including Supplement No. 1, American Society of Civil Engineers, Reston, Virginia.

- ASCE, 2006b, *Seismic Rehabilitation of Existing Buildings*, ASCE/SEI 41-06, American Society of Civil Engineers, Reston, Virginia.
- ASCE, 2013, *Seismic Evaluation and Retrofit of Existing Buildings*, ASCE/SEI 41-13, American Society of Civil Engineers, Reston, Virginia.
- Aschheim, M., 2000, "Towards improved models of shear strength degradation in reinforced concrete members," *Structural Engineering and Mechanics*, Vol. 9, No. 6, pp. 601-613.
- ATC, 1996, *Seismic Evaluation and Retrofit of Concrete Buildings*, ATC-40 Report, Volumes I and II, Applied Technology Council, Redwood City, California.
- ATC, 2012, *Evaluation of the Methodology to Select and Prioritize Collapse Indicators in Older Concrete Buildings*, ATC-78-1 Report, Applied Technology Council, Redwood City, California.
- Baber, T.T., and Wen, Y.K., 1981, "Random vibration of hysteretic, degrading systems," *Journal of Engineering Mechanics*, Vol. 107, No. EM6, pp. 1069-1087.
- Baker, J.W., 2013, "Efficient analytical fragility function fitting using dynamic structural analysis," *Earthquake Spectra*, (in review), Earthquake Engineering Research Institute, Oakland, California.
- Baker, J.W., Lin, T., Shahi, S.K., and Jayaram, N., 2011, *New Ground Motion Selection Procedures and Selected Motions for the PEER Transportation Research Program*, PEER Technical Report 2011/03, Pacific Earthquake Engineering Research Center, Berkeley, California, 106 pages.
- Baradaran Shoraka, M., and Elwood, K.J., 2013 (in review), "Mechanical model for non-ductile reinforced concrete columns," *Journal of Earthquake Engineering*.
- Bashandy, T., Rubiano, N.R., and Klingner, R.E., 1995, *Evaluation and Analytical Verification of Infilled Frame Test Data*, Report No. 95-1, Department of Civil Engineering, University of Texas, Austin, Texas.
- Benuska, K.L., and Clough, R.L., 1973, *Dynamic Analysis of Building Failures, The Great Alaska Earthquake of 1964*, pp. 283-307, National Academy of Sciences, Washington D.C.
- Berry, M., 2006, *Performance Modeling Strategies for Modern Reinforced Concrete Bridge Columns*, Ph.D. Dissertation, University of Washington, Seattle, Washington.
- Bertero, V.V., and Collins, R., 1973, *Investigation of the Failures of the Olive View Stairtowers during the San Fernando Earthquake and their Implications on*

Seismic Design, Report No. EERC 73-26, Earthquake Engineering Research Centre, University of California, Berkeley, California.

Birely, A., Lowes, L.N., and, Lehman, D.E., 2012, “A model for the practical nonlinear analysis of reinforced concrete frames including joint flexibility,” *Engineering Structures*, Vol. 34, pp. 455–465.

Biskinis, D.E., Roupakias, G.K., and Fardis, M.N., 2004, “Degradation of shear strength of reinforced concrete members with inelastic cyclic displacements,” *ACI Structural Journal*, Vol. 101, No. 6, pp. 773-783.

Blackard, B., Willam, K., and Mettupalayam, S., 2009, *Experimental Observations of Masonry Infilled RC Frames with Openings*, ACI Special Publication 265-9, American Concrete Institute, Farmington Hills, Michigan.

Brueggen, B.L., and French, C.W., 2010, “Simplified modeling of non-rectangular reinforced concrete structural walls,” *Proceedings*, Paper 1713, 9th U.S. National Conference and 10th Canadian Conference on Earthquake Engineering, Toronto, Ontario, Canada.

Celik, O.C., 2007, *Probabilistic Assessment of Non-Ductile Reinforced Concrete Frames Susceptible to Mid-America Ground Motions*, Ph.D. Dissertation, Georgia Institute of Technology, Atlanta, Georgia.

CESMD, 2011, *New Zealand Earthquake of 21 February 2011*, Center for Earthquake Strong Motion Data (CESMD), <http://strongmotioncenter.org>, last accessed July 10, 2012.

Chan, M.C., 1972, *Investigation of Collapse of Psychiatric Day Clinic - Olive View Hospital during San Fernando Earthquake*, University of California, Berkeley, California.

Chowdhury, S.R., and Orakcal, K., 2012, “An analytical model for reinforced concrete columns with lap splices,” *Engineering Structures*, Vol. 43, pp. 180-193.

Concrete Coalition, 2013, *Online Database*, Sponsored by the Earthquake Engineering Research Institute, the Pacific Earthquake Engineering Research Center, and the Applied Technology Council, Oakland, California, <http://www.concretecoalition.org>, last accessed August 20, 2013.

CSI, 2013, *Nonlinear Analysis and Performance Assessment for 3D Structures*, PERFORM 3D, Computers and Structures, Inc., Berkeley, California, <http://www.csiamerica.com/perform3d/overview>, last accessed August 20, 2013.

CSSC, 1995, *Northridge Earthquake—Turning Loss to Gain*, Report No. 95-01, California Seismic Safety Commission, Sacramento, California.

- CSSC, 1996, *1994 Northridge Earthquake Building Case Studies Project*, pp. 63-82, California Seismic Safety Commission, Sacramento, California.
- Dawe, J.L., and Seah, C.K., 1989, "Out-of-plane resistance of concrete masonry infilled panels," *Journal of the Canadian Society for Civil Engineering*, Vol. 16, pp. 854-864.
- EERC, 1994, *Preliminary Report on the Seismological and Engineering Aspects of the January 17, 1994 Northridge Earthquake*, Report No. EERC-94/01, Earthquake Engineering Research Centre, University of California, Berkeley, California.
- EERI, 1980, *Reconnaissance Report, Imperial County, California, Earthquake, October 15, 1979*, Earthquake Engineering Research Institute, Oakland, California.
- EERI, 1995, "Guam earthquake reconnaissance report", *Earthquake Spectra*, Supplement B to Volume 11.
- EERI, 1996, "Northridge earthquake reconnaissance report, Vol. 2" *Earthquake Spectra*, Supplement C to Volume 11.
- Elwood, K.J., 2004, "Modeling failures in existing reinforced concrete columns," *Canadian Journal of Civil Engineering*, Vol. 31, No. 5, pp. 846–859.
- Elwood, K.J., 2013, Performance of concrete buildings in the 22 February 2011 Christchurch earthquake and implications for Canadian codes, *Canadian Journal of Civil Engineering*, Vol. 40, No. 3, pp. 759-776.
- Elwood, K.J., and Moehle, J.P., 2005, "Axial capacity model for shear-damaged columns," *ACI Structural Journal*, Vol. 102, No. 4, pp. 578-587.
- Elwood, K.J., and Moehle, J.P., 2008, "Dynamic shear and axial load failure of reinforced concrete columns," *Journal of Structural Engineering*, Vol. 134, No. 7, July 2008, pp. 1189-1198.
- Elwood, K.J., Matamoros, A., Wallace, J.W., Lehman, D.E., Heintz, J.A., Mitchell, A., Moore, M.A., Valley, M.T., Lowes, L.N., Comartin, C., and Moehle, J.P., 2007, "Update of ASCE/SEI 41 concrete provisions," *Earthquake Spectra*, Vol. 23, No. 3, pp. 493-523.
- Fardipour, M., Lam, N., Gad, E., and Wilson, J., 2011, "Collapse limit state assessment of lightly reinforced concrete columns," *Australian Earthquake Engineering Society, 2011 Conference*, 18-20 November 2011, Barossa Valley, South Australia.
- FEMA, 1997a, *NEHRP Guidelines for the Seismic Rehabilitation of Existing Buildings*, FEMA 273 Report, prepared by the Applied Technology Council,

under contract to the Building Seismic Safety Council, for the Federal Emergency Management Agency, Washington, D.C.

FEMA, 1997b, *NEHRP Commentary on the Guidelines for the Seismic Rehabilitation of Existing Buildings*, FEMA 274 Report, prepared by the Applied Technology Council, under contract to the Building Seismic Safety Council, for the Federal Emergency Management Agency, Washington, D.C.

FEMA, 2000, *Prestandard and Commentary for the Seismic Rehabilitation of Buildings*, FEMA 356 Report, prepared by the American Society of Civil Engineers for the Federal Emergency Management Agency, Washington, D.C.

FEMA, 2006, *Techniques for Seismic Rehabilitation of Existing Buildings*, FEMA 547, Federal Emergency Management Agency, Washington, D.C.

FEMA, 2009a, *Effects of Strength and Stiffness Degradation on Seismic Response*, FEMA P-440A Report, prepared by the Applied Technology Council for the Federal Emergency Management Agency, Washington, D.C.

FEMA, 2009b, *NEHRP Recommended Seismic Provisions for New Buildings and Other Structures*, FEMA P-750 Report, prepared by the Building Seismic Safety Council for the Federal Emergency Management Agency, Washington, D.C.

FEMA, 2009c, *Quantification of Building Seismic Performance Factors*, FEMA P-695 Report, prepared by the Applied Technology Council for the Federal Emergency Management Agency, Washington, D.C.

FEMA, 2006, Multi-Hazard Loss Estimation Methodology, Earthquake Module (HAZUS-MH MR2), developed by the National Institute of Building Sciences for the Federal Emergency Management Agency, Washington, D.C.

Flanagan, R.D., and Bennett, R.M., 1999, "Bidirectional behavior of structural clay tile infilled frames," *Journal of Structural Engineering*, Vol. 125, No. 3, pp. 236-244.

GeoNet, 2011. *M 6.3, Christchurch, 22 February 2011, GNS Science, New Zealand*, <http://info.geonet.org.nz/display/quake/M+6.3%2C+Christchurch%2C+22+February+2011>, last accessed July 12, 2012.

Gogus, A., 2010, *Structural Wall Systems – Nonlinear Modeling and Collapse Assessment of Shear Walls and Slab-Column Frames*, Ph.D. Dissertation, University of California, Los Angeles, California.

Grierson, D.E., Xu, L., and Liu, Y., 2005, "Progressive-failure analysis of buildings subjected to abnormal loading," *Computer-Aided Civil and Infrastructure Engineering*, Vol. 20, No. 3, pp. 155-171.

- Gulec, C.K., and Whittaker, A.S., 2011, "Hysteretic modeling of squat reinforced concrete shear walls" *Transactions*, 21st International Conference on Structural Mechanics in Reactor Technology (SMiRT 21), Paper 341, New Delhi, India.
- Hamburger, R. O., 2004, *Supplemental Report: Failure Investigation, Beach Wing, Royal Palm Resort, Tumon, Guam*, EQE International, Oakland, California.
- Haselton, C.B., Baker, J.W., Liel, A.B., and Deierlein, G.G., 2011, "Accounting for ground motion spectral shape characteristics in structural collapse assessment through an adjustment for epsilon," *Journal of Structural Engineering*, Vol. 137, No. 3, pp. 332-344.
- Haselton, C.B., Liel, A.B., Taylor-Lange, S., and Deierlein, G.G., 2008, *Beam-Column Element Model Calibrated for Predicting Flexural Response Leading to Global Collapse of RC Frame Buildings*, PEER Report 2007/03, Pacific Earthquake Engineering Research Center, Berkeley, California.
- Hassan, W., 2011, *Analytical and Experimental Assessment of Seismic Vulnerability of Beam-Column Joints without Transverse Reinforcement in Concrete Buildings*, Ph.D. Dissertation, University of California, Berkeley, California.
- Henkhaus, K., 2010, *Axial Failure of Vulnerable Reinforced Concrete Columns Damaged by Shear Reversals*, Ph.D. Dissertation, Purdue University, West Lafayette, Indiana.
- Holmes, M., 1961, "Steel frames with brickwork and concrete filling," *Proceedings of the Institute of Civil Engineers*, Vol. 19, No. 6501, pp. 473-478.
- Holmes W.T., 2000, "Risk assessment and retrofit of existing buildings," *Proceedings*, Paper No. 2826, 12th World Conference on Earthquake Engineering, Auckland, New Zealand.
- Hortacsu, A., Pujol, S., and Catlin, A.C., 2012, "Development of a database for ground motion and building performance data," *Proceedings of the Fifteenth World Conference on Earthquake Engineering*, Lisbon, Portugal.
- Hueste, M.B.D., and Wight, J.K., 1999, "Nonlinear punching shear failure model for interior slab-column connections," *Journal of Structural Engineering*, Vol. 125, No. 9, pp. 997-1007.
- Hughes, T.J.R., Pister, K.S., and Taylor, R.L., 1979, "Implicit-explicit finite elements in nonlinear transient analysis," *Computer Methods in Applied Mechanics and Engineering*, Vol. 17/18, pp. 159-182.
- Ibarra, L.F., Medina, R.A., and Krawinkler, H., 2005, "Hysteretic models that incorporate strength and stiffness deterioration," *Earthquake Engineering and Structural Dynamics*, Vol. 34, pp. 1489-1511.

ICC, 2012a, *International Building Code*, International Code Council, Washington, D.C.

ICC, 2012b, *International Existing Building Code*, International Code Council, Washington D.C.

Johnson, B., 2010, *Anchorage Detailing Effects on Lateral Deformation Components of R/C Shear Walls*, MS Thesis, Department of Civil Engineering, University of Minnesota, Minneapolis, Minnesota.

Kabeyasawa, T., Kim, Y., Sato, M., Hyunseong, H., and Fukuyama, H., 2012, *Effect of Bi-axial Loading on Flexural Deformability of Reinforced Concrete Walls*, Oral Presentation, 15th World Conference on Earthquake Engineering, Special Session 24-25, September, Lisbon, Portugal.

Kadysiewski, S., Mosalam, K.M., 2008, *Modeling of Unreinforced Masonry Infill Walls Considering In-Plane and Out-of-Plane Interaction*, PEER Report 2008/102, Pacific Earthquake Engineering Research Center, Berkeley, California.

Kadysiewski, S., and Mosalam, K.M., 2009, *Modeling of Unreinforced Masonry Infill Walls Considering In-Plane and Out-of-Plane Interaction*, PEER Report 2008/102, Pacific Earthquake Engineering Research Center, Berkeley, California.

Kang, T.H.-K., Wallace, J.W., and Elwood, K.J., 2009, "Nonlinear modeling of flat plate systems," *Journal of Structural Engineering*, Vol. 135, No. 2, pp. 147-158.

Kato, D., and Ohnishi, K., "Axial load carrying capacity of RC columns under lateral load reversals," *Proceedings*, The Third U.S.-Japan Workshop on Performance-Based Earthquake Engineering Methodology for Reinforced Concrete Building Structures, Pacific Earthquake Engineering Research Center, Berkeley, California.

Kim, J., and LaFave, J., 2009, *Joint Shear Behavior of Reinforced Concrete Beam-Column Connections Subjected to Seismic Lateral Loading*, NSEL Report NSEL-020, Newmark Structural Engineering Laboratory, University of Illinois, Urbana-Champaign, Illinois.

Kojic, S., Trifunac, M.D., and Anderson, J.C., 1984, *A Postearthquake Response Analysis of the Imperial County Services Building in El Centro*, Report No. CE 84-02, University of Southern California, Los Angeles, California.

Kolozvari K., Tran T., Orakcal K., and Wallace J.W., 2012, "Modeling of cyclic shear-flexure interaction in reinforced concrete walls," *Proceedings*, Paper 2471, 15th World Conference on Earthquake Engineering, Lisbon, Portugal.

- Koutromanos, I., 2011, *Numerical Analysis of Masonry-Infilled Reinforced Concrete Frames Subjected to Seismic Loads and Experimental Evaluation of Retrofit Techniques*, Ph.D. Dissertation, University of California, San Diego, California.
- Koutromanos, I., Stavridis, A., Shing, P.B., and Willam, K., 2011, "Numerical modeling of masonry-infilled RC frames subjected to seismic loads," *Computers and Structures*, Vol. 89, pp. 1026-1037.
- Kowalski, M.J., and Priestley, M.J.N., 2000, "Improved analytical model for shear strength of circular reinforced concrete columns in seismic regions," *ACI Structural Journal*, Vol. 97, No. 3, pp. 388-396.
- Krawinkler, H., Medina, R., and Alavi, B., 2003, "Seismic drift and ductility demands and their dependence on ground motions." *Engineering Structures*, Vol. 25, No. 5, pp. 637-653.
- Kreger, M., and Sozen, M.A., 1983, *A Study of the Causes of Column Failures in the Imperial County Services Building during the 15 October 1979 Imperial Valley Earthquake*, Report to the National Sciences Foundation, University of Illinois at Urbana-Champaign, Urbana, Illinois.
- Kreger, M., and Sozen, M.A., 1989, "Seismic response of Imperial County Services Building in 1979," *Journal of Structural Engineering*, Vol. 115, No. 12, pp. 3095-3111.
- LeBorgne, M.R., 2012, *Modeling the Post Shear Failure Behavior of Reinforced Concrete Columns*, Ph.D. Dissertation, University of Texas, Austin, Texas.
- LeBorgne, M.R., and Ghannoum, W.M., 2013, "Analytical element for simulating lateral-strength degradation in reinforced concrete columns and other frame members," *Journal of Structural Engineering*, Vol. 139, No. 8.
- Lee, T.-H., and Mosalam, K.M., 2005, "Seismic demand sensitivity of reinforced concrete shear-wall building using FOSM method," *Earthquake Engineering and Structural Dynamics*, Vol. 34, No. 14, pp. 1719-1736.
- Lee T.-H., and Mosalam, K.M., 2006, *Probabilistic Seismic Evaluation of Reinforced Concrete Structural Components and Systems*, PEER Report 2006/04, pp. 181, Pacific Earthquake Engineering Research Center, Berkeley, California.
- Lehman, D.L., Stanton, J., Anderson, M., Alire, D., and Walker, S., 2004, "Seismic performance of older beam-column joints," *Proceedings*, 13th World Conference on Earthquake Engineering, International Association of Earthquake Engineering, Tokyo, Japan.

- Liel, A.B., Haselton, C.B., Deierlein, G.G, and Baker, J.W., 2009, "Incorporating modeling uncertainties in the assessment of seismic collapse risk of buildings," *Structural Safety*, Vol. 31, Issue 2, pp. 197-211.
- Li, Y., 2012, *Shaking Table Test Column Database and Evaluation of Drift Capacity Models for Non-Ductile Columns*, January 2012, MSc Thesis, University of British Columbia, Vancouver, British Columbia.
- Lotfi, H.R., and Shing, P.B., 1991, "An Appraisal of Smeared Crack Models for Masonry Shear Wall Analysis," *Computers and Structures*, Vol. 41, No. 3, pp. 413–425.
- Lynn, A.C., Moehle, J.P., Mahin, S.A., Holmes, W.T., 1996, "Seismic evaluation of existing reinforced concrete columns," *Earthquake Spectra*, Vol. 12, No. 4, pp. 715-739.
- Mahin, S.A., Bertero, V.V., Chopra, A.K., and Collins, R.G., 1976, *Response of the Olive View Hospital Main Building during the San Fernando Earthquake*, Report No. EERC 76-22, Earthquake Engineering Research Center, University of California, Berkeley, California.
- Mainstone, R.J., and Weeks, G.A., 1970, "The influence of bounding frame on the racking stiffness and strength of brick walls," *Proceedings*, The 2nd International Conference on Brick Masonry, Stoke-on-Trent, England.
- Mander, J.B., Nair, B., Wojtkowski, K., and Ma, J., 1993, *An Experimental Study on the Seismic Performance of Brick-Infilled Steel Frames with and without Retrofit*, Report No. NCEER-93-0001, National Center for Earthquake Engineering Research, State University of New York, Buffalo, New York.
- Massone, L.M., 2006, *RC Wall Shear – Flexure Interaction: Analytical and Experimental Responses*, Ph.D. Dissertation, University of California, Los Angeles, California.
- Massone, L.M., and Lopez, E.E, 2012, "Modeling of global buckling of longitudinal reinforcement," *Proceedings*, 15th World Conference on Earthquake Engineering, Lisbon, Portugal.
- Mazzoni, S., McKenna F., Scott M.H., and Fenves, G.L., 2009, *User Command-Language Manual (OpenSees Version 2.0) Open System for Earthquake Engineering Simulation*, Pacific Earthquake Engineering Research Center, Berkeley, California, <http://opensees.berkeley.edu/OpenSees/manuals/usermanual/index.html>, last accessed August 20, 2013.
- Mehrabi, A.B., Shing, P.B., Schuller, M.P., and Noland, J.L., 1994, *Performance of Masonry-Infilled R/C frames Under In-Plane Lateral Loads*, Report No.

CU/SR-94-6, Dept. of Civil, Environmental, and Architectural Engineering,
University of Colorado, Boulder, Colorado.

Mehrabi, A.B., Shing, P.B., Schuller, M.P., and Noland, J.L., 1996, "Experimental evaluation of masonry-infilled RC frames," *Journal of Structural Engineering*, Vol. 122, No. 3, pp. 228-237.

Melek, M., and Wallace, J.W., 2004, "Cyclic behavior of columns with short lap splices," *ACI Structural Journal*, Vol. 101, No. 6, pp. 802-811.

Mitra, N., and Lowes, L.N., 2007, "Evaluation, calibration, and verification of a reinforced concrete beam-column joint model," *Journal of Structural Engineering*, Vol. 133, No. 1, pp. 105-120.

Moehle, J. P., 1997, *Royal Palm Resort, Guam – An Evaluation of the Causes of the Failure in the Earthquake of 8 August 1993*, Engineering Report, Pacific Earthquake Engineering Research Center, Berkeley, California.

Moehle, J.P., 2003, "Assessment of the collapse of a concrete frame intended to meet U.S. seismic requirements," *Proceedings*, The Fifth U.S.-Japan Workshop on Performance-Based Earthquake Engineering Methodology for Reinforced Concrete Building Structures, Hakone, Japan.

Moehle, J.P., 2007, *The Top Ten List*, Presentation at the Concrete Coalition Meeting, November, 2007, Los Angeles, California.

Mosalam, K.M., and Günay, M.S., 2012, "Behavior and modeling of reinforced concrete frames with unreinforced masonry infill walls," *Structural Engineering and Geomechanics*, Editor S.K. Kunnath, Encyclopedia of Life Support Systems (EOLSS), Developed under the Auspices of the UNESCO, Eolss Publishers, Oxford, United Kingdom, <http://www.eolss.net>, last accessed February 19, 2013.

Mosalam, K.M., and Günay, M.S., 2013, "Modeling Gravity Load Failure in Collapse Simulations," *Review of Past Performance and Further Development of Modeling Techniques for Collapse Assessment of Existing Reinforced Concrete Buildings*, NIST GCR 13-917-28, prepared by the NEHRP Consultants Joint Venture, a partnership of the Applied Technology Council and the Consortium of Universities for Research in Earthquake Engineering, for the National Institute of Standards and Technology, Gaithersburg, Maryland.

Mosalam, K.M., Günay, M.S., and Henry, D.S., 2013, "Simulation of reinforced concrete frames with unreinforced masonry infill walls with emphasis on critical modelling aspects," *Proceedings*, 12th Canadian Masonry Symposium, Vancouver, British Columbia, Canada.

- Mosalam, K.M., Park, S., and Günay, M.S., 2009, "Evaluation of an element removal algorithm for shear critical reinforced concrete frames," *Proceedings*, COMPDYN, Thematic Conference on Computational Methods in Structural Dynamics and Earthquake Engineering, Island of Rhodes, Greece.
- Mostafaei, H., and Kabeyasawa, T., 2007, "Axial-shear-flexure interaction approach for reinforced concrete columns," *ACI Structural Journal*, Vol. 104, No. 2, pp. 218-226.
- Nagae, T., Tahara, K., Matsumori, T., Shiohara, H., Kabeyasawa, T., Kono, S., Nishiyama, M., and Wallace, J.W., Ghannoum, W., Moehle, J.P., Sause, R., Keller, W., and Tuna, Z., 2011, *Design and Instrumentation of the 2010 E-Defense Four-Story Reinforced Concrete and Post-Tensioned Concrete Buildings*, PEER Report No 2011-104, Pacific Earthquake Engineering Research Center, Berkeley, California.
- Naish, D., Fry, A., Klemencic, R., and Wallace, J.W., 2013a, "Reinforced concrete coupling beams: Part I testing," *ACI Structural Journal*, Vol. 110, No. 6.
- Naish, D., Fry, A., Klemencic, R., and Wallace, J.W., 2013b, "Reinforced concrete coupling beams: Part II modeling," *ACI Structural Journal*, Vol. 110, No. 6.
- NEES, 2010, *The Chile Earthquake Database Group*, George E. Brown, Jr., Network for Earthquake Engineering Simulation, Purdue University, West Lafayette, Indiana, NEEShub, <https://nees.org/groups/chileearthquakedatabase>, last accessed August 13, 2013.
- NEES, 2012, *Information on the Drift Capacity of RC Columns*, the George E. Brown Jr., Network for Earthquake Engineering Simulation, NEEShub, http://nees.org/groups/axial_failure, last accessed August 13, 2013.
- NISEE, 2013a, *The Karl V. Steinbrugge Slide and Photograph Collection*, NISEE/PEER/UCB, National Information Service for Earthquake Engineering/Pacific Earthquake Engineering Research Center, Berkeley, California, http://nisee.berkeley.edu/visual_resources/steinbrugge_collection.html, last accessed August 16, 2013.
- NISEE, 2013b, *PEER / Structural Performance Database*, NISEE/PEER/UCB, National Information Service for Earthquake Engineering/Pacific Earthquake Engineering Research Center, Berkeley, California, <http://nisee.berkeley.edu/spd/>, last accessed August 13, 2013.
- NISEE, 2013c, *Earthquake Damage Photographs*, NISEE/PEER/UCB, National Information Service for Earthquake Engineering/Pacific Earthquake Engineering Research Center, Berkeley, California, <http://nisee.berkeley.edu/elibrary/>, last accessed August 16, 2013.

NIST, 2010a, *Evaluation of the FEMA P-695 Methodology for Quantification of Building Seismic Performance Factors*, NIST GCR 10-917-8, prepared by the NEHRP Consultants Joint Venture, a partnership of the Applied Technology Council and the Consortium of Universities for Research in Earthquake Engineering, for the National Institute of Standards and Technology, Gaithersburg, Maryland.

NIST, 2010b, *Program Plan for the Development of Collapse Assessment and Mitigation Strategies for Existing Reinforced Concrete Buildings*, NIST GCR 10-917-7, prepared by the NEHRP Consultants Joint Venture, a partnership of the Applied Technology Council and the Consortium of Universities for Research in Earthquake Engineering, for the National Institute of Standards and Technology, Gaithersburg, Maryland.

NIST, 2011a, *Seismic Design of Cast-in-Place Concrete Special Structural Walls and Coupling*, NIST GCR 11-917-11, prepared by the NEHRP Consultants Joint Venture, a partnership of the Applied Technology Council and the Consortium of Universities for Research in Earthquake Engineering, for the National Institute of Standards and Technology, Gaithersburg, Maryland.

NIST, 2011b, *Selecting and Scaling Earthquake Ground Motions for Performing Response-History Analyses*, NIST GCR 11-917-15, prepared by the NEHRP Consultants Joint Venture, a partnership of the Applied Technology Council and the Consortium of Universities for Research in Earthquake Engineering, for the National Institute of Standards and Technology, Gaithersburg, Maryland.

NIST, 2013a, *Development of NIST Measurement Science R&D Roadmap: Earthquake Risk Reduction in Buildings*, NIST GCR 13-917-23, prepared by the Building Seismic Safety Council for the National Institute of Standards and Technology, Gaithersburg, Maryland.

NIST, 2013b, *NIST Disaster and Failure Studies Program*, National Institute of Standards and Technology, <http://www.nist.gov/el/disasterstudies/index.cfm>, last accessed December 11, 2013.

NZBDH, 2011, *Structural Performance of Christchurch CBD Buildings in the 22 February 2011 Aftershocks*, New Zealand Department of Building and Housing Expert Panel, Ministry of Business, Innovation and Employment, Wellington, New Zealand.

New Zealand Herald, 2011, “Council may be unaware of buildings similar to CTV,” *New Zealand Herald*, article December 11, 2011, article by Kurt Bayer, photographer Sarah Ivey, Auckland, New Zealand, http://www.nzherald.co.nz/ctv-building/news/article.cfm?c_id=1503040&objectid=10853408, last accessed August 13, 2013.

- Olesen, S., Sozen, M., and Siess, C., 1967, *Investigation of Prestressed Reinforced Concrete for Highway Bridges, Part IV: Strength in Shear of Beams with Web Reinforcement*, Engineering Experiment Station Bulletin No. 493, College of Engineering, University of Illinois, Urbana-Champaign, Illinois.
- OpenSees, 2013, *Open System for Earthquake Engineering Simulation, OpenSees*, Pacific Earthquake Engineering Research Center, Berkeley, California, <http://opensees.berkeley.edu>, last accessed on August 13, 2013.
- OpenSeesWiki, 2010, “Infill Wall Model and Element Removal,” *OpenSees*, http://opensees.berkeley.edu/wiki/index.php/Infill_Wall_Model_and_Element_Removal, last accessed October 1, 2010.
- OpenSeesWiki, 2012, “Welcome to the OpenSeesWiki,” *OpenSees*, http://opensees.berkeley.edu/wiki/index.php/Main_Page, last accessed May 10, 2012.
- OSHPD, 2009, *Seismic Retrofit Program Overview*, State of California, Office of Statewide Health Planning and Development, Sacramento, California, <http://www.oshpd.ca.gov/FDD/SB1953/>, last accessed August 20, 2013.
- OSHPD, 2010, *Proposed Changes to the 2010 California Administrative Code*, California Code of Regulations, Title 24, Part 1, Chapters 6 & 7, http://www.oshpd.ca.gov/fdd/Regulations/Title_24_Proposed_and_Approved_Code_Changes/Part1/2010%20ER_Part%201_HAZUS_ET.pdf, last accessed August 20, 2013.
- Otani, S., 1999, “Reinforced concrete building damage statistics and SDF response with design seismic forces,” *Earthquake Spectra*, Vol. 15, No. 3, pp. 485-501.
- Oyen, P., 2006, *Evaluation of Analytical Tools for Determining the Seismic Response of Reinforced Concrete Shear Walls*, Ph.D. Dissertation, University of Washington, Seattle, Washington.
- Panagiotakos, T.B., and Fardis, M.N., 2001, “Deformations of reinforced concrete members at yielding and ultimate,” *ACI Structural Journal*, Vol. 98, No. 2.
- Pantelides, C.P., Hansen, J., Nadauld, J., and Reaveley, L.D., 2002, *Assessment of Reinforced Concrete Building Exterior Joints with Substandard Details*, PEER Report 2002/18, Pacific Earthquake Engineering Research Center, Berkeley, California.
- Park, S., 2010, *Experimental and Analytical Studies on Old Reinforced Concrete Buildings with Seismically Vulnerable Beam-Column Joints*, Ph.D. Dissertation, University of California, Berkeley, California.

- Park, S., and Mosalam, K.M., 2009, *Shear Strength Models of Exterior Beam-Column Joints without Transverse Reinforcement*, PEER Report 2009/106, Pacific Earthquake Engineering Research Center, Berkeley, California.
- Park, S., and Mosalam, K.M., 2012a, "Analytical model for predicting the shear strength of unreinforced exterior beam-column joints," *ACI Structural Journal*, 2012, Vol. 102, No. 2, pp. 149-160.
- Park, S., and Mosalam, K.M., 2012b, *Experimental and Analytical Studies on Reinforced Concrete Buildings with Seismically Vulnerable Beam-Column Joints*, PEER Report 2012/03, Pacific Earthquake Engineering Research Center, Berkeley, California.
- Park, S., and Mosalam, K.M., 2012c, "Parameters for shear strength prediction of exterior beam-column joints without transverse reinforcement," *Engineering Structures*, Vol. 36, No. 3, pp. 198-209.
- Park, S., and Mosalam, K.M., 2013a, "Experimental investigation of non-ductile reinforced concrete corner beam-column joints with floor slabs," *Journal of Structural Engineering*, Vol. 139, No. 1, pp. 1-14.
- Park, S., and Mosalam, K.M., 2013b, "Simulation of reinforced concrete frames with non-ductile beam-column joints," *Earthquake Spectra*, Vol. 29, No. 1, pp. 233-257.
- Pauschke, M., Oliviera, C.S., Shah, H.C., and Zsutty, T.C., 1981, *A Preliminary Investigation of the Dynamic Response of the Imperial County Services Building during the October 15, 1979 Imperial Valley Earthquake*, Report No. 49, Stanford University, Stanford, California.
- PEER, 2010, *Guidelines for Performance-Based Seismic Design of Tall Buildings*, PEER Report 2010/05, prepared by the Tall Buildings Initiative Guidelines Working Group for the Pacific Earthquake Engineering Research Center, Berkeley, California.
- Porter, K.A., Beck, J.L., and Shaikhutdinov, R.V., 2002, "Sensitivity of building loss estimates to major uncertain variables," *Earthquake Spectra*, Vol. 18, No. 4, pp. 719-743.
- Priestley, N.M., and Hart, G.H., 1994, "Seismic Behavior of "As-Built" and "As-Designed" Corner Joints," SEQAD Report to Hart Consultant Group, Report #94-09, Los Angeles, California.
- Pujol, S., Ramirez, J. A., and Sozen, M.A., 1999, "Drift capacity of reinforced concrete columns subjected to cyclic shear reversal," *Seismic Response of Concrete Bridges*, ACI Special Publication 187, American Concrete Institute, Farmington Hills, Michigan.

- Raghunandan, M., and Liel, A.B., 2013, "Effect of ground motion duration on earthquake-induced structural collapse," *Structural Safety*, Vol. 41, pp. 119–133.
- Ranf, R.T., Eberhard, M.O., and Stanton, J.F., 2006, *Effects of Displacement History on Failure of Lightly Confined Bridge Columns*, ACI Special Publication 236, American Concrete Institute, Farmington Hills, Michigan.
- Reuter, H.R., 1964, Collapse of the Four Seasons Apartment Building, March 27, 1964 Earthquake-Anchorage, Alaska, Western Concrete Structures Co., Anchorage, Alaska.
- Rodriguez, M., Botero, J.C., and Villa, J., 1999, "Cyclic stress-strain behavior of reinforcing steel including effect of buckling," *Journal of Structural Engineering*, Vol. 125, No. 6, pp. 605-612.
- Rojahn, C., and Mork, P.N., 1982, "An analysis of strong-motion data from a severely damaged structure—the Imperial County Services Building, El Centro, California," *The Imperial Valley, California, Earthquake of February 9, 1971*, U. S. Geological Survey Professional Paper 1254, Menlo Park, California.
- Ross, B., Osteraas, J., Luth, G., Moncarz, P., and Bozorgnia, Y., 2000, "Seismic collapse of reinforced concrete towers at Royal Palm Resort, Guam, USA", *Proceedings*, 25th Conference on Our World in Concrete & Structures, Singapore, Indonesia.
- Rots, J.G., 1991, "Numerical simulation of cracking in structural masonry," *HERON*, Netherlands School for Advanced Studies in Construction, Netherlands, Vol. 36, No. 2, pp. 49-63.
- Sezen, H., 2002, *Seismic Behavior and Modeling of Reinforced Concrete Building Columns*, Ph.D. Dissertation, University of California, Berkeley, California.
- Sezen, H., and Moehle, J.P., 2004, "Shear strength model for lightly reinforced concrete columns," *Journal of Structural Engineering*, Vol. 130, No. 11, pp. 1692-1703.
- Sharma, A., Eligehausen, R., and Reddy, G.R., 2011, "A new model to simulate joint shear behavior of poorly detailed beam-column connections in RC structures under seismic loads, Part 1: exterior joints," *Engineering Structures*, Vol. 33, pp. 1034-1051.
- Somerville, P., 1997, *Earthquake Ground Motion at the Site of the Royal Palm Resort during the August 8, 1993 Guam Earthquake*, Woodward-Clyde Federal Services, Pasadena, California.

- Somerville, P.G., Smith, N., Punyamurthula, S., and Sun, J., 1997, *Development of Ground Motion Time Histories for Phase 2 of the FEMA/SAC Steel Project*, prepared by SAC Joint Venture for FEMA, SAC/BD-97/04, Federal Emergency Management Agency, Washington, D.C., <http://nisee.berkeley.edu/elibrary/Text/Lib050189>, last accessed August 20, 2013.
- Stafford Smith, B., 1967, "Methods for predicting the lateral stiffness and strength of multi-story infilled frames," *Building Science*, Vol. 2, Issue 3, pp. 247-257.
- Stavridis, A., 2009, *Analytical and Experimental Study of Seismic Performance of Reinforced Concrete Frames Infilled with Masonry Walls*, Ph.D. Dissertation, University of California, San Diego, California.
- Stavridis, A., and Shing, P.B., 2010, "Finite element modeling of nonlinear behavior of masonry-infilled reinforced concrete frames," *Journal of Structural Engineering*, Vol. 136, No. 3, pp. 285-296.
- Stavridis, A., Koutromanos, I., and Shing, P.B., 2012, "Shake-table tests of a three-story reinforced concrete frame with masonry infill walls," *Journal of Earthquake Engineering and Structural Dynamics*, Vol. 41, No. 6, pp. 1089-1108.
- Steinbrugge, K.V., Schader, E.E., Bigglestone, H.C., and Weers, C.A., 1971, *San Fernando Earthquake, February 9, 1971*, Pacific Fire Rating Bureau, San Francisco, California.
- Talaat M., and Mosalam K.M., 2007, *Computational Modeling of Progressive Collapse in Reinforced Concrete Frame Structures*, PEER Report 2007/10, Pacific Earthquake Engineering Research Center, Berkeley, California.
- Talaat, M., and Mosalam, K.M., 2009, "Modeling progressive collapse in reinforced concrete buildings using direct element removal," *Earthquake Engineering Structural Dynamics*, Vol. 38, No. 5, pp. 609-634.
- Takemura, H., and Kawashima, K., 1997, "Effect of loading hysteresis on ductility capacity of reinforced concrete bridge piers," *Journal of Structural Engineering*, Japan, Vol. 43A, pp. 849-858.
- Tashkandi, M.A., and Selna, L.G., 1972, *Failure Analysis of the Olive View Psychiatric Day Clinic*, University of California, Los Angeles, California.
- Thomsen IV, J.H., and Wallace, J.W., 1995, *Displacement-Based Design of Reinforced Concrete Structural Walls: An Experimental Investigation of Walls with Rectangular and T-Shaped Cross-Sections*, Department of Civil Engineering, Clarkson University, Potsdam, New York.

- Thomsen IV, J.H., and Wallace, J.W., 2004, "Displacement-based design of slender reinforced concrete structural walls-experimental verification," *Journal of Structural Engineering*, Vol. 130, No. 4, pp. 618-630.
- Todd, D.R., Carino, N.J., Chung, R.M., Lew, H.S., Taylor, A.W., Walton, W.D., Cooper, J.D., and Nimis, R., 1994, *1994 Northridge Earthquake, Performance of Structures, Lifelines, and Fire Protection Systems*, NIST Special Publication 862, National Institute of Standards and Technology, Gaithersburg, Maryland
- Tran, T.A., and Wallace, J.W., 2010, *Experimental and Analytical Studies of Moderate Aspect Ratio Reinforced Concrete Structural Walls*, Ph.D. Dissertation, University of California, Los Angeles, California.
- Tran, T.A., and Wallace, J.W., 2012, "Experimental study of nonlinear flexural and shear deformations of reinforced concrete structural walls," *Proceedings*, Paper 3913, 15th World Conference on Earthquake Engineering, Lisbon, Portugal.
- Tuna, Z., 2012, *Seismic Performance, Modeling, and Failure Assessment of Reinforced Concrete Shear Wall Buildings*, Ph.D. Dissertation, University of California, Los Angeles, California.
- USGS, 2011, *Magnitude 6.1 - South Island of New Zealand*, United States Geological Survey, Reston, Virginia, <http://earthquake.usgs.gov/earthquakes/eqinthenews/2011/usb0001igm/>, last accessed July 12, 2012.
- USGS, 2012, *1964 Great Alaska Earthquake*, United States Geological Survey, Reston, Virginia, http://earthquake.usgs.gov/earthquakes/states/events/1964_03_28.php, last accessed July 12, 2012.
- USGS, and NOAA, 1971, *The San Fernando, California, Earthquake of February 9, 1971*, Joint publication of the United States Geological Survey and the National Oceanic and Atmospheric Administration, U.S. Government Printing Offices, Washington D.C.
- Vamvatsikos, D., and Cornell, C.A., 2006, "Direct estimation of the seismic demand and capacity of oscillators with multi-linear static pushovers through incremental dynamic analysis," *Earthquake Engineering and Structural Dynamics*, Vol. 35, Issue 9, pp. 1097-1117.
- Walker, S., 2001, *Seismic Performance of Existing Reinforced Concrete Beam-Column Joints*, M.S. Thesis, Department of Civil and Environmental Engineering, University of Washington, Seattle, Washington.

- Wallace, J.W., Elwood, K.J., and Massone, L.M., 2008, "An axial load capacity model for shear critical RC wall piers," *Journal of Structural Engineering*, Vol. 134, No. 9, pp. 1548-1557.
- Wallace, J.W., Massone, L.M., Bonelli, P., Dragovich, J., Lagos, R., Luders, C., and Moehle, J.P., 2012, "Damage and implications for seismic design of RC structural wall buildings," *Earthquake Spectra*, Vol. 28, No. S1, pp. S28-S300.
- Wallace, J.W., Segura, C., and Tran, T.A., 2013, "Shear design of RC structural walls," *Proceedings*, 10th International Conference on Urban Earthquake Engineering, Tokyo Institute of Technology, Tokyo, Japan.
- Wight, J.K., and Sozen, M.A., 1975, "Strength decay of RC columns under shear reversals," *Journal of Structural Engineering*, Vol. 101, No. 5, pp. 1053-1065.
- Yang, T.Y., Moehle, J.P., Bozorgnia, Y., Zareian, F., and Wallace, J.W., 2012, "Performance assessment of tall concrete core-wall buildings designed using two alternative approaches," *Earthquake Engineering and Structural Dynamics*, Vol. 41, Issue 11, pp. 1515-1531.
- Yavari, S., Lin, S.-H., Elwood, K.J., Wu, C.-L., Hwang, S.-J., and Moehle, J.P., 2013, "Shaking table tests on reinforced concrete frames without seismic detailing," *ACI Structural Journal*, Farmington Hills, Michigan, Vol. 110, No. 6, pp. 1001-1012.
- Youssef, M., and Ghobarah, A., 2001, "Modeling of RC beam-column joints and structural walls," *Journal of Earthquake Engineering*, Vol. 5, No. 1, pp. 93-111.
- Zeris, C.A., 1984, *Investigation of the Response of the Imperial County Services Building to the 1979 Imperial Valley Earthquake and its Implications to Earthquake Resistant Design*, University of California, Berkeley, California.

Project Participants

National Institute of Standards and Technology

John (Jack) R. Hayes Jr.
Engineering Laboratory (MS8604)
National Institute of Standards and Technology
100 Bureau Drive
Gaithersburg, Maryland 20899

Steven L. McCabe
Engineering Laboratory (MS8604)
National Institute of Standards and Technology
100 Bureau Drive
Gaithersburg, Maryland 20899

NEHRP Consultants Joint Venture

APPLIED TECHNOLOGY COUNCIL
201 Redwood Shores Parkway, Suite 240
Redwood City, California 94065
www.ATCouncil.org

CONSORTIUM OF UNIVERSITIES FOR
RESEARCH IN EARTHQUAKE ENGINEERING
1301 S. 46th Street, Building 420
Richmond, California 94804
www.CUREE.org

Joint Venture Management Committee

James R. Harris
J.R. Harris & Company
1775 Sherman Street
Denver, Colorado 80203

Christopher Rojahn
Applied Technology Council
201 Redwood Shores Parkway, Suite 240
Redwood City, California 94065

Robert Reitherman
Consortium of Universities for Research in
Earthquake Engineering
1301 S. 46th Street, Building 420
Richmond, California 94804

Andrew Whittaker
University at Buffalo
Dept. of Civil, Structural, and Environ. Engin.
230 Ketter Hall
Buffalo, New York 14260

Joint Venture Program Committee

Jon A. Heintz (Program Manager)
Applied Technology Council
201 Redwood Shores Parkway, Suite 240
Redwood City, California 94065

William T. Holmes
Rutherford + Chekene
55 Second Street, Suite 600
San Francisco, California 94105

Michael Constantinou
University at Buffalo
Dept. of Civil, Structural, and Environ. Engin.
132 Ketter Hall
Buffalo, New York 14260

Jack Moehle
University of California, Berkeley
Dept. of Civil and Environmental Engineering
775 Davis Hall
Berkeley, California 94720

C.B. Crouse
URS Corporation
1501 4th Avenue, Suite 1400
Seattle, Washington 98101

James R. Harris (ex-officio)
Andrew Whittaker (ex-officio)

Project Management

Christopher Rojahn
Applied Technology Council
201 Redwood Shores Parkway, Suite 240
Redwood City, California 94065

Jon P. Kiland
Applied Technology Council
201 Redwood Shores Parkway, Suite 240
Redwood City, California 94065

Project Technical Committee

Kenneth J. Elwood (Technical Director)
University of British Columbia
Dept. of Civil Engineering
6250 Applied Science Lane
Vancouver, British Columbia V6Z 1Z4

Jack Baker
Stanford University
Dept. of Civil and Environmental Engineering
473 Via Ortega
Stanford, California 94305

Craig D. Comartin
CDComartin Inc.
7683 Andrea Avenue
Stockton, California 95207

William T. Holmes
Rutherford + Chekene
55 Second Street, Suite 600
San Francisco, California 94105

Jack Moehle
University of California, Berkeley
Dept. of Civil and Environmental Engineering
775 Davis Hall
Berkeley, California 94720

Peter Somers
Magnusson Klemencic Associates
1301 Fifth Avenue, Suite 3200
Seattle, Washington 98101

Project Review Panel

JoAnn Browning
University of Kansas
Dept. of Civil, Environ., and Arch. Engineering
1530 W. 15th Street
Lawrence, Kansas 66045

Nicholas Luco
U.S. Geological Survey
P.O. Box 25046 – DFC – MS 966
Denver, Colorado 80225

Gregory Deierlein
Stanford University
Dept. of Civil and Environmental Engineering
Blume Earthquake Engineering Center, M3037
Stanford, California 94305

Terry Lundein
Coughlin Porter Lundeen, Inc.
413 Pine Street, Suite 300
Seattle, Washington 98108

James O. Jirsa
University of Texas at Austin
Dept. of Civil, Arch., and Environ. Engineering
ECJ Hall, Suite 4.726
Austin, Texas 78759

Mike Mehrain
URS Corporation
915 Wilshire Boulevard, Suite 700
Los Angeles, California 90017

Laura N. Lowes
University of Washington
Dept. of Civil and Environmental Engineering
233C More Hall, Box 352700
Seattle, Washington 98195

ATC-78-1 Project Representatives

Michael Mahoney
Federal Emergency Management Agency
500 C Street SW, Room 416
Washington, D.C. 20472

Robert D. Hanson
FEMA Technical Monitor
5885 Dunabbey Loop
Dublin, Ohio 43017

Abbie Liel
University of Colorado, Boulder
Dept. of Civil, Arch. and Environ. Engineering
ECOT 411
Boulder, Colorado 80309

Workshop Participants

Daniel Abrams
University of Illinois
Dept. of Civil and Environ. Engineering
2118 Newmark Civil Engineering Laboratory
Urbana, Illinois 61801

Ibrahim Almufti
Arup
560 Mission Street, Suite 700
San Francisco, California 94105

Jack Baker
Stanford University
Dept. of Civil and Environ. Engineering
473 Via Ortega
Stanford, California 94305

Majid Baradaran Shoraka
University of British Columbia
6250 Applied Science Lane
Vancouver, British Columbia V6T 1Z4

Russell Berkowitz
Forell/Elsesser Engineers, Inc
160 Pine Street, 6th Floor
San Francisco, California 94111

Craig D. Comartin
CDCComartin Inc.
7683 Andrea Avenue
Stockton, California 95207

Panagiotis Galanis*
University of California, Berkeley
Dept. of Civil and Environmental Engineering
325 Davis Hall
Berkeley, California 94720

Siamak Sattar*
University of Colorado, Boulder
Dept. of Civil, Arch. and Environ. Engineering
Boulder, Colorado 80309

*Graduate Student, Member of Working Group

Gregory Deierlein
Stanford University
Dept. of Civil and Environ. Engineering
Blume Earthquake Engineering Center, M3037
Stanford, California 94305

Kenneth J. Elwood
University of British Columbia
Dept. of Civil Engineering
6250 Applied Science Lane
Vancouver, British Columbia VT6 1Z4

Robert Fleischman
University of Arizona
Dept. of Civil Engineering and Engineering Mech.
1209 East Second Street
Tucson, Arizona 85721

Panagiotis Galanis
University of California, Berkeley
Dept. of Civil and Environmental Engineering
325 Davis Hall
Berkeley, California 94720

Wassim Ghannoum
University of Texas at Austin
Dept. of Civil, Arch., and Environ. Engineering
301 E. Dean Keeton Street, Stop C1747
Austin, Texas 78712

Selim Günay
University of California, Berkeley
Dept. of Civil and Environmental Engineering
733 Davis Hall
Berkeley, California 94720

Bernadette Hadnagy
Applied Technology Council
201 Redwood Shores Parkway, Suite 240
Redwood City, California 94065

Robert D. Hanson
5885 Dunabbey Loop
Dublin, Ohio 43017

Curt Haselton
California State University, Chico
Dept. of Civil Engineering
270 Langdon Hall
Chico, California 95929

William T. Holmes
Rutherford + Chekene
55 Second Street, Suite 600
San Francisco, California 94105

MaryBeth Hueste
Texas A&M University
Dept. of Civil Engineering
808U CE/TTI Building, MS 3136
College Station, Texas 77843

James O. Jirsa
University of Texas at Austin
Dept. of Civil, Arch., and Environ. Engineering
ECJ Hall, Suite 4.726
Austin, Texas 78759

Insung Kim
Degenkolb Engineers
235 Montgomery Street, Suite 500
San Francisco, California 94104

Michael Korolyk
Tipping Mar
1906 Shattuck Avenue
Berkeley, California 94704

Sashi Kannath
University of California, Davis
Dept. of Civil and Environmental Engineering
2001 Engineering III
Davis, California 95616

James LaFave
University of Illinois
Dept. of Civil and Environmental Engineering
2118 Newmark Civil Engineering Laboratory
Urbana, Illinois 61801

Dawn Lehman
University of Washington
Dept. of Civil and Environmental Engineering
214B More Hall, Box 352700
Seattle, Washington 98195

Abbie Liel
University of Colorado, Boulder
Dept. of Civil, Arch. and Environ. Engineering
ECOT 411
Boulder, Colorado 80309

Laura N. Lowes
University of Washington
Dept. of Civil and Environmental Engineering
233C More Hall, Box 352700
Seattle, Washington 98195

Nicholas Luco
U.S. Geological Survey
P.O. Box 25046 – DFC – MS 966
Denver, Colorado 80225

Stephen Mahin
Pacific Earthquake Engineering Research Center
University of California, Berkeley
777 Davis Hall, MC 1710
Berkeley, California 94720

Michael Mahoney
Federal Emergency Management Agency
500 C Street SW, Room 416
Washington, D.C. 20472

Adolfo Matamoros
University of Kansas
Dept. of Civil, Environ., and Arch. Engineering
2150 Learned Hall
Lawrence, Kansas 66045

Frank McKenna
Pacific Earthquake Engineering Research Center
University of California, Berkeley
777 Davis Hall, MC 1710
Berkeley, California 94720

Jack Moehle
University of California, Berkeley
Dept. of Civil and Environmental Engineering
775 Davis Hall
Berkeley, California 94720

Khalid Mosalam
University of California, Berkeley
Dept. of Civil and Environmental Engineering
733 Davis Hall
Berkeley, California 94720

Santiago Pujol
Purdue University
School of Civil Engineering
550 Stadium Mall Drive
West Lafayette, Indiana 47907

Christopher Rojahn
Applied Technology Council
201 Redwood Shores Parkway., Suite 240
Redwood City, California 94065

P. Benson Shing
University of California, San Diego
Dept. of Structural Engineering
409 University Center
9500 Gilman Drive – MC0085
La Jolla, California 92093

Peter Somers
Magnusson Klemencic Associates
1301 Fifth Avenue, Suite 3200
Seattle, Washington 98101

Jonathan P. Stewart
University of California, Los Angeles
Dept. of Civil and Environmental Engineering
5731 Boelter Hall
Los Angeles, California 90095

John Wallace
University of California, Los Angeles
Dept. of Civil and Environmental Engineering
5731C Boelter Hall
Los Angeles, California 90095

Eric B. Williamson
University of Texas at Austin
Dept. of Civil, Arch., and Environ. Engineering
301 E. Dean Keeton Street, Stop C1747
Austin, Texas 78712

Bryan Zagers
Coughlin Porter Lundeen, Inc.
413 Pine Street, Suite 300
Seattle, Washington 98101

Farzin Zareian
University of California, Irvine
Dept. of Civil and Environmental Engineering
E/4141 Engineering Gateway
Irvine, California 92697